A SEMI-CONTINUOUS CHROMATOGRAPHIC PROCESS FOR THE SEPARATION OF CARBOHYDRATES

A thesis submitted for the degree of

Doctor of Philosophy

by

CHI BUN CHING

Department of Chemical Engineering
University of Aston in Birmingham

April 1978

A SEMI-CONTINUOUS CHROMATOGRAPHIC PROCESS FOR THE SEPARATION OF CARBOHYDRATES

CHI BUN CHING APRIL 1978

A Thesis submitted for the Degree of Doctor of Philosophy

SUMMARY

A review is given of general chromatographic theory, the factors affecting the performance of chromatographic columns and aspects of scale-up of the chromatographic process. The chemi-adsorption separation mechanism employed in this research study for the separation of glucose and fructose is outlined. A review of various industrial processes for manufacturing high fructose syrups is also included so as to serve as a basis for comparison.

The design and construction of a sequential continuous chromatographic separation unit (SCCR4), for liquid-solid chromatography applications, is described. Counter-current operation was simulated by sequencing a system of inlet and outlet port functions around ten, 2.54 cm internal diameter x 70 cm long, glass columns.

Operation of the unit for continuous separation of glucose and fructose by chemi-adsorption chromatography is reported, using 150 - 300μm diameter calcium charged ion exchange resin (Zerolit SRC14) as packing, and distilled water as the mobile phase. The effects of feed and purge flowrates, mobile phase temperatures and feed concentration have been investigated. A feed of 50% w/v of glucose and fructose solution has been successfully separated, at a rate of 3 cm^3 min^{-1}, into a glucose-rich and a fructose-rich product of purity 86.4% w/w and 88.7% w/w respectively. This throughput, on an equal cross-sectional area basis, is approximately 2½ times that achieved by an equivalent batch process operated by the Boehringer Mannheim Company.

A temperature dependence of the equilibrium distribution coefficient (K_D) of fructose, established from small-scale batch column work, provides an explanation for the higher contamination of the glucose-rich product observed in SCCR4 runs conducted at elevated mobile phase temperatures.

A theoretical treatment, based on an equilibrium stage concept, of the counter-current liquid-solid chromatographic process has been attempted. A batch column study was conducted to acquire the necessary equilibrium data and plate heights for the computer simulation work. Results achieved from the theoretical study indicated partial agreement with the experimental findings.

KEY WORDS

CHROMATOGRAPHY, CONTINUOUS, GLUCOSE, FRUCTOSE.

Acknowledgements

The author is indebted to the following:

Professor G.V. Jeffreys and the Department of Chemical Engineering for making available the facilities for research.

Professor P.E. Barker, who supervised the work, for his advice and guidance.

Mr. M.F. Lea for construction of the electronic equipment.

Mr. N. Roberts and other members of the departmental technical staff who assisted in the manufacture and construction of the sequential unit.

Dr. S. Holding, Dr. B.W. Hatt and other research students in the Separation and Purification Group for many thought provoking discussions.

Dr. P.J. Somers and Mr. R. Woodbury of Birmingham University, for their advice on the analytical techniques.

Miss J. Morton for her diligence in typing this thesis.

The University of Aston for provision of a scholarship.

CONTENTS

1 Introduction

Sugar is an extremely important food ingredient. In 1972 about 90 million tonnes/year of sucrose was produced worldwide and of this 3 million was consumed in the United Kingdom. Traditionally, the main source of sucrose is either from cane, grown in tropical and sub-tropical areas such as the Caribbean, or from beet in more temperate zones such as the United Kingdom, France and Belgium. Most sucrose is sold in the form of granulated sugar of normal purity 99.95% However, quite a large part of sugar used in the food industry as a sweetening substance and also as preserving agent is handled as a liquid product. Liquid sugar is usually partially or wholly inverted, i.e. the sucrose is hydrolysed into its two component sugars, D-glucose and D-fructose.

In the past few decades, world sugar prices have fluctuated widely. Consequently, in nations that relied heavily on sugar imports such as Japan (80%) and Britain (60%), there has been a strong desire for an economic alternative means of producing synthetic liquid syrups. As in these countries, home-grown starch sources in the form of rice, maize and potatoes are readily available, emphasis has been centered on converting such starch into a syrup with an acceptable sweetness. Although, through a combined acid-enzyme process, a complete

conversion of starch into glucose has been achieved, the product is only 70-75% as sweet as sucrose. Hence other means of increasing the sweetness of starch syrups has been sought. As fructose is much sweeter than its isomer glucose, the corn wet-milling industry has spent many years trying to develop corn syrups containing sufficient fructose to increase the sweetness. Since Marshall and Kooi (68) disclosed a microbial enzyme capable of isomerizing glucose into fructose in 1957, there have been various attempts to commercialize the techniques. The most successful isomerisation process was reported by Clinton Inc, a division of Standard Brands of the U.S.A. In May 1970, a high fructose corn syrup containing 71% w/v solids of which 50% w/w was glucose, 42% w/w fructose and the balance higher saccharides was manufactured by the Company. This syrup had a sweetness comparable with sucrose but was marketed at a lower price. However, the enzyme, glucose isomerase, only acts on one anomer of D-glucopyranose, namely the α-amomer. The product fructose also is produced in only one anomeric form. Consequently, the limit of equilibrium with this process is around 50% and the economic conversion is even lower (42-44%).

Due to its sweetness property (-D fructopyranose in cold dilute solutions is twice as sweet as an equivalent amount of sucrose), very high fructose content syrups are desired by industries for producing low calorie foods and drinks. Since the maximum fructose content of syrups derived from both the sucrose inversion process and the enzymatic conversion process is approximately 50% w/w, an additional enriching process is necessary if a very high fructose content product is desired.

The similarities in physical and chemical properties between glucose and fructose molecules have posed difficulties in applying the conventional means of separation for resolving the two components. In the past decade, large scale separations of glucose from fructose have been performed on chromatographic columns packed with calcium charged resins. The basic separation mechanism involved was the formation of complexes between calcium ions and fructose molecules. However, it is understood that all these operations were conducted in the batch mode, the most notable processes being those of the Colonial Sugar Refining Company (64) and the Boehringer Mannheim Process (65). Hence, a continuous process for separating fructose from glucose would therefore merit investigation.

Since the original work of Tswett (162), chromatography has developed into two main forms : liquid chromatography and gas chromatography. Most of the effort in the 1950's and 1960's was placed upon the development of gas chromatography equipment and techniques. However, in the past decade, the significance of liquid chromatography as a separation means for production scale purposes, has gradually been realised. Their applications include the resolution of materials such as proteins, enzymes, polysaccharides and monosaccharides. It is believed that all such operations were performed in a batch co-current mode. Despite the use of repeated sample injections, the batch nature of operation tends to limit column utilization. Consequently, many novel designs for both cross and counter-current continuous chromatography have been proposed. The designs for cross-current operation have subsequently been proved difficult to implement on a large scale.

Recently, more effort has been directed towards the development of chromatographic schemes based on a counter-current operating mode. In these schemes, the mobile phase fluid, and the stationary phase solid, are moved counter-currently, and the feed mixture usually introduced at mid-point of the separating section. The feed component with the less-affinity for the stationary phase travels with the eluting solvent, to emerge from

one end of the separating section, while the feed component with the strong affinity for the stationary phase travels preferentially with the stationary phase, and emerges from the other end of the separating section. The advantage of counter-current operation is that the entire column length can be effectively utilized, and, within a major part of the separation section, only partial resolution of components is required to achieve pure products at column outlets. This allows severe overloading, by conventional batch standards, to be tolerated.

Barker and co-workers (1-23) have been actively involved in the development of counter-current chromatographic processes, particularly in the field of gas-liquid chromatography. The latest experimental scheme, reported by Barker and Deeble (20), was based on simulating the relative phase movement by sequencing a system of inlet and outlet port functions around a closed loop of twelve 7.6 cm diameter columns. Successful separations of an equivolume mixture of 1, 1, 2-trifluoro-1, 2, 2-trichlorothane and 1, 1, 1-trichloroethane have been achieved at product purities in excess of 99.7% and feed throughput of up to 1400 cm^3 hr^{-1}.

In the present research programme, a semi-continuous counter-current liquid-solid chromatographic unit, based

on the flow scheme of Barker and Deeble (20), is to be designed, constructed, and commissioned for the separation of fructose from glucose. Due to a possible industrial link with the isomerization process, the experimental programme of this research study will be devoted to maximizing feed throughput. However, the effect of increasing mobile phase temperature, which will lead to a reduction of pressure drop, on the separation performance of the chromatographic unit, is also to be investigated. Finally, attempts to simulate the system, possibly based on an equilibrium stage concept, will be made. It is anticipated that batch column studies will also be necessary for acquiring the necessary equilibrium data and separation efficiencies in terms of plate height.

The semi-continuous counter-current liquid-solid chromatographic unit constructed for the present research study is referred to throughout this thesis as the SCCR4 unit.

Chapter 2

Literature Survey - Part 1

Theory of Chromatographic Process

2 Theory of Chromatographic Process

2.1 Scope

The work of James and Martin in 1951 (26) has prompted a spectacular growth of interest in the general field of chromatography. At present, publications on the subject exceed two or three thousand per annum and will continue to increase. Hence, it is necessary to be restricted in the summary of relevant literature. The first part of this survey serves to provide a general introduction to the basic concept and terminology in chromatography. This is followed by a review of the various theoretical models concerned with chromatographic zone spreading.

Scale up of the chromatographic process is reviewed in Chapter Four and in two sections : batch chromatography and continuous chromatography.

2.2. Introduction to General Chromatography

In chromatography, two or more constituents of a sample are separated from each other by virtue of the difference in their distribution ratio between a stationary phase and a mobile phase in intimate contact. Modern liquid chromatographic methods can be classified, according to the mechanism of retention, into four main categories:

(i) Ion exchange chromatography
(ii) Exclusion chromatography
(iii) Partition chromatography
(iv) Adsorption chromatography

Ion exchange chromatography involves a continuous reversible exchange of ions between the electrolytes and the ion exchangers. Separation is achieved through a difference in the affinities of the solute ions for the resin. In exclusion chromatography, separation results because of the difference in the size of the sample molecules; those that are small enough are able to penetrate the porous matrix of the packing; whereas the larger components remain in the interstitial regions between the particles. Consequently, the largest components elute first, followed by those of smaller molecules. Partition chromatography relies on the absorption of solutes by an inert solid support coated with a liquid stationary phase. Finally, adsorption chromatography depends on the association formed between the solutes and the active sites of the solid packing.

Such associations can be physical or chemical. In recent years, most of the latter applications are performed with ion exchanger, charged to an appropriate form, as the stationary phase. The actual mechanism does not involve any exchange of ions and in ion exchange field such a separation is sometimes known as ligand exchange.

2.2.1. Basic Theories and Definitions

There are three modes of general chromatographic practice namely, elution, frontal and displacement. In liquid chromatography operation, elution is the only mode that can result in a quantitative separation. As such, most of the established theories in the field are related to elution chromatography.

In elution chromatography, the sample components are injected at the beginning of the chromatographic column and development occurs through the bed. Each individual component will elute from the column according to its equilibrium distribution coefficient between the stationary and the mobile phases. If a very small sample size is used (a linear distribution isotherm), the concentration profiles of the products are symmetrical and Gaussian.

Under such conditions it is possible to relate directly the time of elution of the peak maximum to the equilibrium distribution coefficient. As shown in

Fig. 2.1 A Typical Chromatogram

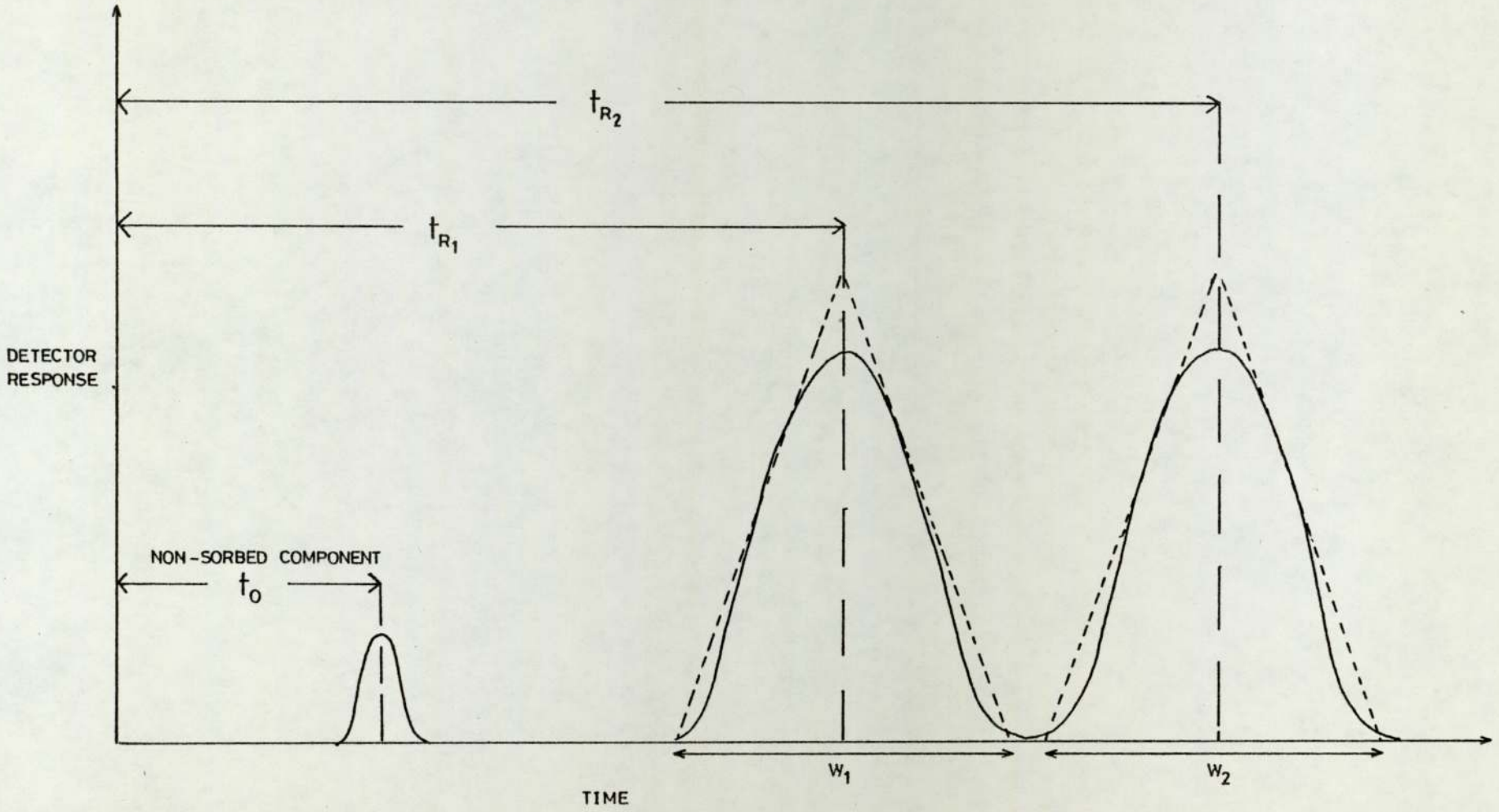

Figure (2.1), this time is called the retention time, and the method is classified as linear elution chromatography. However, such ideal conditions are difficult to achieve in practice.

As the elution time is a function of the velocity of the mobile phase, a more fundamental parameter of retention is the retention volume, V_R. This represents the total mobile phase volume required to elute the sample from the column. The fundamental retention equation for a chromatographic process (25) is

$$V_R = V_M + K_D V_S \qquad (2.1)$$

where, V_R = Elution volume of a component

V_M = Total volume of the mobile phase in the column

= Void + Pore Volume

V_S = Volume of stationary phase (resin's solid matrix)

K_D = equilibrium distribution coefficient

$$= \frac{\text{concentration of solute in stationary phase}}{\text{concentration of solute in liquid phase}}$$

V_M can be determined from the elution time of a non-retained component, t_o (Fig 2.1):

$$V_M = t_o . F' \qquad (2.2)$$

F' = mobile phase flowrate

Another important retention parameter is the capacity factor, K', defined:

$$K' = K_D \frac{V_S}{V_M} = \frac{\text{amount of solute in stationary phase}}{\text{amount of solute in mobile phase}}$$

Sub into equation (2.1)

$$V_R = V_M (1 + K') \qquad (2.3)$$

If $K' = 0$, the retention volume is equal to V_M.

Expressing equation (2.3) in time units and assuming the flowrate is constant:

$$t_R = t_o (1 + K') \qquad (2.4)$$

The time of a non-sorbed component, t_o, is equal to the column length divided by the mobile phase velocity, L/u. Hence equation (2.4) can be arranged to:

$$t_R = L/u (1 + K') \qquad (2.5)$$

This equation provides the fundamental relationship between retention and equilibrium distribution coefficient, column length, and mobile phase velocity.

2.2.2. Resolution

In chromatography, the degree of separation is quantified through a resolution term, R_s. In a binary chromatogram, two characteristics namely, the distance between the peak maxima and the widths of the bands, are used to describe resolution. Figure (2.2) shows the influence of these two characteristics on resolution.

Fig. 2.2 Chromatogram Illustrating Resolution

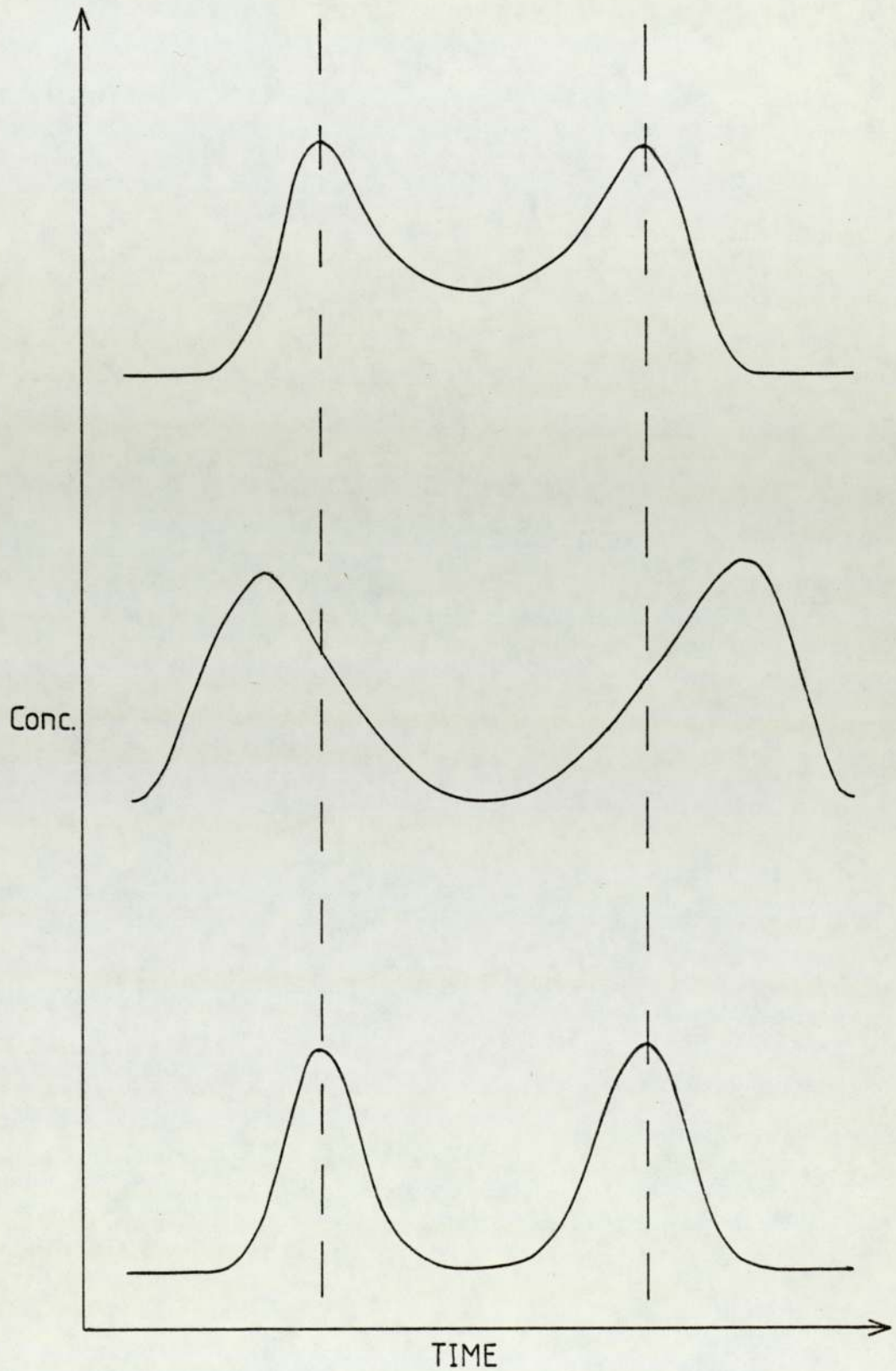

In the top chromatogram, the bands overlap and thus indicates a poor separation. In the middle chromatogram, the two bands are well separated but the band widths and the distance between peaks are large. This implies a complete resolution is only achieved through a long elution time and during which solute bands spreading occur. In the lower chromatogram, the two bands are separated and also both the individual band width and the distance between peaks are narrow. This represents a good separation.

A conventional form of expressing resolution is:

$$R_s = \frac{t_{R_2} - t_{R_1}}{\frac{1}{2}(W_1 + W_2)} \qquad (2.6)$$

σ = standard deviation of the Gaussian Distribution. The peak width, W, for individual component in a Gaussian distribution is equal to 4σ. In an ideal binary chromatogram, where σ_1 equals σ_2, the peak to peak separation is equal to $4\sigma_2, (2\sigma_1 + 2\sigma_2)$, if $R_s = 1$ and there will be only 2% band overlap. In high speed liquid chromatography, $R_s = 1$ is taken as a satisfactory separation. If a better resolution is required, a 6σ separation ($R_s = 1.5$) is selected. Conversely, as R_s becomes less than unity the bands overlap more and more. When it is below 0.8, the separation is usually unsatisfactory.

Equation (2.6) although useful in measuring R_s, does not relate the fundamental chromatographic parameters.

Purnell (98), based on a binary chromatogram with equal band widths, derived a relationship between resolution and three fundamental parameters:

$$R_s = \frac{1}{4} \left\{ \frac{\alpha - 1}{\alpha} \right\} \left\{ \frac{K'_2}{1 + K'_2} \right\} \left\{ N \right\}^{\frac{1}{2}} \qquad (2.7)$$

where, N = number of theoretical plates

$\alpha = \frac{K'_2}{K'_1} = \frac{K_{D_2}}{K_{D_1}}$ = relative retention

K_{D_2} = distribution coefficient for the more retarded component

K_{D_1} = distribution coefficient for the less retarded component

K'_2, K'_1 = are the capacity factors.

2.3. Theory of Zone Spreading

2.3.1. Introduction

Chromatographic separations are governed by two criteria, thermodynamic equilibria and column dynamics. It is the latter which determines the width of the solute zones and which the theories of chromatography attempt to define. Efforts by various researchers have succeeded in demonstrating the dependence of zone spreading on various factors. However, a perfect quantitative relationship linking both has yet to be developed.

2.3.2. The Theoretical Plate Concept

The theoretical plate model was introduced into chromatography by Martin and Synge (168) because of its effectiveness in describing distillation processes. In their work, a chromatographic column is assumed to consist of a number of layers each of which is equivalent to one theoretical plate, and the height of such layer is called the H.E.T.P. or 'height equivalent to one theoretical plate'. The solution issuing from each plate is assumed to be in equilibrium with the mean concentration of solute in the stationary phase throughout the plate. It is also assumed that the diffusion of solute from one plate to another must be negligible and that the mobile phase flow is discontinuous, consisting of the stepwise additions of volumes of the mobile phase equal to the mobile phase volume per plate. Further assumptions include that at equilibrium, the distribution ratio of one solute between the two phases must be independent both of the absolute value of its concentration and of the presence of other solutes.

From the above assumptions, Martin and Synge (168) postulated that a single solute band will spread into a Gaussian distribution curve. The degree of spreading of this solute band is quantified by the second moment,

or the variance of the curve.

A parameter used to characterize the efficiency of the chromatographic column is the plate height:

$$H = \frac{d\sigma_z^2}{dZ}$$

σ_z^2 = length based second moment

Z = distance along a column of length L.

Martin and Synge also observed the dependence of H.E.T.P. (H) on the mobile phase velocity (u) and the particles diameter (dp)

$$H = f\ (u, dp^2) \qquad (2.7)$$

Furthermore, as the longitudinal diffusion from plate to plate becomes relatively more significant at a reduced flowrate, they emphasised that for any given separation there is an optimum mobile phase flowrate. From the results of their experimental work on higher mono-aminoacids in protein hydrolysates, the separation chromatograms obtained were worse than that by theoretical prediction.

Glueckauf (27) converted the discrete plate model into a continuous one by reducing the plate volume to an infinitessimally small value. The concentration profile exhibits a Poisson distribution and could, if

the number of plates, N, is large enough (>100), be approximated to a Gaussian distribution. The standard deviation (σ) of this Gaussian distribution (a direct measure of zone spreading) is given by:

$$\sigma = (H. L_m)^{\frac{1}{2}} \qquad (2.8)$$

where H is the plate height and L_m is the distance migrated.

Rearranging Equation (2.8)

$$H = \frac{\sigma^2}{L_m} \qquad (2.9)$$

Equation (2.9) shows that H varies directly with σ^2, i.e. the variance of the distribution and an important statistical property of σ^2 is that it is additive and hence various independent contributions can be summed:

$$\text{i.e. } \sigma^2 = \sigma_1^2 + \sigma_2^2 + \sigma_3^2 + ... \qquad (2.10)$$

Hence the H.E.T.P. can be expressed as

$$H = \Sigma_i \frac{\sigma_i^2}{L_m} \qquad (2.11)$$

As such, various contributions to the plate height may be determined independently and summed to give an overall value for H.

The most significant deviation of the plate model concept from real column processes rests on the assumption of plate wide equilibrium. In actual situations, equilibrium is only reached at the peak maximum point. In addition, the plate model fails to account for the contributions of molecular structure, sorption phenomenon, temperature, molecular diffusion, and flow pattern towards zone spreading. However, the plate height is a useful and widely accepted parameter for the characterization of zone spreading and column efficiency.

2.3.3. Zone Spreading Rate Theories

2.3.3.1. Van Deemter Theory

In 1952, Lapidus and Amundson (28) developed a mathematical theory which incorporated mass transfer and diffusion terms into a model. This theory was later to become the foundation for the well known treatment by Van Deemter, Zuiderweg and Klinkenberg (29) of estimating plate heights. In their expression relating the column parameter to the H.E.T.P.

$$H = 2\lambda d_p + \frac{2\gamma' D_m}{u} + \frac{8}{\pi^2} \cdot \frac{K' d^2}{(1+K')^2 D_s} \cdot u \qquad (2.12)$$

λ = packing characterization term for eddy diffusivity such that eddy diffusivity, E, = $\lambda . u . d_p$.

d_p = mean particle diameter.

γ' = labyrinth factor to allow for the torous flow path.

D_M = mobile phase molecular diffusivity.

D_s = stationary phase molecular diffusivity.

d = thickness of stationary phase liquid film.

u = interstitial gas phase velocity.

$K' = \frac{F_M}{F_s}$. K_D= mass distribution coefficient.

K_D = distribution coefficient.

F_M = Fractional volume of mobile phase.

F_s = Fractional volume of stationary phase.

In a shortened form Equation (2.12) is often expressed as:

$$H = A + \frac{B}{u} + C_s.u \qquad (2.13)$$

A, B, and C_s are the eddy diffusion, axial diffusion and stationary phase mass transfer resistance terms respectively. Van Deemter introduced a further term (C_m.u) to allow for resistance to mass transfer resistance in the mobile phase. Equation (2.13) can be represented graphically is shown in Figure (2.3a).

In gas chromatography it shows that the gas phase longitudinal diffusion term becomes significant at low gas velocities. At higher gas velocities the dependence

Fig. 2·3a Graphical Representation Of The Van Deemter Equation

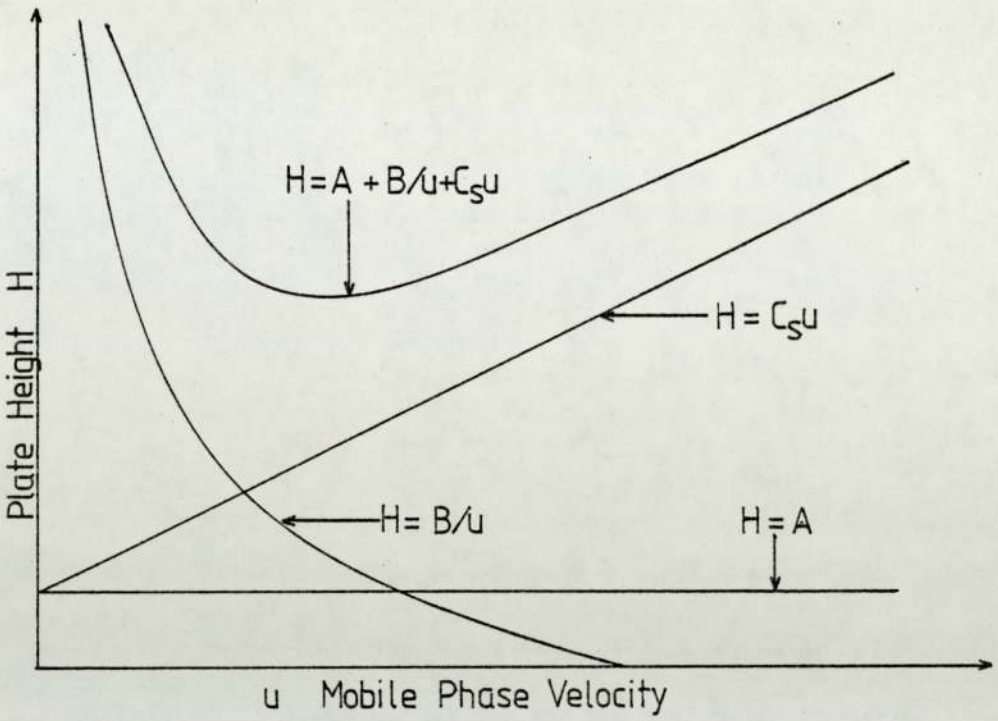

Fig. 2·3b Comparision Of The Chromatographic Plate Height Curves For Gas Chromatography And Liquid Chromatography

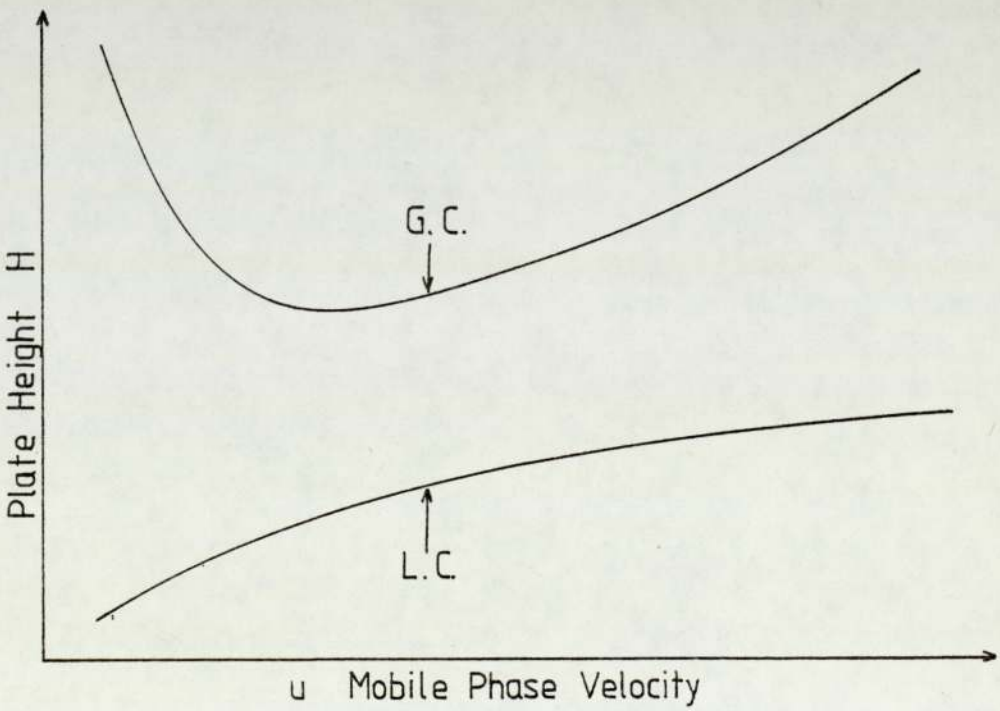

of H on B/u disappears and the stationary phase resistance to mass transfer (C_s.u) becomes controlling. Hence, Equation (2.12) is extensively applied in gas chromatography for predicting the optimum flowrate that would lead to a minimum H.E.T.P. value.

In Figure (2.3b), a similar graph for liquid chromatography illustrates how its shape differs from that of gas chromatography. The major reason being that the longitudinal diffusion coefficients in liquids are 10^4 - 10^5 times smaller than those in gases and hence contributes negligible effect towards zone spreading. Consequently, no decrease in H with increasing velocity is observed at low velocities such as with gaseous systems.

The major assumptions of Van Deemter model include a flat velocity profile for the mobile phase and no contribution from radial diffusion.

2.3.3.2. Random Walk Model

Giddings and co-workers (30-37) have conducted extensive studies on the mechanism of zone spreading, and details are fully documented in his well known text (30). With his random walk approach, Gidding attempted to explain and correlate various individual molecular processes occuring in a chromatographic column. In his model, he claimed that solutes are in constant

random movement. Each particle can move either in a forward or backward direction in varying step magnitudes. However, for simplification, all step lengths are assumed to be equal (l'). If there is an exactly equal chance for moving in either direction, the random walk is symmetrical and hence will result in a Gaussian distribution of molecular spreading. The variance, σ^2 is equal to $l'^2 n'$, where n' is the number of steps taken. Each process occurring in the column has its own value of l' and n' which can be summed to give a total variance

$$\sigma^2_{TOTAL} = \Sigma\sigma_i^2 = \Sigma l_i'^2 n_i' = H \qquad (2.14)$$

Giddings uses the variance due to the molecular diffusion process, and given by Einstein (38) as:

$$\sigma^2 = 2Dt_D$$

t_D = Diffusion time

D = Diffusion coefficient

To determine the contribution to the plate height from longitudinal mobile phase diffusion

$$H = \frac{2\gamma' D_m}{u} \qquad (2.15)$$

γ' is the obstructive factor (<1) and its inclusion is the result of a reduction in the actual distance

diffused by the molecule caused by its need to skirt the granules of the solid phase. Similarly, the contribution from the longitudinal stationary phase diffusion can be calculated. However, it is usually insignificant.

Giddings evaluates absorption and desorption kinetics as

$$H = 2R\,(1-R)\,\frac{d^2 u}{D_s} \qquad (2.16)$$

d = thickness of stationary phase film.

R = is the fraction of time of solute in the mobile phase.

Diffusion processes occurring in the mobile phase are significantly more complicated than those in the stationary phase. Part of the difficulty can be traced to the fact that diffusion is occurring in a very complex network of interconnected channels and void spaces. In addition, the flow velocities vary over wide limits when moving across a channel or from one channel to another. Giddings (30) identifies five different types of velocity inequalities which can lead to zone spreading in the mobile phase, Figure (2.4).

(1) Transchannel effects caused by a higher velocity in the centre of the channel than at the wall.

Fig. 2.4 Contributions To Velocities Inqualities In Large Diameter Column

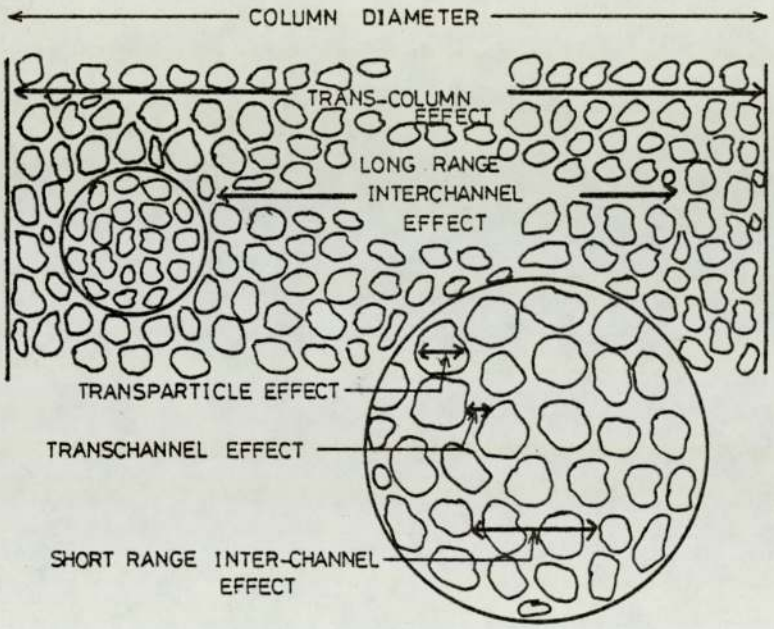

(2) Transparticle effects caused by the stagnant mobile phase in the pores of the support particles.

(3) Short-range inter channel effects.

(4) Long-range inter channel effects.

(5) Transcolumn effects between central and outer regions of the column.

By assuming a step to a faster streamline is a forward step and a step to a slower streamline a backward step, Gidding established that the overall mobile mass transfer resistance term was as follows:

$$H = \frac{W.d_p^{\,2}.u}{D_M} \qquad (2.17)$$

d_p = particle diameter.

D_M = Diffusivity of solute in mobile phase.

$$W = \sum_{i=1}^{5} W_i = \frac{W_\alpha^2\, W_\beta^2}{2}$$

W_α = (distance between velocity extremes)/d_p.

W_β = (difference between extreme and average velocity)/u.

By using the classical theory of solute molecules being locked in fixed stream paths, the individual eddy diffusion contribution from each of the five categories of velocity inequalities are defined as:

$$H = 2d_p \sum_{i=1}^{5} \lambda_i = 2d_p\lambda \qquad (2.18)$$

where, $\lambda_i = \frac{W_\beta^2 . W_\lambda}{2}$

W_λ = a structural parameter.

Summing all the plate height contributions:

$$H = 2\lambda d_p + 2\gamma' \frac{D_M}{u} + 2R(1-R) \frac{d^2 u}{D_2} + \frac{W\, d_p{}^2 u}{D_M} \qquad (2.19)$$

In simpler form

$$H = A + B/u + C_s . u + C_m . u \qquad (2.20)$$

Equation (2.20) is of the same general form as the Van Deemter equation (2.13) except for the addition of a mobile phase mass transfer resistance term. Implicit in equation (2.20) is the assumption that individual contributions to plate height, H are independent and additive. Recognising the close relationship between eddy diffusion and flow inequalities, Gidding proposed a "Coupling Theory", in which the resistance to mass transfer in the mobile phase and the eddy diffusion term are coupled. The simplified form of the equation is

$$H = \frac{B}{u} + C_s u + \frac{1}{1/A + 1/C_m . u} \qquad (2.21)$$

Fig.2.5 Comparison Between Classical And Coupled Equation For Plate Height

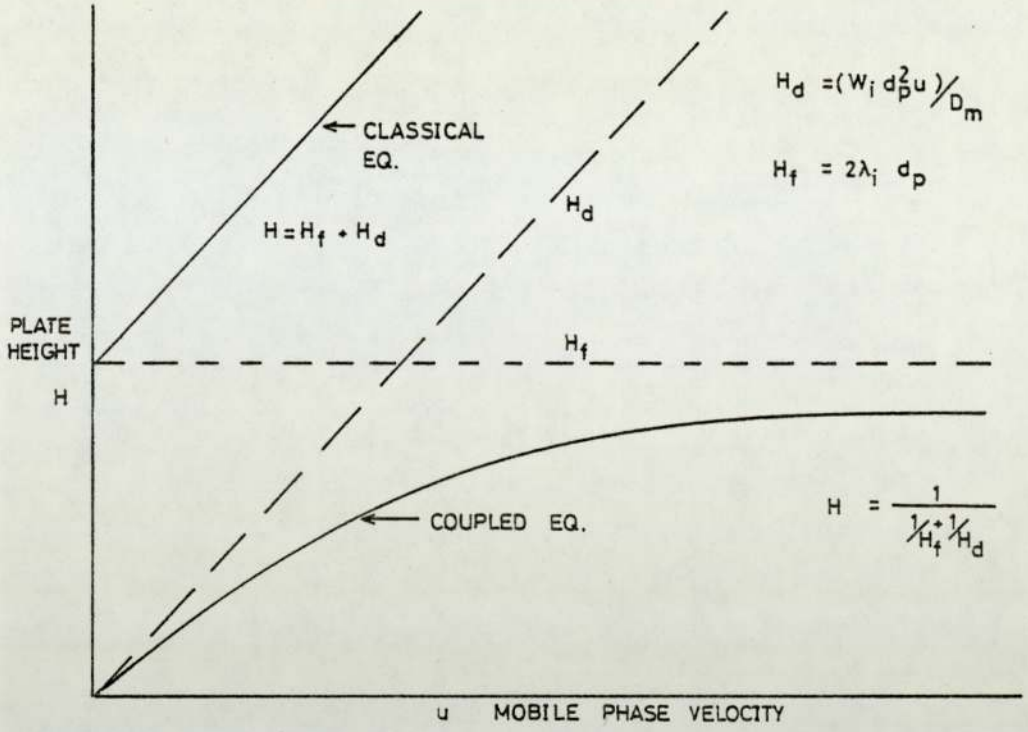

Fig.2.6 Comparison Between Actual Equilibrium Component Zone Concentration Profiles For Normal Elution Chromatography

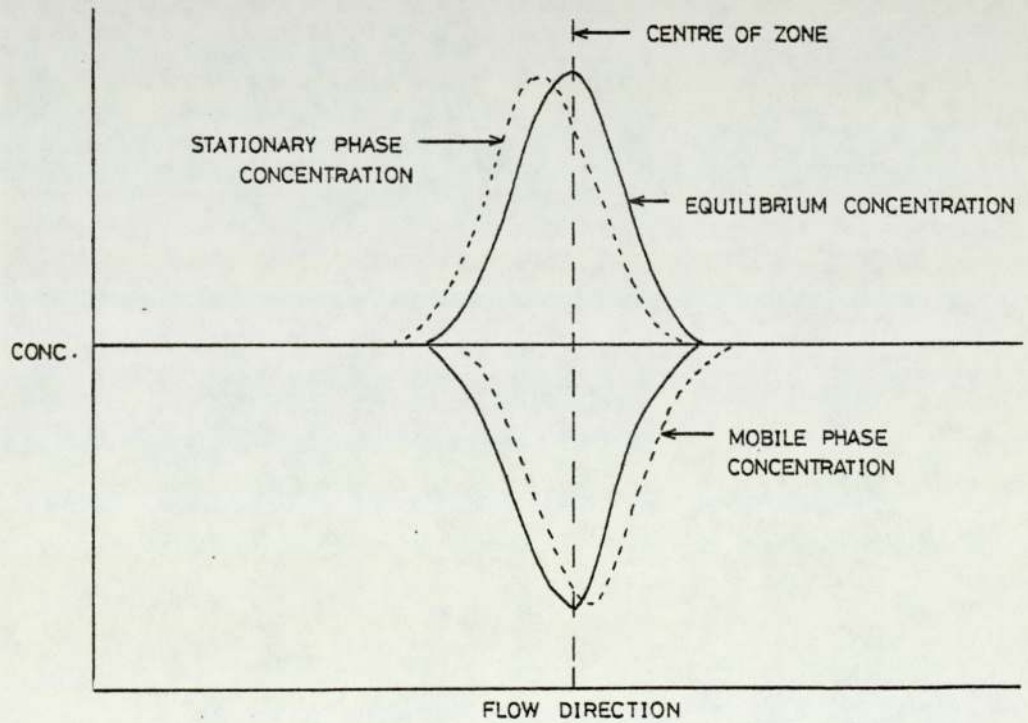

The total value of the contribution to H of the coupled term is always less than that obtained from either of the component parts. (Figure 2.5) and equation (2.19) have been extensively applied by many workers in the general field of chromatography for the successful prediction of plate height. However, the main drawback of this random walk approach is the assumption of an equal step magnitude and that a fixed number of steps are taken by all the participating molecules. In actual practice, particularly in reference to sorption - desorption kinetics a variable number of steps and step lengths are taken by individual molecules. Giddings, realising such limitations of the random walk approach, further developed the more powerful generalised non-equilibrium theory for zone spreading.

2.4. Generalised Non-equilibrium Theory

Giddings (30) claims that true equilibrium between two phases only exists at the centre of the zone, as shown in Figure (2.6). The stationary phase concentration has a lag in its equilibrium value, whilst the mobile phase concentration will always be ahead of its equilibrium concentration. The main cause for such a non-equilibrium situation arises from the slow rate of mass transfer between the two phases. The extent of non-equilibrium

can be reduced by having the zone migrating slowly and thus preventing rapid concentration changes. Giddings, based on such a non-equilibrium concept, succeeds in replacing the single molecular events of the random walk method by the gross processes of mass transfer. The final relationship for H derived from non-equilibrium theory is given as:

$$H = \frac{2\gamma' D_M}{u} + g' R(1-R) \frac{d^2 u}{D_s} + \left\{ \frac{1}{2\lambda d_p} + \frac{D_M}{W d_p^2 u} \right\}^{-1} \qquad (2.22)$$

where D_M = diffusivity of solute in mobile phase

g' = configuration factor of the packing.

Equation (2.22) differs from the resulting plate height equation (equation (2.21)) derived from the random walk approach, only by the inclusion of an extra term to account for packing geometries. It provides an insight into the non-equilibrium dynamics of chromatography and serves as a guideline on column optimization. For instance, in liquid chromatography, the first term of equation (2.22) shows that eddy diffusion contribution is insignificant due to a very small liquid diffusion rate. The second term indicates that at a higher flowrate, the time available for achieving equilibrium is reduced. This, coupled with

the increase of the stagnant liquid film around the particle (larger) at a high liquid loading, results in a greater departure from equilibrium and an increase in plate height. Furthermore, the term R(1-R) has a maximum value when R = 0.5, i.e. when the solute spends half of its time in the mobile phase, and tends to be zero when R becomes unity or zero. Consequently, for a low H.E.T.P. value, it is essential to choose a mobile phase within which the solute diffusion coefficient is large. Finally, in the coupled eddy diffusion term, the direct dependence of H on both d_p and d_p^2 reflects a desire to choose the diameter of the packing material to be as small as possible.

To summarize, the preceeding theoretical concepts provide a detailed account of the mechanism involved in zone spreading. However, the contribution to the plate height from sample size, column geometries etc. are ignored. A theoretical treatment of these factors will be discussed in Chapter 4.

Chapter 3

Literature Survey - Part 2

Chemi-adsorption Chromatographic Separation of Monosaccharides

3. Chemi-adsorption Chromatographic Separation of Monosaccharides.

3.1. Scope

In the main studies of this research programme, fructose is continuously separated from an equal mixture of glucose and fructose. Both the molecules of glucose and fructose are of identical molecular size and weight, and would therefore be eluted at the same rate from a bed of porous type packing. However, if the mixture is developed through a bed of calcium charged cationic resins, fructose, due to its complex formation with calcium ions, is retarded and glucose will emerge first from the column. Such a chemi-adsorption effect is employed in this research work for producing a high purity fructose solution.

The complexing of fructose with the alkaline earth metals has been demonstrated by a number of workers, but no conclusive report has ever been published regarding the exact mechanism involved. However, the hypothesis proposed by Angyal (39-45) provides a logical explanation for the non-complexing effect between glucose and the calcium ions. Hence the first part of this survey includes the various studies on metal complexing and the Angyal hypothesis, and aims to establish the existence of such a chemi-adsorption separation effect between the two monosaccharides.

Although, only the separation of fructose from glucose is investigated in this research programme, it has always been a belief on the part of the author that the semi-continuous chromatographic system can be developed into an industrially viable process for manufacturing a high purity fructose syrup from either a sucrose or corn starch hydrolysate feedstock. As such, included in this survey is a detailed account of various processes and methods from which high fructose syrup are being manufactured. These can serve as guidelines for comparing the performance of the SCCR-4 process.

3.2. Metal Complexing of Fructose

3.2.1. Proof of Existence of Sugar Complexing

Complex formations between various metals and sugars have been known and studied as early as the ninteenth century. However, most of the chemical formulas suggested by the early investigators for compounds formed by the interaction of carbohydrates with metal bases are mere assumptions, based on insufficient evidence. Von Lippman (47), Vogel and Georg (48) has compiled a very comprehensive account of the work achieved by the early researchers. Later studies of the D-glucose - sodium chloride - water system by Matsuura and Tegge (49), and of the sucrose - sodium iodide -

water system by Wiklund (50), furnish a more conclusive proof of the existence of 2D-glucose. NaCl. H_2O, 2sucrose. 3NaCl. $3H_2O$, and sucrose. NaCl. $2H_2O$. These authors demonstrate not only the presence of sugar-salt complexes, but also how the formation of complexes affects the solubilities of both the carbohydrates and the salt. Tegge and Lebedev (51) have extensively studied the relation between temperature and the stabilities of 2D-glucose. NACl. H_2O in aqueous systems. The fact that this complex crystallizes better than the pure D-glucose from aqueous solution is important industrially.

Saltman and Charley (52) have shown by dialysis experiments that the Calcium, Magnesium, Barium and Strontium ions form soluble chelates in aqueous alkaline solution with D-galactose, D-fructose, D-arabinose, D-rilose, maltose and lactose. Charley and Sarkar (52) showed that the absence of any precipitation of alkaline earth metal hydroxide when an aqueous solution containing D-fructose and an alkaline-earth salt is made alkaline (pH12) is additional evidence for the existence of such complexes.

The existence of sucrose. BaO, sucrose. SrO are shown by Nushizawa and Hachihama (53) in phase studies. Other studies in the changes in the physical phenomena

of the carbohydrates as a result of metal complexing, include an alteration of specific optical rotation, as reported by Rendlemen (54), an increase in the viscosity of the resulting solution, as reported by Naffia and Frege (55). Finally, Stokes et al. (56) has demonstrated an increase of sucrose concentration in an aqueous solution of potassium or sodium chloride results in a decrease in the solution's electric conductivity.

3.2.2. The Angyal Hypothesis

All the above studies have provided sufficient evidence for complex formation existing between various sugars and cations, they have not, however, succeeded in revealing the basic mechanism, nor provided information on the conditions required for such complexing.

S.J. Angyal (39) reported that the coordination complexes of sugars and cations are formed by the displacement of water molecules in the solvation sphere of cations by the hydroxyl groups of the sugar, which is a polyalcohol. Since water solvates ions much better than does a monoalcohol, the latter will not displace water to any considerable extent. If two or more hydroxyl groups in a compound, namely sugar, are in a sterically favourable arrangement, they may displace two or more molecules, respectively, of water from the solvation sphere. There are no cases known,

however of di-alcohol complexing strongly with cations in aqueous solution, it appears that at least three hydroxyl groups in favourable steric arrangement are required for complex formation. His work (39-45) over several years has established the fact that for complex formation with alkaline earth (Ca^{++}, Ba^{++}, Sr^{++}) cations, sugars in their ring forms require either:

(i) an axial-equatorial-axial arrangement of three hydroxyl groups on successive carbon atoms of the tetrahydropyran ring (Fig 3.1a).

or (ii) a cis-cis relationship on successive carbon atoms of the tetrahydrofuran ring (Fig 3.2a).

In the axial-equatorial-axial arrangement, the sequence can be two hydroxyl and one methoxyl group.

Angyal (39,44) experiments have shown that various members of the aldohexose family, for example α-D-Gulose and α-L-Talose (Fig 3.1b, 3.1c), form complexes with the calcium ions in aqueous solution. However, under the same conditions, no calcium complexes are reported for D-Glucose and D-Mannose (Fig 3.1e, 3.1d). These sugars lack the required ax-eq-ax sequence of hydroxyl groups.

Parrish and Angyal (45) further investigated the formation of complexes of D-glucose, D-xylose, sugars which do not possess the required configuration in their

Fig. 3.1 Molecular Structure Of Aldohexoses

(a) α-D-Allo-Pyranose

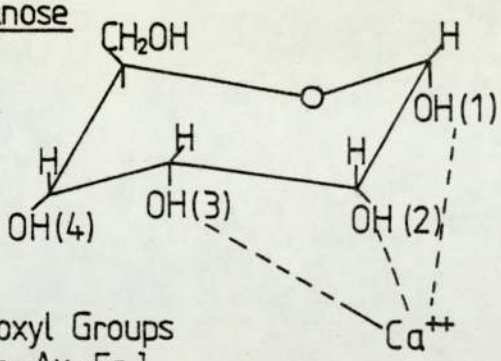

Orientation Of Hydroxyl Groups
NO. 1,2,3,4, : [Ax-Eq.-Ax-Eq.]

(b) α-D-Gulo-Pyranose

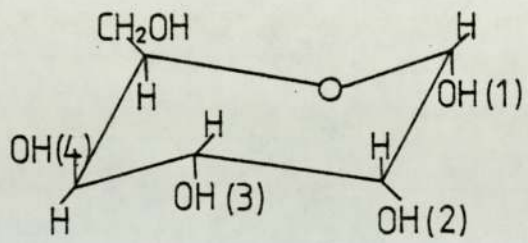

[Ax-Eq.-Ax-Eq.]

(c) α-L-Talo-Pyranose

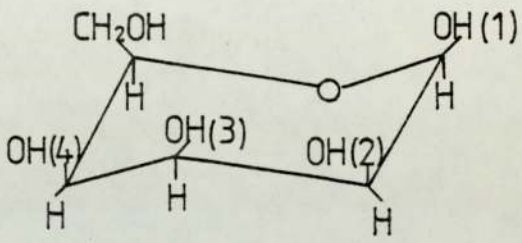

[Eq.-Ax-Eq.-Ax]

(d) α-D-Manno-Pyranose

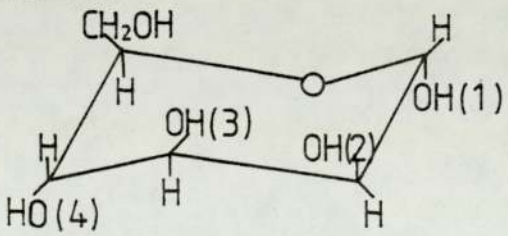

[Ax - Ax-Eq.-Eq.]

(e) α-D-Gluco-Pyranose

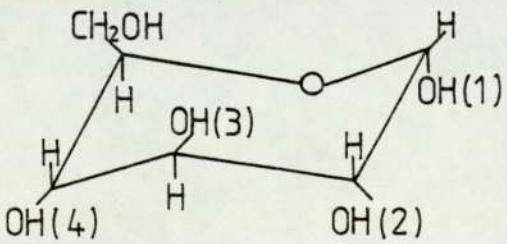

[Ax-Eq.-Eq.-Eq.]

β-D-Gluco-Pyranose

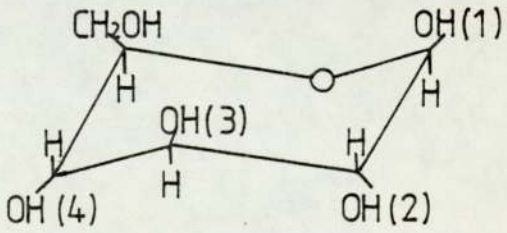

[Eq.-Eq.-Eq.-Eq.]

six member ring form. Their findings have revealed that in the presence of methanol and hydrochloric acid, D-glucose reacts and the corresponding methyl glycosides or dimethyl acetals are formed. However with the addition of either Strontium or Calcium Chloride to the reaction mixture, the proportions of the products obtained are altered. Consequently, it is deduced that D-glucose forms a complex with the metals under such conditions and shifts the equilibrium of the reaction. Similar observations have been reported by Domovs and Freund (57).

Reports on the complexing between D-glucose and the alkaline metal Na^+ are numerous. The formation of a complex between the two in aqueous solution has been reported by Matsuura (49). Recently, investigation on the system in ethanol medium is conducted by Rendleman (54). The most notable application of this complexing effect is reported by Tatuki (58), who claims that glucose can be separated from a mixture of glucose and fructose by complexing the former with sodium chloride and crystallizing it out. However, until recently, no attempts and conclusive evidence have established an actual mechanism of such complexing between D-glucose and the sodium ions.

Fructose, a member of the Ketohexose family, exists in both the α, β pyranose and furanose forms. The latter

Fig. 3·2 Molucular Structure Of Allose And Fructose

(a) α-D-Allose-Furanose

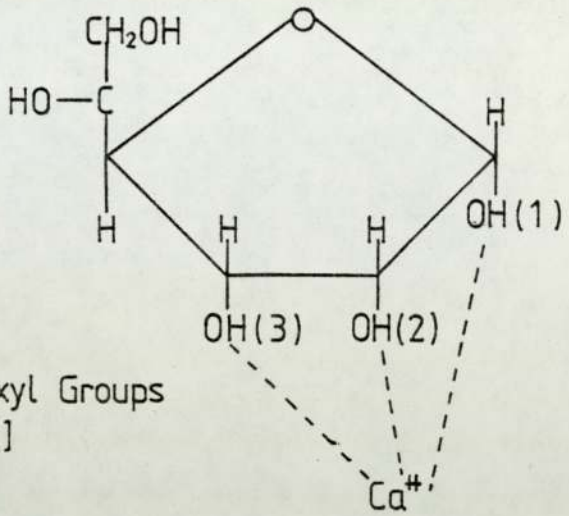

Orientation Of Hydroxyl Groups
Of 1,2,3, :[Cis - Cis]

(b) ß-D-FructoFuranose

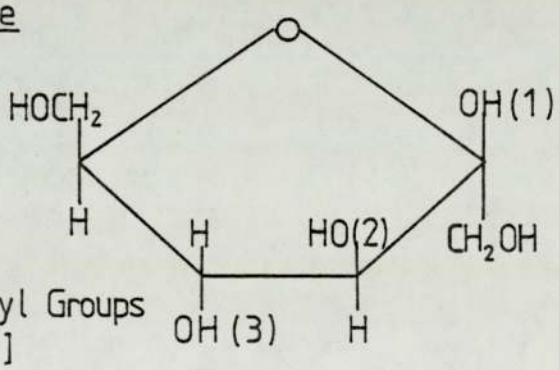

Orientation Of Hydroxyl Groups
Of 1,2,3, :[Cis-Trans]

(c) α-D-FructoPyranose

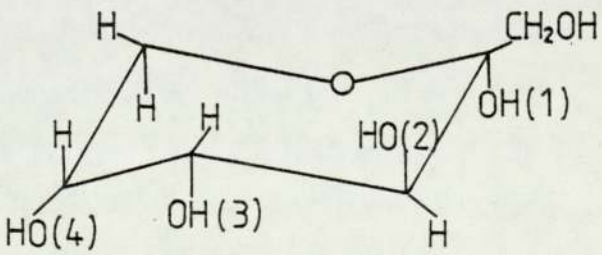

Orientation Of Hydroxyl Groups
Of 1,2,3,4,:[Ax-Ax-Ax-Eq.]

form is found to occur in most oligo and poly-saccharides, probably because of the greater stability of this form of the sugar as compared with its pyranose form.

As explained in Figure (3.2b), both the α and β forms of fructopyranose and fructofuranose do not possess either a sequence of ax-eq-ax or a cis-cis arrangement of hydroxyl groups. Indeed, such a favourable steric sequence does not appear in any optical isomers (α, β, D and L form) of fructose. Consequently, the hypothesis proposed by Angyal for the complex formation between the calcium ions and the aldohexoses could not be generalised to account for the ketohexose complexing with the alkaline earth metals.

However, reports on the subject are numerous and the application of the calcium-fructose complexing effect as a means for separating fructose from a mixture of sugars is already a proven success. Smith and Tollen's (59) studies on the reaction of fructose with various alkaline earth metal (Ca^{++}, Ba^{++}, Sr^{++}) in aqueous medium has provided the early evidence of the existence of the Ca^{++} fructose complex. Additional confirmation is achieved through the investigation by Domovs and Freund (57) on the same system in a methanol medium. The oustanding chelating ability is further illustrated by Verstraiten in his studies with

Germanic acid, telluric acid and boric acid (60). Antikainen (61) reports the formation of a 1:2 germanate-fructose chelate during studies of the interaction of $H_2 \cdot Ge \cdot O_3$ and D-fructose in the pH range 6-10. Recent studies appear to have placed more emphasis upon the application of the calcium fructose complexing effect as a means of separation. These processes will be discussed in more detail in the following section.

In conclusion, Angyal's hypothesis of a sequence of ax-eq-ax arrangement of hydroxyl groups provides a logical explanation for the non-complexing of D-glucose with calcium ions. However, the actual complexing mechanism between D-fructose and calcium ions is still open to further hypothesis.

3.3. High Fructose Syrups

3.3.1. The Need for the Fructose Syrup

Fructose (laevalose or fruit sugar) appears naturally in many different plants particularly in ripe fruit and honey. It is also a significant component part of sucrose, raffinose, inulin and various similar starch containing polysaccharides. Of all the known "sugars", fructose contains the highest sweetening potential. The sweetness of the β-D-fructose in cold dilute solution is up to twice that of sucrose. Hence

with regard to a low caloric diet, fructose offers the possibility to produce a low calorie food without reducing its enjoyment value. The calorific value of fructose (3.73 cal/gm) is similar to that of sugar (3.94 cal/gm).

More benefit is derived from fructose from a synergistic effect in combination with saccharin . A mixture of 0.01 gm of saccharin and 1.0 gm of fructose provides a sweetness level of 7 gm of sucrose in one-seventh the bulk and have only one-seventh the calories. Similarly with sucrose, a 10% water solution of 60% fructose and 40% sucrose is 1.3 times as sweet as 10% pure sucrose and 1.1 times as sweet as 10% pure fructose. Furthermore, high fructose syrup offers a greater storage stability compared with liquid sucrose. Hence, more recently fructose syrup is now widely used in confectionary, cake, beverages and ice-cream industries.

From the medical viewpoint, the fact that fructose causes no hyperglycaemia and no insulin release is the reason for its important role in diabetic diets and in diets for patients with hepatic billiary and heart diseases.

3.3.2. Processes for Manufacturing High Fructose Syrup

Methods for producing high fructose syrup are classified into three main categories according to the

raw materials:

(i) Hydrolysis of sucrose

(ii) Enzymatic conversion of corn starch

(iii) Hydrolysis of inulin, a polyfructosan.

3.3.2.1. Hydrolysis of Sucrose

The conventional method for manufacturing fructose syrup is the hydrolysis of sucrose, which is a disaccharide. The main source of sucrose is from either sugar canes or sugar beets. The hydrolysis process is called sugar inversion and can be achieved by directly contacting the feed with mineral acids, or by passing the sugar through columns of cation exchange resin charged to the H^+ form. In the former case, all the free acid ions in the hydrolysate have to be removed subsequently by an anion exchanger.

As the structure of sucrose consists of one molecule of glucose and one molecule of fructose, the product from the inversion process contains an equal amount of both sugars. However, a complete conversion is difficult to attain, and the resulting solution usually contains some residual disaccharide. The purity of fructose in the syrup produced from such processes rarely exceeds 40%. Consequently, a further refining process is required to enrich the fructose content.

In 1969, Jones and Wall (62,63) reported that columns of neutral forms of sulphuric acid type ion-exchanger resins could be employed to separate mono-saccharides mixtures with water as the developing solvent. In their work, columns (70 x 2.2 cm I.D.) of Dowex 50W x 8% Divinyl benzene (200 - 400 mesh, Ba^{++}) are used and the mono-saccharides are eluted by water in the order D-Glucose, D-Sorbose, D-Galactose, D-Xylose, D-Mannose, D-Fructose and D-Sorbitol. Their results have shown that if the difference between the elution volumes is more than 25 cm^3 the corresponding pair of sugars are readily separable. The recorded volumes of D-Glucose and D-Fructose are 157 cm^3 and 200 cm^3 respectively. As such, it can be predicted that a complete resolution of the two sugars is possible. The discovery of Jones and Wall has prompted various attempts to incorporate such separation mechanisms as a means of enriching fructose syrup. The most notable processes are now recorded.

3.3.2.1.1. The Colonial Sugar Refining Co. Process (64)

The Colonial Sugar Refining Co. claimed a new process and apparatus for the separation of fructose and glucose from syrups containing them. In their work, a 1.8 m resin bed length (no mention of column diameter) was used. Dowex 50W, a sulphonated polystyrene cation

resin, cross-linked with 4% Divinylbenzene and having a particle size of 420 - 210μm is reported to be a suitable packing. The ion exchanger is charged with the calcium ions, however it is reported that other alkaline earth metals like Strontium or Barium are equally suited to the process. The selection of the calcium salts is made based on their cheapness and non-toxic property. The feed employed is invert sugar solution.

The process includes the recycling of certain fractions of product and can be identified in four main steps. Firstly, predetermined volumes of the feed syrup and water are admitted to the column sequentially with the control of various valves. At the start of the operation the column is half filled with a water immersed resin bed. The water level is lowered to the upper surface of the resin and the syrup is fed to the top of the column. Elution water is then introduced into the column just before the syrup level drops to the upper surface of the resin. The second step is the separation of the effluent from the column sequentially into various fractions:

(i) a dilute solution of glucose

(ii) a concentrated glucose-rich solution

(iii) recycle (I) consisting of concentrated glucose-rich solution but highly contaminated with fructose.

(iv) recycle (II) consisting of concentrated fructose-rich solution highly contaminated with glucose.

(v) a concentrated fructose-rich solution

(vi) dilute fructose-rich solution.

The next step is the re-admitting sequentially of recycle (I), recycle (II), additional feed and elution water to the column. The final step is the repeat of step two and three in a cyclic manner.

The total product outlet flowrate is reported to be approximately 0.195 $m^3 . h^{-1} . m^{-2}$ of resin bed. As stated in the patent, in spite of the fact that a greater separation of fructose and glucose can be achieved at ambient temperature (20°C) than at elevated temperature (60°C), the latter is preferred. This is related to the fact that concentrated syrups are viscous and slow moving at low temperature and their dilution entails increased evaporation costs. Hence, all the storage tanks containing feed syrups are equipped with heating devices. The operating column is also lagged to minimize heat losses. There are two sets of results presented in the patent with each representing a different fresh syrup to total feed ratio.

In the first one, in which a ratio of 1:4.68 is chosen, the effluent analysis is as follows:

the concentrated glucose-rich fraction has a total solids concentration of 24% w/w, of which 78% is glucose and 22% is fructose; the concentrated fructose-rich fraction has a total solids concentration of 29% w/w, of which 82% is fructose and 18% is glucose; the dilute solutions has a total solids concentration of 1% w/w substantially all of which is fructose.

In the second set of results, a fresh syrup to the total feed charge ratio of 1:6 is used. The product analysis is as follows: the concentrated glucose-rich fraction has a total solids concentration of 23% w/w, of which 75% is glucose and 25% is fructose; the concentrated fructose-rich fraction has a total solids concentration of 24% w/w, of which 95% is fructose and 5% is glucose; the loss in the dilute solutions, mainly fructose, is equivalent to a solid concentration of 2% w/w.

The amount of recycle is shown to affect the purity of the products and for a given volume of resin bed and elution water, increasing the fresh syrup quantity will lead to a poorer resolution.

The process has been automated. However, as the raw feed employed in this process is invert sugar, a preliminary hydrolysis step is required.

3.3.2.1.2. Boehringer Process (65)

In 1967, Boehringer Mannheim Company was granted

a patent for a process from which glucose and fructose can be obtained from sucrose or sucrose containing invert sugars. In comparison, the previous Colonial Sugar Refining Co. process only has technical importance when the starting materials can be produced in a simple and cheap way and, in particular, free from impurities, for example, inorganic salts. It is known that invert sugar solutions through an ion exchanger in the pure H-form suffer undesirable discolourations at elevated temperature and long residence times. Similar effects are observed in solutions of glucose and fructose produced by inversion with mineral acids and subsequently passed over a basic exchanger for the purpose of removing the excess acid ions.

Such adverse effects are eliminated in the Boehringer process for the feed employed is an aqueous solution of sucrose. In operation, the feed is passed over a cation exchanger which has been charged, at room temperature, as fully as possible with calcium ions, but still containing 1 to 30% of free H^+ ions. The residue acid ions serve to hydrolyse the sucrose, whereas the calcium ions form complexes with the fructose molecules and thus separation results. It is reported that, such cation exchanger columns show no detectable difference in the ability to separate glucose and fructose as compared to columns which are fully charged with Ca^{++} ions. In addition, a complete hydrolysis is also achieved.

Since the success of such a process hinges on the preparation of the ion exchanger, the resin is charged under controlled conditions. It is stated that if a cation exchanger, in its initial H^+ form, is charged at a room temperature with 10% calcium chloride solution at a pH value lower than 8, it can still retain 3 to 5% of the H^+ ions. A complete saturation with calcium ions is only possible if the charging is conducted at 60°C or with a calcium chloride solution with a pH value greater than 8 at room temperature.

In the reported experiments, Dowex 50W x 4, a sulphonated polystyrene resin with 4% DVB crosslinkage, is used. The equipment consisted of 6 glass columns (15cm x 2m) connected in series. The depth of the resin bed in each of the columns is 1.5 m giving an overall bed length of 9.0 m and a total volume of 0.17 m^3. The operating temperature is 60°C so as to reduce the system's viscosity and pressure drop. Individual columns are heated to the required temperature with the help of a water recirculation unit.

Water is the eluent and the preferred rate is reported to be 1 to 2 $cm^3 \cdot cm^{-2} \cdot min^{-1}$. The concentration of the feed is 50% w/w and its ratio to the eluent flow is approximately 1:2. Under the above mentioned conditions, the first sugar-containing fraction (mainly glucose) emerges from the column after 3 to 5 hours, and

after a further 3 to 5 hours, the last sugar-containing fraction (mainly fructose) emerges from the column. Two sets of experimental results have been published, in the first one, pure sucrose solution is used as feed, whereas in the second run, it is replaced by a mixture of sucrose, glucose and fructose. As illustrated in chromatogram (Fig. 3.3), the two results are almost identical and no sucrose is detected in the product. This implies a complete hydrolysis is achieved.

This simultaneous hydrolysis and separation process offers a more flexible and efficient alternative for the production of fructose syrup from sucrose. Shortly after the disclosure of the Boehringer patent, various European countries have plants of such a process under construction, and the majority are installed by BMA under licence from Boehringer Mannheim GmbH.

In the pamphlet published by BMA (66), it is stated that both crystallised fructose or syrup with a 70% dry substance of pure fructose can be achieved by their plants through various stages of filtration and evaporation. A study of this industrially implemented process can provide an insight into the technical viability of the SCCR4 process being operated at a production scale.

Fig.3.3 Results Published By Boehringer Patent

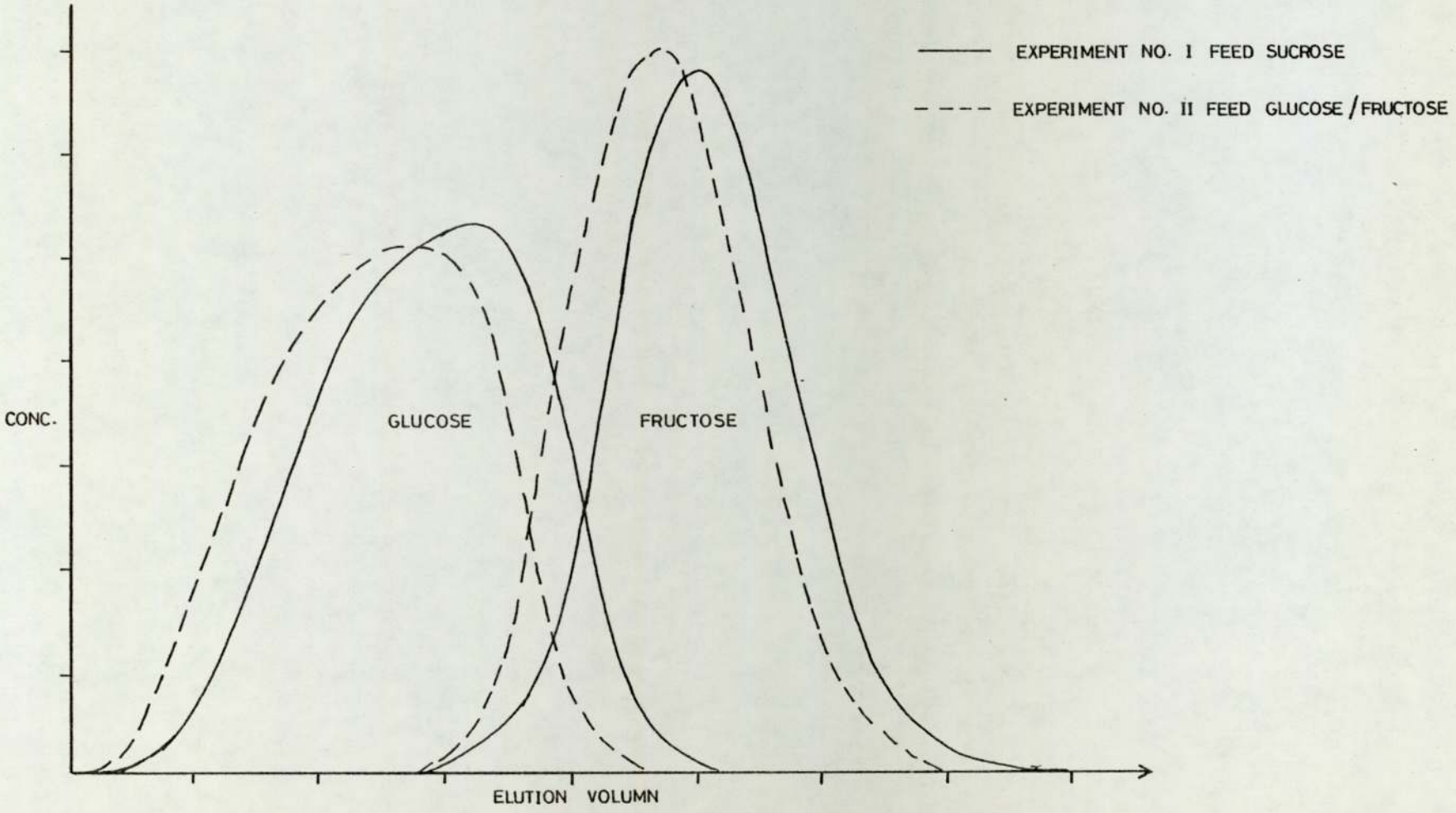

The BMA plant can be separated into three main sections namely (i) the feed preparation and purification section, (ii) the hydrolysis and separation section, and (iii) the product collection, concentration and storage section. A flow scheme of the plant is illustrated in (Fig. 3.4).

In the separation section, the sucrose is separated into the two monosaccharides and the product is divided into four main fractions (Fig. 3.5):

(i) Intermediate component group (I) - rich in glucose but contaminated with fructose.

(ii) Glucose-rich group.

(iii) Intermediate component group (II) - rich in fructose but contaminated with glucose.

(iv) Fructose-rich group.

In the feed handling and purification section, the sucrose is taken from the silo and fed to an intermediate bunker by means of a worm-screw conveyor, from which it is fed by means of dosing equipment into a dissolving apparatus. Deionised water and the sugar-containing intermediate component - group (II), recycled from the separating plant, serve as dissolving agents. The prepared sugar syrup is subjected to a filtration stage with either filter processes as a layer filtration, or with filtering agents as alluvial filtration. The filtrate is then passed through various columns of

Fig. 3.4 Schematic Digram Of The BMA Process

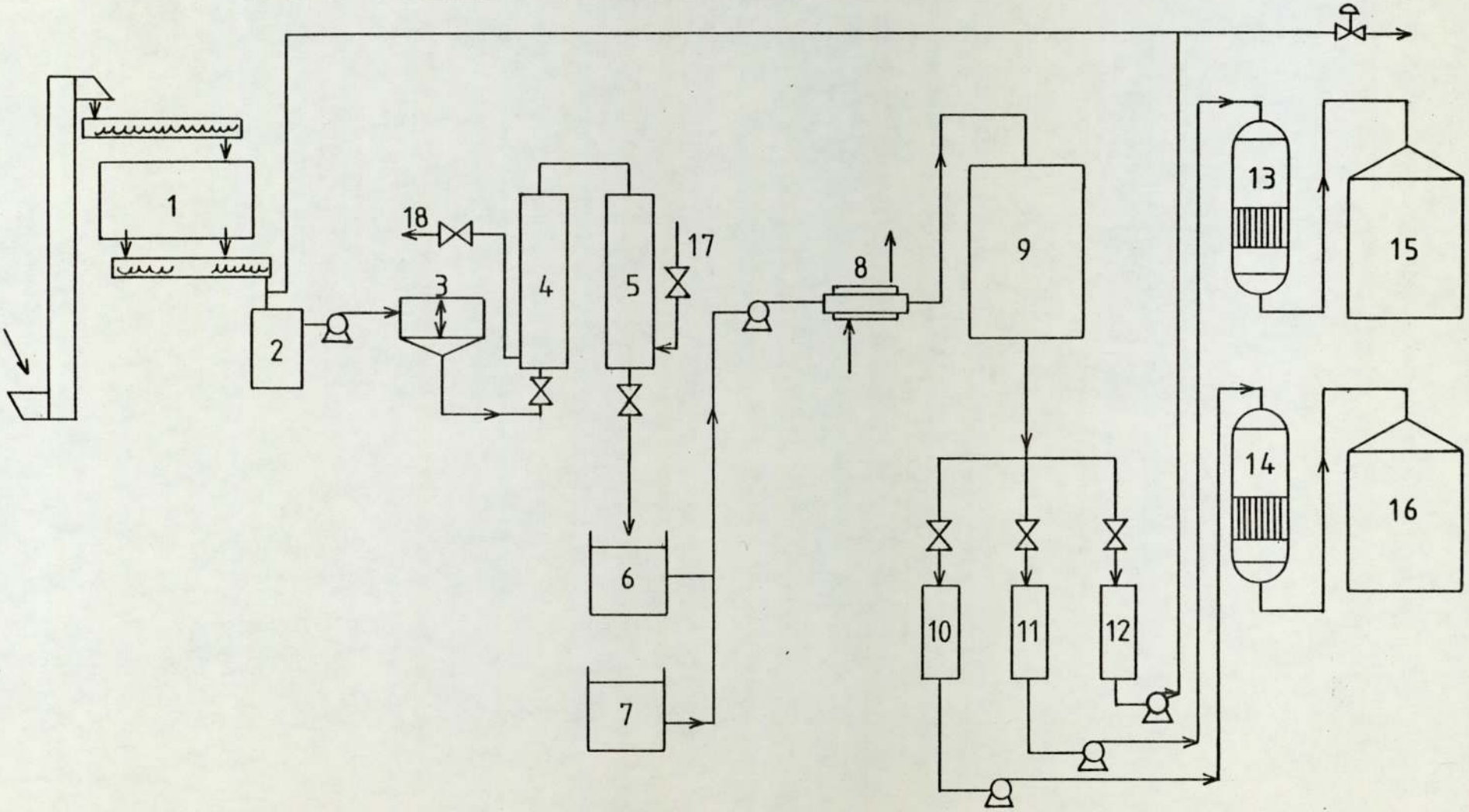

Fig. 3.5 Chromatogram Illustrating The BMA Process Product Fractionation

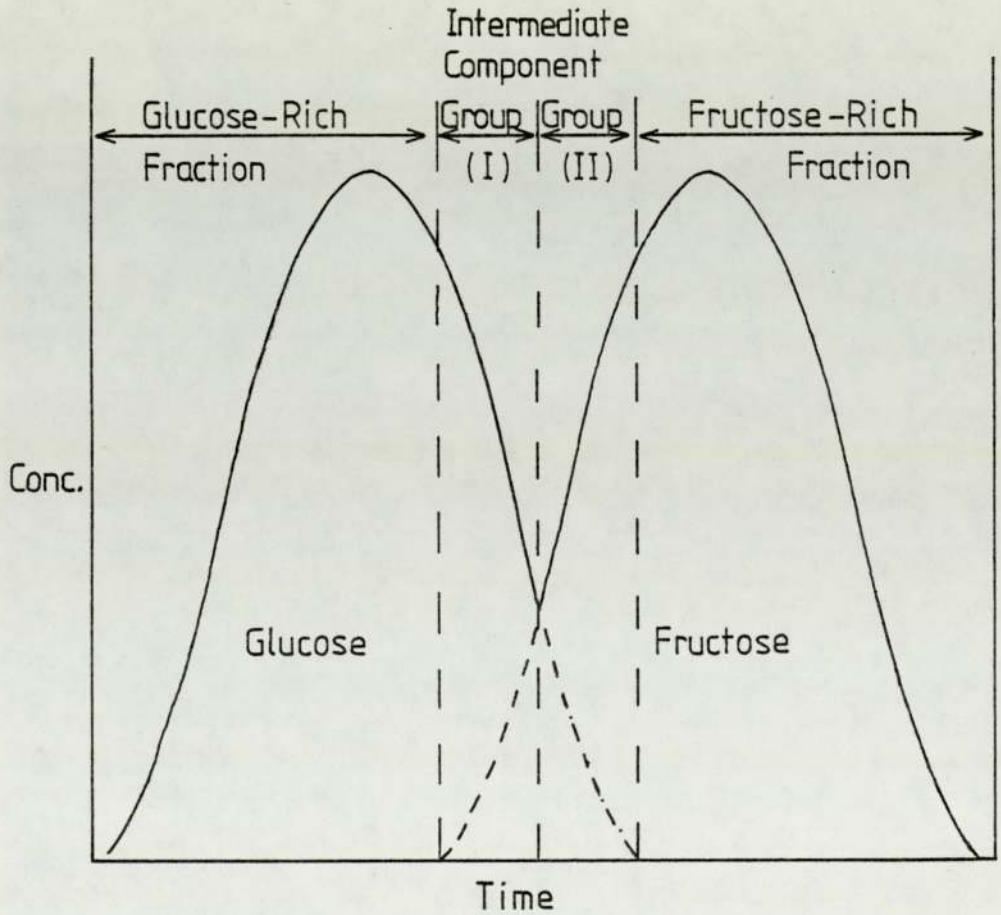

different resins for demineralising. The dimineralised sucrose is stored in the intermediate tanks and is then fed periodically to the separating column via the heat exchanger. Immediately after the sugar solution has been transferred to the component separating columns, the demineralising resins are washed out with water. Elution water is then fed to the separation column via the same heat exchanger.

In the product collection, concentration and storage stage, the glucose-rich fraction and the intermediate component - group (I) are pumped into the same container pending to be fed to a continuous two-stage evaporating plant and, under vacuum, concentrated to a glucose syrup of 50% w/w. However, the fructose-rich fraction and the intermediate component - group (II) are collected in separate containers. Subsequently, the fructose-rich fraction, with a fructose purity in excess of 96%, is concentrated in a two-stage evaporation plant to a syrup of 70% dry-substance. The resulting syrup is then subjected to a carbonisation process for decolourising purposes. After the purification, the warm fructose syrup is put through a final safety filtration stage, cooled off in the heat exchanger to the storage temperature and pumped to the storage tanks which are installed with air conditioning and exterior heating facilities. The further processing

of the 70% w/w syrup to fructose crystals are carried out by using methanol as a total crystallization from water.

The intermediate component group (II) is recycled back to the mixing tank for dissolving the fresh sucrose. In the event that liquid sugar is used as the raw material, the recycle (II) can be concentrated in a separate evaporator plant.

3.3.2.1.3. Tatuki's Patent

In 1970, R. Tatuki in his U.S. Patent (58) claimed an alternative method for separating glucose from fructose which involves the complex formation effect of the former mono-saccharide with sodium ions. He reported that methods for separating fructose in the form of calcium chloride double salt from an invert sugar solution is operationally and economically disadvantageous since a large quantity of methanol is needed in the final recovery of the fructose. In his proposed method, an invert sugar solution prepared from the acid treatment of sucrose or the isomerization of glucose is used. The above sugar solution has to be adjusted to a pH value between 7 and 9 so as to allow the glucose to form a double salt with the added sodium chloride. An alkaline substance, for example, sodium hydroxide may be added for the adjustment of the

pH of the solution. The amount of sodium chloride required could be calculated according to the amount of glucose present, however, in practice an excess quantity is used. The Na·glucose complexes are crystallised out by concentrating the solution under vacuum. Finally, the remaining solution containing the fructose and the excess sodium chloride, is deionized and concentrated to produce fructose crystals.

In summary, this process offers an alternative method for extracting fructose crystals from an invert sugar solution. Unfortunately, the presence of the excess sodium chloride in the final solution requires a further demineralisation process that would result in a change in the sugar's qualities. Furthermore, the argument put forward by the author against the use of the calcium fructose complexing technique was based entirely on the uneconomic quantities of methanol required to crystallize out the fructose. However to most food and drink industries, a syrup product is already acceptable. Finally, the results published in the patent are based on small scale batch experiments and until recently no industrial implementation of this technique is ever recorded.

3.3.2.2. Enzymatic Conversion of Corn Starch

3.3.2.2.1. Introduction

There has long been a need for an economic alternative

method of producing synthetic invert sugar from a source other than sucrose itself. As most of the nations that rely heavily on sugar imports such as Japan (80%) and Britain (60%) have readily available home-grown carbohydrate sources in the form of starch from rice and potatoes, the search has centred for several decades on the glucose from that starch. Maize can be used as an alternative source of glucose in countries like the U.S.A. because it is less labour intensive. The isolation of wheat starch is another source of glucose.

In order to convert the glucose into fructose without the production of by-products of alkaline degradation of both the sugars, a perfect chemical catalyst has yet to be developed. However, the biologists have already applied naturally occurring enzymes for the purpose.

3.3.2.2.2. The Development of Glucose Isomerase and its Application

The enzymatic isomerization of sugars is practised as far back as in the late 1930's. This involves the use of saccharifying enzymes to produce a sweeter corn syrup. In the early enzymatic process, starch is partially hydrolysed with acid and subsequently allowed to isomerize with a saccharifying enzyme. This method

produces a syrup which is significantly sweeter than syrups made by acid hydrolysis. The innovation at the time, was a real breakthrough and was protected by patent (67).

The actual mechanism of fructose isomerization is the rearrangement of a glucose molecule (aldohexose) in an equilibrium reaction by an isomerase enzyme. The transformation, which involves an intramolecular transfer of H^+ between adjacent carbon atoms in the sugar molecule can be expressed in a simplified manner as shown in Fig (3.6).

Early work in the thirties and forties on enzymatic isomerization was mainly concerned with five carbon sugars, such as xylose. In 1957, Marshall and Kooi (68) discovered an enzyme for converting D-glucose to D-fructose. The enzyme as described in their report as a specific 'xylose isomerase', would in fact, function also as 'glucose isomerase", and is prepared from Pseudomonas hydrophilia. The article emphasized the biological significance of their discovery rather than its industrial importance. It was not until 1960 that commercial appreciation was evident when a patent (69), was issued for Marshall and Kooi's invention. However, from an industrial development viewpoint, the patented process has various discouraging operational requirements. Firstly, the costly xylose is required in the bacterial

Fig. 3.6 Isomerization Of Glucose Into Fructose

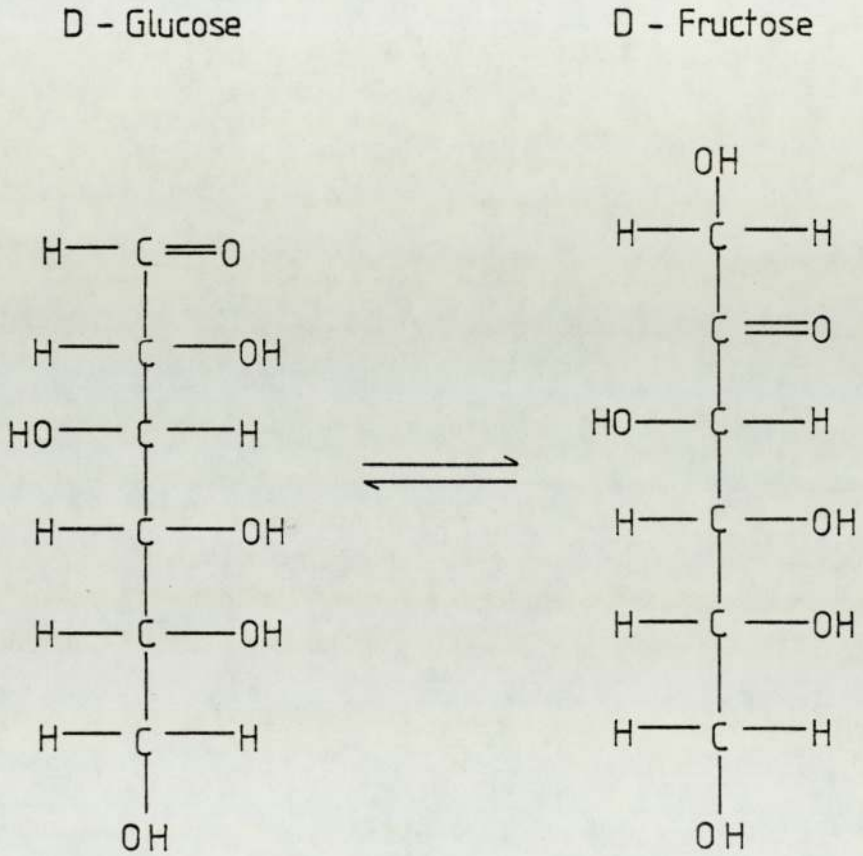

fermentation for producing the enzyme and its yeild is low. In addition, arsenate, an unacceptable food ingredient, is needed in the use of the enzyme. Finally the equilibrium conversion of glucose to fructose is low in the order of 35% or less. Overall, the described process has never been accepted as technically or commercially feasible by the U.S. technologists and no major industrial implementation is ever recorded.

The discovery by Marshall has generated enormous interest in the subject in Japan. Publications on glucose isomerization enzymes have been very prevalent since the early sixties. One of the most notable achievements from an industrial standpoint is the discovery of immobilised enzymes (70,71). This is based on the fact that the glucose isomerase enzyme, unlike most other enzymes is usually retained within the bacterial cell rather than being excreted into the medium. As such it is more advantageous in practice to use the whole bacterial cells containing the immobilised enzyme as the isomerizing agent. This differs from using cell free extracts of the enzyme, which is the common practice in enzyme technology.

In 1965, T. Sato (73) discovered a more stable form of the enzyme. He reported that a filamentous bacteria, Streptomyces phaeochromogenes, will produce "glucose

isomerase" when grown on xylose. The enzyme when used in the presence of magnesium (for activation) and cobalt (for heat stability) exhibits exceptional activity and stability. A patent was granted to Tsumura and Sato (74) in 1966 on the use of Streptomyces species.

Despite such development in the field of glucose isomerase, the process, at the time, was still generally believed to be too costly for commercialisation. The enzymatic conversion of glucose only gained industrial recognition after Takasaki published a commercial process (72) at the Fermentation Research Institute in Chiba City. In all previous methods of cultivating glucose isomerase, the costly xylose is essential and this results in the entire conversion process to be economically unfavourable. In the report, it is proposed that such cost could be reduced by growing special strains of Streptomcyces on crude xylose such as cereal bran or straw, in place of xylose. A patent was applied for (75). Later, Takasaki and co-workers (76), outlined in detail a proposed commercial isomerization process in which enzyme-containing cells of Streptomyces albus are added directly to the glucose substrate. When the isomerization is completed, the cells are recovered and reused in the subsequent batch reaction. Alternatively, the cells could be used continuously in columns.

Due to Takasaki's success in producing the glucose isomerase more economically, interests in the commercialisation of the enzymatic conversion process was aroused. Standard Brand Inc., purchased the Takasaki know-how and patent rights, and after a programme of technological development, brought the process into commercial production in 1967 (77).

Clinton's, a subsidiary of Standard Brand Inc., first commercial high-fructose corn syrup is introduced in 1967. Called Isomerase 30, it contains 15% fructose and is produced in a batch process using soluble glucose isomerase. The product syrup is about 75% as sweet as an equivalent sucrose solution. In 1968, syrup Isomerase 100, is introduced and contains 42% fructose. It is also manufactured in a batch process - initially with soluble glucose isomerase and later with the enzymes immobilised on an insoluble substrate.

In November 1972, a continuous system (77) using the immobilised enzyme was put into operation and subsequently has reduced the required contact time from more than two days for the batch process to a matter of hours for the continuous process. The commercial process, as shown in Fig (3.7), includes liquifying raw cornstarch, saccharifying to dextrose, refining, isomerising the glucose to fructose, refining again and concentrating the refined high-fructose corn syrup. The saccharification and feed preparation steps are

Fig. 3.7 Clinton Continuous Glucose Isomerization Process Flow Scheme

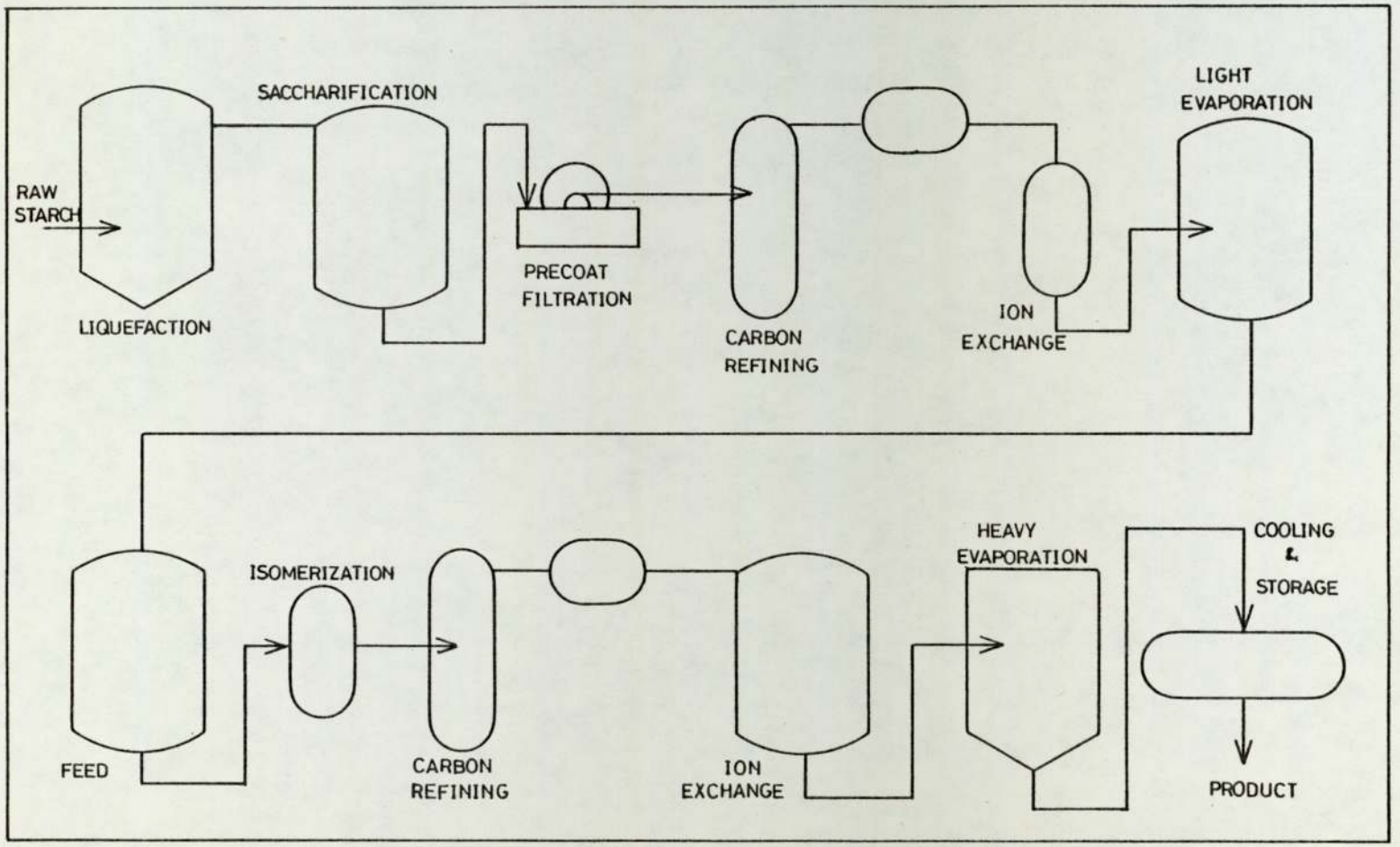

batch operations; the liquefaction, isomerization and evaporation steps are continuous operations; and the remaining steps are semi-continuous operations. The complete process is fully automated (77, 78).

The fructose content in the final product is mainly governed by the performance of the saccharification and the isomerization steps. During the former step, a higher glucose content of the syrup prior to the enzyme treatment will lead to a higher fructose content of the resulting product. Whilst in the isomerization stage, a high activity together with a minimum loss of enzyme will ensure a maximum throughput of high purity syrup. Hence enormous efforts have been placed by Clinton upon the enzyme immobilization technology. The two primary methods applied in their commercial process are both protected by patents. In the first method, described in U.S. Patent 3,694,134 (79), Streptomyces is grown under submerged aerobic conditions. The finished fermenter broth is pH-adjusted and heated to fix the glucose isomerase within bacterial cells. Then the broth is filtered and washed with water. The resulting filter cake is dried, then slurried with a glucose-containing cornstarch hydrolysate, $MgSO_4$, and $NaHSO_4$. The slurry is pumped through a pressure-leaf filter until each leaf is coated with a 2.5 to 3.8 x 10^{-2} m layer of the fixed isomerase preparation. The filter is then used in the reactor.

In the second method, described in U.S. Patent 3,788,945 (80), the glucose isomerase is adsorbed into diethyl amino ethyl cellulose or other absorbents. The resulting powder is filtered on a pressure-leaf filter, and the filter is used subsequently in the reactor.

After the reactor is loaded with the filter cake, corn syrup is pumped through at such a rate that 45% of the glucose is converted to fructose. The flowrate is gradually reduced as the activity of the fixed isomerase preparation diminishes, so that the conversion still remains at 45%. The high fructose corn syrup, Isomerase 100, manufactured from this continuous process contains 71% dry solids made up from 42% of fructose, 50% of glucose and 8% of other saccharides. It has a sweetness equivalent to sucrose in a comparable solid basis; but is marketed at only a fraction of the price of sucrose. Consequently, the new sweetener is widely accepted by various food and beverage industries. By 1980, Clinton forecasts the high fructose corn syrup will replace up to 30% of the United States market that would be supplied by sucrose products. Consequently, various companies have announced plans to begin or expand production of high fructose corn syrup.

In Europe, the conventional form of sweetener is supplied by sucrose products derived from sugar beets.

In order to protect the sugar beet industries, the European Economic Community has imposed a premium on the high fructose syrup derived from corn or other forms of starch so as to make the corn syrup less economically attractive to the food, drinks and other related industries. However, the long term strategy developed by industries to exploit the financial gain with the new sweetener is well reflected in the construction of the isomerization plant by Albion Sugar Company Ltd. of Holland in 1975 at Tilbury (81). This refinery is equipped to process 200,000 tons of starch per annum and the supply of immobilised glucose isomerase is by KSH of Holland.

3.3.2.2.3. The Development of Sweetzyme and its Application

The latest development in the isomerization process is the entry of Novo Industri (82) into the field with Sweetzyme - their trade name for an immobilised glucose isomerase produced from Bacillus coagulons. This enzyme is active up to 90°C but exhibits its high activities at about 65°C. While the premium pH range is 8 to 8.5, a useful 70% of the activity is maintained at pH7. But, the most significant advantage of using Sweetzyme is that

no cobalt ions are required for heat stabilising and hence reduces the costs for refining the final isomerised syrup.

In the previous Takasaki and Clinton technique of immobilisation, the entrapment of the glucose isomerase into insoluble cells, like the DEAE cellulose, is by heat treatment. Such an intracellular immobilisation is unlikely to produce sufficient high yields. But, Sweetzyme is immobilised in a way in which the enzyme protein and the other cell components are converted into an insoluble matrix by crosslinking with glutaraldehyde. This extracellular enzyme can be produced in much higher yeilds by genetic manipulation, substrate improvements and other advanced fermentation techniques. Furthermore, in the above described Clinton process, the enzyme for the isomerization reactor is prepared in a leaf filter and the process is conducted by pumping syrup continuously through the filter cake. However, with Sweetzyme, the crosslinked cell mass can be made into pellets by extrudation in an axial extruder, and the size of the particles can range from 6 to 700 µm in diameter. Consequently, a wider choice of reactor for the process is possible.

In a paper by Zitten et al. (82) describing a continuous Sweetzyme isomerization process, the efficiencies in terms of activities and conversion of the various

basic types of reactor are compared. The authors report that the continuous stirred tank is less effective than the fixed bed reactor as the back mixing, for kinetic reasons, gives a poorer utilization of the enzyme activity. Their proposed reaction scheme and rate expression for the design of enzymatic isomerization reactor is:

$$E' + G \rightleftharpoons E'G \rightleftharpoons E'F \rightleftharpoons E' + F$$

$$\text{Activity} = \frac{d(\text{Fructose})}{dt} = -\frac{d(\text{Glucose})}{dt}$$

At equilibrium

$$= \frac{\text{Flow } (G_o X - (B + C G_o) \text{ In } (1 - \frac{X}{X_{eg}}))}{k.w}$$

B, C, k = constants

X = degree of conversion = F/Go

G_o = initial glucose concentration

X_{eg} = degree of conversion at equilibrium

w' = amount of enzyme

In general,

$$\text{Activity} = \frac{\text{Flow} \cdot (Go\ X - k\ \text{In}\ (1 - X))}{k.\ w.\ \phi(X)} \qquad (3.1)$$

$\phi(X)$ = empirical function of X

$\phi(X) \rightarrow 1$ for $X \rightarrow 0$

$\phi(X) \rightarrow 0$ for $X \rightarrow X_{eg}$

$\phi(X) \rightarrow 0.6$ for $X = 0.45$

Based on Equation (3.1), the authors attempted to estimate the theoretical requirement of Sweetzyme required

Fig. 3.8 Molecular Structure Of Inulin

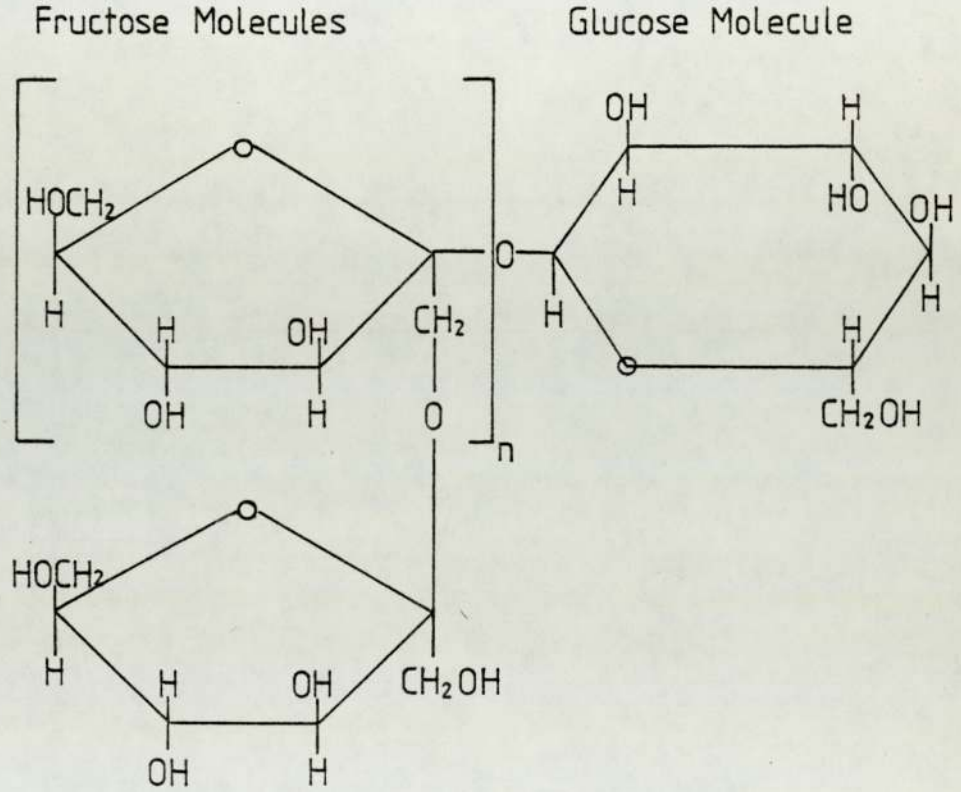

for a plant with a production capacity of up to 100,000 kg per day (as dry substance). The flow scheme is similar to the Clinton process (Section 3.3.2.2.2.) except that six fixed bed reactors, arranged in two parallel lines, are used instead of the filter cake type reactor as in the previous scheme. Their calculations predicted the enzyme consumption for manufacturing a 42% pure fructose product from a 93% pure glucose raw syrup is approximately 83 kg per day.

3.3.2.3. Hydrolysis of Inulin, a polyfructosan

Inulin is a polysaccharide that exists in the roots of the Compositae like Jerusalem artichoke, dandelion and dahlia tubers. Its molecule is unbranched and consisted of about thirty D-fructofuranose units linked together. More recent work has led to the belief that one end fructose is joined through C(2), to a D-glucose unit. Consequently, the breaking down of inulin into its monomers will produce an extremely high purity fructose syrup (Figure 3.8).

Work on how to improve crop yields of tubers as well as on the technique of saccharifying have been conducted simultaneously by both the plant geneticists and the chemists, but published information on the subject is very limited. In a paper by Yasuki et al. (83) of the Asaki Chemical Industry Company Ltd., it was

stated, based on laboratory work, fructose can be produced from inulin with a Helminthosporium Species.

In conclusion, Inulin offers a possible source of almost pure fructose syrup. However, further work is needed to show if the process is economically viable.

Finally, fructose can be obtained as a by-product when dextran, a polysaccharide, is synthesized from sucrose using Leuconostoc Mesenteroides B512. However, as the starting material is sucrose, this process is uneconomical as a direct method of producing fructose syrup.

Chapter 4

Literature Survey - Part 3

Scale up of Chromatographic Process

4. Scale up of Chromatographic Process

In the previous chapter, theories of chromatography have been reviewed. However, most of the theories are derived for analytical scale work. Their applications in separations at the laboratory ('preparative') or production-scale level are only possible if factors governing scale up can be identified and accounted for. Hence, included in the following chapter is a survey of such factors. As studies on continuous chromatographic processes are very limited, findings for batch chromatographic processes are employed as a practical guideline to highlight the most important aspects of scale up.

4.1 Factors Affecting Scale up

4.1.1 Effect of the Flow Pattern in Large Diameter Columns

In Giddings' (30) random walk approach, five sources from which velocity inequalities may occur in packed column are identified. In large diameter columns, the most significant contribution to zone spreading is the transcolumn effect. In order to account for such unevenness in flow velocity, an extra term H_c, is incorporated into the Van Deemter plate height equation (2.5):

$$H = (A + \frac{B}{u} + C_m u + C_s u) + H_c \qquad (4.1)$$

The exact form of the velocity profile across a large column is still an open subject. Based on the concept of a velocity profile convex to the direction of flow, Giddings(84) found the plate height contribution from flow inequalities to be:

$$H = G_2 \left\{ \frac{r_c^2 \; u}{96 \; \gamma_r' \; D_m} \right\} \qquad (4.2)$$

u = mobile phase velocitiy

G_2 = constant

γ_r' = radial labyrinth factor

r_c = radius of column

D_m = Diffusivity of solute in mobile phase

This correlation is found to give good agreement with experimental results obtained for 0.6 cm to 5.1 cm diameter columns (85). Huyten (86) extended the study to columns with a 7.5×10^{-2} m diameter. Similar expressions are obtained by Higgin and Smith (87), and Rijinders (88).

In contrast, Bayer, Hupe and Mack (89), based on a velocity profile concave to the flow direction, developed an empirical expression for H_c as follows:

$$H_c = 2.83 \left\{ \frac{r_c^{0.58}}{u^{1.886}} \right\} \qquad (4.3)$$

which gave good experimental agreement for columns

between 1.3 cm and 10.2 cm diameter.

The band spreading caused by the non-uniform velocity profile can be reduced by lateral diffusion. Littlewood (90) and Sie and Rijinder (91) described the lateral diffusion in terms of a molecular diffusion expression ($\gamma' D_m$) and a convective diffusion term ($\alpha' . d_p . u$). Combining these with the longitudinal diffusion terms they obtain

$$H_c = \frac{0.5\ I'\ d_c^2 u}{\gamma' D_m + \alpha'\ d_p\ u} \qquad (4.4)$$

α' = constant for packing geometry

I' = complex double definite integral of the velocity profile gradient.

All the preceding expressions for H_c predict a decrease of efficiency with increase in column diameter. Pretorious and De Clerk (92) suspected these correlations and maintained that the 'wall effect' and the 'particle to column diameter ratio' are the factors governing the velocity profile. The resultant profile they developed is of a 'w' slope with maximum velocity being experienced several particle diameter into the bed, and the plate height expression was found to be:

$$H_c = \frac{M'\ d_c^2\ u}{2\ D_r . d_p} \qquad (4.5)$$

where $M' = \frac{1}{100}\ \mathrm{EXP}\left\{ - \frac{d_c}{10\ d_p} \right\}$

The results of their study indicated that H_c increases with d_c at constant $\frac{d_p}{d_c}$. However when the ratio reaches a maximum at $\frac{d_p}{d_c} = 0.5$, H_c then decreases with increasing d_c and implies an increase in efficiency.

The concept is supported by the results of Spencer and Kuckarski (93) and Knox (94). Bayer et al. (89) reported a lessening of the rate of increase in H.E.T.P. as column diameter is increased from 1 to 5 cm. Gidding (71) suggested that this effect could be due to the fact that if radial equilibrium is not achieved in large diameter columns, then plate height becomes independent of diameter.

To summarize, the effect of column diameter on operating efficiency is still a debatable subject. However, the majority of opinion indicates a loss of efficiency when columns are scaled to the production level.

4.1.2 Effect of Increased Sample Size

In ideal elution chromatography, a small sample of feed, spreading over a narrow inlet band, is eluted from a column. This produces a Gaussian outlet profile, the width of which is independent of the inlet band width. However, as suggested by Van Deemter and Glueckauf (29, 27), if the ratio of the widths of the feed inlet band and the product outlet bands increases

Fig.4.1 Illustration Of The Operating Modes Of Chromatography

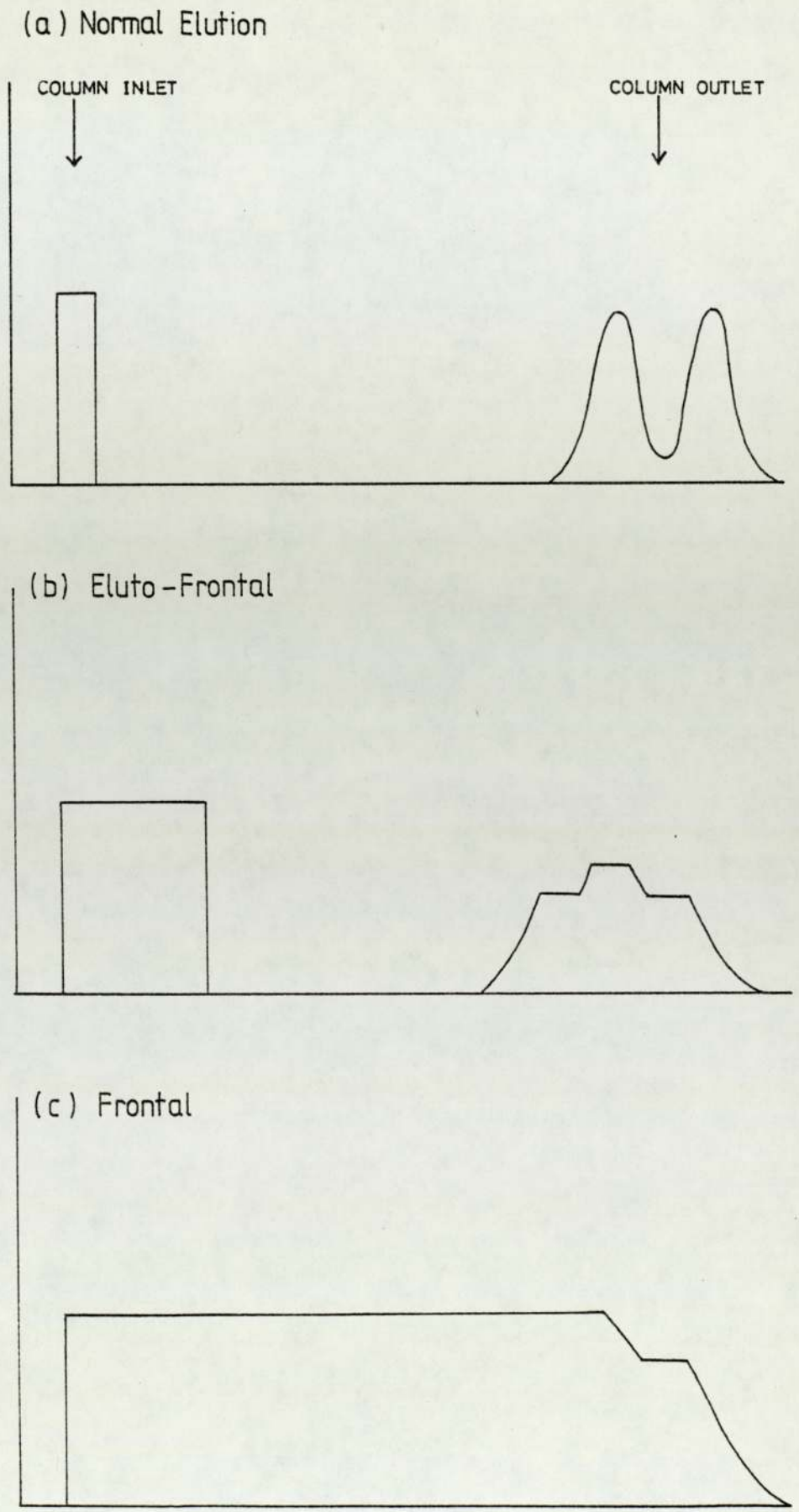

above 1/4, the Gaussian distribution profile will be altered. If the ratio is further increased, eventually the outlet profile will have a shape as shown in Fig (4.1b). Such a mode of operation is called eluto-frontal. This method offers a direct recovery of the least retarded component from the front of the outlet band and the most retarded from the rear of the band. Finally a continuous input of feed will produce a plateau profile led by a multi-stepped front boundary (Figure 4.1c). This mode of operation is called frontal analysis. In this mode of operation, only the least retarded component can be recovered from the leading edge of the boundary, and within the plateau region no separation is achieved.

Conder and Purnell (95,96) suggested the following limits for the various modes of operation;

$$\theta < \frac{1}{2} \qquad \text{ELUTION}$$

$$\frac{1}{2} < \theta < 6 \qquad \text{OVERLOAD ELUTION}$$

$$\theta > 6 \qquad \text{ELUTAL-FRONTAL}$$

where $\theta = \dfrac{N_f}{\sqrt{N}}$

N_f = number of plates occupied by feed inlet band

N = total number of plates in column.

Overload elution is the intermediate mode.

In production scale chromatography, it is more economical to use a larger feed input so as to achieve a maximum column utilization of the packing. From their latest studies, Conder and Purnell (96) reported that the eluto-frontal mode of operation offers the same degree of separation as the elution mode, but with at least a six fold increase in throughput at only a three fold increase in column length. They further indicated that the most economical mode of operation is likely to be in the overload region if expensive packing and column pressure drop contribute significantly to costs.

In conclusion, an increased sample size leads to a drop in column efficiency in terms of the number of theoretical plates. However, this is compensated for by a more complete utilization of packing. Consequently, production scale co-current batch process is most advantageous if operated in the overload elution mode.

4.1.3. Finite Concentration Effects

In the previous discussion on general chromatographic theories (Section 2.2.1), a linear absorption isotherm is assumed, i.e. the distribution of solute between the two phases is independent of the solute concentration. In reality, such distributions may vary with the external solute concentration, and in these cases the isotherm is

Fig. 4.2 The Relationship Between The Solute Zone Boundary Concentration Profile And The Type Of Distribution Isotherm

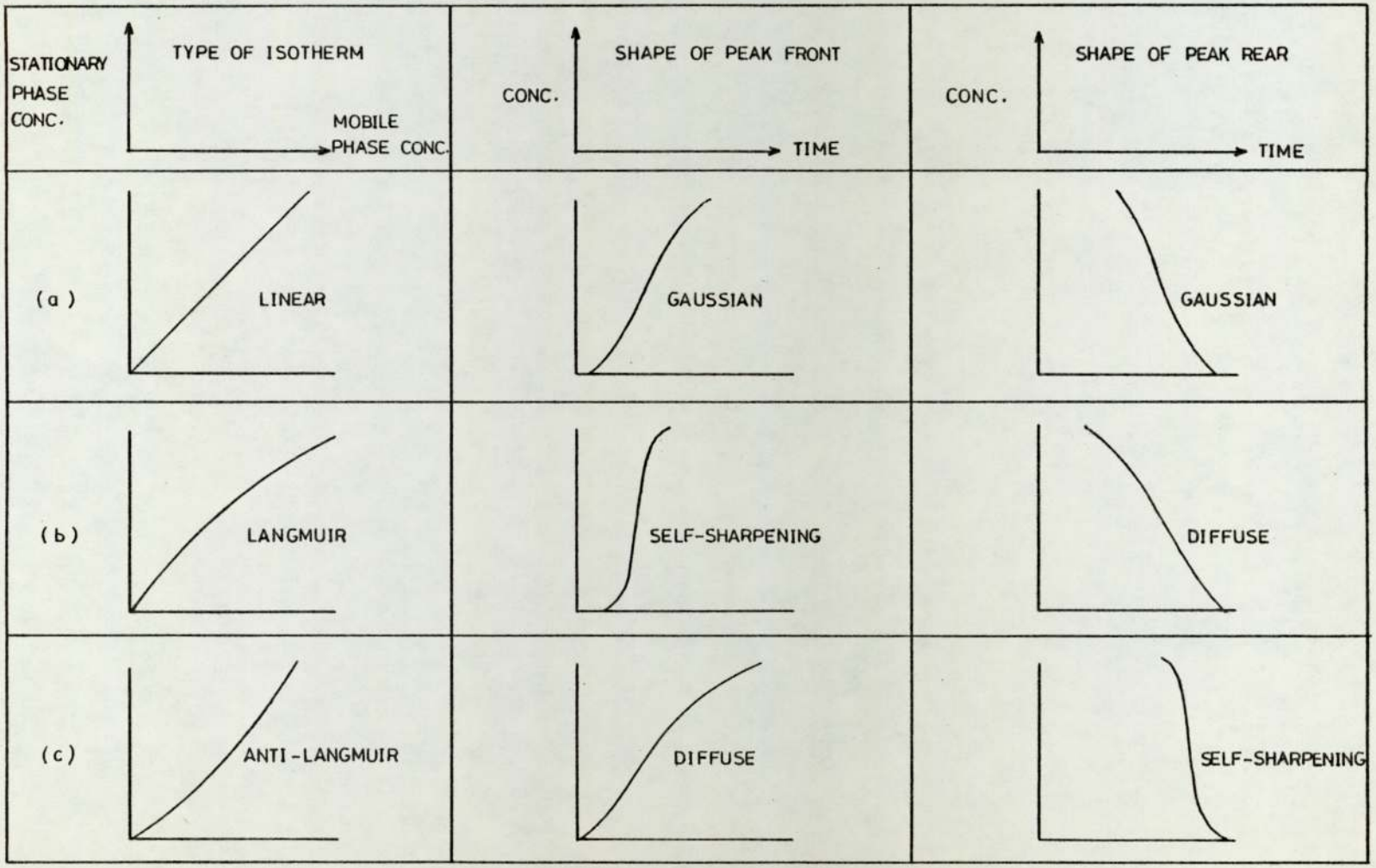

non-linear. For non-linear chromatography, Helfferich (97) redefined the elution equation (c.f. Equation 2.1) as:

$$V_R = V_M + V_S \frac{\partial q}{\partial c} \qquad (4.6)$$

q = solute concentration in stationary phase

c = solute concentration in mobile phase

Operations under non-linear conditions produce peak distortion due to the variation in the distribution coefficients across the solute zones. Figure (4.2) illustrates the two commonest forms of non-linear isotherms and the resulting solute boundary shapes.

For a Langmuir isotherm, both the retention volume and K_D(= $\frac{q}{c}$) decrease with increasing concentration. The product profile has a sharpened leading edge and a diffuse trailing edge. Conversely, for an anti-Langmuir isotherm, in which both the retention volume and K_D increase with increasing concentration, the outlet profile is characterized by a diffuse front and a sharpened tail. Operation in the non-linear region requires an extra column length to compensate the decrease in resolution. However, in production scale operations, it is unlikely that all of the solutes are needed to be separated completely from one another, and usually a certain degree of contamination can be tolerated. Consequently, a maximum feed throughput is the desire of most industrial

processes so that by increasing the feed concentration, the corresponding liquid volume that has to be handled is reduced. Finally, an increase in feed concentration will undoubtedly lead to an increase in viscosity and pressure drop. Hence, the maximum feed concentration limit is usually governed by the permissible process pressure drop, and it is a common practice in industries to operate large scale chromatographic columns at an elevated temperature.

4.1.4. Effect of the Mobile Phase Velocity

An increase in the mobile phase flowrate leads to a higher H.E.T.P. value (Figure 2.3), and consequently requires extra column length for maintaining the same degree of resolution. However, such an increase will also result in the feed being eluted in a shorter time and this implies an increase in throughput. Therefore, in large scale operations, a maximum velocity is employed provided the resulting separation is acceptable. Similar to the feed concentration effect, pressure drop across the system is usually the critical factor in selecting the mobile phase velocity to be used.

4.1.5. Effect of Column Length (Number of Theoretical Plates).

In elution chromatography, an increase in column

length will lead to a better resolution, but also an increase in elution time. (Section 2.2.2). Purnell (98) suggested that the number of theoretical plates required to separate two peak centres by 6σ, can be calculated as follows:

$$N_{REQ} = 36 \left\{\frac{\alpha}{\alpha-1}\right\}^2 \left\{\frac{1+K'_2}{K'_2}\right\}^2 \qquad (4.7)$$

K'_2 = refers to the capacity factor of the most retarded component.

$\alpha = \frac{K'_2}{K'_1}$ = relative retention factor.

Equation (4.7) shows that if $\alpha=1$, an infinite number of plates is required for the separation. As α becomes larger, the corresponding column length (theoretical plates) needed is reduced. Similarly, the magnitude of K'_2 also affects the plate's requirement. These illustrate, in elution chromatography, that the column length is solely dictated by the thermodynamics of the system.

For operations outside the elution mode, a similar direct dependence of the number of plates on the thermodynamics of the system has been shown and discussed by Conder and Purnell (95,96).

For separation involving a very difficult system,

i.e. when α is very close to unity and that K'_2 is very small, it is a common practice in industries to incorporate a recycling process. (c.f. BMA Process in Section 3.3.1.1). Although such methods will reduce the annual throughput, the problems, namely high pressure drop and expensive packing, associated with extra long columns can be avoided.

4.2. Practical Methods of Improving Column Efficiency

4.2.1. Methods of Packing

The low efficiencies in large diameter columns is very often the result of a poor method of packing. Hence, many workers have sought to achieve a packing technique giving both high and reproducible column efficiency.

In gas chromatography, Higgin and Smith (87) studied several methods of packing such as "bulk", "snow" and "mountain" packing and reported that the "mountain" technique produces the best results, with H.E.T.P. in the order of 1×10^{-3}m being obtained. The fluidization technique of Guillemin (99) produced a very high initial efficiency but beds packed by this technique are very prone to collapse. Bayer (89) introduced mechanical tapping and vibration to improve efficiencies. In Verzele's (100) well known "shake-turn-pressure" method, the column is shaken in the radial direction and is rotated along its own axis whilst being packed and periodically pressured.

In liquid chromatography, two main types of packing methods, namely dry and slurry technique, have been used to achieve more uniform and densely packed columns. Studies of dry packing have been carried out using absorbents (101) for small particles in small diameter columns. With larger diameter columns, slurry packing technique is often preferred. This is the technique adopted for the SCCR4 unit and will be discussed in a later section.

To summarize, a gain in efficiency with careful packing of chromatographic columns is possible, but opinions differ on the best packing technique to use.

4.2.2. The Use of Repeated Feed Injections

In analytical elution chromatography, a small sample of feed is injected and eluted subsequently. This ideal technique involves only a very small part of the packing being utilised and would therefore be unacceptable to any industrial scale operation.

To maximize column utilization, a repetitive way of sample feeding has been commonly employed. This involves the introduction of subsequent charges of feed into the column at controlled time intervals. The sequence and rate of injection is extremely critical if excessive overlapping is to be avoided. Studies on the subject have been conducted by various workers.

In general, their common goal is to achieve a maximum throughput. However, such a desire is governed by two factors, firstly, the overlapping of individual component profiles within a sample, and, secondly, the contamination between subequent charges of feed. In a linear liquid system, Timmins et al. (102) defined a throughput prediction expression, for the case when the front running peak of a given injection just begins to catch the late running peak of the previous injection, as: (Figure 4.3).

$$Q = \frac{0.4}{R_s} \left\{ A' \phi u \rho x \right\} \left\{ 1 - \left(\frac{l_{min}}{l} \right) \right\}^{\frac{1}{2}} \qquad (4.8)$$

Q = Production rate

A' = Column area

ϕ = Column porosity

ρ = mobile phase density

x = Concentration of feed in mobile phase during injection

R_s = resolution

u = mobile phase velocity

l_{min} = minimum column length that will still achieve separation = $N_{min}.H$

H = Plate height obtained from an experimental equation of the Van Deemter form.

$$N_{min} = 16 (R_s)^2 \left(\frac{\alpha}{\alpha - 1} \right)^2 \left(\frac{K^1 + 1}{K^1} \right)^2$$

The above equation correlates throughput directly with the physical geometry of the packed column and the thermodynamics of the system. Timmins (102) further developed from Equation (4.8) a mobile phase utilisation efficiency, η_L, defined as the ratio of feed rate to carrier rate, and also a column utilisation efficiency, ε_L, defined as the ratio of feed rate to column volume:

$$\eta_L = 0.4 \left\{\frac{x}{R_s}\right\} \left\{1 - \left(\frac{l_{min}}{l}\right)\right\}^{\frac{1}{2}} \qquad (4.9)$$

$$\varepsilon_L = 0.4 \left\{\frac{x}{R_s}\right\} \left\{\frac{\rho u \phi}{l_{min}}\right\} \left\{\frac{l_{min}}{l}\right\} \left\{1 - \left(\frac{l_{min}}{l}\right)\right\}^{\frac{1}{2}} \qquad (4.10)$$

Implicit in Equation (4.9) is an inverse dependence of the mobile phase velocity on the column length. The authors have shown that by increasing the column length by a factor of four, the mobile phase flowrate is reduced by a factor of 2.1. However, results calculated from Equation (4.10) show that ε_L increases substantially up to $\left(\frac{l}{l_{min}}\right) = 1.5$, after which ε_L decreases in contract to the continual increase in η_L. Hence, a compromise between maximum η_L and ε_L has to be decided for the most economic operating conditions.

From their calculations, Timmins et al. (102) suggested that for such repetitive sample injection

operation, it is best to choose a relatively high flow-rate and an optimum value of $(\frac{l}{l_{min}})$ lying in the range 1.5 to 3.

The above equation illustrates how the total throughput can be predicted in a repetitive sample feeding system, the actual recovery of individual component not being accounted for. The purities of individual components in the products rest also on how the different streams of the eluent are collected.

In a binary system, Pretorius and de Clerk (92) suggest the recovery rate of an individual component can be predicted, if two cuts, one between the component peaks, and the other between samples are made on the chromatogram (Fig (4.3)), as

$$E_p = \frac{(m - \Delta_m)\, u}{W_{to}\,(1 + K_{D_1})} \qquad (4.11)$$

E_p = production rate of a given component

m = total mass of component in sample

Δ_m = mass of component lost during fraction cutting

W_{to} = total chromatogram width per sample at the column outlet

To ensure that samples do not overlap, the distance between samples is taken as being twice the distance between the two peaks within the sample. Therefore, to separate the peaks by six standard deviations, the

Fig.4.3 Illustration Of Repetitive Injection Technique For Two Components System

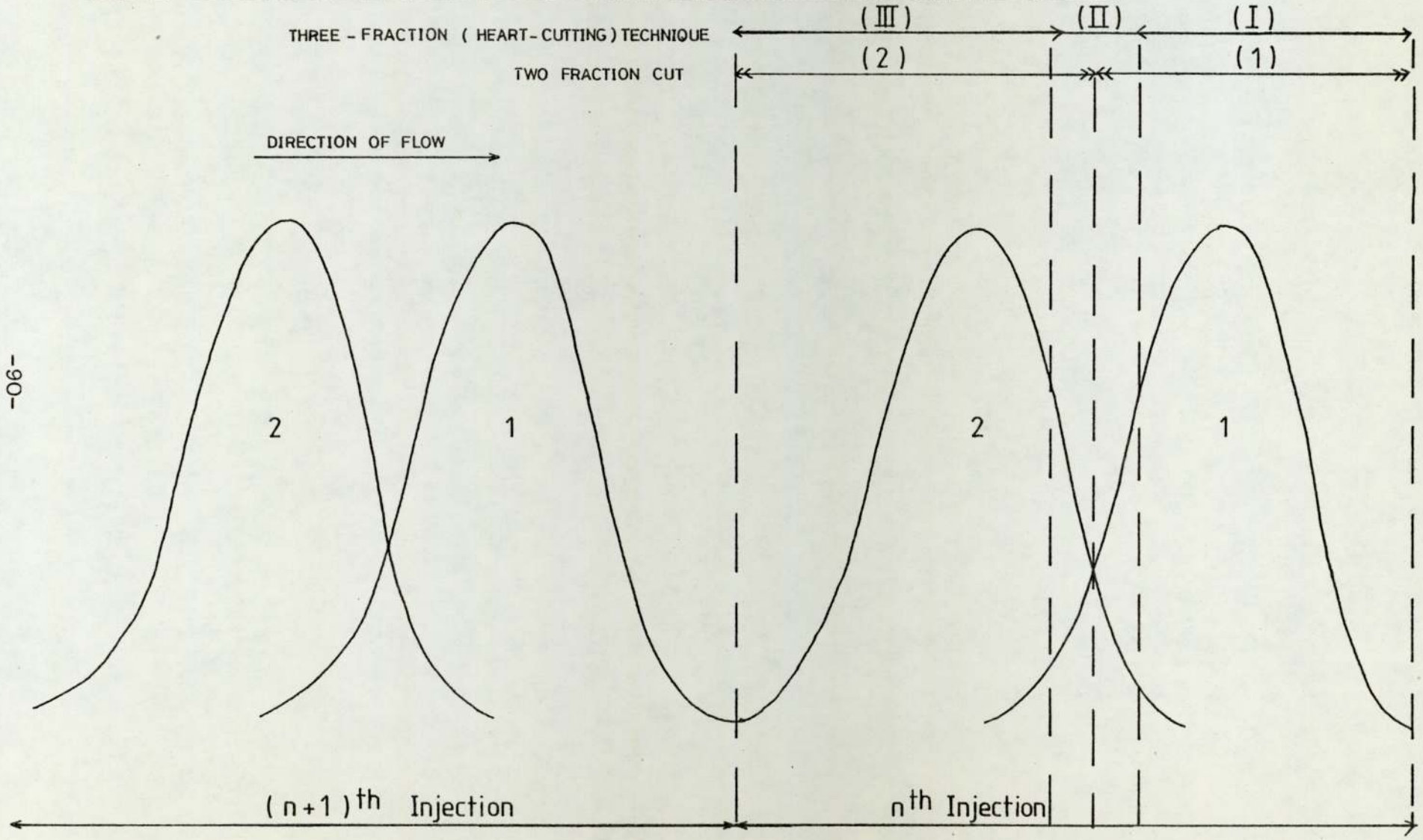

parameter W_{to} is fixed as

$$W_{to} = 12.\ R_s\ \sigma_{to}$$

σ_{to} = standard deviation at column outlet.

Operation under the above conditions was shown by the authors to have a product contamination of about 0.15%.

Gordon et al. (103) proposed an alternative "heart cutting" technique (Figure 4.3) that can lead to higher throughputs provided a drop in resolution is accepted. The product is separated into three fractions, the highly contaminated portion is usually recycled and re-introduced through the column for further resolution. However such recycling procedures involve sophisticated instrumentation and has to be weighed carefully against the need of either an increase in the feed throughput or the desirability of an ultra pure product.

Finally, Conder (104) has reported that it is always preferable to overlap the component bands rather than to avoid the need for cutting by increasing column length and resolution. It is indicated that a 60% recovery of the injected sample is an optimum, with the remaining contaminated 40% being recycled.

4.2.3. The Use of Flow Distributors

In large diameter columns, the velocity profile of the mobile phase varies considerably across the cross-section of the column. It is generally accepted that the installation of flow distributors at the column inlet will enhance radial mixing and consequently lead to a more uniform profile. Musser and Spark (105) investigated the performance of inlet cones and their results indicated that wide angle cones (60^{o} - 90^{o}) packed with inert material to about 80% of their volume, provide the most efficient means of distribution. Huyten et al. (86) reported similar findings, and established that if chromatographic packing was used in the inlet and exit cones, column efficiency is improved. Albrecht and Verzele (106) also found an improvement of efficiency by packing the inlet cone of a 7.5 x 10^{-2}m diameter column with glass spheres.

4.2.4. The Use of Homogenizer, Baffles and Washers

Besides the use of inlet cones, the adverse effect of the velocity inequalities across the cross-section of column can be minimized by remixing the solute stream at intervals along the column. The most popular device is the mixing chambers proposed by Carel and Perkins (107, 108). In their work, the mixing devices consist of

porous discs on either side of a plate with a single central hole and are installed in the column at various predetermined intervals. The porous discs provide redistribution whilst the "doughnut" plate serves to remix the mobile phase. Plate heights of 2 mm in a 10 cm diameter column have been reported (108). The spacing of the homogenizer as reported by Pescar (109) is not critical, but in contrast to his opinion, Golay (110) suggested that excess mixing devices could actually contribute to zone spreading and that the law of diminishing return applied. Mir (111) has equated the gain in efficiency in terms of plate height for n_1 mixing devices as:

$$\frac{H'_{CN} - H'}{H'_{C} - H'} = \frac{1}{n_1}$$

H' = Intrinsic plate height for packing as measured on an analytical column

H'_C = Plate height obtained for large diameter column without mixing devices

H'_{CN} = Plate height obtained for the same large diameter column with mixing devices.

The introduction of baffling in production scale chromatographic columns is a common practice.

Abcor Inc., Massachusetts (102), proposed a "disc and doughnut" system. The disc, of smaller diameter than the column, forces the mobile phase to the walls, after which strikes the "doughnut" and is redirected to the centre. Improved efficiency of large diameter columns have been reported with the use of such baffles.

Further methods of in-column mixing include the use of washers, as reported by Bayer et al. (89) and Amy and co-worker (112). Friscone (113) used filter paper washers coated with stationary phase to retard the normally advanced solute profile near the column wall. To summarise, the gain in efficiency for various mixing devices has been proved and their installation in large diameter columns is desirable.

4.3. Continuous Chromatography

Chromatography was discovered by Tswett in 1903 (162), and since then has been developed from a powerful analytical tool into an industrial viable process. Most of the early large scale attempts are confined to a batchwise operation. Although repeated sample injection (c.f. Section 4.2.2.) and feed size and concentration can improve batch column utilization, it has been established from all other branches of separation that a continuous operation allows a more efficient column utilization.

Figure (4.4) illustrates the increased throughput for a counter-current flow scheme relative to a conventional co-current batch system. If "pure" products are to be collected in the batch process then, either the eluted components must be fully resolved or the "overlapped" fraction must be removed and recycled. In contrast, for the counter current flow scheme, the solute concentration profiles need only be partially resolved within the chromatographic column to allow the collection of pure products at the column exits. A complete column utilisation is achieved and therefore severe overloading by co-current standards of the solid phase is possible.

In addition, greater throughputs, higher purities and low costs are normally inherent in continuous mass transfer processes when compared with the equivalent batch processes. All these factors have prompted many workers to design and perfect chromatographic systems capable of operating in a continuous manner. A review of various different schemes and operations is given below and all the achievements can be identified into three main groups, namely fixed bed, moving bed and simulated moving bed operations.

Fig. 4.4 Chromatographic Concentration Profiles Obtained For The Separation Of Two Components

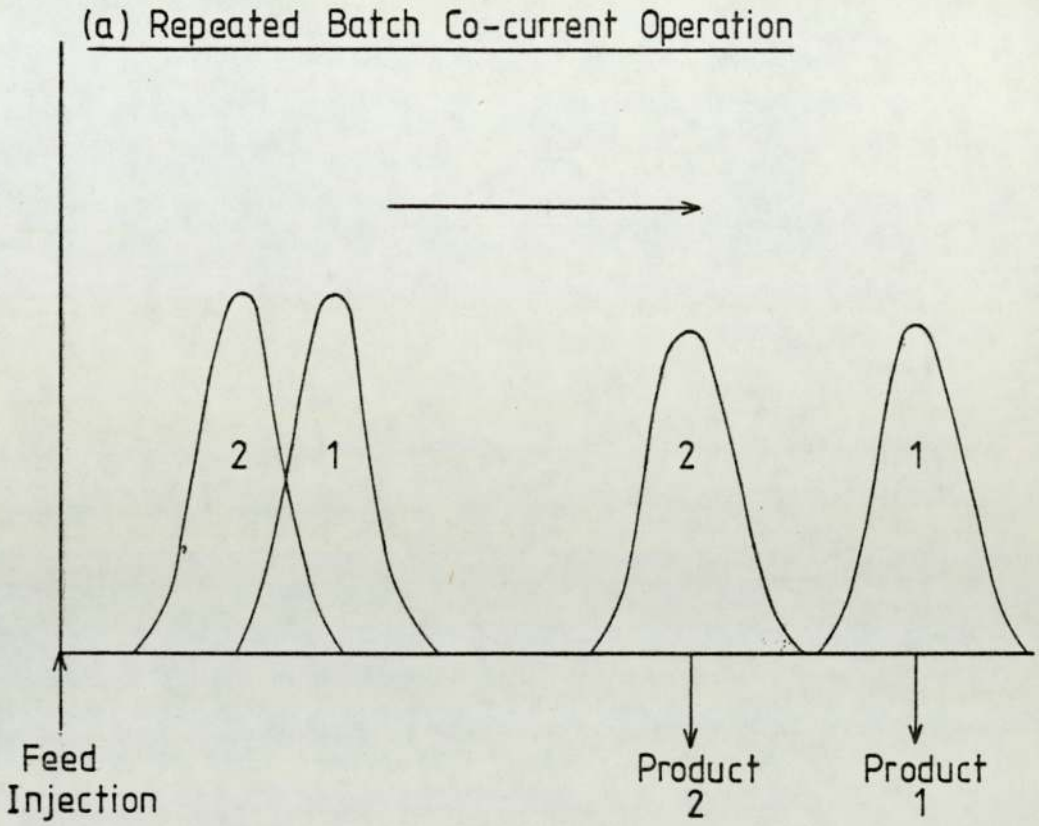

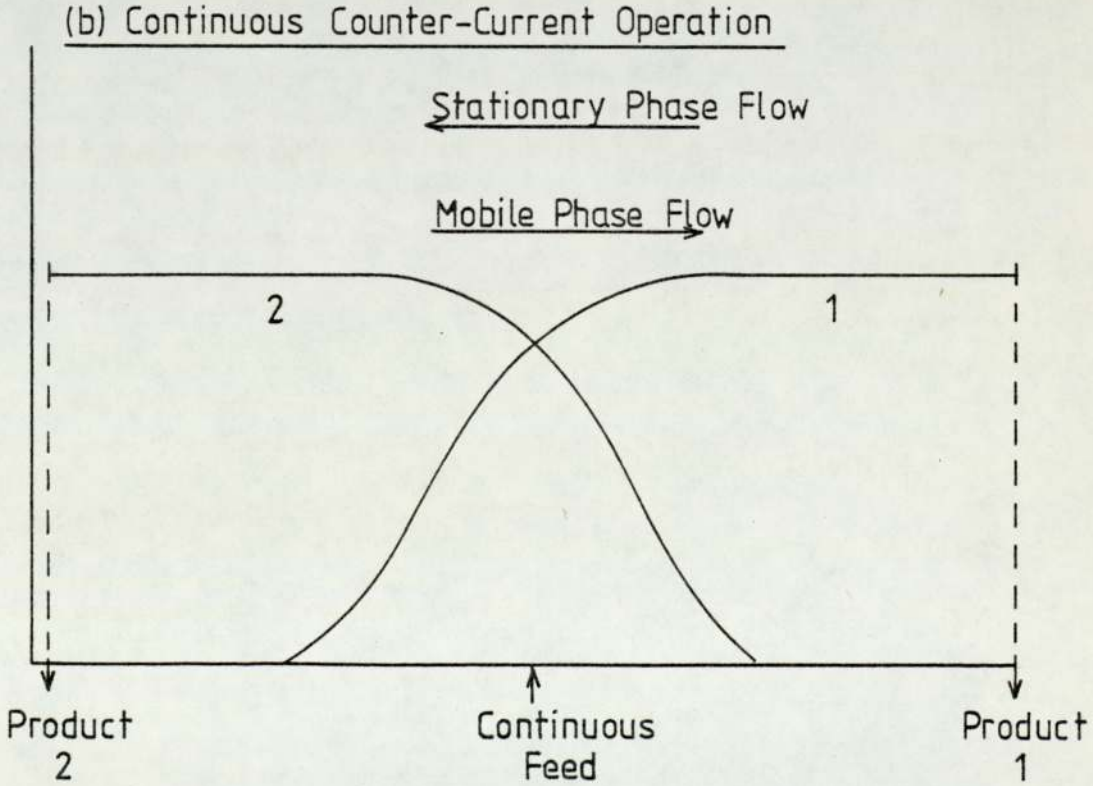

4.3.1. Fixed Bed Systems

4.3.1.1. Non-cyclically Operated

Tiley and co-workers (114-116) investigated a counter-current fixed bed system using a 2.5 cm diameter column. In this the stationary phase of dinonyl-phthalate flowed downwards over the packing element of "Knitmesh", against the carrier gas flow. The product purities were reported to be in excess of 99.9% at a feed rate of up to 5 cm^3hr^{-1}. Column efficiencies expressed in terms of H.E.T.P. were however much higher than those obtained from counter current chromatographic columns in which the packing was flowing under gravity.

A similar scheme was practised by Kuhn et al. (117-118) who superimposed a temperature gradient onto the column to exploit the temperature dependence of the partition coefficients so as to improve the separation of multi-component systems. Such products were collected at different places along the column. Purities of 95% were achieved during a continuous separation of a ternary mixture of n-valeric acid/n-butyric acid, using paraffin oil containing 10% stearic acid as the stationary phase. In common with Tiley, a high H.E.T.P. value and low throughput were obtained.

A cross current operation was achieved by Turina et al. (119) by using two parallel glass plates 1 mm

Fig. 4.5 Chromatographic Slabs

(a) Scheme Of Turina et. al.

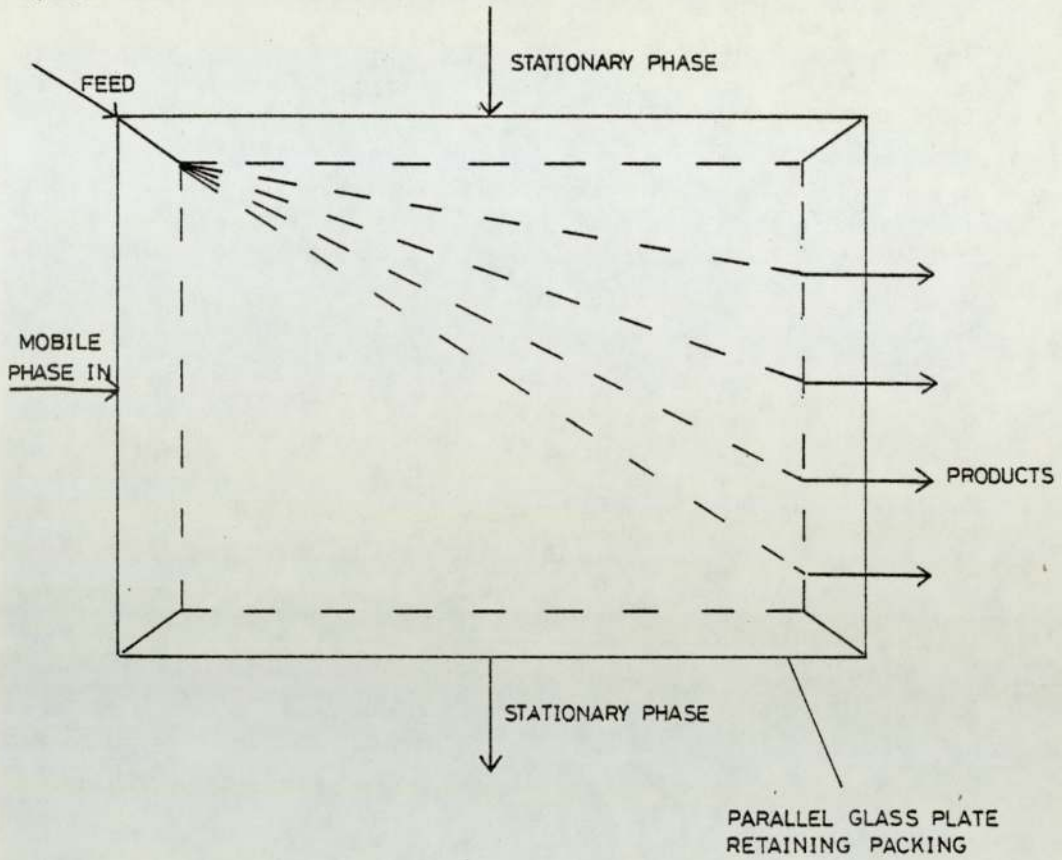

(b) Scheme Of Tuthill

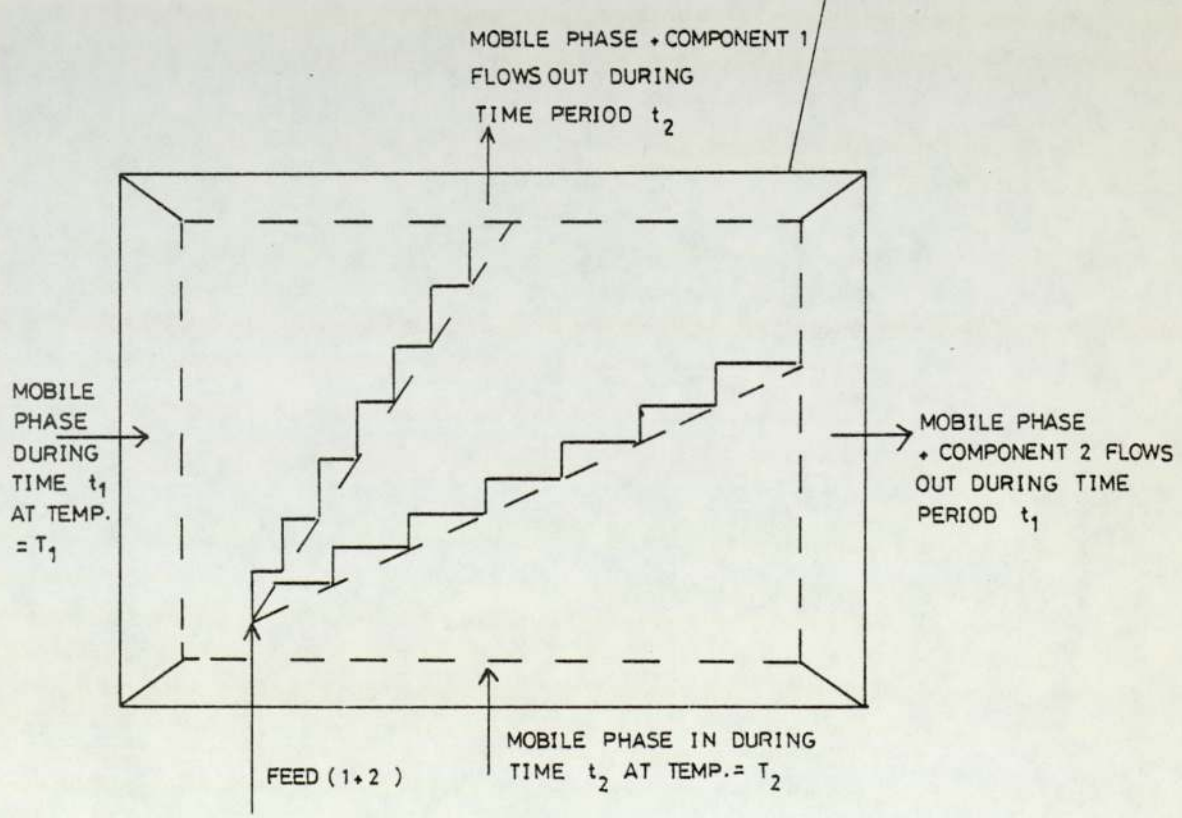

apart, containing the inert support (Figure 4.5a). Both the carrier gas and the stationary phase were introduced into the system at right angles to one another. The feed mixture enters at the corner between the carrier gas and stationary phase inlets. Each individual component travels at a different angle through the bed according to its retention time in the stationary phase. The products are collected via a series of outlet ports opposite to the carrier gas inlet. The main advantage of this scheme is its potential in separating a multi component mixture into individual components in one single operation.

4.3.1.2. Cyclically Operated (Parametric Pumping)

Recent operation of separation processes in a cyclic manner and under unsteady state conditions has shown to enhance column efficiencies. Cyclic operation may involve the flow of various phases to be varied intermittently or sinusoidally with time. Further variables include temperature, pressure and concentration.

Temperature cycling was first employed by Pigford et al. (120,121). In their studies, a constant mobile phase was passed through a fixed bed of solid adsorbent. Temperature cycling within the column was created by the continual introduction of a feed mixture which was alternatively heated and cooled. Due to the temperature

dependence of the partition coefficient, the difference in the solute affinities for the stationary phase increase during the hot cycle. Consequently, the product outlet stream's concentration cycled between being rich or poor in the preferentially-absorbed component.

A further process of parametric cycling has been reported by Wilhelm et al. (122). The direction of the mobile phase through a solid adsorption bed is changed periodically from upwards to downwards. During the downflow period, the column is heated so as to utilize the temperature dependence of the partition coefficient mentioned earlier. Although successfully operated, the efficiency is greatly reduced when continuous feeding and product removal are employed.

Tuthill (123) incorporated a temperature variable into Turina's (119) scheme. The feed mixture is introduced continuously into one corner of a rectangular chromatographic slab, and the entry of the mobile phase alternates between the two sides of the slab adjacent to the feed entry point. The temperature of the system is cycled in phase with the direction of the flow of the mobile phase. This change of temperature results in a change in the ratio of the component velocities through the slab, and, by selecting the appropriate flowrate and temperature, components can be made to move

preferentially in the horizontal or vertical direction (Figure 4.5b).

Extensive studies on parameter pumping techniques have been conducted by Wankat (124,125) and a survey of other attempts are included in the author's review (125).

4.3.2. Moving Bed System

4.3.2.1. Cross-Current Flow Processes

In cross-current flow systems, the movement of the chromatographic bed is at right angles to that of the mobile phase. The development of such processes can be classified into two forms, helical flow through annular columns and radial flow between parallel discs.

4.3.2.1.1. Helical Flow System

This scheme was first proposed by Martin (126) is illustrated in Figure (4.6). The column is formed by packing an annular space between two concentric cylinders. The feed and the mobile phase fluid enter the top of the column, and as the column rotates, each component of the feed follows a helical flow path. Various streams of the product are collected at points around the circumference of the base. From his studies, Giddings(127)

Fig. 4.6 Helical Flow Scheme For Continuous Chromatography

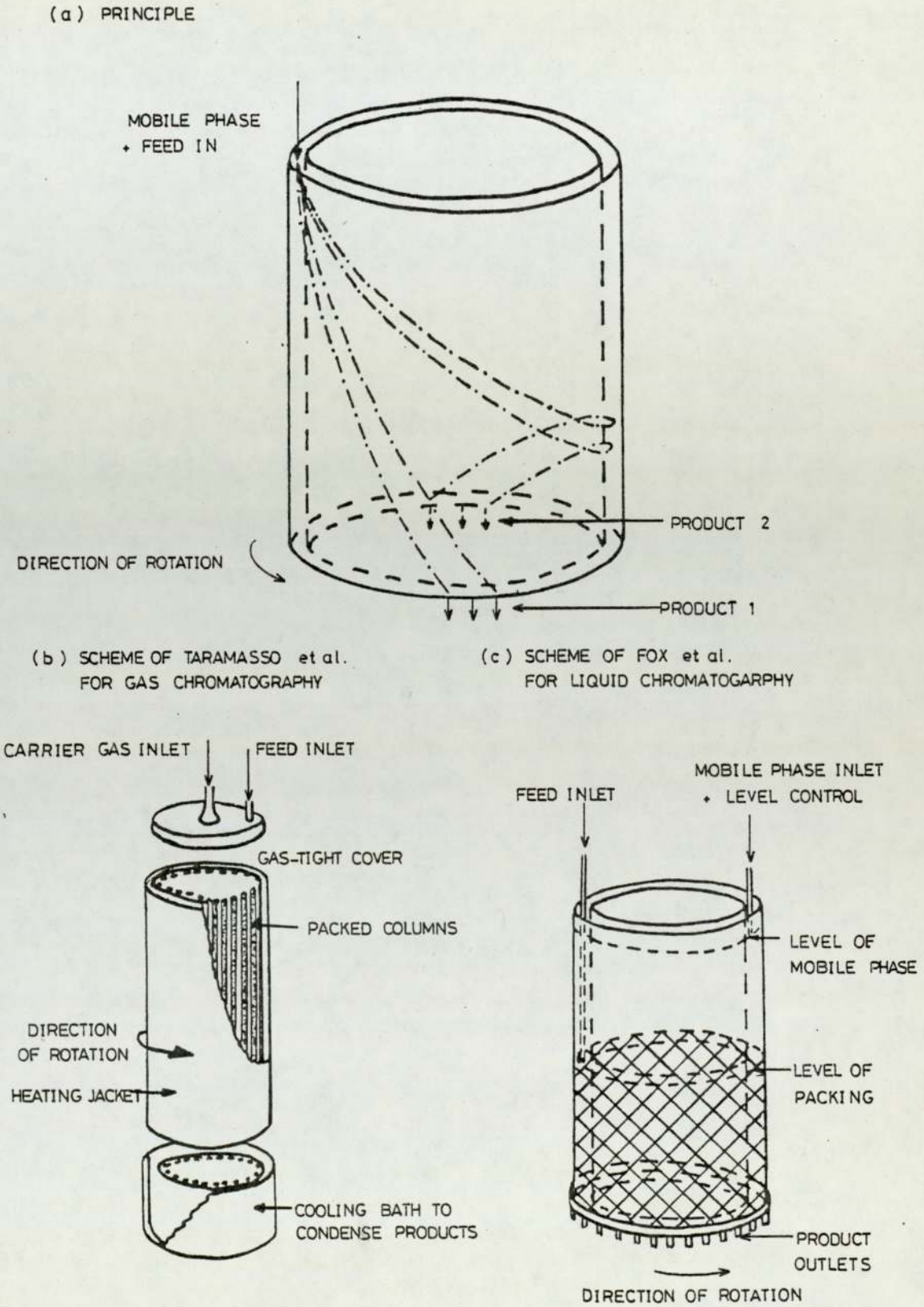

concluded that this scheme is capable of better resolution and throughput than a conventional column of similar geometry.

Dinelli, Taramasso (128,129) (Figure 4.6) constructed a unit based on the above principle which consists of 100 columns, 6 mm in diameter and 1.2 cm in length, to form an annulus of parallel columns. The combined unit is rotated at speeds of 1 - 50 resolutions per hour past a fixed feed inlet and product outlet ports. In their studies with cyclohexane-benzene, throughputs of up to 200 cm^3hr^{-1} were obtained at product purities of 99.9%. An enlarged unit using 36 tubes of 2.4 m length has been used for separation of isomers and close boiling points mixtures (130-132).

Further application of the helical flow system was illustrated by Fox et al. (133-135) for the separation of proteins. The annular column employed had an inner diameter of 27.3 cm and an outer diameter of 29.2 cm and was of length 30.5 cm. Product purities of 97% at a feed rate of up to 22 cm^3hr^{-1} was claimed.

4.3.2.1.2. Radial Flow System

Mosier (136) has patented a rotating annular chromatographic unit into which the feed is radially introduced. Figure (4.7). The unit has to be rotated past a fixed feed inlet and outlet to produce a separation

Fig. 4.7 Radial Flow Schemes For Continuous Chromatography

(a) Principle

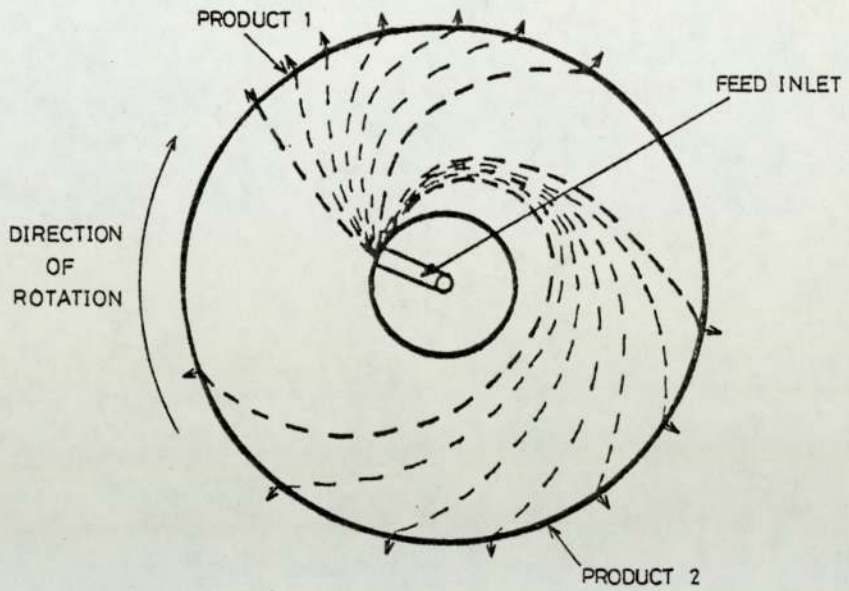

(b) Scheme Of Sussman

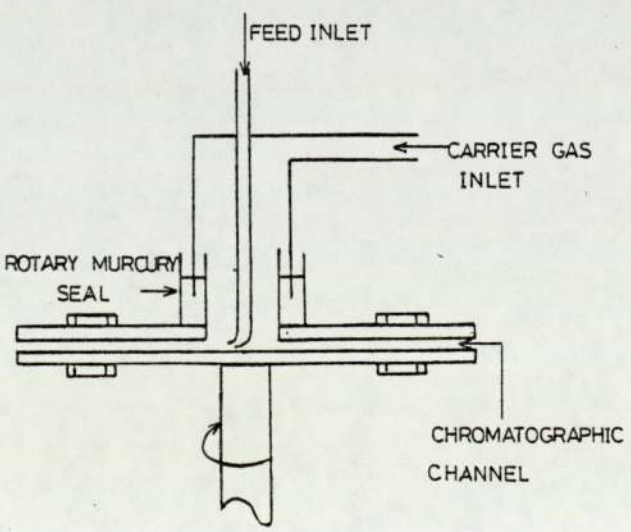

(c) Scheme Of Mosier

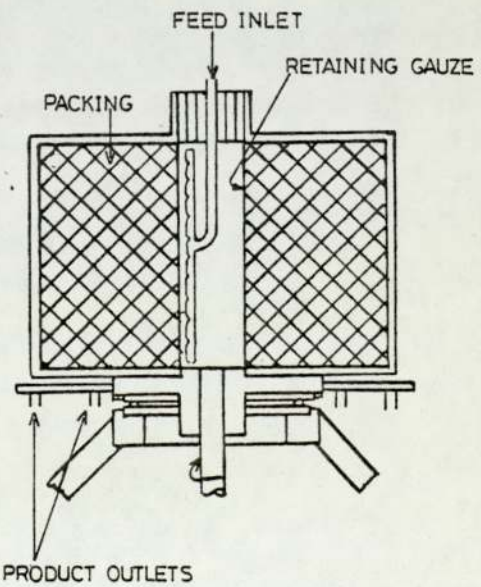

as illustrated in Figure (4.7). Several product outlets are installed at the base. Individual components follow a different radial path towards the circumference and subsequently are removed from the base of the unit. Adapting the above principle, Sussman (137) developed an annular disc system Figure (4.7). Separation occurs between a stationary phase coated onto surfaces between 50μm and 150μm apart. Successful studies on the separation of hydrocarbon mixtures with the unit have been reported. (138,139).

In conclusion, scaling up of the above helical or radial flow equipment require a high degree of precision engineering and because such equipments may lack reliability it is thought industrial interest may be limited.

4.3.2.2. Counter-Current Flow System

In counter-current flow systems, the stationary phase is moved in the opposite direction to that of the mobile phase by a variety of methods. The development of mechanical systems based on such a principle can be classified into two main types, namely the moving bed system and the moving column system.

4.3.2.2.1. Moving Bed System

The continuous movements of the two phases in

opposing directions present the most simple method of achieving a counter-current process. Considerable work in this field has been conducted by Barker and co-workers (3, 4, 5). Figure (4.8) illustrates the equipment they developed. The column in the system is 2.5 cm in diameter and 2.74 m long. The packing, coated with a suitable liquid stationary phase, was introduced downwards under gravity, and the carrier gas packed upwards through the column. The flow of packing was regulated by a variable orifice at the column base and by the rotating of the attached table, the packing was removed and subsequently recycled to the top of the column. Vibration was employed to ensure a steady flow of packing.

For a binary system, the least absorbed components were carried in the mobile phase to be collected at the top of the column. The more strongly absorbed component remains in the stationary phase and was removed in the stripping action at the bottom of the column. Details of the successful gas-liquid chromatographic separations carried out using this equipment are given in the literature (3-8). Schultz (140), Scott (141) and Tiley et al. (115-116) have also reported successful operations of small diameter units functioning on the same principle.

Industrial implementation of such a method can be traced back to the "Hypersorption Process" developed by the Union Oil Company, California. Activated carbon

Fig. 4.8 Counter-Current G.L.C. Apparatus With Circulating Packing

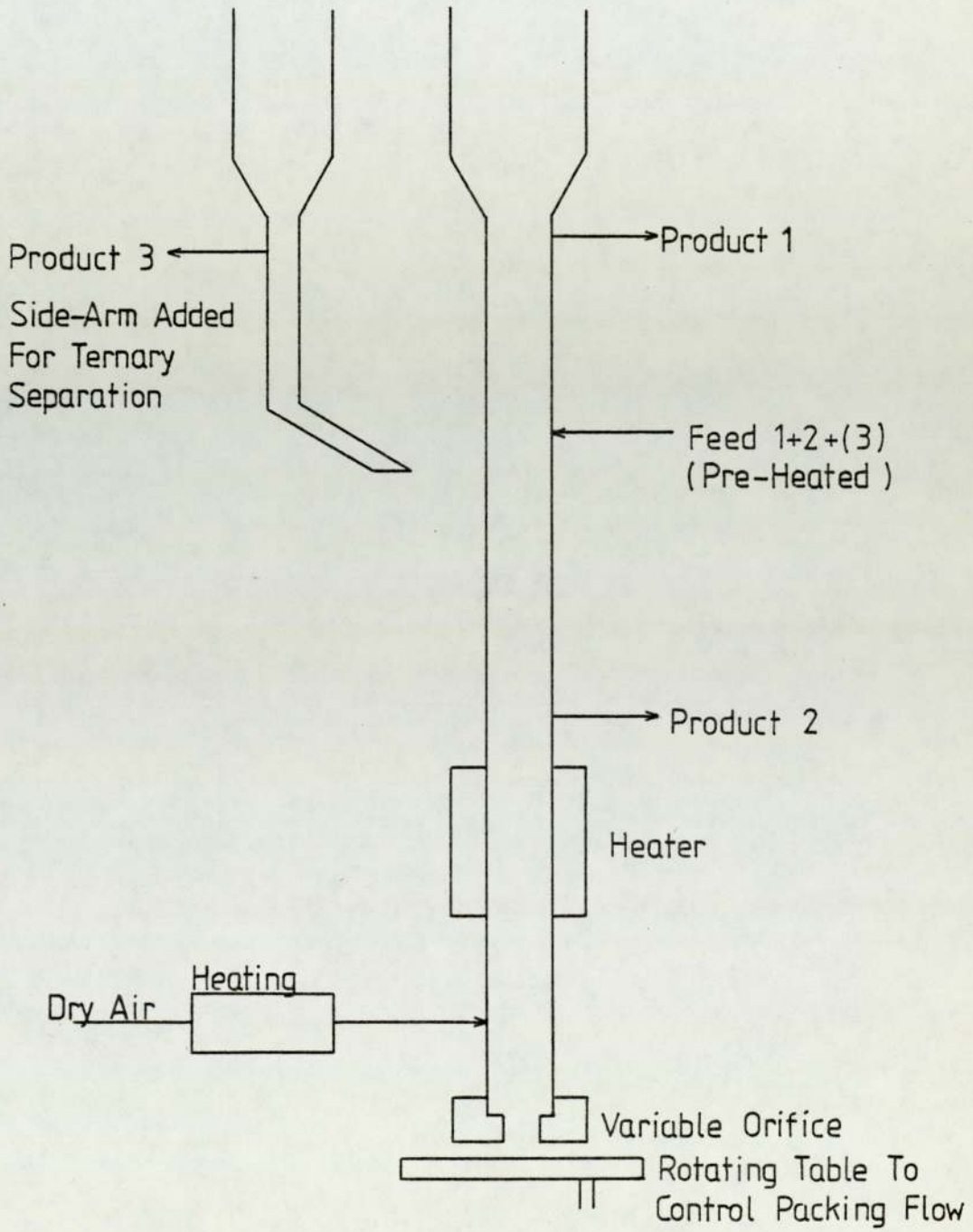

adsorbent was used as the down-flowing solid phase. The process was previously operated commercially for the recovery of ethylene, but has subsequently proved uneconomic (142), since the development of low temperature distillation. Similar plants have been constructed by both the Dow Chemical Company, Michigan, U.S.A., and by Phillips Petroleum Company. (143) for the separation of light hydrocarbons. However, both plants are no longer in operation for economic and technical reasons.

To summarize, moving bed systems have the following inherent disadvantages:

(i) Handling of large quantities of solid packing.

(ii) Attrition and elutriation of packing.

(iii) Mobile phase velocity has to be below the minimum fluidisation velocity of the packing.

(iv) Back mixing and low uneven packed densities resulted in low column efficiency.

4.3.2.2.2. Moving Column System

Attempts to avoid the above mentioned problems, have led to the development of the moving column system. This technique involves the rotation of a circular column past fixed inlet and outlet ports, and against the direction of a mobile phase flow in the separating region. Figure (4.9) illustrates a number of such

Fig. 4.9 Circular Column For Counter-Current Flow Processes

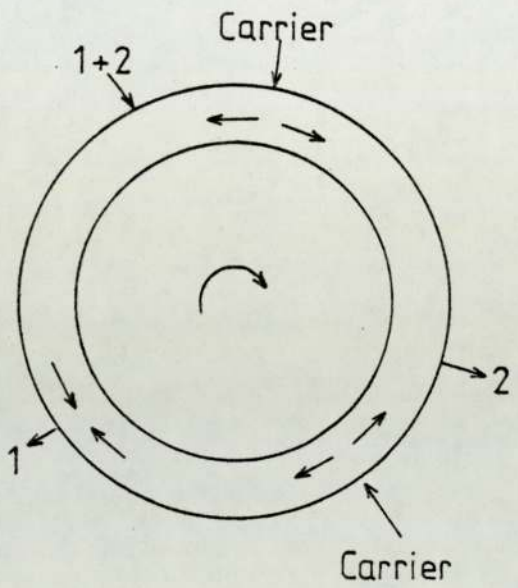

(a) Pichler Glasser

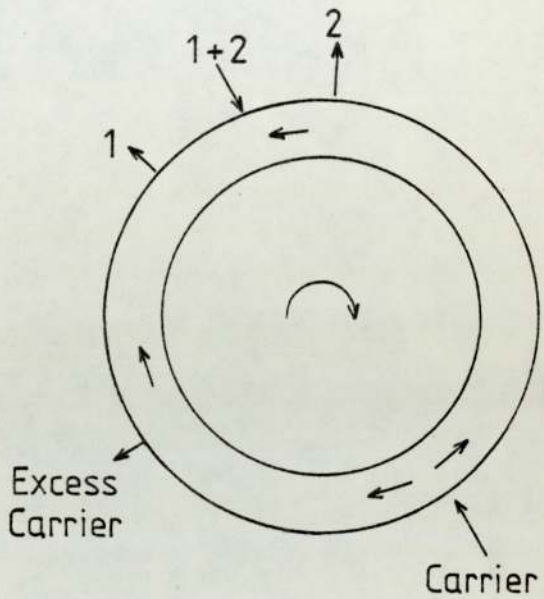

(b) Luft

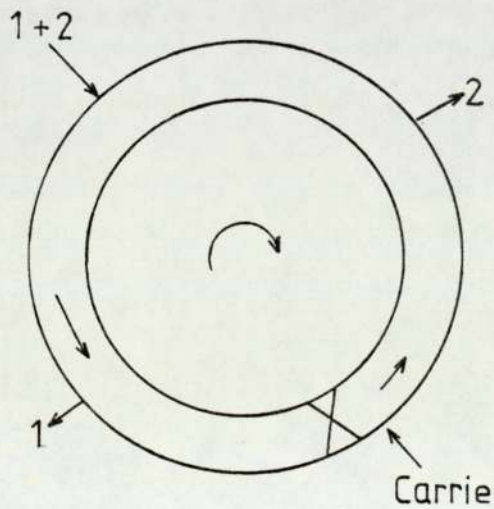

(c) Barker

schemes. The designs of Pichler and Schultz (144), Luft (145), Glasser (146) and Gulf Research and Development (147) are very similar but differ in the flow direction in the stripping/purging sections and the means of controlling the flow direction generally within the column. However, all the designs proposed that the relative port positions and carrier gas flow-rates be selected such that the direction of flow was correctly maintained by balancing pressure drops within the system.

By introducing a cam-operated lock between the two product outlets, Figure (4.9c), Barker (9) succeeded in ensuring the mobile phase travels in one direction only. In addition, the column length available for separation was also increased.

Based on Barker's principle, Barker and Huntington (9), constructed with the assistance of the Universal Fisher Engineering Company Limited, a unit of light equal square cross-section chambers each side of length 3.8 cm, linked end to end by external valves to form a toroid, 1.5 m in diameter, (Figure 4.10). Each chamber was installed with helical copper-tubing through which heating or cooling fluid could be passed. 180 gas packages in and out of the column were opened or closed by poppet valves. Sealing between the ports and rotating toroid was obtained by an oval shape graphlon ring set in the toroid face. This unit was successfully operated for

Fig. 4.10 Circular Moving Column Chromatograph

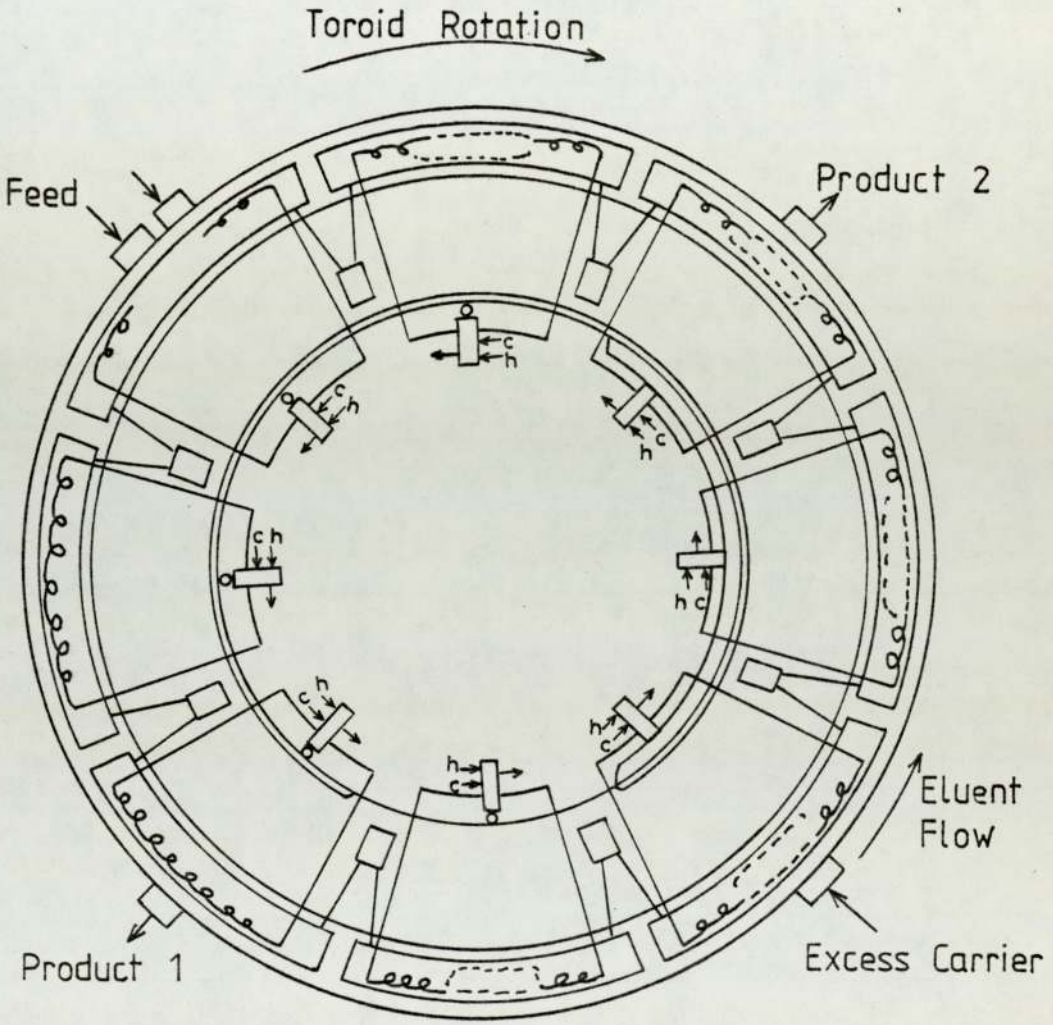

the separation of azeotropic and close boiling point system at feed rates of up to 450 cm^3hr^{-1}. Barker (15) and Hatt (14) used the same equipment for liquid-liquid chromatographic separations. Ion exchange resins, charged in the Li^+ form, were used as a stationary phase and distilled, deionised water as the eluent. D-glucose was successfully separated from starch at feed rates of up to 2.4g. hr^{-1} with this equipment.

To enable a more compact equipment to be built, Barker and the Universal Fisher Group Ltd. (9) replaced the toroid with a tube bundle of 44 tubes arranged as shown in Figure (4.11). The tubes were 2.5 cm in diameter, 22.8 cm length and linked in series to form a closed loop. The bundle of tubes were held between two stainless steel annular rings. The transfer of the mobile phase between columns was controlled by poppet valves. As the bundle rotates, two poppet valves were closed by a cam control so as to provide the necessary lock and also maintain unidirectional mobile phase flow. Inlets for the feed, the mobile phase and both product outlets, were all located on the upper face of the top ring.

Spring-loaded "graphlon" (P.T.F.E. - carbon composite) face seals were employed at the inlet and outlet ports to prevent leakage from the unit when the valves were open. The separations performed on this unit were

Fig. 4.11 Compact Moving Column Chromatograph

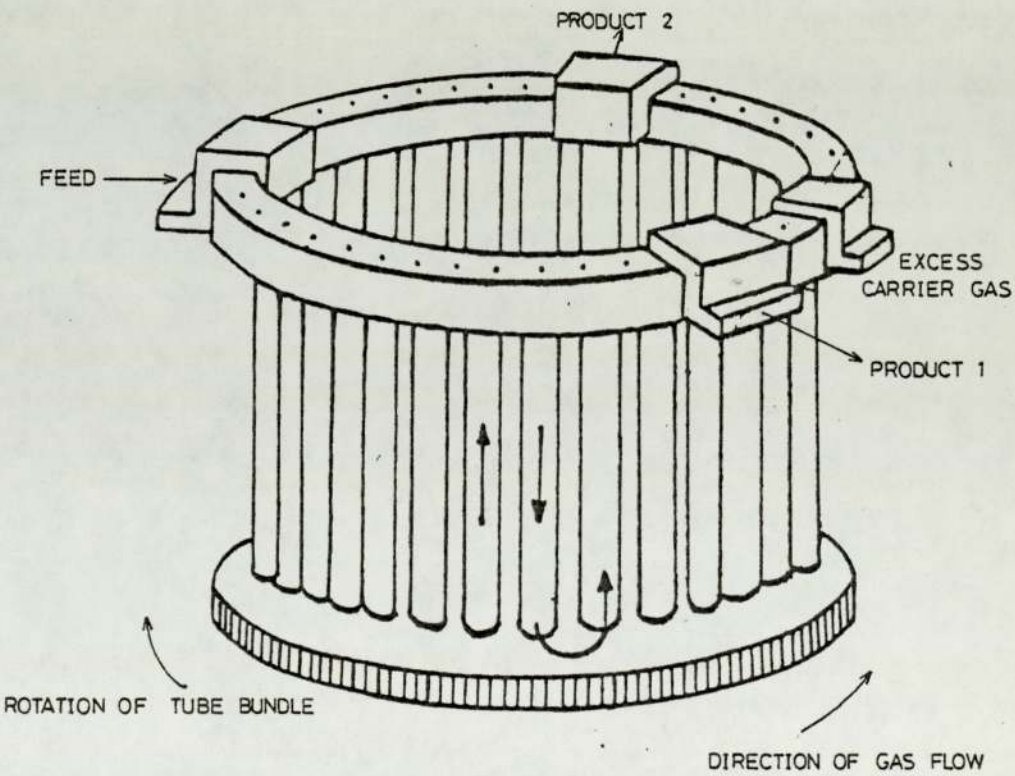

demonstrated by Barker and co-workers (10,11) to be better than the previous toroid unit due to the extra mass transfer length available. Products with high purities and at feed rates of up to 154 $cm^3 hr^{-1}$ were obtained (10-13).

The successful operation of the bundle unit relies heavily on the proper functioning of both the poppet valves and the face seals. Under conditions of stress, temperature and corrosive chemicals, the poppet valves were found to be unreliable. Consequently, such inlet and outlet valves were replaced by a "graphlon seal", and a bench scale unit was constructed accordingly. Barker and Hatt (14,15) applied this equipment for the separation of glucose from starch. Barker, Hatt and Williams (22), used similar equipment for Dextran fractionation studies.

A more recent system is under development by Barker, Hatt and Knoechelmann (24). This involves the replacement of the bundle of vertical columns by individual U-shape glass columns. Hence, the lower sealing face is eliminated and the transfer of fluid between columns is achieved through holes in the upper ring. The sequence of inter-linking columns is controlled by a large graphlon sealing plate operated by a pneumatic actuator.

Industrial utilization of such moving column systems were made by Unidiv Ltd., Crewley and also Precision Engineering Co. Ltd. In their small scale sequential

separators (148), the relative movement of the column bundle past inlet and outlet ports was achieved by indexing the columns at a predetermined time interval. Operators of this equipment for gas and liquid chromatographic separations have been reported (149).

4.3.3. Simulated Moving Bed Counter-Current Systems

The mechanical complexities involved in rotating a large bundle of columns coupled with the unreliability of the seals, have made the moving column system difficult and expensive to be implemented industrially. Therefore more recent designs have achieved a counter-current scheme through simulated bed movement.

Szepesy et al. (150) proposed a scheme (Figure 4.12a) in which a switching valve was centrally mounted on a rotary P.T.F.E. disc. Rotation of the valve alters the relative positions of the inlet and outlet ports to a series of stationary columns. In such a manner, counter-current column movement is simulated. Maximum flowrate through the valve has been reported to be about 330 cm^3 min^{-1}.

Similar rotating valve method has been employed industrially by Universal Oil Products (151,152) for the separation of light hydrocarbons. A typical flow scheme

Fig. 4.12 Equipment For Continuous Chromatography Using A Rotary Valve

(a) Scheme Of Szepesey et al

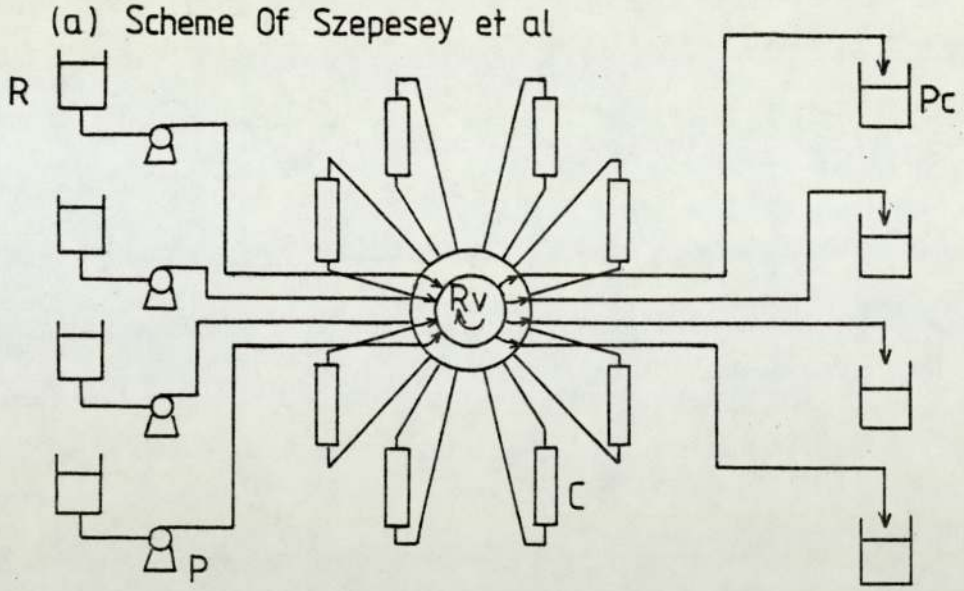

C COLUMNS
Rv ROTARY VALVE
R RESERVOIRS
P PUMPS
Pc PRODUCT COLLECTION

(b) V.O.P. Process Scheme

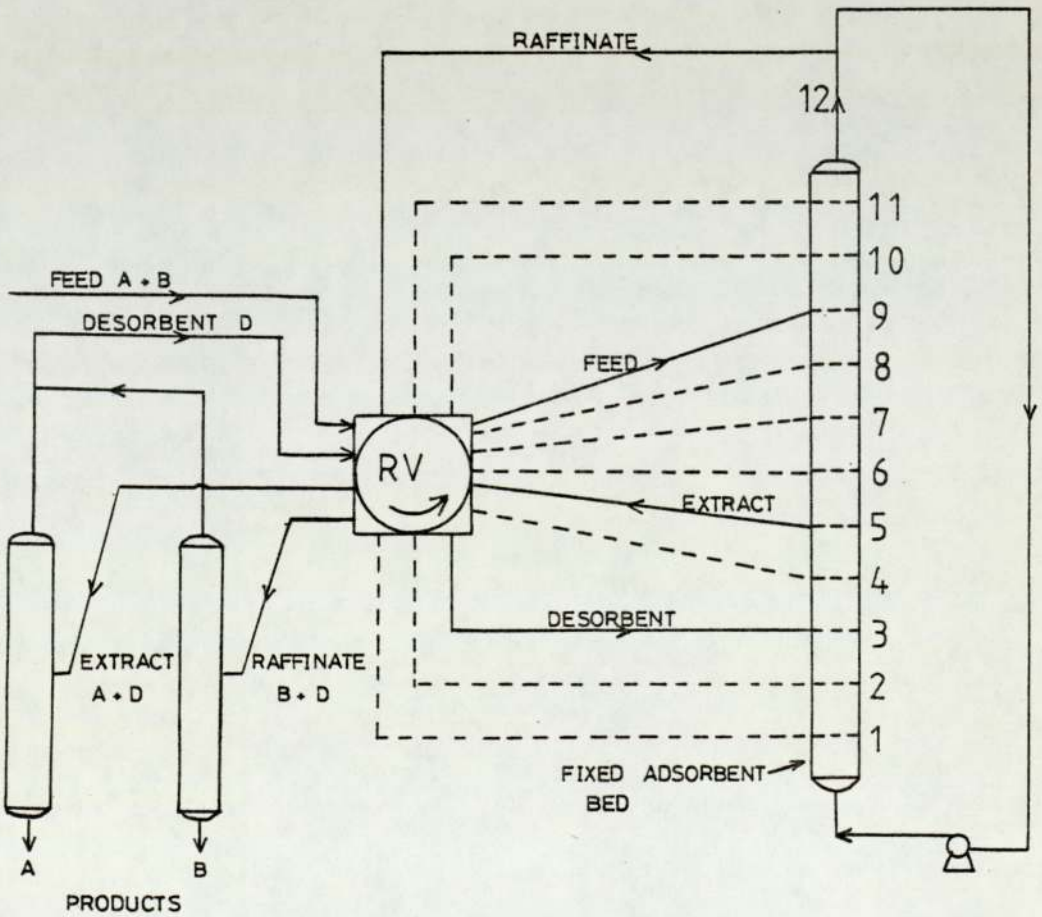

is illustrated in Figure (4.12b) and a single column is used. The simulated movement of column packing is achieved by indexing the column inlet and outlet ports. Pilot plant studies produced p-xylene purities of 99.5% from a feed mixture containing only 14.3% w/w of the component.

Barker and Deeble (20) have designed a novel process scheme where all moving ports except for the closing and opening of seven valves, are eliminated. The counter-current movement of both phases is simulated using solenoid or pneumatically operated valves. In their equipment, twelve 7.6 cm diameter, 0.61 m long vertical columns were connected together to form a closed loop. Six valves are assigned to each column to control the flow of fluid in and out of the system and between columns. Studies with this unit on binary halocarbon mixtures have proved to be successful at feedrates of up to 1400 cm^3hr^{-1}. A second machine has been constructed for the study of high temperature gas-liquid chromatographic separations involving labile materials (153).

Liquid-liquid chromatographic studies with the same process scheme have been conducted by Ellison (21), Barker et al. (23). The development of the semi-continuous chromatographic refiner used for the study of liquid-solid (chemi-adsorption) chromatographic separations throughout

this research programme also follows a similar operating principle as patented by Barker and Deeble (19).

Chapter 5

Analytical Techniques and Experiments

5.1. Introduction

This chapter consists of three main sections. The first section outlines the general techniques and equipment associated with the use of colorimetry as an analytical tool. The second section deals with an experimental study conducted, with analytical scale columns, to select the appropriate ion exchange resin for the SCCR4 machine. Included in this section is also a brief account of ion exchange resin's properties which also formed part of the selection criteria.

The final section deals with the analytical work conducted with the chosen packing, to acquire the equilibrium data and H.E.T.P. values of use in both the setting of the operating conditions of the SCCR4 unit and the subsequent mathematical modelling work.

5.2. Analytical Equipment and Techniques

5.2.1. Analytical Equipment

The analytical technique employed was colorimetry and the main detection system was a Technicon Autoanalyser unit. The unit is based on the chemical reaction of a continuous sample stream with metered quantities of reagents, designed to produce a chromophore, the optical density (O.D.) of the chromophore being proportional to the sample concentration.

Three assays were used in this research:

(1) The Glucose oxidase/Peroxidase assay (154), which produces a green chromophore, was used to determine the concentration of glucose in the sample. The O.D. of the chromophore was measured at a wavelength of 420 nm. This assay responds exclusively to glucose (Figure 5.1).

(2) The Resorcinol/Hydrochloric acid assay (155,156), which produces a pink chromophore, was used to determine the concentration of fructose in the sample and was measured at a wavelength of 550 nm. This assay was developed primarily for the detection of fructose but was found to provide a response of 2% to other carbohydrates in the sample (Figure 5.2).

(3) The Cysteine hydrochloride/sulphuric acid assay (157), which produces a yellow chromophore, was used to determine the total concentration of carbohydrates in the sample and was measured at a wavelength of 420 nm (Figure 5.3).

As illustrated in the schematic diagrams (Figures 5.1, 5.2, 5.3), a multi-channel proportionating pump was employed to meter the sample and reagent streams. The pump functioned on a peristaltic principle, and the liquid delivery rates were governed by the size of the pump tubes chosen. These tubes, which were PVC or

Fig. 5.1 Glucose Oxidase Assay

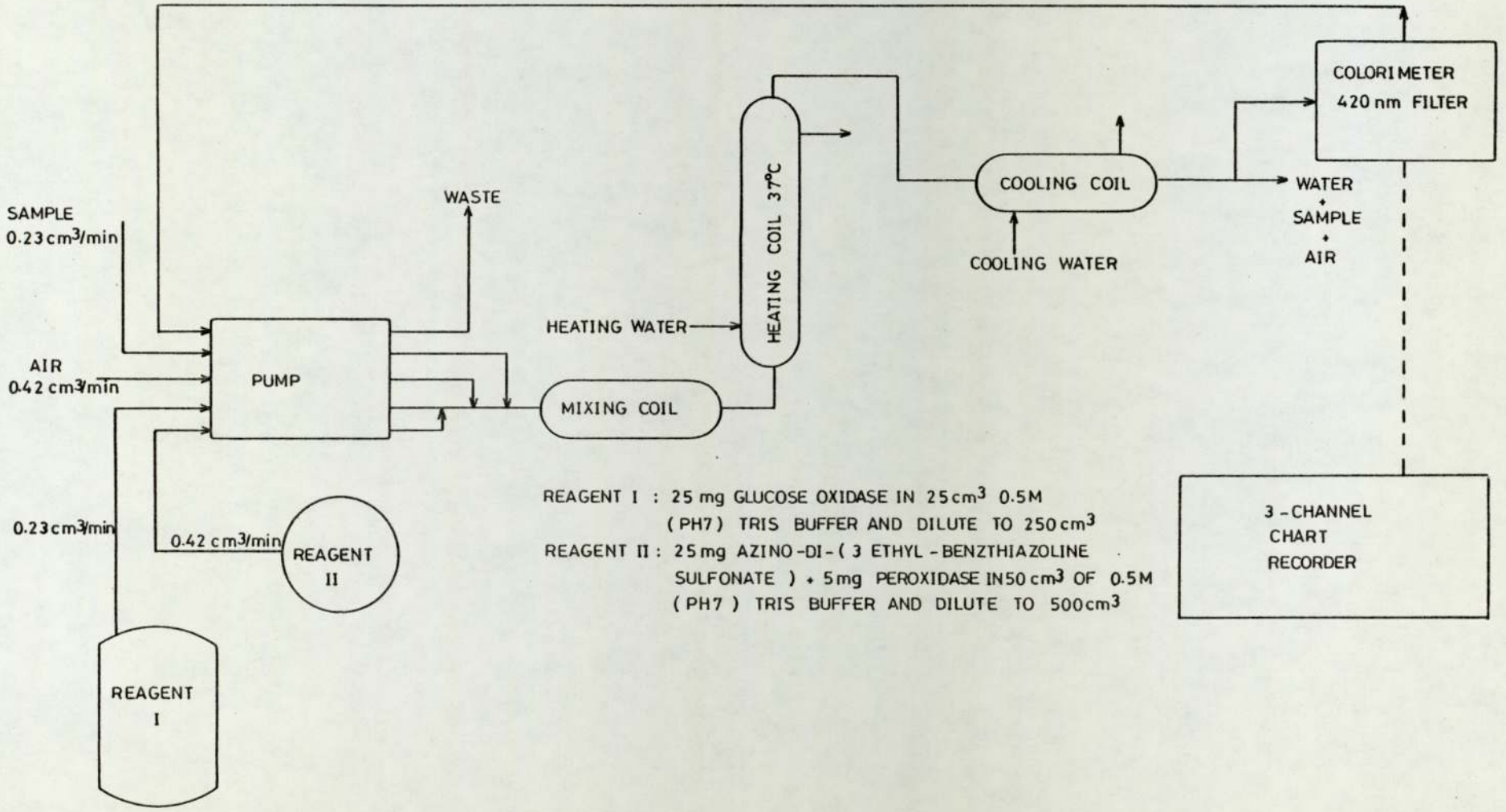

Fig. 5.2 Resorcinal Assay

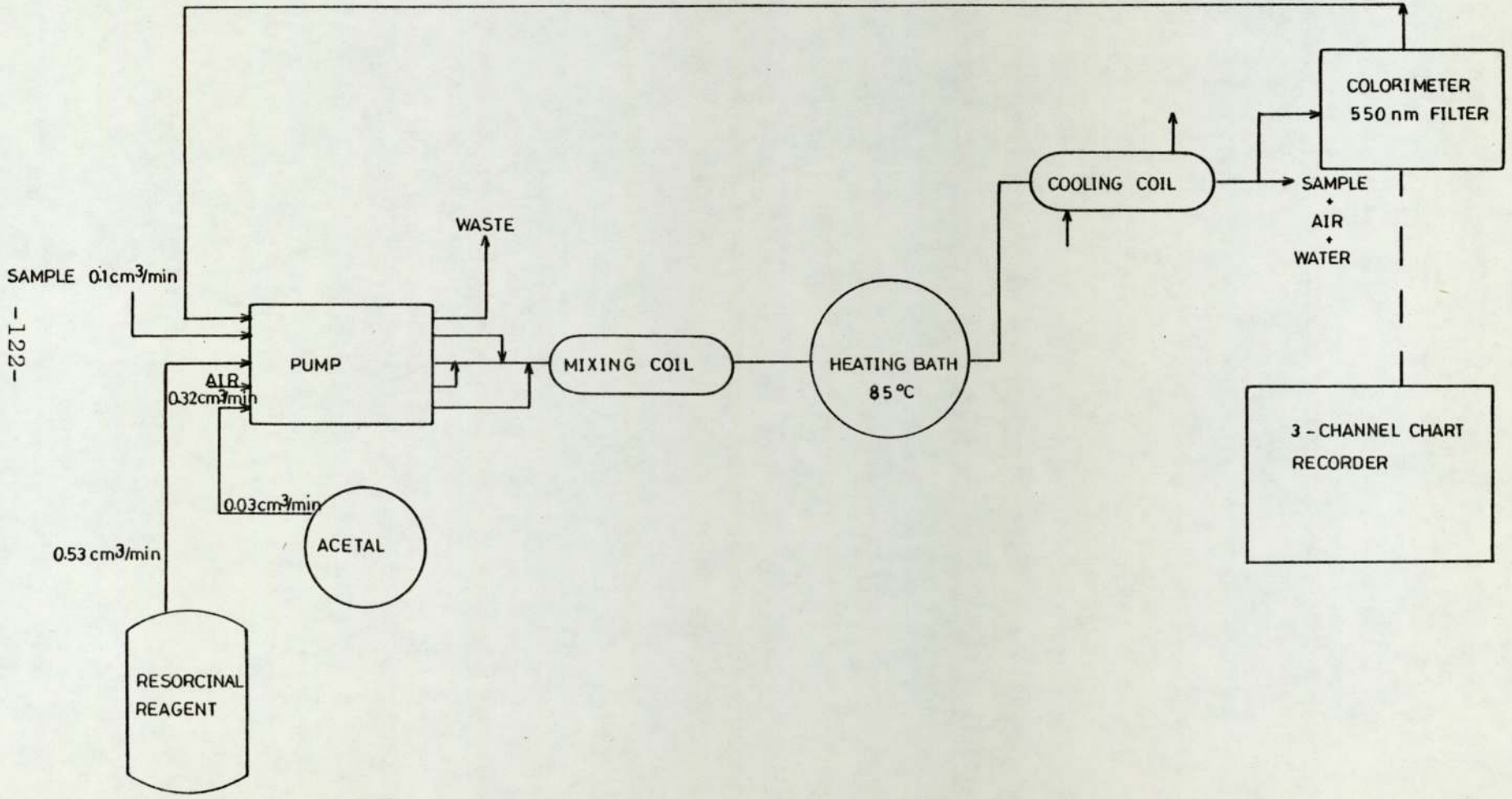

Fig. 5.3 L-Cysteine / H_2SO_4 Assay

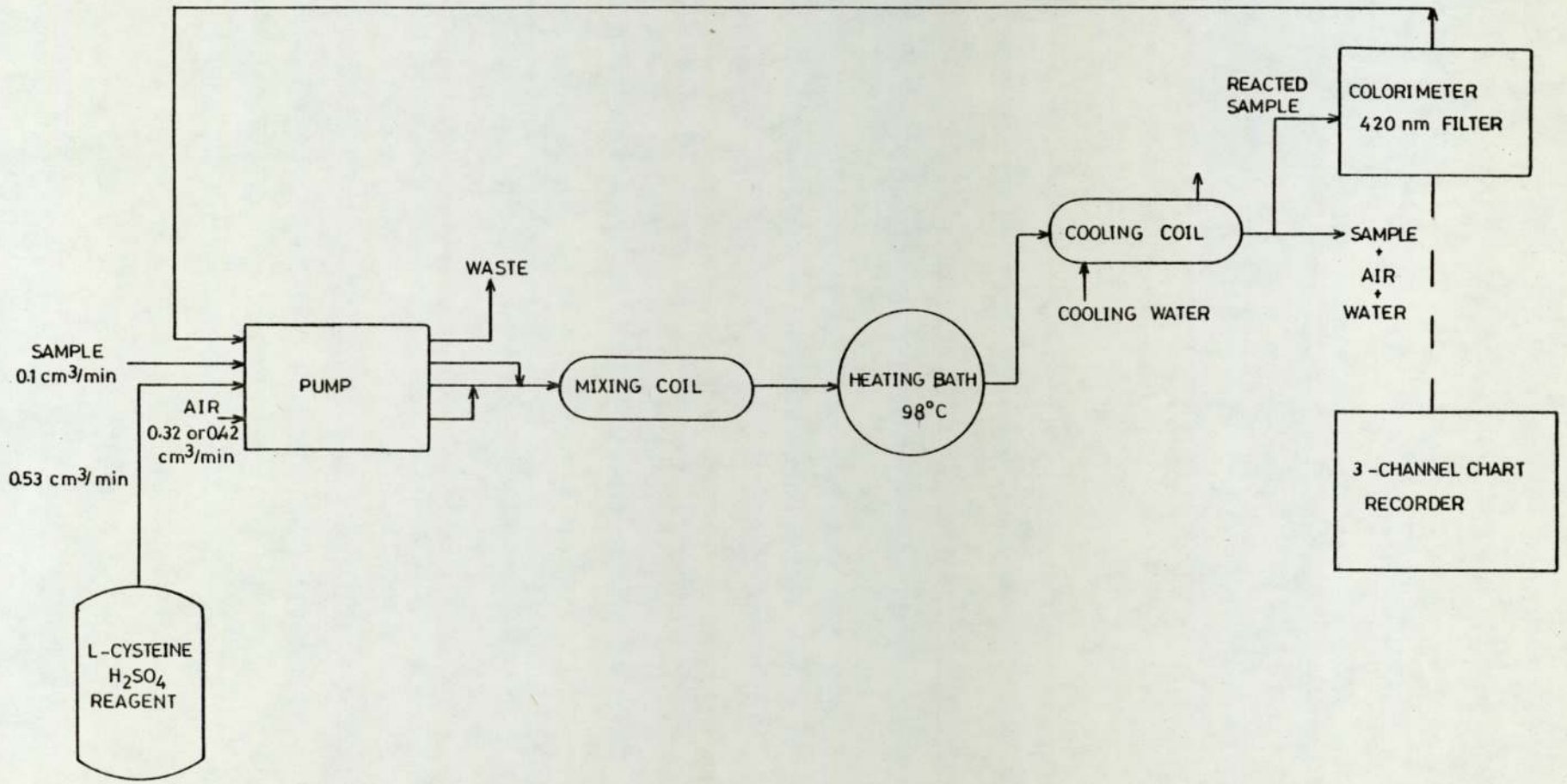

Acidflex, were precision bore and had a life of approximately 200 hours.

Sample and reagent streams were merged together in a glass T-piece and the combined streams were separated into small fractions, so as to minimize longitudinal back mixing, and were subsequently introduced through a mixing coil. Emerging from the mixing coil, the sample fractions were passed through a heating and a cooling stage. The former stage included the use of a heating bath whose temperature was set according to the requirement of each assay (Figures 5.1, 5.2, 5.3). The resident time of the sample through the heating bath can be altered by changing the length of the passage coil. After passing the cooling stage, achieved by jacketing a length of the transfer tube with cooling water, the sample fractions were analysed in the colorimeter. A continuous flow cell (1.5 cm path length), a reference beam to give a continuous zero balance, and a pair of filters were incorporated in the colorimeter to enable the measurement of the O.D. of the chromphore at the correct wavelength to be made continuously.

5.2.2. Analytical Technique

5.2.2.1. Assay Calibration

Each assay was individually calibrated by placing the sample tube in various solutions of known concentrations,

ranging from 0.005 mg cm^{-3} to 0.080 mg cm^{-3}, and allowing the chart recorder responses to reach a plateau value. These values, in optical density (O.D.) were read directly from the charts, by means of a logarithmic scale on the chart paper:

$$\text{Absorbance, or O.D.} = -\log_{10} {}^{I}/_{Io} = -\log_{10} T' \qquad (5.1)$$

I_o = Intensity of radiation incident upon a sample

I = Intensity of radiation emerging from the sample

T' = Transmittance.

Calibration curves for all the assays are listed in Figures (1, 2, 3) in Appendix (I).

5.2.2.2. Product Analysis

5.2.2.2.1. Product From the SCCR4 Machine

As the products from the SCCR4 machine were collected in batches, the determination of the concentration of one particular component in each batch was achieved by placing the sample tube of the appropriate assay into that batch and allowing the chart recorder response to reach a plateau value. In order to maintain the product concentrations within the linear operating range (Figures 1, 2, 3 in Appendix I) of the Autoanalyser Unit, it was necessary to dilute each sample up to 200 - 300 times.

5.2.2.2.2. Product from Analytical Columns (Qualitative Analysis)

The product stream eluting from the batch analytical scale columns was connected by a stainless steel needle to the sample tube of the Cysteine hydrochloride/sulphuric acid assay for the development of the chromatograms for glucose and fructose. The techniques and measurement associated with batch column work will be given in the next section (Section 5.3.1.).

5.3. Experimental Study with Analytical Columns

5.3.1. Column Techniques and Measurements

5.3.1.1. The Batch Column.

The batch, analytical-scale columns used in this research were 1.15 cm internal diameter, 65 cm long, made from glass, and surrounded by a constant temperature water jacket (Figure 5.4). The columns were tapered to a narrow outlet at the bottom, which held a small plug of glass wool to retain the packing. The top of the column was sealed with a rubber bung fitted with a 5 cm length of 0.1 cm I.D. stainless steel tube, connected to the PVC mobile phase inlet line. A glass T-piece was fitted onto the column outlet. One arm of the T-piece contained a stainless steel sampling needle and the other arm conducted excess mobile phase to waste. The

Fig.5.4 Typical Chromatographic Column

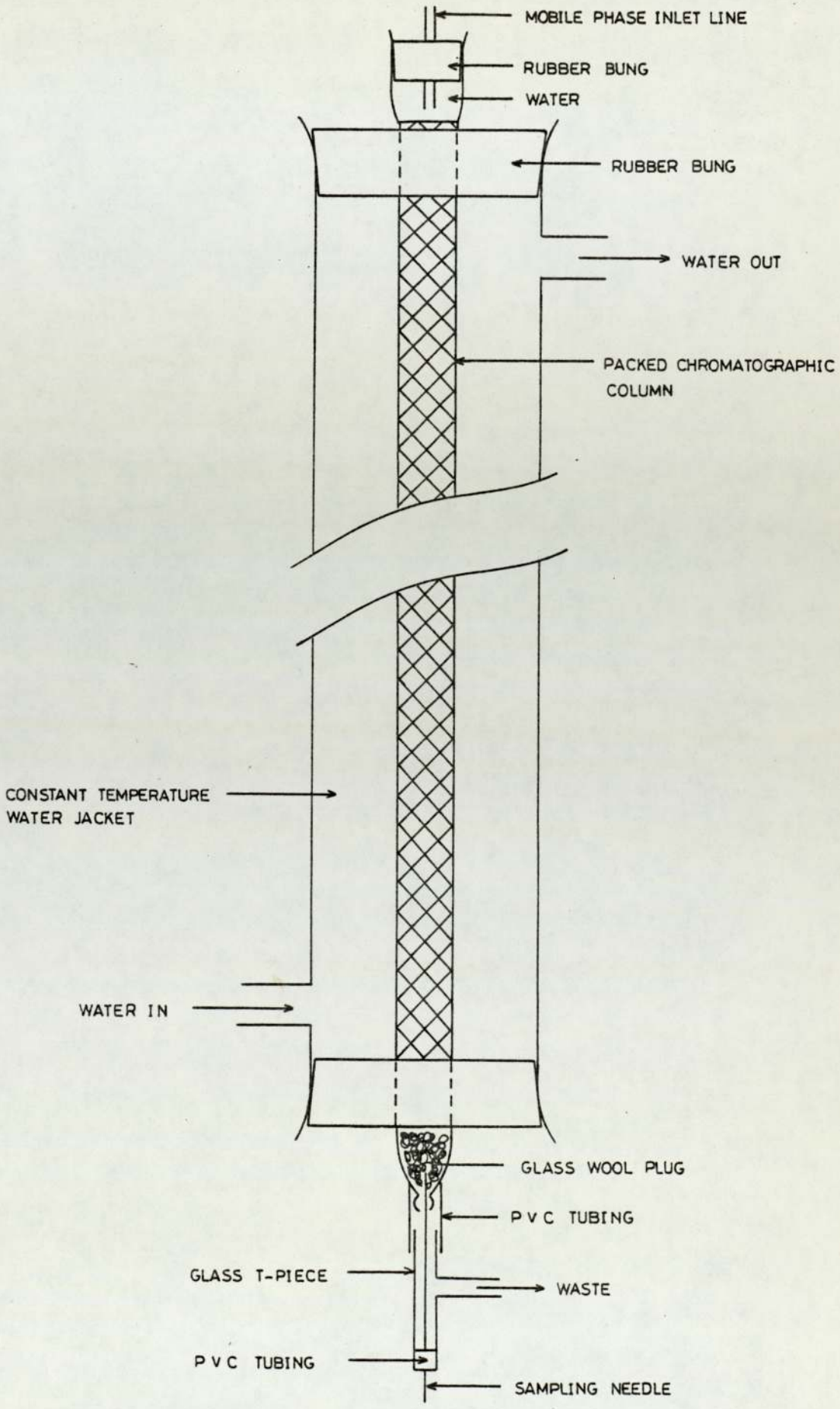

sampling needle was placed very close to the bottom of the packing, to reduce column 'dead volume', and to transport the product stream to the detector.

5.3.1.2. Column Packing Procedure

A slurry-filling method was employed for packing all analytical columns. Initially, the column was filled with distilled water and the outlet plugged. The packing slurry was then introduced into the top of the column using a glass funnel and simultaneously, water was allowed to flow out from the column. To ensure the water level in the column did not drop below the top of the funnel, distilled water was continuously added. Finally, the column was vibrated manually until the packed section reached a constant volume.

5.3.1.3. Sample Loading

The rubber bung and mobile phase inlet tube were removed from the top of the column. The sealing screw clip, located at the column outlet, was opened to allow the liquid level in the column to drop until it revealed the top of the resin bed and subsequently closed again. A micro-pipette was then used to introduce the sample solution onto the centre of the packing. The liquid

level was again allowed to fall until it reached the top of the packing. A volume of distilled water approximately equal to the sample volume, was next injected onto the top of the pack, and once again the liquid level was lowered. The column, above the packed section, was next filled with distilled water, and the rubber bung replaced. This displaced excess distilled water from the column through the stainless steel tube fitted in the bung. Finally the mobile phase inlet line was connected to the stainless steel tube, and at the same time the column outlet clip was opened and the chart recorder started. During the above procedure, care was taken to ensure that the resin bed was not disturbed.

During the analytical studies, 50 µl samples of -0.3 - 0.6 mg cm^{-3} were used. The elution rate and temperature varied from 0.018 to 0.57 cm^3 min^{-1} and from 25°C to 60°C respectively.

5.3.1.4. General Measurements

The mobile phase flowrate was measured, both before and after each elution, by weighing the amount of water leaving the column outlet over a timed interval. The delay time of the detection system, that is the time

interval between the sample leaving the column and the chart recorder responding to the sample, was also checked and recorded twice per day. This was achieved by placing the sample needle in a solution of glucose or fructose and starting the recorder simultaneously. This delay time, measured from the chart, was subtracted from the measured total sample elution time to provide the net elution time of the sample from the column. Recorded delay times for the Cysteine hydrochloride/sulphuric acid assay were usually 10 - 15 minutes. Elution volumes of starch, glucose and fructose were calculated by multiplying the individual net elution times by the mobile phase flowrate. The distribution coefficient, K_D^F, of fructose, was calculated from Equation (5.9) in Section 5.3.3.1.

5.3.2. Experimental Study for Packing Selection

5.3.2.1. Introduction

There are many different types of ion-exchange resins commercially available. In liquid chromatography, the most commonly employed resin is produced from polystyrene crosslinked with divinyl benzene (D.V.B.). Polar groups, acidic (cationic) or basic (anionic) in nature, are introduced either before or after the polymerisation stage. In general, a high percentage linkage represents

a high structural strength, but has a much smaller effective pore size, permeability and tendency to swell. The most popular types of resin have a nominal 8% DVB content.

In this research study, the selected resin must be the type with an acidic polar group that can accept calcium ions as its counter-part. This excluded the choice of anionic type of resins (with a basic polar group). In cationic resins, the acidity of the functioning polar group was commonly used to distinguish between the strongly and weakly acidic types. The most frequently used form of a weak acid resin consists of a carboxyl functional group. Whereas, the most popular strong acid resin contains a sulfonic functional group. In general, the latter type of resin offers a wider pH and temperature operating range, and therefore the various resins chosen for the following studies were confined to this type only.

5.3.2.2. Resins Chosen for Comparison

Four different resins were acquired for a comparative study. Their selections represented a combination of variations of particle sizes, percentages of linkage and costs. Experiments have been conducted, with columns of the same geometries, to evaluate the

Table 5.1 Properties Of Various Resins

Type	Grade	Form Supplied	Size Range μm	Exchange Capacity [Wet : meq/cm³ Dry : meq/g]	Cross-Linking %	Maximum Operating Temperature °C	PH Range
Lewatit SC 104	Standard	H^+	1203$^+$	Dry 4.5	4	120	1 - 14
Zerolit '225' SRC 13	Standard	Na^+	1203 ~ 294	Dry 4.5 ~ 50	8	140	1 - 14
Zerolit 225 SRC 14	Standard	Na^+	294 ~ 150	Dry 4.5 ~ 50	8	140	1 - 14
Amberlite Type I	Chromatographic	Na^+	150 ~ 76	Wed : 1.9 Dry : 5	8	120	1 - 14

separation efficiency of individual resins. Standardised techniques for column packing (Section 5.3.1.2), sample loading (Section 5.3.1.3) and resin conditioning (Section 7.1), were maintained throughout the study. The properties of the resins were tabulated in Table 5.1.

5.3.2.3. The Criterion for Selecting the Most Efficient Packing

Although pressure drop and costs contributed partly towards the final choice of resins, the main criteria for this comparative study was based on the ability of individual packings to separate glucose and fructose. The resolution of a binary mixture, described in terms of both bands and peak-to-peak widths, was discussed in Section 2.2, and was employed as a guideline for evaluating the performance of each resin. Samples of glucose/fructose were loaded onto and eluted, at various flowrates but at ambient temperature, from columns packed with the different resins.

5.3.2.4. Results and Discussion

A typical set of chromatograms is shown in Figure 5.5. At an elution rate of 0.23 cm^3/min, only two

Fig. 5.5 Elution Chromatograms Of Glucose/Fructose From Various Resins

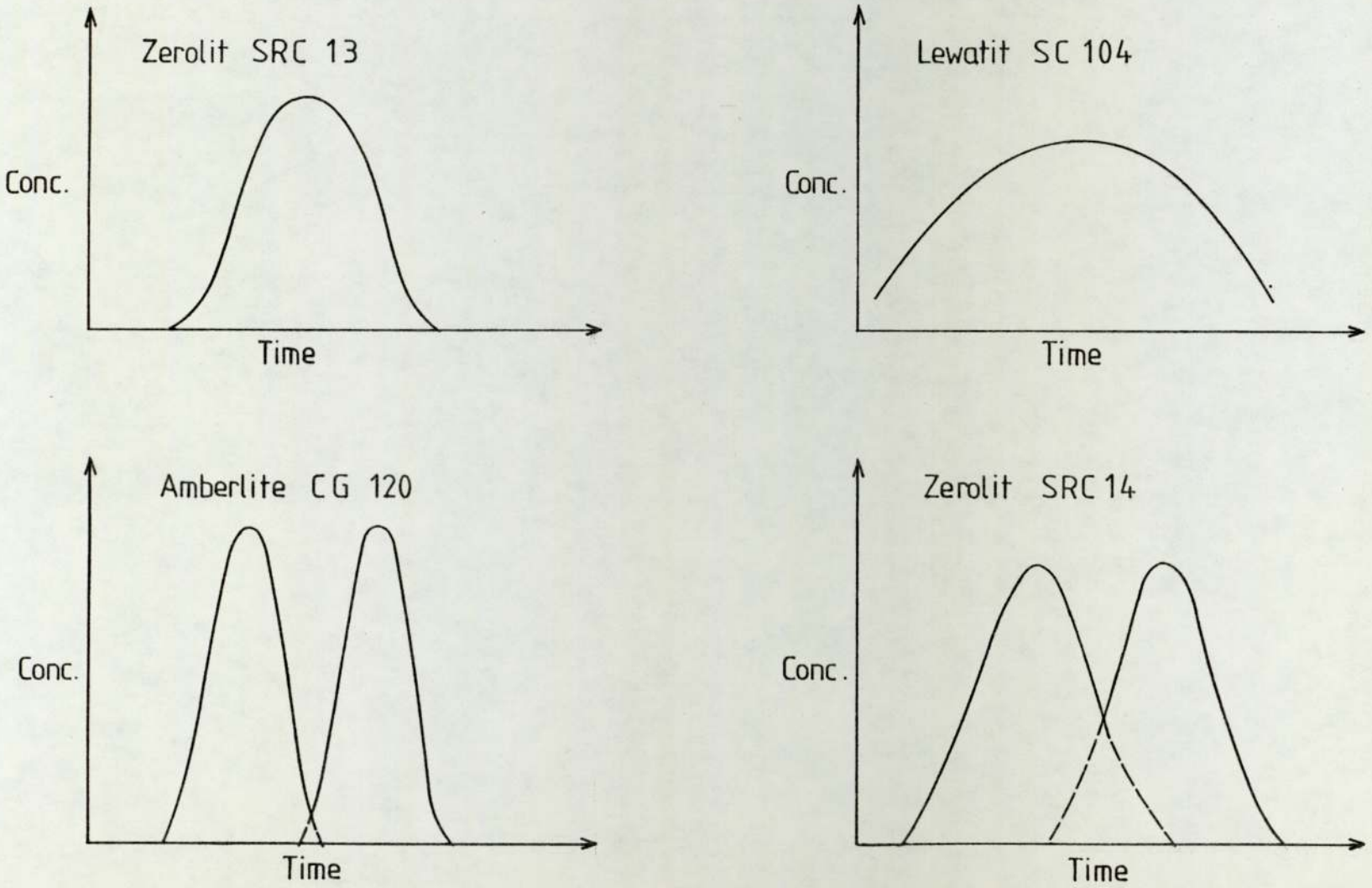

resins, namely Zerolit SRC14 and Amberlite CG120, succeeded in resolving the sample mixture into its separate components. The latter resin provided a more complete resolution of glucose from fructose than the former resin.

At higher elution rates, the sample resolving power of all the resins decreased, and at a flowrate of 0.57 cm^3/min, Amberlite CG120 was the only resin still retaining a partial resolution which was marked with excessive overlapping between the glucose and fructose bands.

By eluting samples at a slower flowrate of 0.1 cm^3/min, there were still no indications that resolution was achieved by both the Zerolit SRC13 and Lewatit SC104 resins. However, at this flowrate, a complete separation of the glucose band from the fructose band was achieved with the Zerolit SRC14 resin, and the similar chromatogram developed from the Amberlite CG120 indicated, besides a complete resolution, also an increased peak-to-peak width between the two components.

From the results of the batch experiments, and between a flowrate of 0.1 - 0.5 cm^3/min, Amberlite CG120 resin offered the best resolving capability. But a cost survey revealed that this resin was marketed at about 6 - 10 times the cost of the other three resins. In addition, the particle size range of the Amberlite CG120

resin(150μm - 76 μm) was the smallest. From the Kozeny equation (158), the pressure drop, p, through a packed bed under laminar flow conditions, and assuming no wall effect, may be written:

$$\Delta p = \frac{K'' S_p^2 (1-\varepsilon)^2 \mu \, l \, U}{\varepsilon^3} \qquad (5.2)$$

K'' = Kozeny's constant ($\simeq 5$)

S_p = Specific surface area of packing particles
= $6/d_p$ for spheres

d_p = particle diameter

μ = fluid viscosity

l = bed length

U = average fluid velocity, defined as $\frac{1}{A'} \frac{dV}{dt}$

V = volume of fluid flowing in time, t

A' = total cross-sectional area of bed

ε = voidage.

For spherical particles, Equation (5.2) becomes:

$$\Delta p = \frac{180 (1-\varepsilon)^2 \mu \, l \, U}{\varepsilon^3 d_p^2} \qquad (5.3)$$

Equation (5.3) shows the relationship between pressure drop and particle size. Halving the size of

the particle employed in a system will result in a four folds increase in pressure drop. Hence, after compromising performance against cost and pressure drop, Zerolit SRC14 resin was selected to be the SCCR4 packing.

5.3.3. Experimental Study with Analytical Column Packed with Zerolit SRC14 Resins

The study was conducted with a primary aim of acquiring equilibrium data and H.E.T.P. values which were essential to both the prediction of the operating conditions of the SCCR4 machine and future simulation work. This included firstly, the determination of the elution volumes of glucose and fructose to establish a relative distribution factor (K_D^F) and secondly, the calculation of the number of theoretical plates (N) per column in the sequential separator, to indicate on-column dispersion. In addition, the variation of such data with elution rates and temperatures were also investigated.

5.3.3.1. Determination of Relative Distribution Factor

From Section 2.1, the distribution coefficient of a component in elution chromatography is defined as:

$$K_D = \frac{V_R - V_M}{V_S} \qquad (5.4)$$

V_R = retention volume of the component

V_M = total volume of mobile phase in the column

= V_i (Pore volume) + V_o (Void volume)

V_S = volume of solid stationary phase; (The resin's solid matrix)

Applying Equation (5.4) for eluting glucose from a Ca^{++} charged ion exchange resin column;

$$K_D^G = \frac{V_R^G - V_M}{V_S} \qquad (5.5)$$

As the glucose molecule form no complexes with the Ca^{++} ions, it will emerge from the column after diffusing through the pore (intraparticle) and void (interparticles) volumes. Hence, in this case,

$V_R^G = V_M$ (Total mobile phase volume in the column). (5.6)

and from Equation (5.5) $K_D^G = 0$

Applying Equation (5.5) to fructose will result:

$$K_D^F = \frac{V_R^F - V_M}{V_S} \qquad (5.7)$$

From Equation (5.6)

$$V_R^G = V_M$$

$$K_D^F = \frac{V_R^F - V_R^G}{V_S} \qquad (5.8)$$

V_S = volume of resin matrix, and is:

$$V_S = V_{TOTAL} - (V_i + V_o)$$

V_{TOTAL} = Total column volume

V_i = pore volume

V_o = void volume.

Since $V_M = V_i + V_o$

and $V_R^G = V_M$ from Equation (5.6)

$$K_D^F = \frac{V_R^F - V_R^G}{V_{TOTAL} - V_R^G} \qquad (5.9)$$

5.3.3.2. Calculation of On-Column Dispersion

Values for the number of theoretical plates (N) were calculated, for both glucose and fructose, from the chromatograms obtained. For a Gaussian Peak (159)

$$N = 8 \left(\frac{t_R}{W_{h'/e}} \right)$$

t_R = Peak retention time of the component

$W_{h'/e}$ = width of the components peak

h' = height of the component peak

Corresponding H.E.T.P. values were calculated from

$$\text{H.E.T.P.} = \frac{l}{N}$$

l = length of packed column section.

5.3.3.3. Results and Discussion

Results of all the experiments are illustrated in both tabular (Table 5.2) and graphical (Figures 5.6, 5.7, 5.8) form. In Table 5.2, the peak elution volume of glucose is shown to be constant (41.4 cm^3) over a range of elution rates and temperatures. Similarly, the peak elution volume of fructose (60.9 cm^3) was found to remain constant at all elution rates. However, at elevated temperatures, a decrease in the corresponding elution volume was detected. From the chromatograms developed at higher temperatures, closer peak-to-peak distances between glucose and fructose bands were observed. This implies that the resolution (Section 2.2) of the two components becomes more difficult with

Table 5.2 Results Of Analytical Study With Zerolit SRC 14 Resin

TEMPERATURE °C	ELUTION RATE cm³/min	ELUTION VOLUME OF GLUCOSE V_R^G (cm³)	ELUTION VOLUME OF FRUCTOSE V_R^F (cm³)	RELATIVE DISTRIBUTION COEFFICIENT K_D^F	NO. OF THEORETICAL PLATES w.r.t. GLUCOSE N^G	NO. OF THEORETICAL PLATES w.r.t. FRUCTOSE N^F	H.E.T.P. FOR GLUCOSE H^G (mm)	H.E.T.P. FOR FRUCTOSE H^F (mm)
25	0.576	41.5	60.8	0.613	62	34	10.52	19.35
25	0.460	41.2	61.0	0.620	87	43	7.50	1.50
25	0.232	41.4	60.8	0.613	211	86	3.08	7.59
25	0.180	41.6	60.9	0.617	289	119	2.25	5.45
32	0.180	41.3	58.7	0.550	361	200	1.80	3.25
40	0.180	41.3	57.1	0.500	455	315	1.43	2.06
43	0.180	41.3	56.6	0.481	504	348	1.29	1.87
52	0.180	41.4	55.8	0.456	613	401	1.06	1.62

Column Dimension : 1.14 cm I.D. * 65 cm ; Total Column Volume : 73 cm³; Total Resin Weigh : 93 gm.

Fig. 5·6 Variation Of K_D^F With Temperature

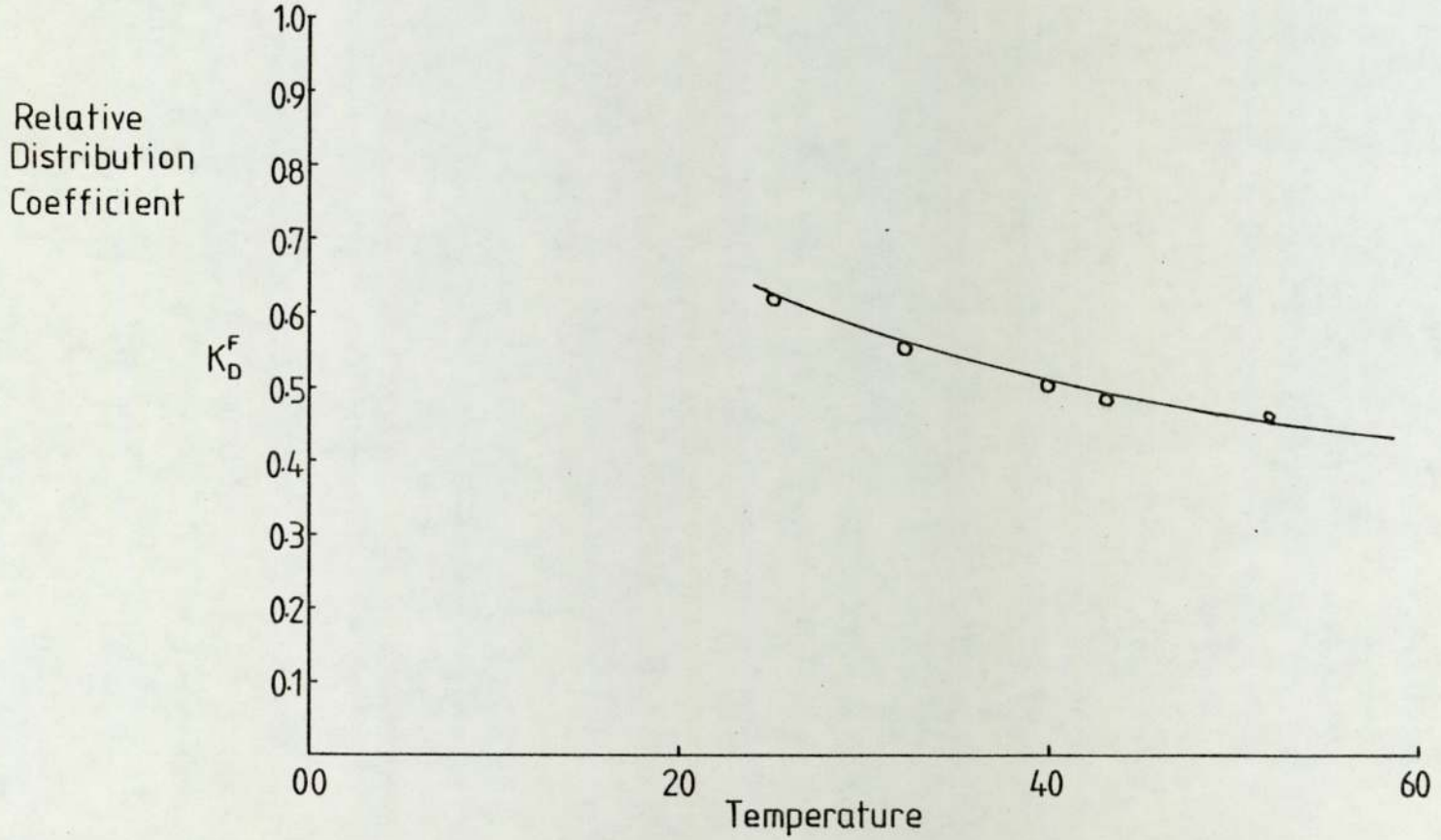

Fig. 5.7 Variation Of Plate Height With Flowrates

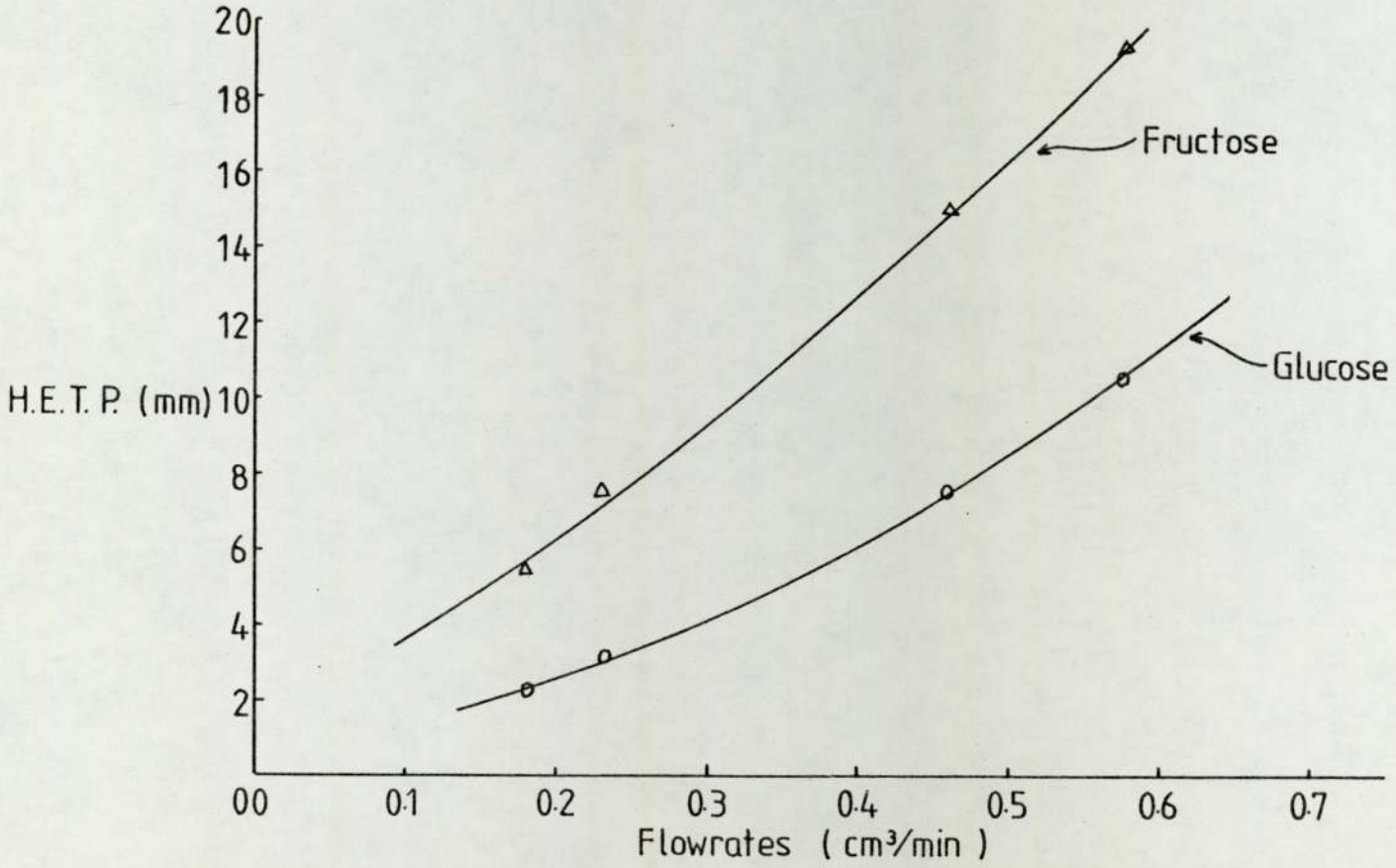

Fig. 5.8 Variation Of Plate Height With Temperature

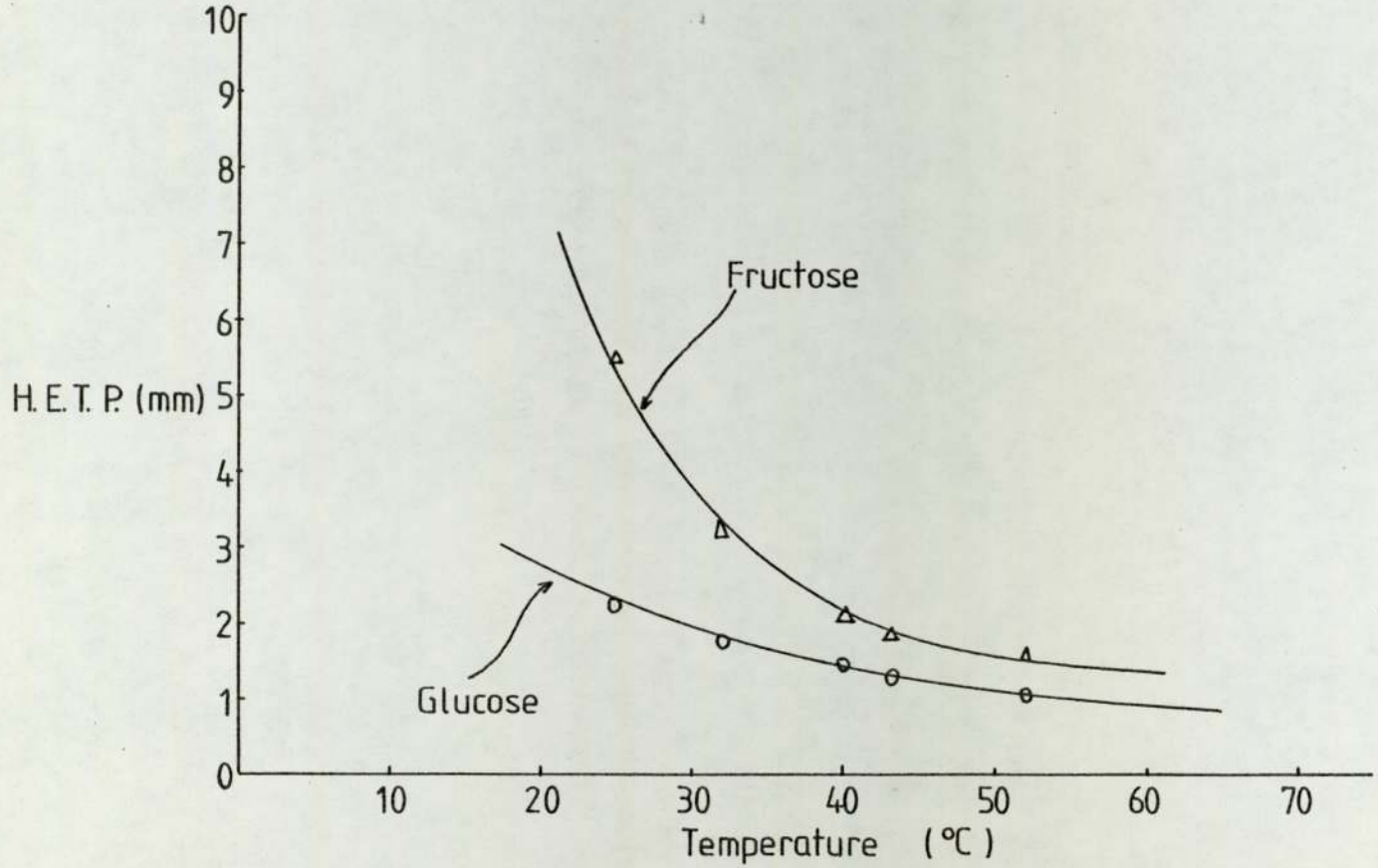

increasing temperature. Figure 5.6 illustrates the variation of the relative distribution coefficient (K_D^F) with temperatures. The significance of K_D^F on the separation were investigated in the mathematical simulation work and will be discussed in a later section, (Section 9.3).

Results from this experimental study also revealed a dependency of the theoretical plate height, for both glucose and fructose on flowrates (Figure 5.7) and temperatures (Figure 5.8). The increase of plate heights with elution rates is a well established fact in liquid chromatographic practice, and results of this study indicated (Figure 5.7) that a decrease of the elution rate by a third will provide a four-fold reduction in the corresponding plate height.

The gain from plate height reduction with temperature is more prominent with fructose than glucose. By elevating the temperature from 25°C to 52°C, the plate height of fructose drops from 5.45 mm, to 1.62 mm. Whereas, the corresponding drop in glucose plate height is only from 2.25 mm to 1.06 mm.

Chapter 6

Design and Construction of the Sequential Continuous Chromatographic Refiner (SCCR4)

6. Design and Construction of the Sequential Continuous Chromatographic Refiner (SCCR4)

6.1. Introduction

The successful operations of both the continuous gas-liquid chromatographic process by Barker and Deeble (20), and the liquid-liquid chromatographic process by Barker, Hatt and Ellison (21), have led to the belief that a similar flow scheme could be undertaken for the study of a liquid-solid chromatographic process.

6.1.1. Principle of Operation of the SCCR4 Equipment

Figure 6.1 schematically shows the operation of the SCCR4 machine for the separation of a binary feed mixture. A mixture of components 1 and 2 is fed into the system at port D. The less strongly adsorbed component, (component 1) is preferentially moved with the mobile phase fluid towards product 1 offtake port A. A section of the closed loop column is isolated by locks T and TT; an independent purge fluid stream enters at port E and exits with the more strongly adsorbed component (component 2) from port B. Figure 6.1a represents the distribution of the two components within

Fig.(6·1) Principle of Operation of SCCR4 Machine

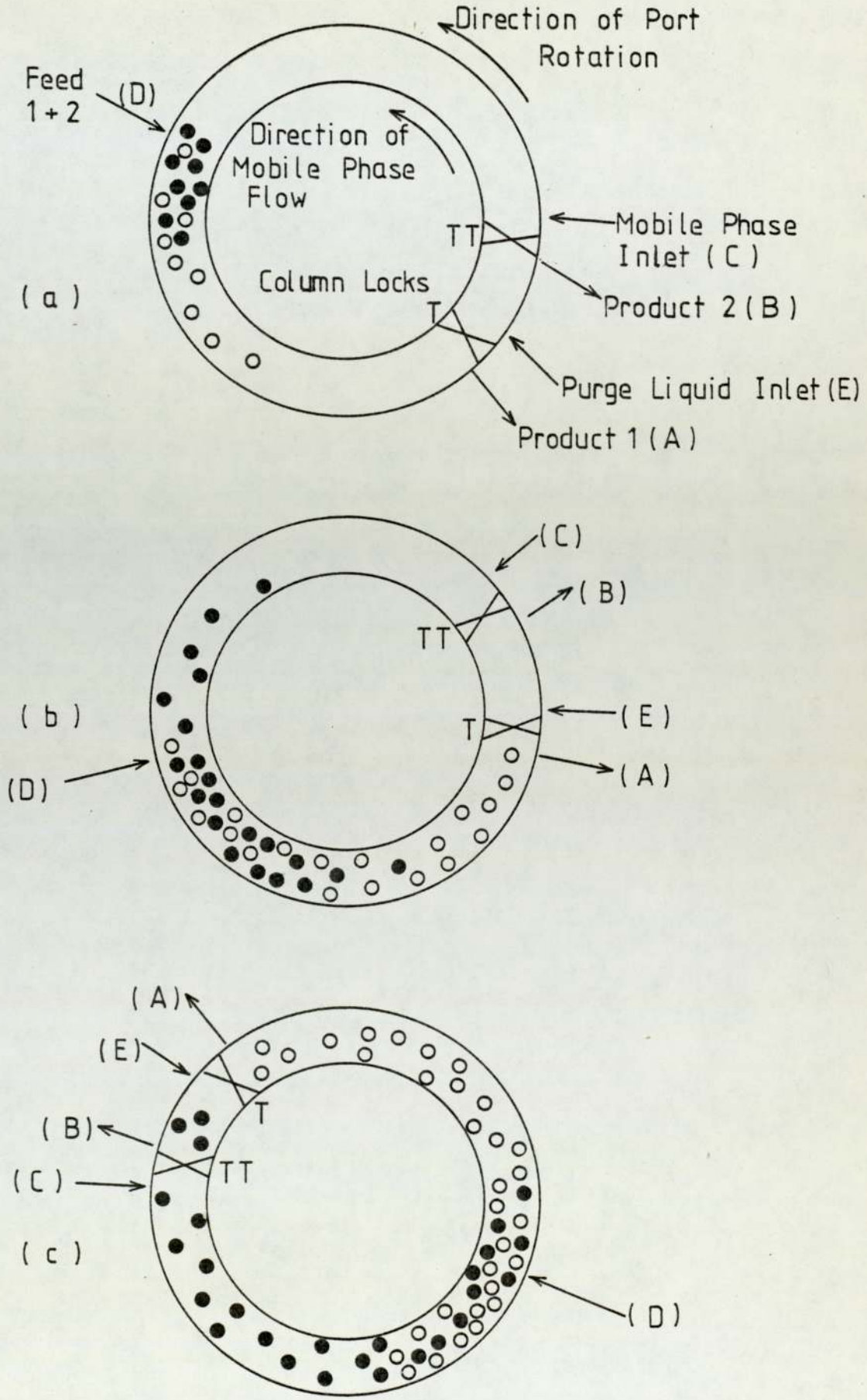

the system soon after 'start up'. In Figure 6.1b, all the port functions have been advanced one position in a direction co-current to the direction of mobile phase flow. This port advancement results in an 'effective' movement of the packed column in a direction counter-current to the direction of the mobile phase flow. The rate of advancing the ports must be less than the velocity of the less strongly adsorbed component through the packing, but greater than that of the more strongly adsorbed component. As such, component 2 is being 'held' preferentially on the resin bed while component 1 is emerging from port A. The last diagram (c) of Figure 6.1 shows the fully established operating condition of the unit.

From Figure 6.1, it may be seen that seven valves need to be opened or closed simultaneously, namely, the feed inlet, the mobile phase inlet, the product 1 outlet, the purge fluid inlet and outlet and two column isolation locks. Based on the above principle, it was found mechanically convenient to construct a liquid solid chromatographic fractionation unit with separate columns, with the valves placed around and between each column. A more detailed description of the ten column unit that was built now follows.

6.1.2. Development of SCCR4 Unit

The special features incorporated into the design of the SCCR4 can be summarised:

(i) The use of pneumatic valves, which can be activated to open or close, operating in a programmed sequence to provide a fixed bed, moving port system of operation. The success of such a scheme has been demonstrated by previous workers (20,21), but the incorporation of the pneumatic operated valves and its control system was expected to offer additional operational reliability, safety and flexibility over the former SCCR designs adopting solenoid operated valves.

(ii) The use of materials of construction not only resistant to water and carbohydrate solution, but also inert to dilute mineral acids, thus ensuring a wider range of systems that can be conducted on the SCCR4 unit.

(iii) The incorporation of a plunger head device, operated by midget pneumatic cylinders, to accommodate any swelling or contracting of the resin bed due to variations of the ionic strength of the external solution.

(iv) A separate purge section, independent of the main mobile phase stream, to purge the more strongly adsorbed component. The temperature of the purge liquid in the SCCR4 unit to be elevated to a maximum of 85^{o}C. This implies a more efficient purging in a 'shorter switch time'.

(v) Heating tapes to be mounted on the glass columns for achieving higher temperature operations, and any heat loss from the column being minimized by a 50 mm diameter fibre glass jacket. Each column's temperature to be independently controlled and indicated by a thermoster and a thermocouple respectively mounted on the wall of the column.

6.1.3. Overall Description

An overall view of the SCCR4 unit is shown in Figure 6.2, Figure 6.3 and Figure 6.4. The two photographs show the unit before and after heating facilities were incorporated. The main separation unit is a closed loop of ten (QVF 25.4 mm I.D. x 700 mm) glass columns. Six pneumatic operated poppet valves, Section (6.2.1.3), four of which (the feed, the purge, the mobile phase and the transfer valve) were mounted at the inlet to each column, whilst the other two (product 1 and product 2) were mounted at the outlet of each column. Isolation of an individual column was achieved by energizing, to close, two consecutive double acting pneumatic transfer valves. Inlet and outlet lines were arranged in a ring distribution network (Section 6.2.3), connected respectively to the metering pump (Section 6.2.4) and product collection device (Section 6.4.2) of the system.

Fig. 6·2 Schematic Diagram Of SCCR 4 System

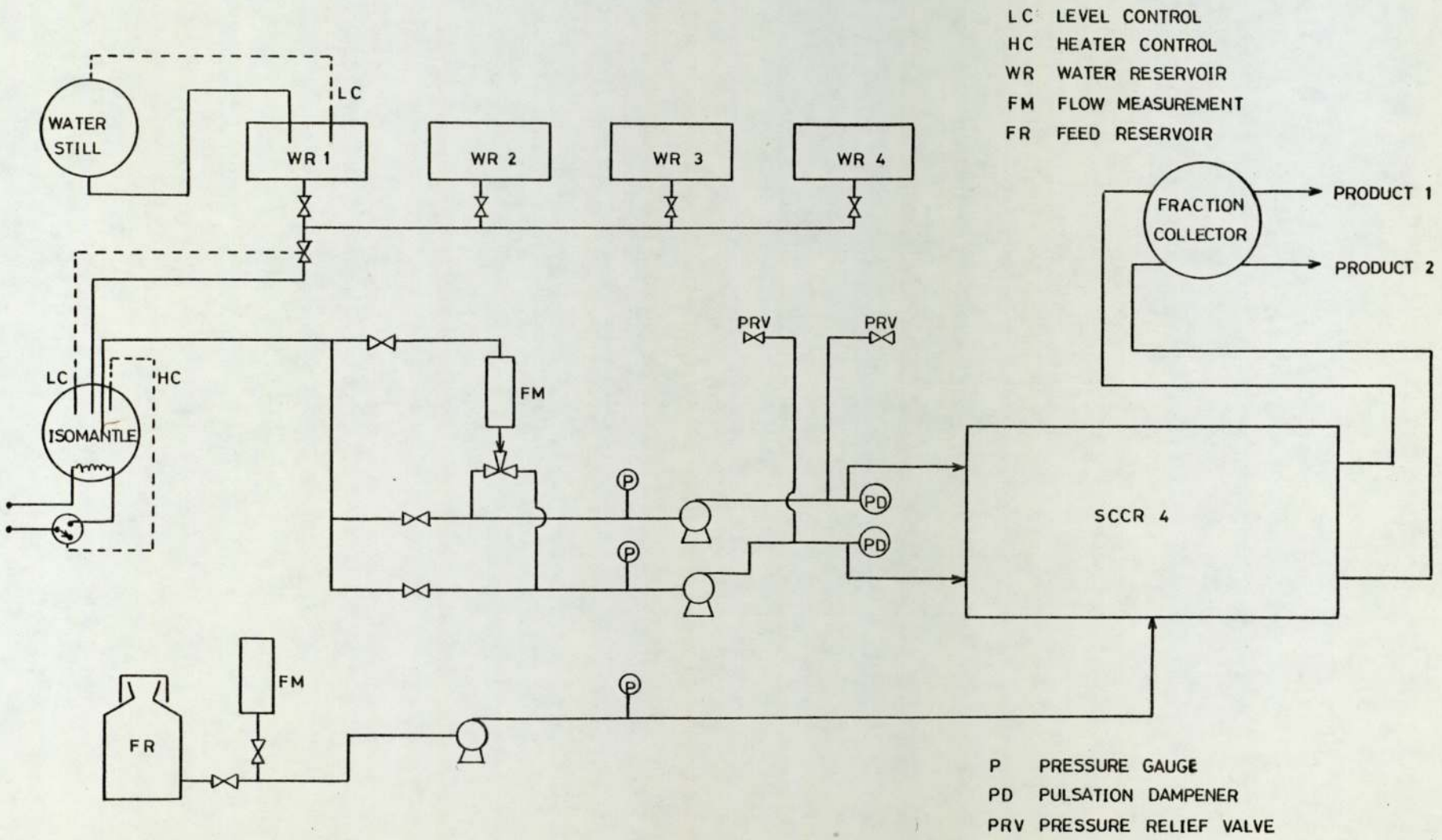

Key For Fig. 6.3 & Fig. 6.4

A	Control Box
B	Digital Timer
C	Purge Liquid Pump
D	Feed And Mobile Phase Liquid Pump
E	Packed Column
F	Pneumatic Cylinder & Plunger Unit
G	Valve
H	Relief Valve
I	Pressure Gauges
J	Pneumatic Pressure Regulator
K	Pulsation Dampener
L	Column With Heating Tape & Jacket

Fig. 6.3 Overall View Of SCCR 4

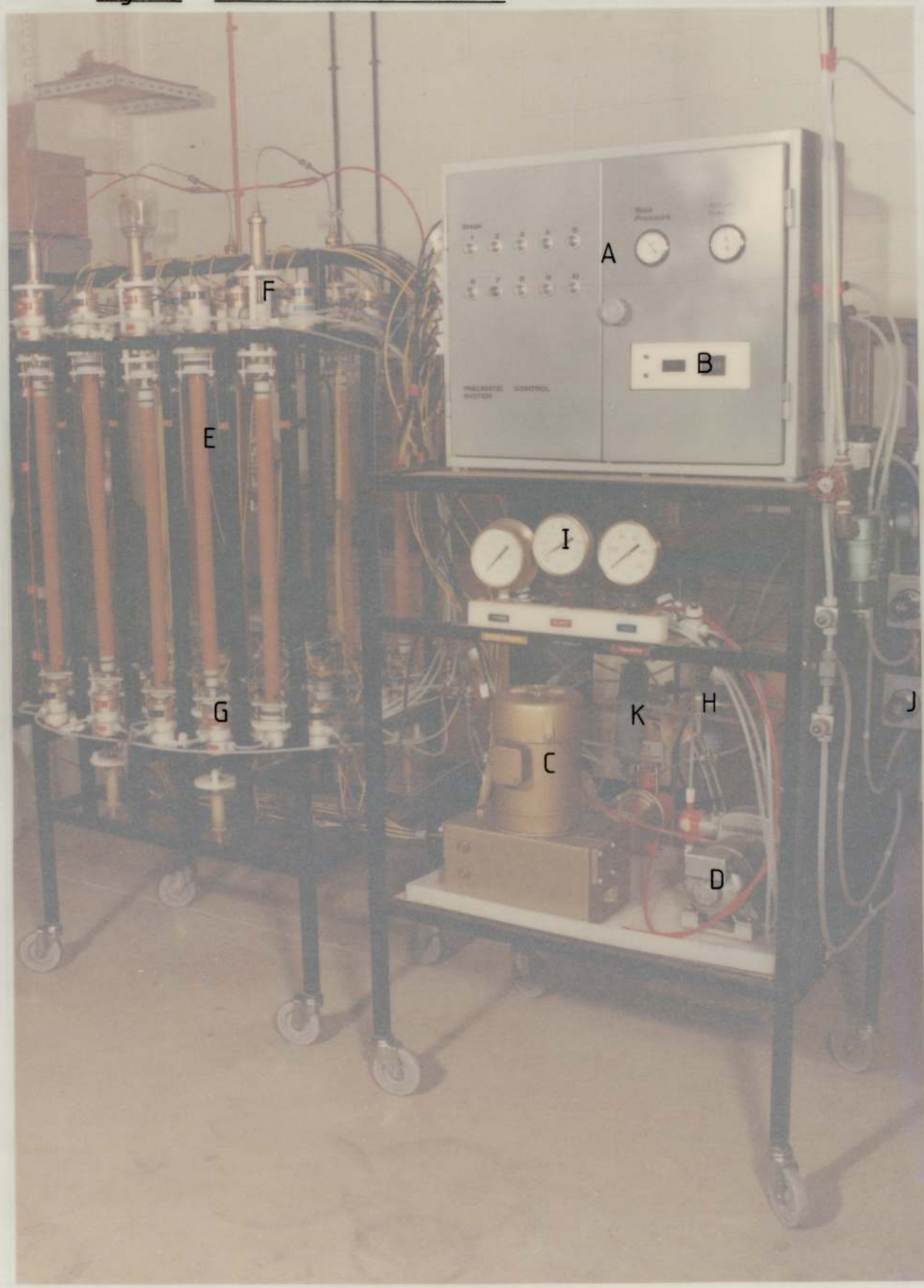

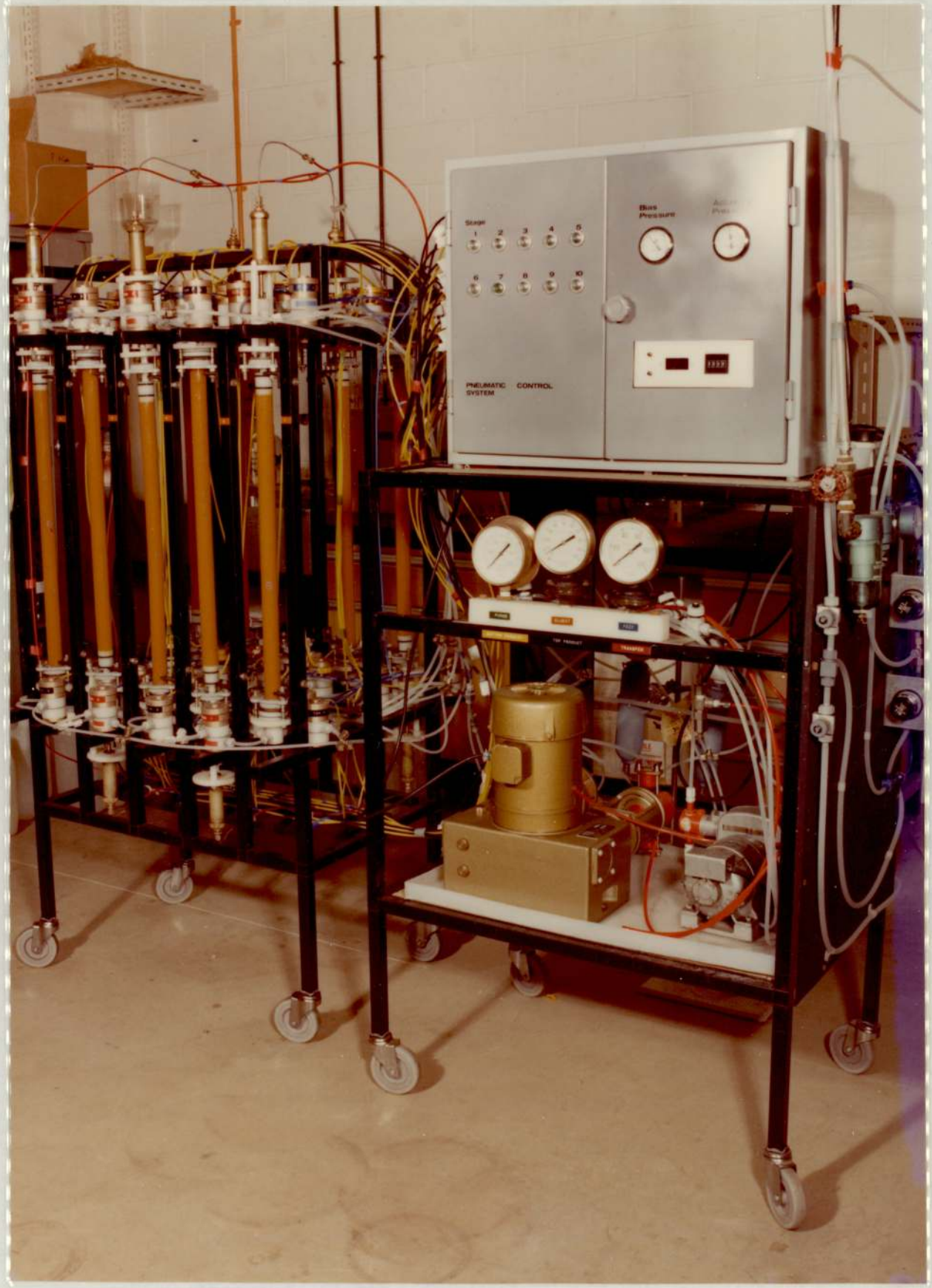
Stage
1
2
3
4
5
6
7
8
9
10
Bias
Pressure
PNEUMATIC CONTROL
SYSTEM

Fig. 6.4 Overall View of SCCR4 Unit With Heating Facilities

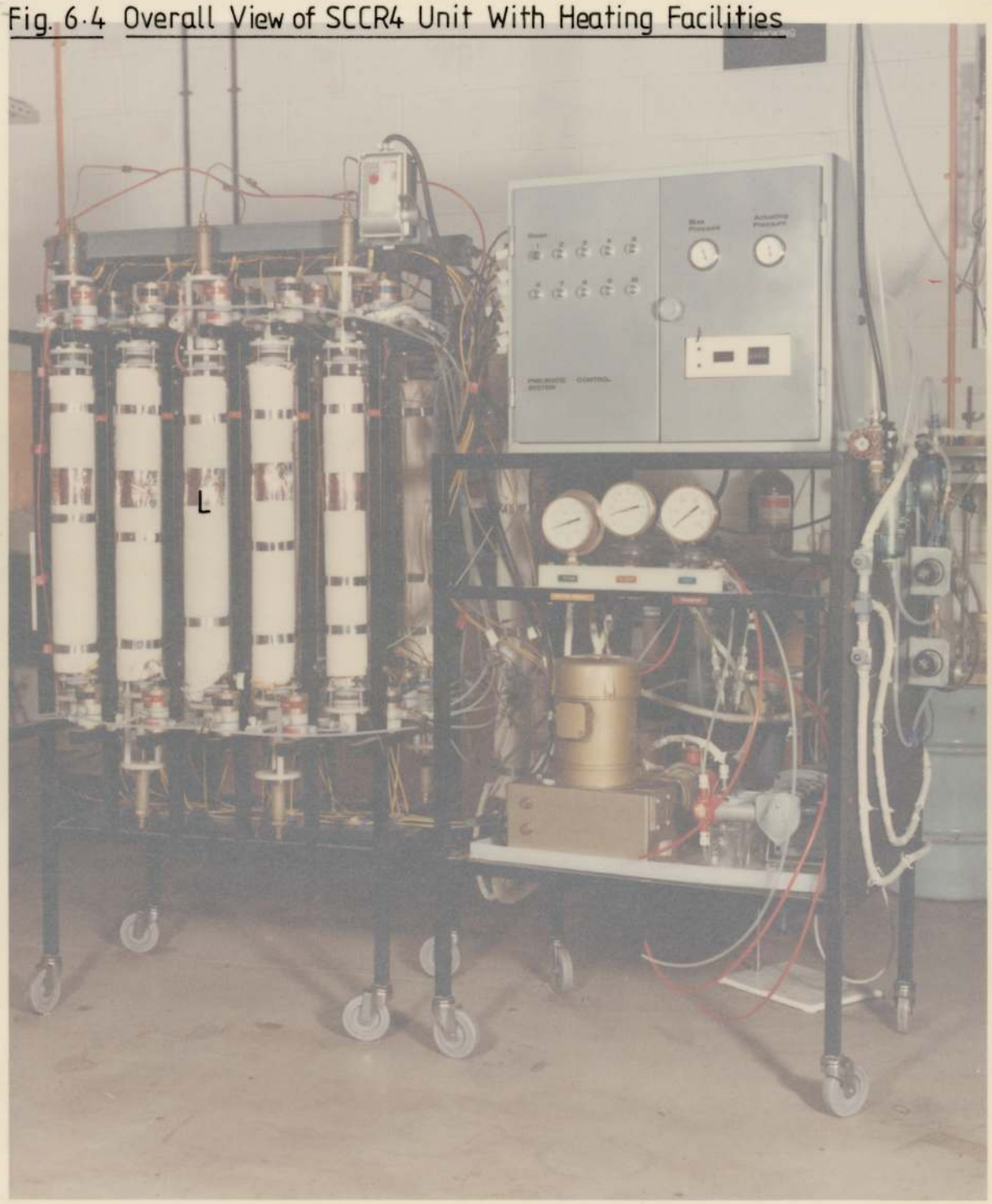

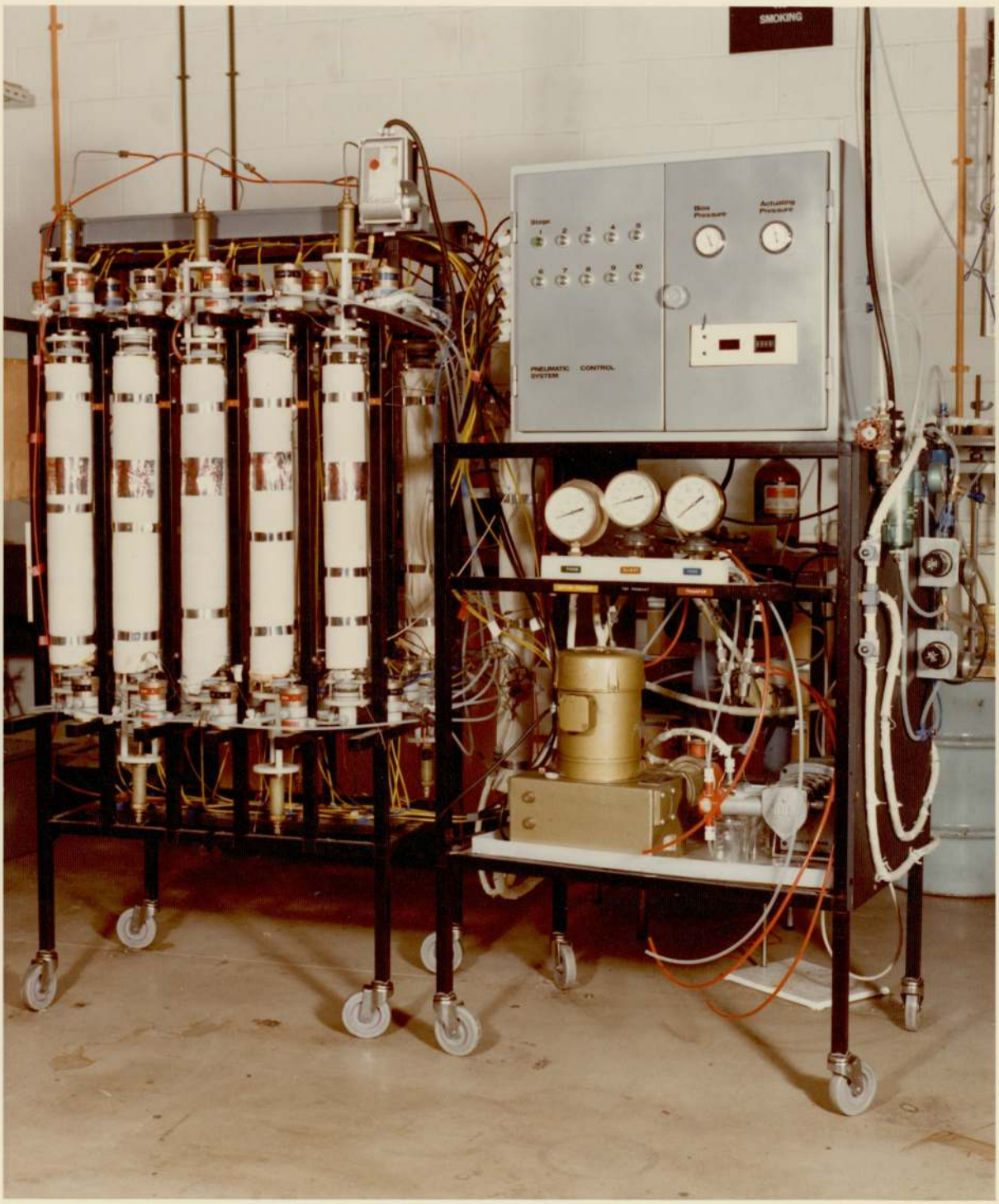
SMOKING
Step
Bias Pressure
Actuating Pressure
PNEUMATIC CONTROL SYSTEM

The actuation and advancement of valve functions are governed by a central cam unit (Section 6.2.2.1). The rectangular supporting framework was constructed of 'Handy' square tubes and joints supplied by 'Handy Tube' of Middlesex. Detailed design features of the SCCR4 unit are given in the following sections.

6.2. The Separation Unit

6.2.1. The Valves

Previous work on the SCCR machine (20,21) has led to the conclusion that a double pneumatically actuated poppet valve would offer not only a higher degree of reliability but also a wider range of operating conditions. After the fabrication, testing and modification of two prototypes, a valve was finally designed to have satisfied the selection criteria.

In the course of developing the valves for the SCCR4 machine, advice on detailed mechanical design was sought from Dr. B. Jones of the Mechanical Engineering Department of Birmingham University. All the machining and fabrication work of the valves was conducted by Aston Technical Services Ltd., a Company associated with the University of Aston. Figures (6.5 and 6.6) photographically illustrate the final design of both an assembled and a dismantled valve.

In the following sections, the term "bias pressure" refers to the air pressure applied constantly during operations, to maintain the valve to be either open or closed. The "actuating pressure" refers to that pressure required to close or open the appropriate valves during a particular sequence. The net difference of the two is referred as the "differential pressure".

Fig. 6·5 View of An Assembled Valve

A	Diaphragm Chamber - Upper
B	Diaphragm Chamber - Lower
C	Neoprene Diaphragm
D	Body
E	Inlet Chamber
F	Viton Gasket
G	Poppet & Stem
H	Adjustment Nut
I	Viton O Ring
J	Thrust Washer
K	Sealing Ring Washer
L	Neoprene O Ring
M	4 BA Hex. Nut
N	Diaphragm Backing Plate
O	2 BA Cheese Head Screw
P	4 BA Cap Screw
Q	Valve Mounting Plate

Fig. 6.6 Parts of The Pneumatic Poppet Valve

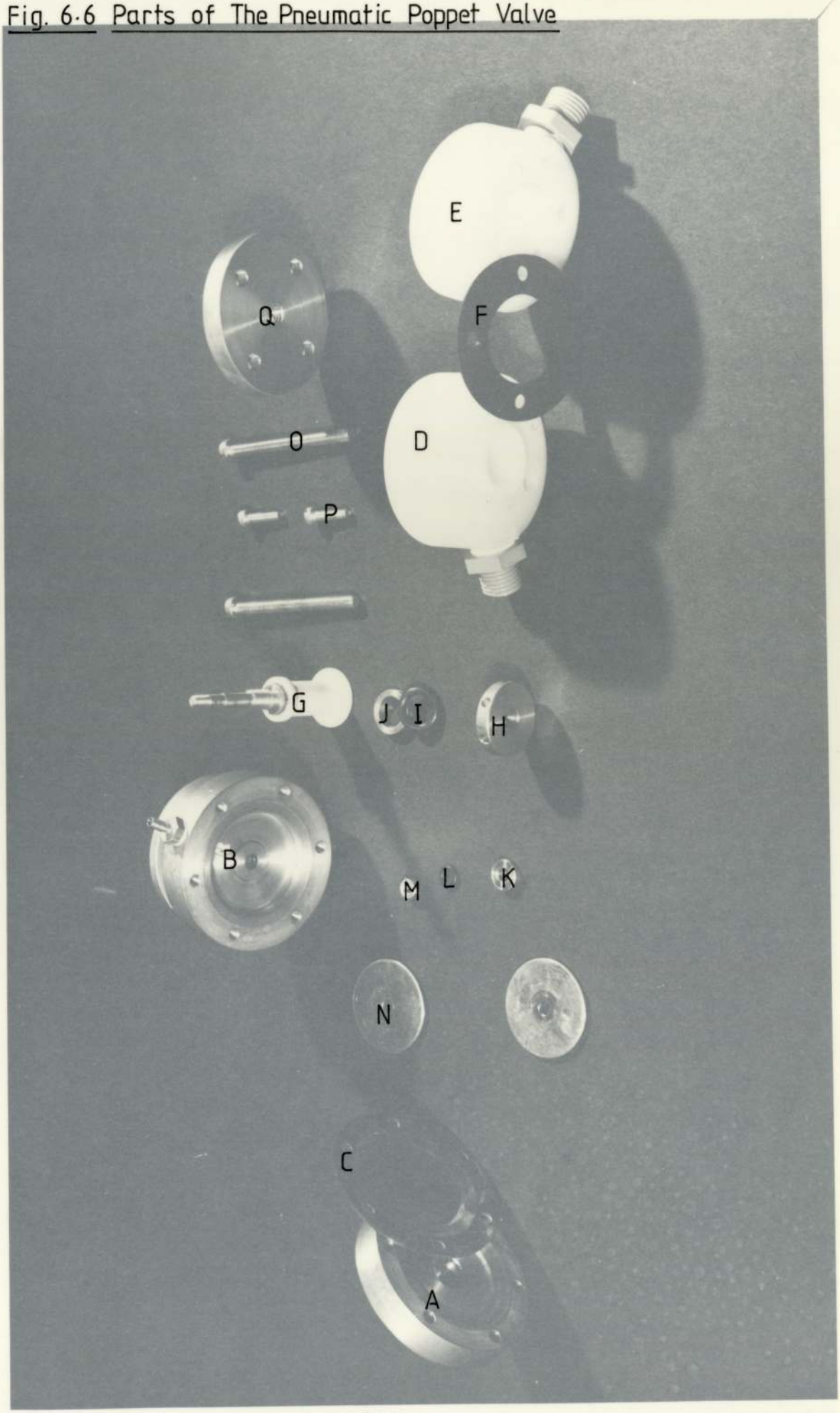

Item No.	Part Name	Material
1	Diaphragm Chamber-Upper	Brass
2	Diaphragm	Neoprene
3	Body Gasket	Viton
4	Diaphragm Chamber-Lower	Brass
5	Diaphragm Backing Plate	Brass
6	Sealing Ring Washer	Brass
7	Body	Polypropylene
8	Inlet Chamber	Polypropylene
9	Mounting Plate	Brass
10	Poppet Valve	P.T.F.E. Glass Filled
11	Adjustment Nut	Brass
12	Valve Stem	Brass
13	Thrust Washer	Brass
14	O Ring BS 007	Neoprene
15	O Ring BS 008	Neoprene
16	O Ring BS 110	Viton
17	4 BA Cap Screw	Brass
18	2 BA Cheese Head Screw	Brass
19	4 BA Hex. Nut	Brass

Fig. 6.7 Technical Drawing of The Final Design of The Pneumatic Poppet Valve Used In SCCR4 Unit

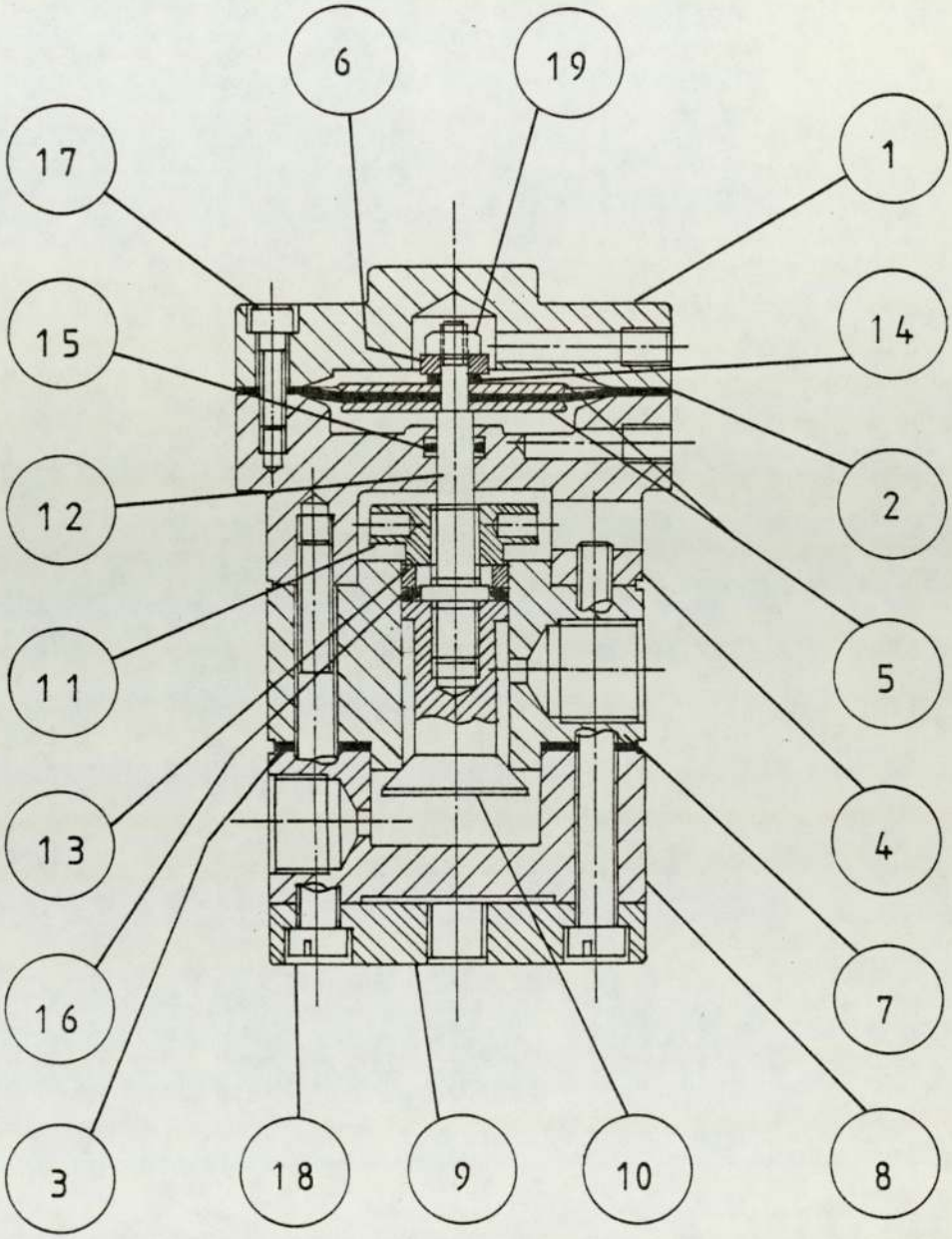

The pneumatically operated poppet valve (Figure 6.7), incorporated in the SCCR4 unit, consists primarily of a pneumatic and a process fluid section. The pneumatic section is fabricated from brass and consists of lower and upper chambers. The two chambers are held together by six 4BA screws with a neoprene diaphragm sandwiched in between. Air can be separately introduced into or exhausted from individual chambers. The process fluid section also consists of two sections and is made from polypropylene, a plastic which is resistant to most corrosive solvents. Process fluid enters the valve from the lower port, and, after flowing past the poppet, leaves the valve from the upper port. Closure of the valve is achieved by movement of the poppet upwards against the edge of the central core of the upper plastic section using an air pressure below the diaphragm. A viton gasket is placed between the two plastic sections of the valve to prevent the leakage of process fluid to the surroundings. The poppet is linked to the diaphragm of the pneumatic chamber by a specially designed stem, one end of which is permanently attached to the poppet and the other is guided through the central hole of the diaphragm where it is locked in position by a nut and washer. Three 'O' rings are positioned along the stem for sealing purposes. The first 'O' ring (Figure 6.7 (16)) is situated on the top

of the poppet and, under the thrust of a metal ring (Figure 6.7 (13)) and a screw type expander (Figure 6.7 (11)), prevents process fluid leaking into the pneumatic chambers. The second 'O' ring (Figure 6.7 (15)) is located in a recess in the body of the lower pneumatic chamber and serves as a seal against air leakage through the stem. Finally, in order to prevent air escaping from one pneumatic chamber to the other through the centre hole, a third 'O' ring is placed (Figure 6.7 (14)), under the stem's lock nut and washer, and on top of the diaphragm. The entire valve is held together by four long screws. The opening of the valve rests on the introduction of air into the upper pneumatic chamber closing the valve. The poppet (Figure 6.7 (10)) is fabricated from glass loaded Telfon.

With a bias and actuating pressure of 120 kNm^{-2} and 240 kNm^{-2} respectively, the valve can seal and open against a process differential pressure of up to 700 kNm^{-2} in both forward and backward direction. Under such conditions, the valve has been continuously tested for five hundred hours. No leakage was observed and the neoprene diaphragm showed no sign of rupture. As such, this design was considered to have satisfied the selection criterion and a total of sixty valves were fabricated.

6.2.2. Pneumatic Supply and Control System

The main supply of air is from the Department's compressor, but a switch valve (Figure 6.8b) is installed so as to enable the use of standby "bottled air" in case the former pressure drops below 300 kNm^{-2}. Air emerging from the switch valve is divided into two streams, namely the actuating and the bias streams. Their pressures are regulated to 240 and 120 kNm^{-2} respectively. The bias air supply is linked directly to the valves and pressure is applied continuously throughout the entire operation. Whilst the actuating air supply is introduced through a central controlling system and is applied only to the appropriate valves during a particular sequence. In order to avoid the rupture of the neoprene diaphragms caused by excessive differential pressure, a side stream of the bias air supply is employed as a pilot to ensure that the actuating pressure is shut off if the former supply fails (Figure 6.9).

The heart of the central control system (Figure 6.8a) is a cam unit, with ten programmable discs operating on ten on/off valves. Figure (6·10) illustrates how the on/off valves are controlled by the discs. The gaps on consecutive discs are set at 36^{o} out of phase and each valve represents one sequence of the SCCR4 process. The

A Cam Unit

B On/Off Valve

C Motor

D Pilot Valve

E Pneumatic/Electric Signal Convertor

F Double Return Valve

G Switch Valve Controlling Air Supply From Either Main Compressor Or Bottle

H Regulator For Air Supply From Main Compressor

I Regulator For Actuating Air

J Regulator For Bias Air

Fig. 6·8 Pneumatic Control & Auxillary Equipments

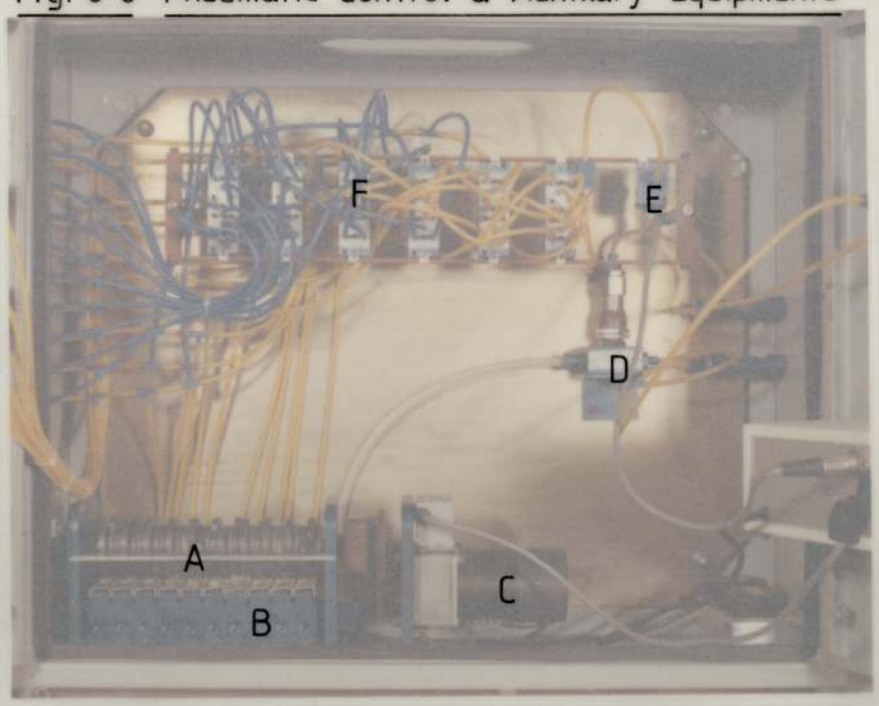

(a) Controller

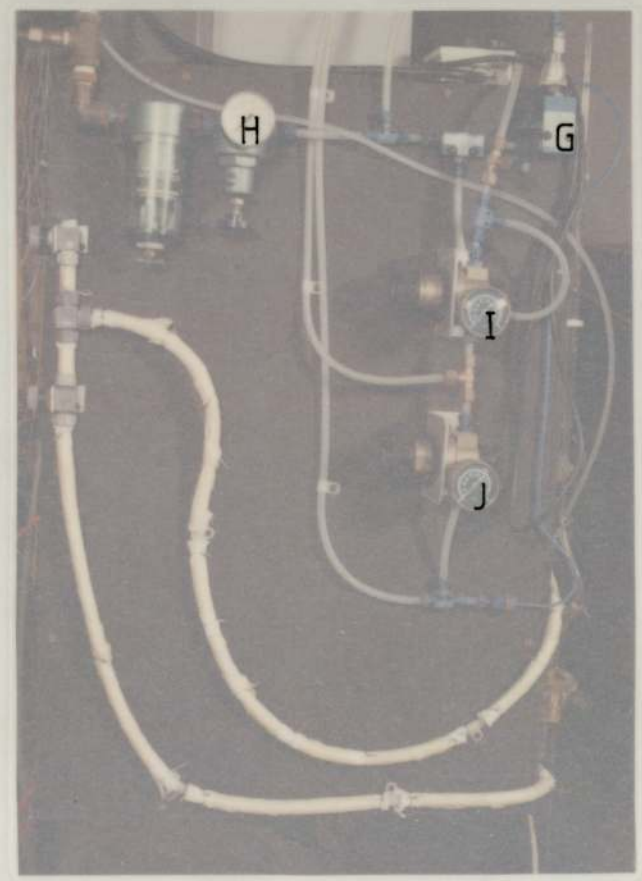

(b) Air Supply

(c) Pneumatic Cylinder & Plunger Unit

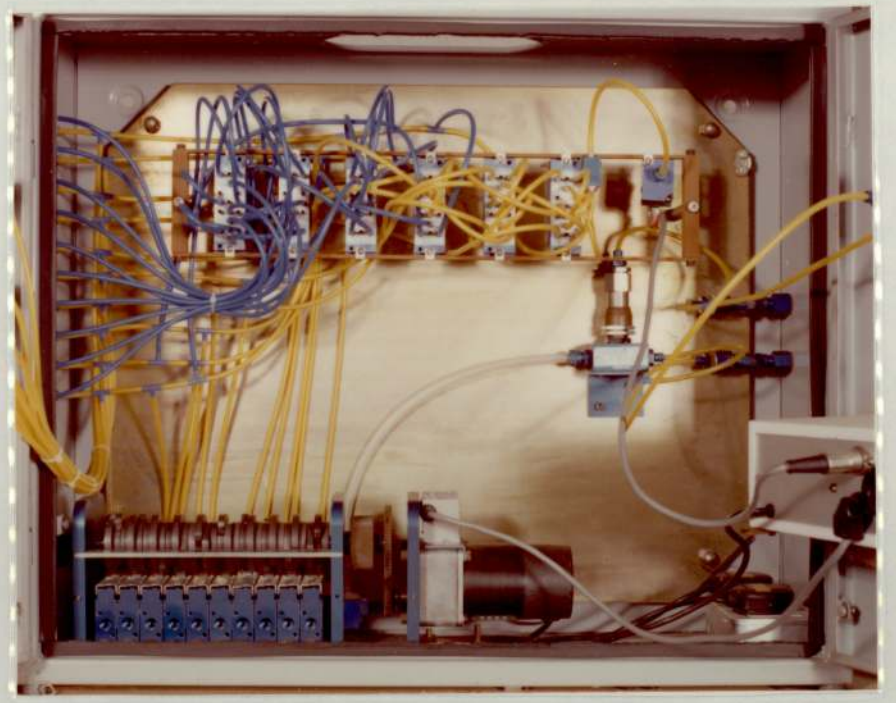

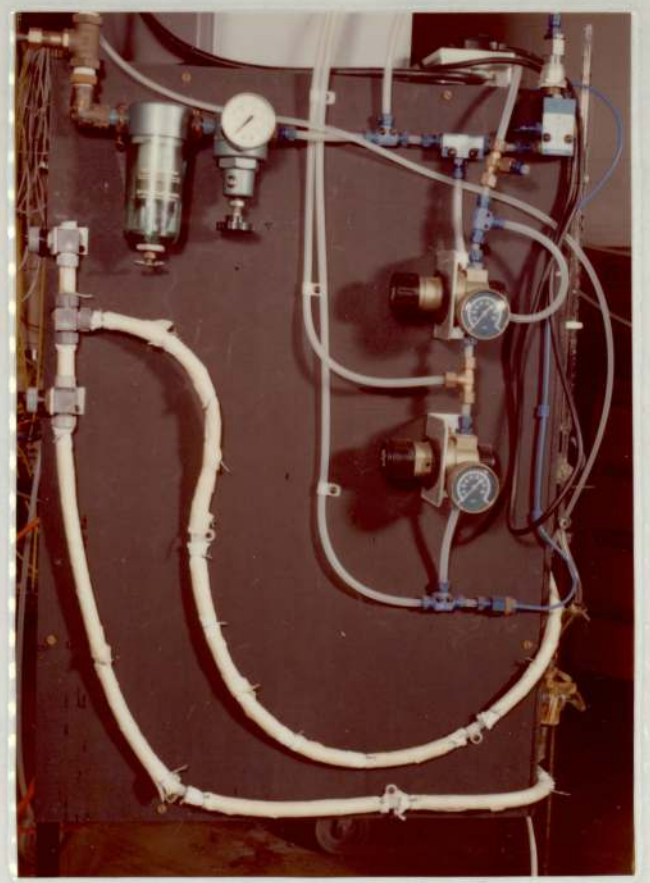

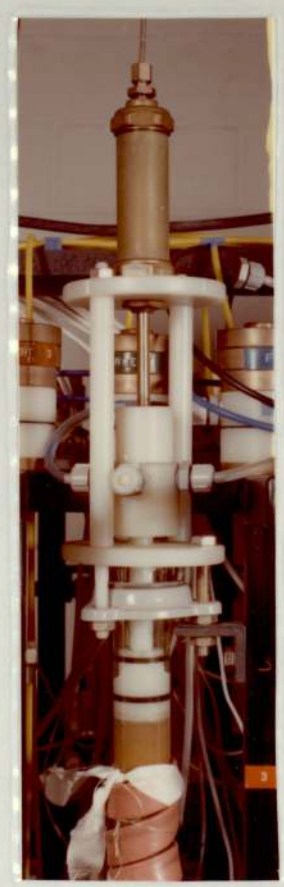

Fig. 6.9 Flow Scheme Of Pneumatic Control System

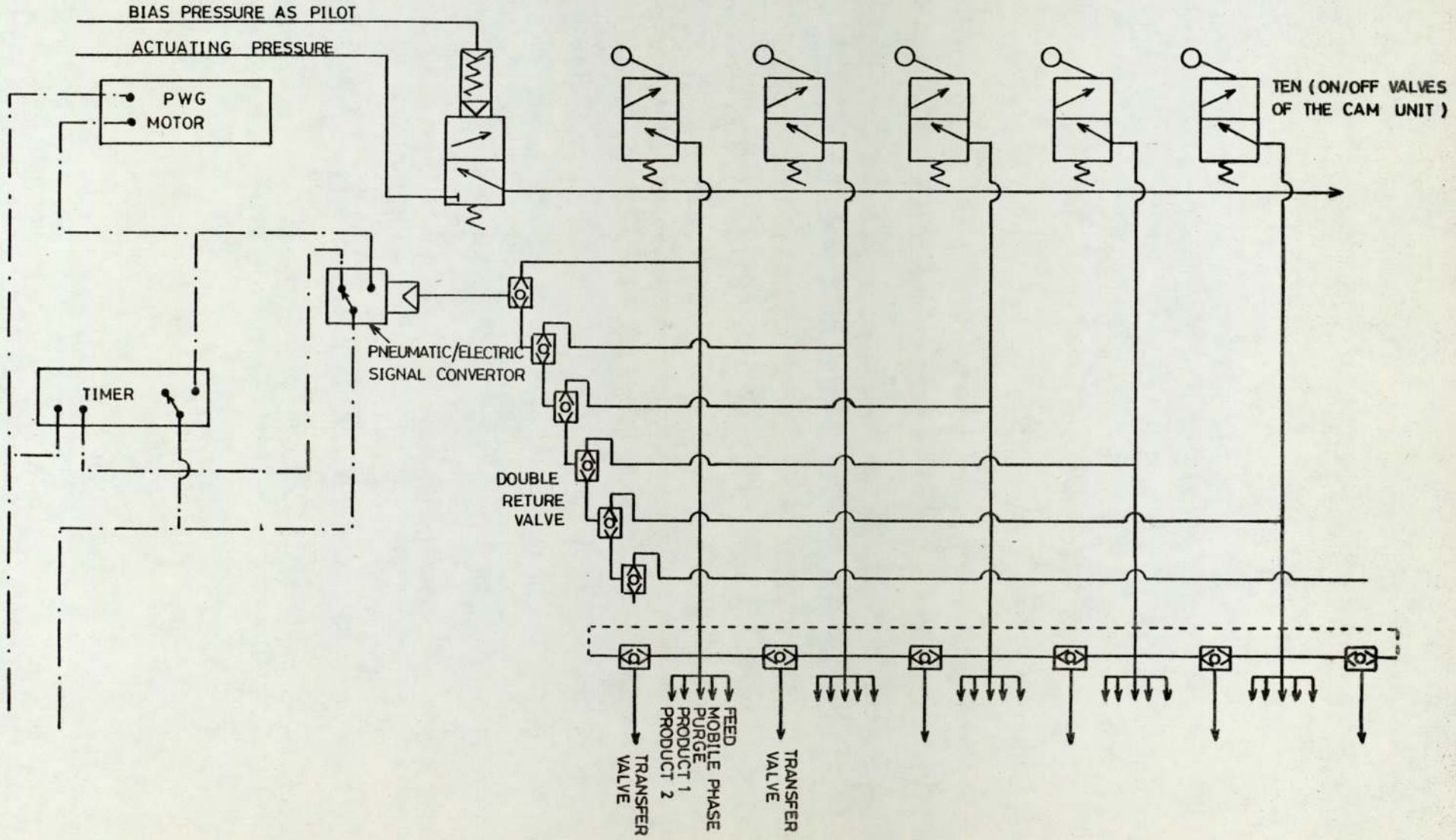

Fig. 6.10 Diagrams Illustrating The Functioning Of The CAM Unit

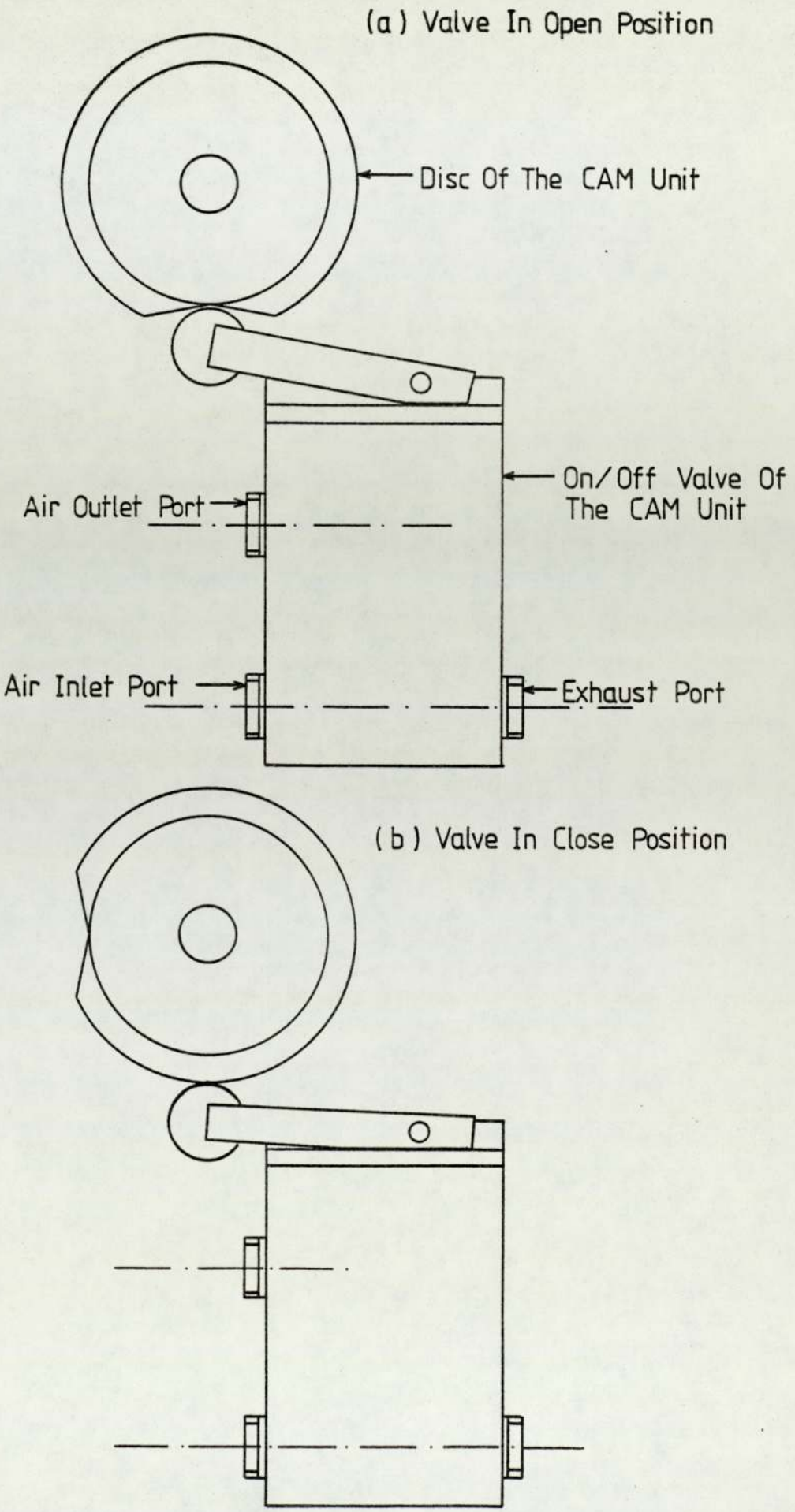

cam unit is driven by a single speed motor.

A schematic diagram of the complete control system is shown in Figure 6.9. Besides the cam unit, the other main items include nineteen double return valves, a digital timer and a pneumatic/electric signal convertor. A double return valve has two inlet and one outlet port. Air can be introduced from either of the inlet ports and is exhausted through the outlet port. Simultaneously, the opposite inlet port is automatically sealed off. The first group of these valves (ten) serves to provide instructions to the timer. Whilst the second groups of the double return valves (nine) enables the energising of consecutive transfer valves. The digital timer was assembled in the Departments' Electronics Section and governed the on/off of the cam unit motor according to a pre-set time limit.

In operation, when one of the cam units on/off valves reaches its open position, the actuating air is allowed through the valve and subsequently split, (Figure 6.9), with the aid of two double return valves into seven streams to actuate the appropriate valves. The actuating pressure is also used, through a series of double return valves, to energise the pneumatic/electric signal convertor. Under pressure, this convertor will not only re-zero and re-start the timer, but also

disconnect the electricity supply to the motor. At the end of the pre-set time limit, the timer will automatically re-connect the current supply to the motor which then rotates the cam shaft through a further 36^{o} until a new opening position for a second valve is reached and the sequence repeats itself.

Ten Schrader midget pneumatic cylinders were mounted at the beginning of each column, on top of the plunger device to act as the counter force against the swelling or contracting of the resin bed caused by any variation of ionic strength in the solution around the resin particles. The air pressure applied to the cylinders during operation was 250 kNm^{-2}. The complete unit is shown in Figure 6.8c.

6.2.3. Columns and Fittings

The dimension and number of columns decided for the SCCR4 machine was a result of compromising cost against continuity. The 'ideal' continuity of the sequential process can only be achieved by incorporating an infinite number of small columns. As such, a maximum number of columns is desirable if the discontinuity imposed by the discrete operating nature of the SCCR4 machine is to be reduced. However, each additional column introduced into the system requires

six further valves plus their respective pipe networks and fittings.

Within the budget allowed for the research, ten (QVF 25.4 mm I.D. x 700 mm) glass columns were used giving a total bed length of approximately 6.5 m. The glass columns were supplied by Jobling Limited, Stoke-on-Trent, and were quoted to be capable of withstanding a process pressure of 700 kNm^{-2}.

Transparent PVC tubings, 6.4 mm O.D. and 4.2 mm I.D. were employed in the fluid ring-main distribution network. A detailed layout of all pipelines of the SCCR4 process unit is shown in Figure 6.11. Connecting lengths of PVC tube together, was achieved by using polypropylene T-pieces, supplied by Delta Platics Ltd. All joints were lightened by No.10 'Unex' stainless steel clips. Such connections have been tested to withstand a process fluid pressure of up to 700 kNm^{-2}.

Connections of the PVC tubing to the SCCR4 columns was achieved using specially designed column end fittings. An assembled inlet fitting is illustrated in Figure 6.12, and an outlet fitting is shown in Figure 6.13. Both types of fitting were machined from polypropylene rods supplied by G.H. Bloore Ltd. of Birmingham.

The inlet fitting was also designed to accommodate the swelling and contracting effect of the ion exchange

Fig. 6.11 Flow Lines Arrangement Of SCCR 4 Machine

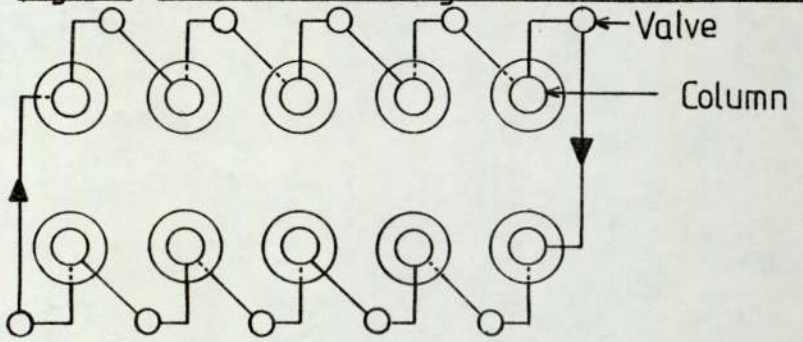

Transfer Lines

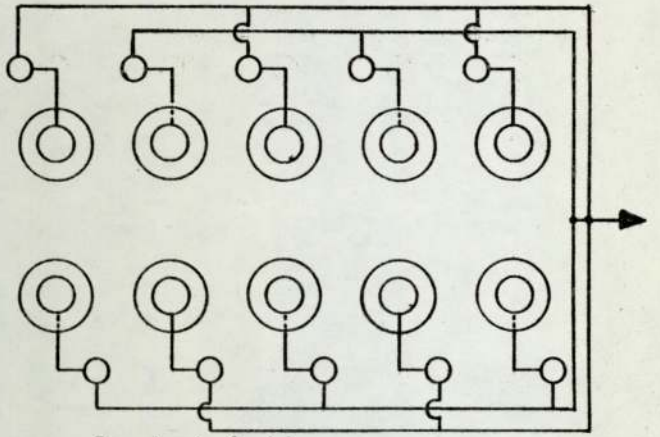

Product 1 Lines

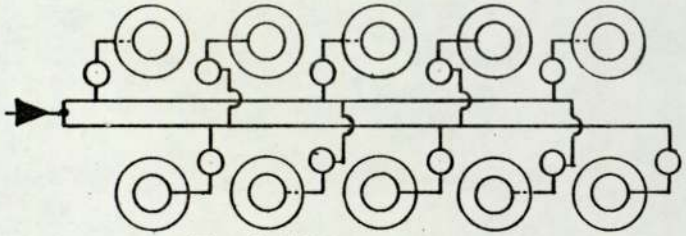

Feed Lines

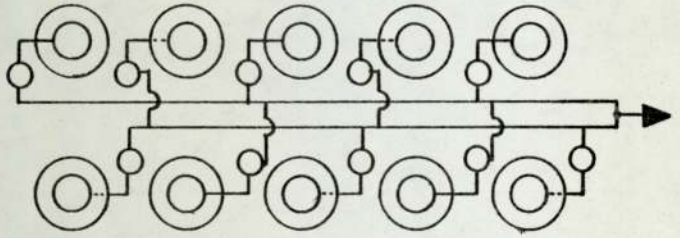

Product 2 Lines

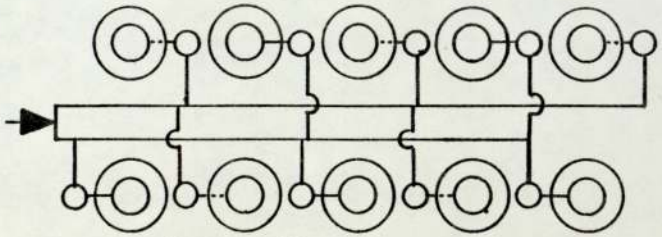

Purge Lines

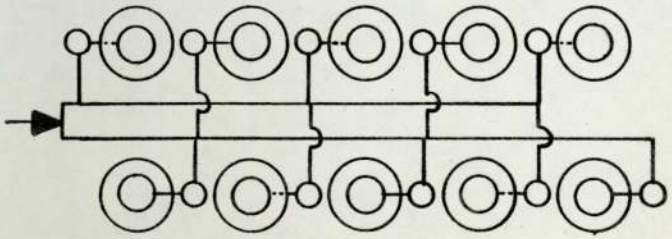

Mobile Phase Lines

Fig. 6.12 Assembled Inlet Column Fitting

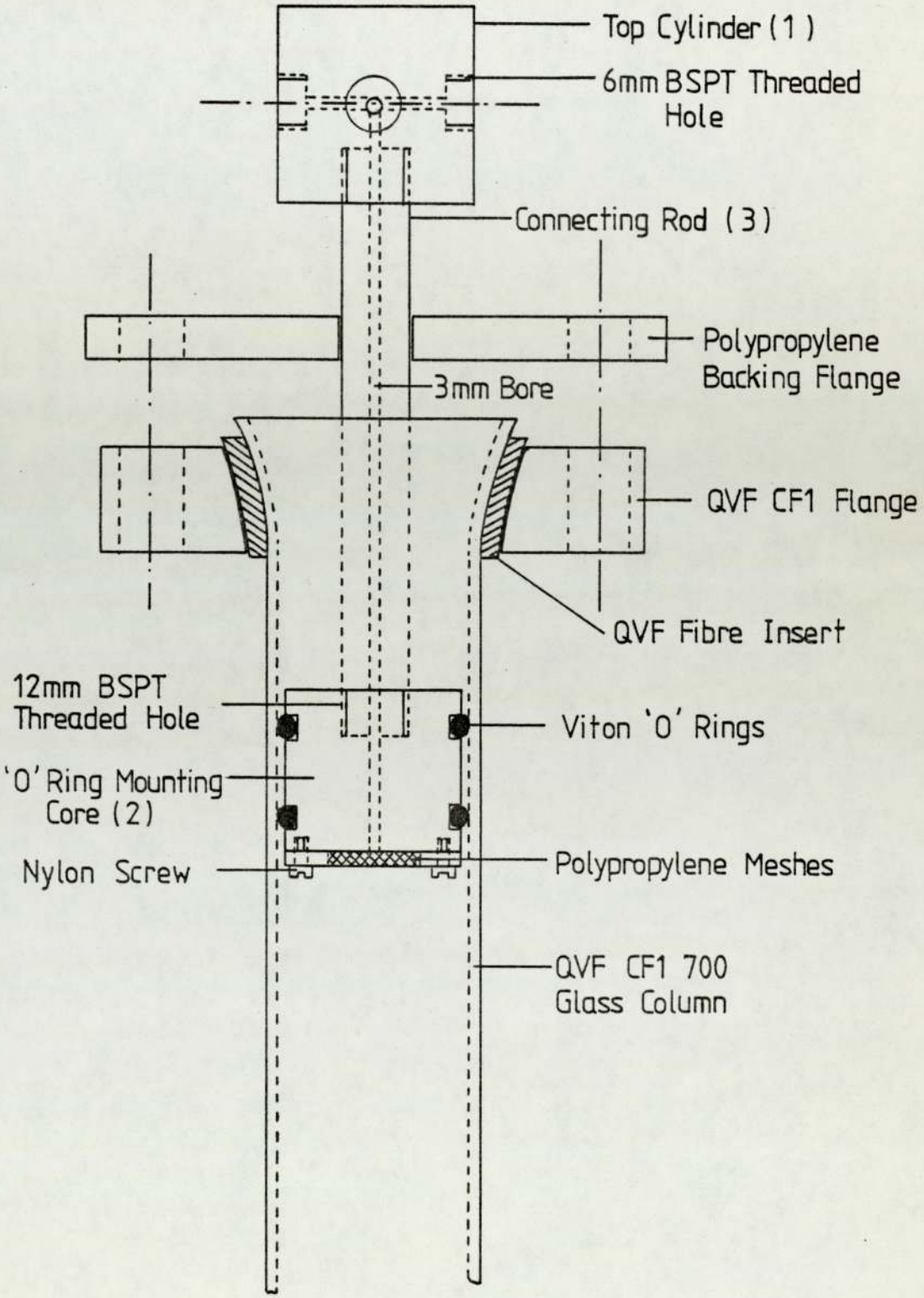

resin bed. It can be identified into three main sections namely, the top cylinder (Figure 6.12 (1)), the connecting rod, (Figure 6.12 (3)), and the 'O' ring mounting core (Figure 6.12 (2)). The process fluid was introduced into the column through one of the four 6 mm BSPT threaded holes, drilled at right angles to one another, on the cylinder. The connecting rod, with a 3 mm bore, transferred the fluid into the 'O' ring mounting core in which two Viton 'O' rings, supplied by Dowty Ltd, were mounted into the two grooves (Figure 6.12) at a distance of 20 mm apart. When the plunger device was inserted into the column, the 'O' rings, under compression, formed an effective seal against both the inner wall of the column and the grooves. The securing of the inlet fitting onto the column was achieved by a polypropylene backing flange bolted with three stainless steel screws, to a QVF CF1 plastic column flange fitted around the neck of the column. The former flange, with a central hole through which the connecting rod of the plunger device could travel freely, also served to centralise the entire inlet fitting. Finally, a backing plate was bolted with four nylon (4BA) screws, onto the 'O' ring mounting core. Sandwiched between the two was a polypropylene mesh which served firstly to retain the packing, and secondly to produce a uniform distribution of solute across the

Fig. 6.13 Assembled Column Outlet Fitting

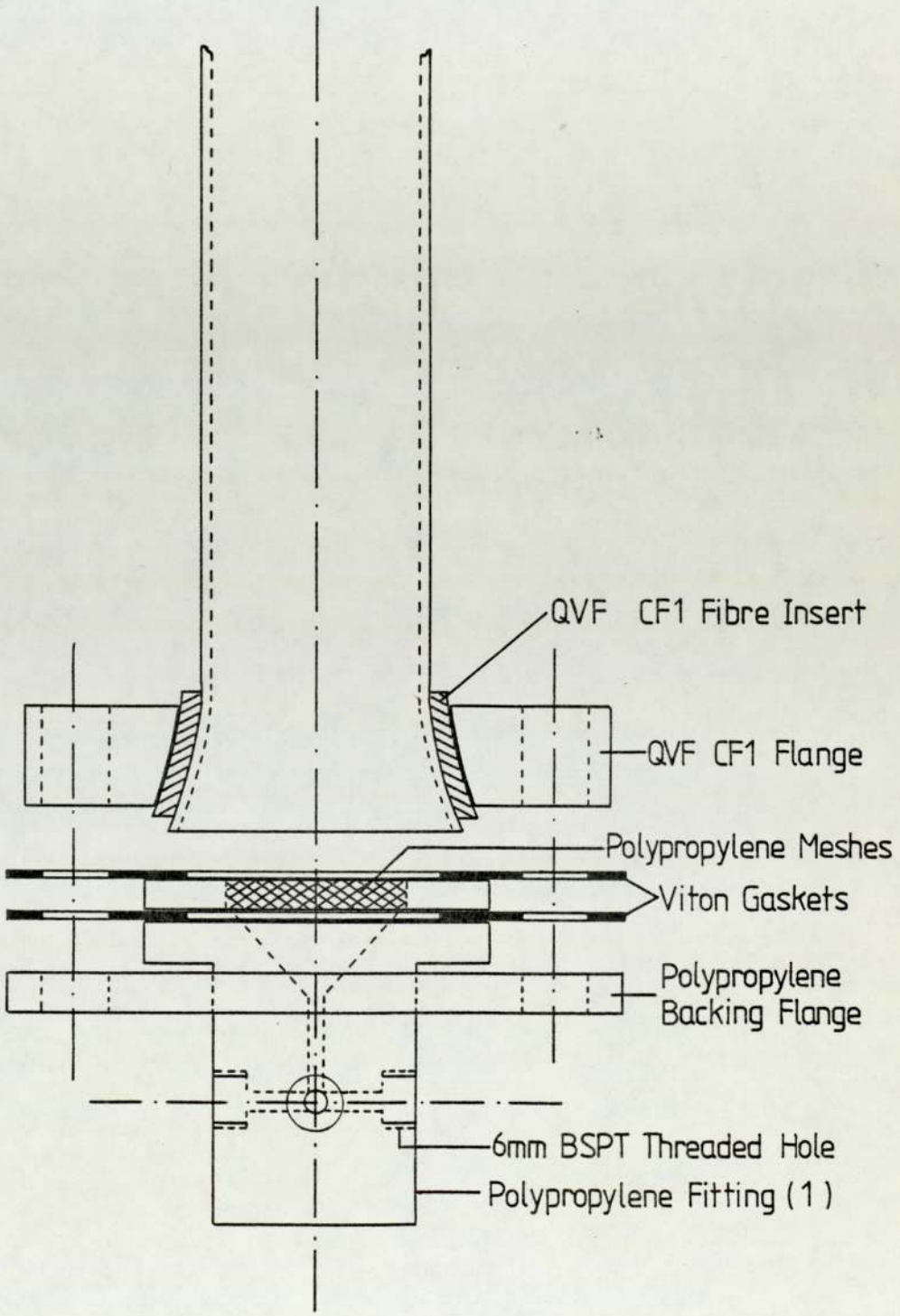

column. The polypropylene mesh, supplied by Henry Simon Limited, Stockport, was arranged in two layers, one of 150μm to retain the packing in the column, and one of 1500μm for support.

To counteract the swelling and contracting of the resin bed, a pneumatic midget (25.4 mm diameter) cylinder (Section 6.2.2.2. and Figure 6.8 (c)) was mounted onto the top receptacle of the plunger device. The 'O' rings were lubricated with silicone grease. During tests with water, the entire unit had been proved to be capable of moving in both upward and downward directions, subjected to the differential pressure of the midget pneumatic cylinder and in the column, and no leakage of water through the 'O' ring was recorded.

The shape of the outlet fitting resembled a 'top hat' (Figure 6.13 (1)). The wider top was aimed to provide the necessary area upon which the thrust of a polypropylene backing flange could be applied to secure the fitting onto the column. Three threaded holes, which accept 6.35 mm B.S.P. taper polystyrene stud fittings, were cut in the body of the outlet fitting to allow the process fluids to leave the column. Between the top of the outlet fitting and the bottom of the column was a two-layer polypropylene mesh (described previously) sandwiched between a viton gasket on each side to provide an effective seal. These

meshes were fixed between two 'O' shaped pieces of polypropylene and were plastic welded together. Standard QVF CF1 plastic flange and fibre inserts, fitted around the neck of the column, were used to connect bolts linking the polypropylene backing flange. When the bolts were tightened, the whole assembly was pulled together, compressing the viton gaskets, forming a seal.

The column assemblies were supported on a metal frame by mild steel angle brackets. These brackets have 13 mm long slots in the vertical face to allow the columns to 'hang' fairly loosely from the frame, as a rigid connection could result in excessive stress being applied to one of the glass columns which could result in its cracking. The frame was constructed from 'Handy' mild steel square tubes and joints, the entire structure resting on four castors. The total weight of the SCCR4 machine was estimated as approximately 100 kg. The maximum loading on each castor, as quoted by the manufacturer was 75 kg.

6.2.4. Pumps

The success of the SCCR4 scheme rested heavily on the accurate and reliable operation of the pumps. A general survey revealed that pumps with a high degree

of accuracy, ± 0.2% or below, are marketed at a high price. Within the budget limit for the research, the best possible pumps available are those with an accuracy in the region of ± 1%. Consequently, two positive displacement metering pumps, supplied by Metering Pumps Ltd., London, were chosen which had an accuracy specification of approximately ± 1%, between 10% and 100% of the maximum stroke of the pump. Several pump heads can be driven simultaneously by the motor of each pump.

The mobile phase and purge liquids were pumped by an MPL KV Twin Metripump fitted with a 1400 r.p.m. motor operating at 24 strokes per minute. The two plastic metering heads are a PG 13G, plunger type head, and a D45P, diaphragm type head, for the mobile phase and purge respectively. The maximum flowrate delivered by the plunger head was 100 cm^3min^{-1} which was below the requirement of the purge. Hence a diaphragm head, with a maximum delivery of 500 cm^3min^{-1} was used for the purge. This type of head was less accurate than the conventional plunger type of head, but, as thepurge does not control the flow in the separating section of the SCCR4 process, a very accurate flowrate was not essential.

The K-twin pump was only used for the mobile phase when flowrates greater than 10 cm^3min^{-1} (above 10% of the maximum stroke) were required, as the accuracy was found to decrease below this level.

The second pump for use with the SCCR4 machine was an MPL Series 2 positive displacement metering pump fitted with one plastic PC4G and one stainless steel pump head. The former head was for delivering the feed solution and was driven by the pump's motor via a reduction (five to one ratio) unit to give a maximum flowrate of 10 cm^3min^{-1}. The stainless steel head was used for pumping the mobile phase at flow-rates lower than 10 cm^3min^{-1}, as it has an operating range of approximately 1.25 - 12.5 cm^3min^{-1}. The materials, for all pump heads, in contact with the process fluids were resistant to dilute acids and this may be used for future work with the SCCR4 unit, if required.

6.3. Heating Facilities

6.3.1. Introduction

In the initial design of the SCCR4 machine, no heating facilities were included. The addition of various heating and insulation devices were undertaken in two stages. The first stage, based on the results of the preliminary runs that a hot purge will lead to a more complete purging of columns within a shorter time, included:

(i) the insulation of all the columns and the inlet liquid lines.

(ii) the use of an isomantle for supplying purge and mobile phase at an elevated temperature.

(iii) the incorporation of seven thermocouples to indicate the temperatures of the incoming purge and mobile phase liquids and five other points along the transfer lines (Figure 6.16).

The second stage, designed near the end of the research programme, aimed at investigating the temperature effect on the separation of glucose and fructose and included:

(i) the mounting of plastic heating tapes on individual columns.

(ii) the incorporation of thermostatic control to govern the on and off of individual heating tapes.

(iii) the installation of a preheater and its thermostatic control for the mobile phase inlet.

(iv) the use of thermocouples to record the temperature of each column.

The author was aware of the fact that within a column, temperature profiles existed in both the longitudinal and radial direction. To record the former, various thermocouples have to be inserted, at separate levels, into the centre, or at equal distances from the centre of a column. Whereas the study of the latter profile required the placing of a few thermocouples on the same level but at various distances from the column's centre. As the incorporation of the second stage of heating facilities was conducted near the end of the research programme, any drilling for the insertion of thermocouples into the column would require the emptying and refilling of the column packings. A re-packed column system offers a new separation efficiency and such results obtained at elevated temperatures would fail to demonstrate, when compared with the results achieved previously, the temperature effect on the separation of glucose and fructose.

Consequently, within the time and budget remaining for the research, a single thermocouple was adhered onto the surface, at the mid-point of a column, to record the temperature of the column wall. This recorded temperature

was found to be 1 - 2°C higher than that of the mobile phase exiting the column.

A detailed description of individual heating equipment is given in the following sections.

6.3.2. Isomantle for Heating Up the Purge and Mobile Phase Liquid

Figure 6.14 (a) illustrates the isomantle resting on its support which was installed with four (4 K-Watts each) heating elements. The capacity of the isomantle was approximately 7.5×10^{-2} m^3. Distilled water flows from the reservoirs (Section 6.4.1) under gravity into the isomantle which was installed with two control devices to govern its water temperature and level. The level control device includes a pressure sensing tube acting on a pneumatic diaphragm to provide an electrical contact for the solenoid operated on/off valve located at the outlet of the water reservoirs.

In the start-up period, all four heating elements of the isomantle were required to boost the water to the desired temperature. During operation, only two of such heating elements were connected to a copper thermostat switch to maintain the required temperature. In order to avoid the introduction of copper ions into the distilled water, the thermostat was inserted into

A Fraction Collector

B Isomantle

C Level Control Box

D Thermostat Sensor

E Thermoster Control Box

F Multipoint Selector Switch

G Digital Millivolt Display Unit

H Thermostat Control For Mobil Phase Preheater

I Voltmeter For Preheater

Fig. 6·14 Heating Facilities

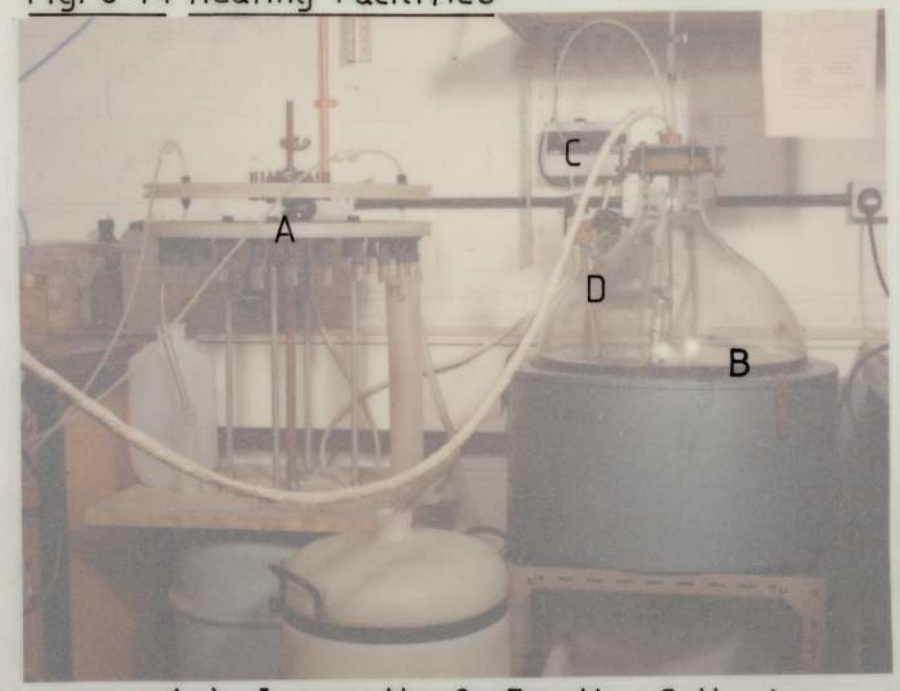

(a) Isomantle & Fraction Collector

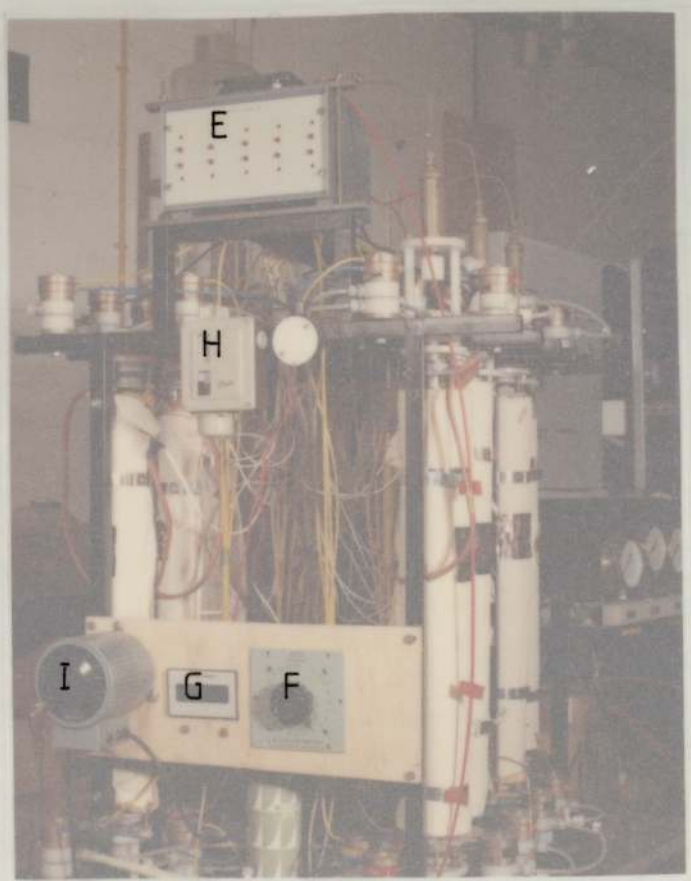

(b) Proportional Temperature Controller System

(c) Heating Tape

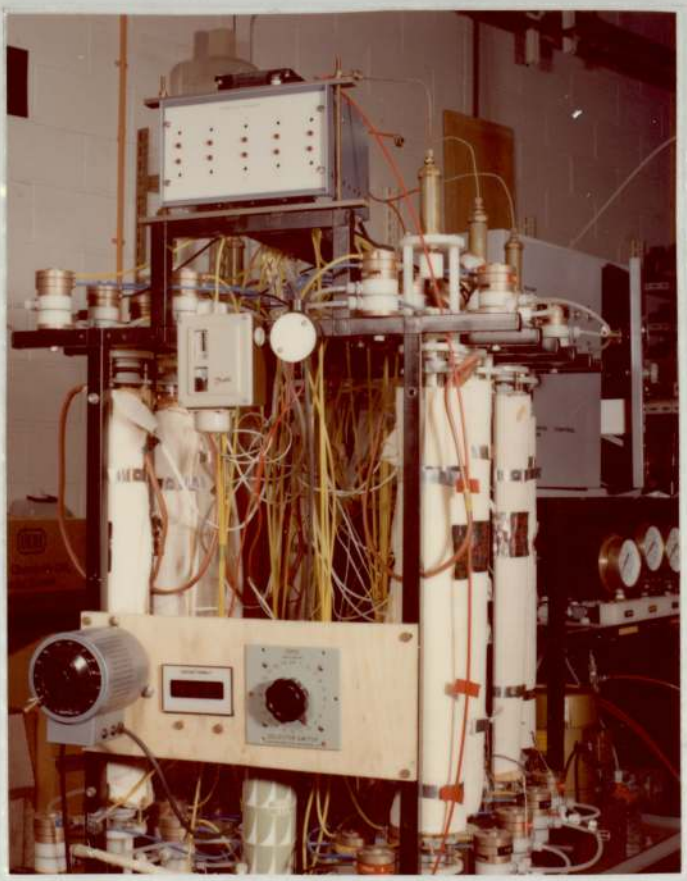

a glass tube filled with silica oil to provide better thermal contact.

At the bottom of the isomantle a QVF stop cock was mounted and water was drained periodically to ensure a regular supply of fresh water.

6.3.3. Heating Tape for Columns

The heating tapes mounted on the column (Figure 6.14 (c)) were supplied by Hotfoil Ltd, Wolverhampton and were of dimensions 20 mm in width, 3 mm in thickness and 1.8 m in length. The tape was insulted with glass cloth and extruded silicone rubber and was designed to function up to a temperature of 200°C. The loading of each heating tape was 80 watts.

6.3.4. Preheater for the Mobile Phase Liquid

Due to a slow liquid flowrate, the temperature of the mobile phase liquid dropped from that acquired in the isomantle to about ambient just before entering the SCCR4 machine. Hence a preheater was necessary to raise the temperature of the mobile phase liquid to that of the mean column operating temperature. This necessitated the use of 6 mm bore stainless steel tubing wrapped round with a glass heating tape and enclosed in

40 mm fibreglass jacket. The electric supply to the heating tape was governed by a variable voltmeter.

6.3.5. The Controlling Devices and Insulation

The column heating tapes were independently controlled by proportional temperature controllers which were designed and assembled in the Department's Electronics Workshop. Figure (6.15) illustrates the control circuit in which a thermoster bead, mounted on the wall of the column, sensed the latter temperature and relayed it back to a proprietary Zero Voltage Switch. The function of the switch was to convert the incoming signal into electric energy which was subseqently supplied to a Triac in bursts. In the Triac, the received energy was compared with the pre-set value and thus determined the on or off of the heating tapes. All ten of the controllers were housed in a metal box (Figure 6.14 (b)) with each tape being individually indicated by a neon light. Adjustment of the control valve of the Triac was made via a screw type device accessed from the front panel of the control box. The proportional controller was capable of maintaining the column temperature to within $\pm$ 1^{o}C of that of the set figure.

Fig. 6.15 Schematic Diagram Of The Proportional Temperature Controller

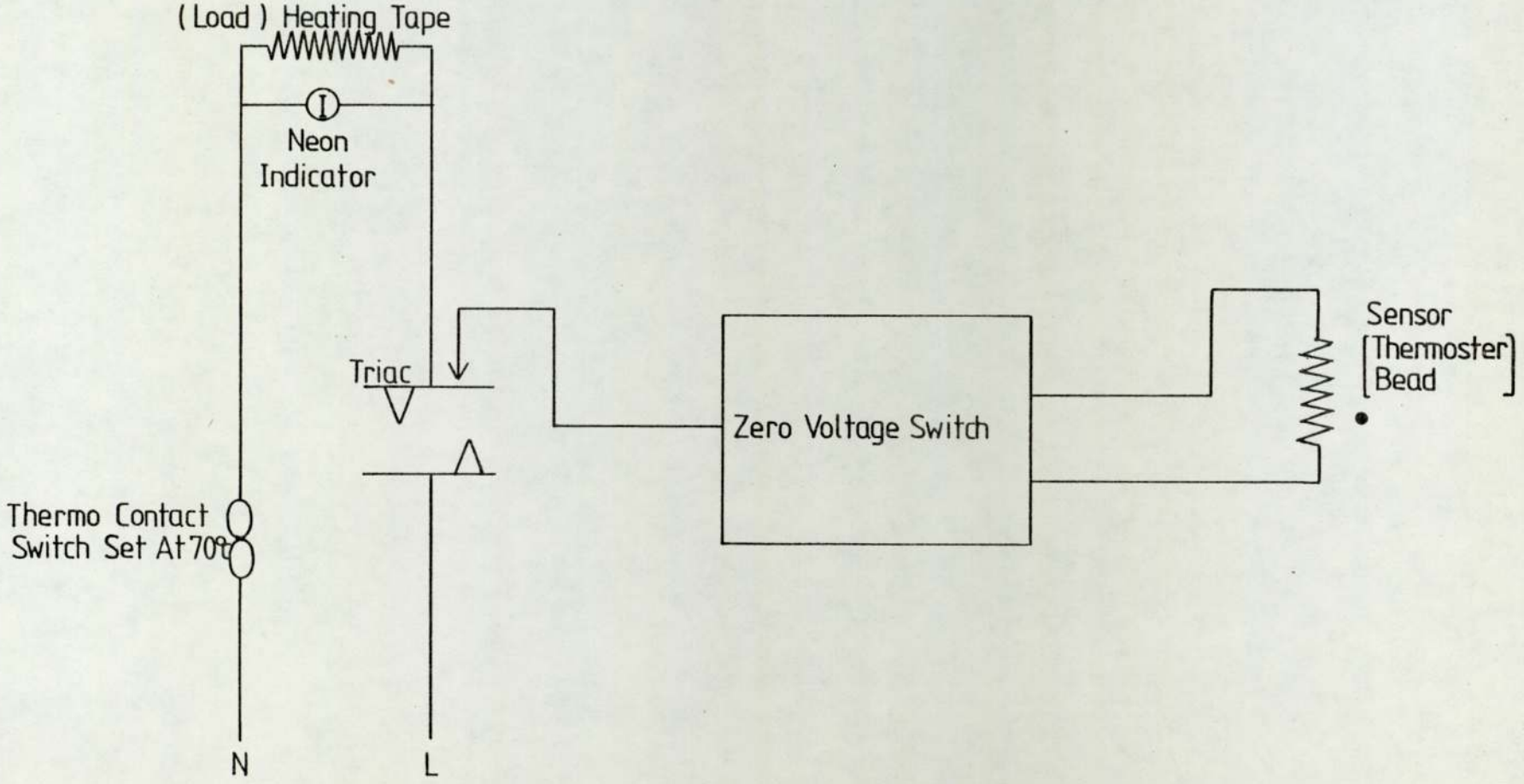

The preheater for the mobile phase liquid was controlled by a Type DF Thermostat, supplied by Hot Foil Ltd, Wolverhampton. The stainless steel sensing tube was inserted into the flowline via a plastic T-joint. The accuracy of the thermostat was within ± 5°C of the set value.

All the columns were fitted with a 50 mm diameter fibre glass jacket.

6.3.6. Thermocouple Networks

Two different thermocouple networks can be identified in the SCCR4 machine. The first network, installed during the first stage of incorporating heating facilities, consists of seven Chromium-Nickel thermocouple probes inserted into the flow lines of the SCCR4 machine as shown in Figure 6.16. The corresponding positions of the thermocouples in the multipoint selector switch is from 1 to 7.

The second network consists of ten Chromium-Nickel self-adhesive thermocouple patches, supplied by Comark Electronics Ltd., Rustington and were attached onto the wall of each column in the same position as the thermoster bead of the controller. The corresponding positions of the thermocouples in the multipoint selector switch is from 11 to 20.

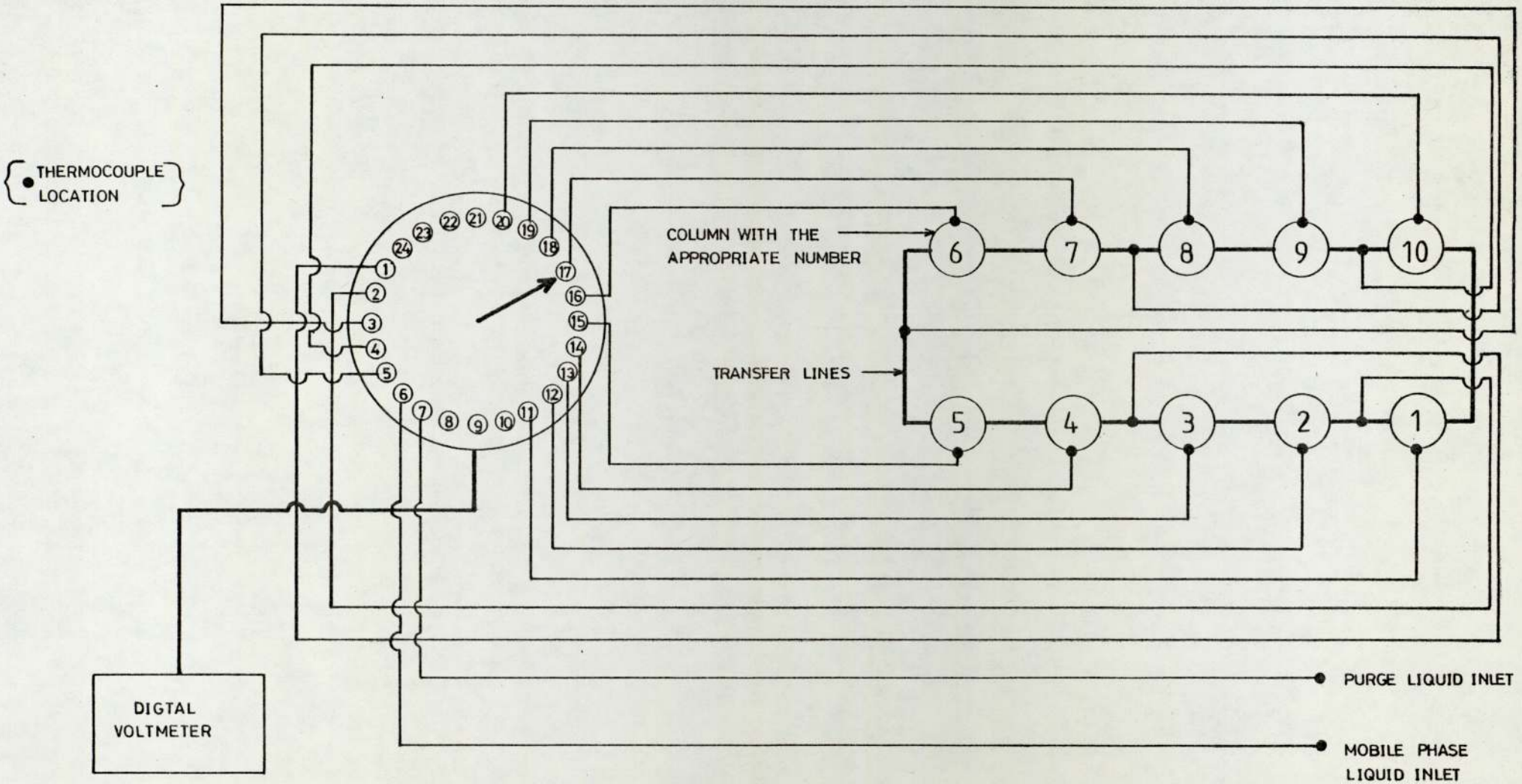

Fig. 6.16 Thermocouples Network

The cold junction for all the thermocouples was a Dewar flask containing a well stirred mixture of ice and water. Calibration of the thermocouples was performed with the Dewar flask as the cold junction, by inserting the measuring junction into a stirred liquid bath. The liquid bath provides the best medium for establishing a controlled environment up to 100°C.

Calibration charts for the thermocouples are given in Figure (1) Appendix II.

6.4. Auxillary Equipment

6.4.1. Mobile Phase, Purge and Feed Supply

The liquid supply to the SCCR4 machine was distilled water obtained from an 8000 cm^3 hr^{-1} automatic water still, marketed by Fisons Scientific Apparatus, Loughborough. In chromatographic separations involving ion exchange resins, the liquid mobile phase should ideally be free of all ions. However, within the budget constraints, the purchasing of a large scale water deioniser was not possible. In Boehringer's (Section 3.3.2.1.2) large scale batch work on fructose/glucose separation involving Ca^{+} charged ion exchange resins, distilled water, instead of deionised water, was employed as the liquid mobile phase. Finally, the adverse effect of the minute percentage of free ions in the distilled water, if indicated in subsequent experimental results, would be nullified with the periodical recharging of the resin with $CaCl_2$ solution.

The distilled water from the still was stored in two stages. The first stage, a series of eight rigid polythene reservoirs linked together by PVC tubing, received all output directly from the still. The water level in the reservoirs was automatically controlled via a pressure sensor, by solenoid switch governing the on or off of the still. The reservoirs were installed at

an elevated level from which the distilled water flows, under gravity and via a solenoid operated on/off valve, into a 7.5×10^{-2} m^3 isomantle where the distilled water was heated to the required temperature before being introduced into the SCCR4 machine. The isomantle and its controlling devices were described in Section 6.3.1.1.

Feed inlet to the SCCR4 machine was supplied as a solution which was stored in a 2×10^{-2} m^3 glass aspirator.

6.4.2. Product Collection

The two product streams from the SCCR4 machine were collected in plastic containers of 6, 10 and 80×10^{-3} m^3 capacity. Switching of the product streams from one container to the next was achieved using the fraction collector (Figure 6.14 (a)). The operating principle consisted of moving the product outlet lines, at desired time intervals, from delivering to one pair of collection vessels to delivering to the next pair. The fraction collector was designed to function automatically through the drive of an electric motor. However, during the course of this research, it was operated manually to collect a bulk sample per cycle.

6.4.3. Flowrate, Pressure and Temperature Measurement

Feed inlet flowrate was measured using 25 cm^3 glass burrettes. Measurement of both the inlet mobile phase and purge flowrate was recorded using a calibrated glass QVF pipe section of 2.54 cm diameter and 0.5 m length.

Inlet pressures to the SCCR4 machine were continuously monitored by Bourdon gauges. One 0 -690 kNm^{-2} gauge, was installed after the pumpheads, in each of the mobile phase and feed inlet lines. Whereas, the inlet purge pressure was recorded by a 0 -1380 kNm^{-2} gauge. Stainless steel pulsation dampeners with a nitrile rubber diaphragm, supplied by Fawcett Engineering Company, Bromborough, were incorporated in the inlet purge and mobile phase lines to minimize the pulsation effect which may damage this type of pressure gauge. This, coupled with the use of polystyrene needle valves to restrict sudden fluid surges to the gauges, succeeded in smoothing out the pulsations and enabled steady pressure readings to be recorded.

Outlet flowrates from the SCCR4 machine were measured by weighing the products, and outlet pressures were equal to atmospheric pressure.

A total of seventeen thermocouples were incorporated into the SCCR4 machine and their respective locations

were mentioned in Section 6.3.1.5. All these thermocouples were wired back to a 24 point selector switch. The temperature of one particular location can be displayed in multi-volt units, on a digital voltmeter, by setting the selector switch to the appropriate position. The conversion of the multi-volt units into temperature units was accomplished through a calibration curve.

6.5. Safety

6.5.1. Pressure Equipment

The maximum operating pressure envisaged for the SCCR4 machine was 620 kNm^{-2}. All the columns and fittings were tested with water as the working fluid after assembly up to a 770 kNm^{-2}.

In case of a blockage occurring in one of the flow lines or a pneumatic valve failing to open, adjustable stainless steel pressure relief valves, supplied by Hokes International Ltd, were installed in the inlet lines of the SCCR4 machine. The relief pressure was set at 600 kNm^{-2}.

6.5.2. Heating Equipment

Although the maximum safety operational temperature of the QVF columns was quoted by the manufacturer to be 120°C, the highest temperature in the SCCR4 studies was set only to be 70°C so as to avoid any generation of steam. Furthermore, a fail-safe contact switch was incorporated in series with the heating tape to prevent the latter overheating the column due to any malfunctioning of the control system. The contact switch was mounted on the surface of the column and, at temperatures higher than 70°C, would discontinue the current supply to the heating tape.

Chapter 7

Commissioning of SCCR4 Unit

7.1. Treatment of Packing

In order to ensure each column would contain packing of approximately the same size distribution, the 4Kg of moist Zerolit 225 SRC 14 (295- 149μm) resin (supplied by BDH Chemicals Ltd.) was divided into sixteen batches by the use of a sample splitter.

Ten batches of the resin were individually conditioned to the Ca^{++} form and subsequently used in packing the SCCR4 columns. Two of the remaining six batches were set aside for sieve analysis and a tabulated result is given in Appendix (III, Figure 1).

The apparatus used in conditioning the Zerolit resin consists of a sintered glass funnel (1000 cm^3 capacity) and a filtering flask (10000 cm^3 capacity). Both items were supplied by Fison Scientific Apparatus Ltd. Figure 7.1 illustrates the arrangement of the apparatus. The outlet of the filtering flask was connected with a flexible PVC tubing. A screw clamp was used to close or open the tubing and thus controlled the flow of regenerant through the resin bed. After regeneration, the resin bed was rinsed with distilled water until excess regenerant has been removed. Checking for completeness was by means of a pH meter.

Although the scope of this research project concerns only the separation of fructose from a mixture

Fig. 7.1 Apparatus For Conditioning Of SCCR 4 Resin

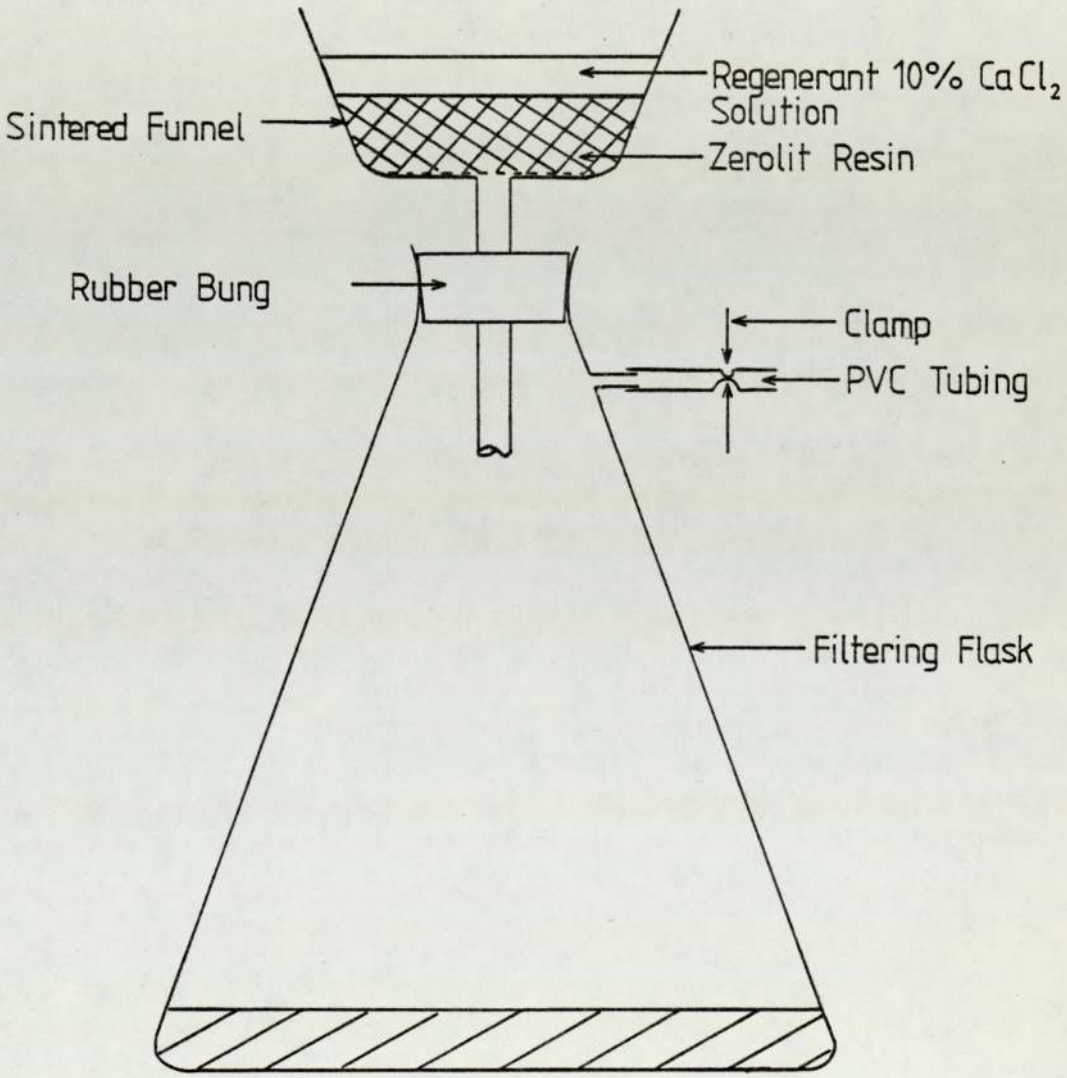

containing an equal amount of glucose, there was an intention for a future worker to operate the SCCR4 machine to separate fructose directly from a sucrose feed which would consequently involve an additional hydrolysis mechanism. In order to allow for the latter mechanism, the Zerolit 225 SRC14 resin was conditioned, according to the procedures published in the Boehringer Mannheim Patents (65), to contain 3 - 5% free Hydrogen ions.

As the Zerolit resin was supplied in Na^+ form, it was necessary to convert the resin first to a hydrogen form. To effect this, 10% w/v hydrochloric acid solution was used as the regenerant. Each of the ten batches of Zerolit resin to be treated has a wet volume of appoximately 320-350 cm^3. In ion exchange practice, the ratio meq. regenerant/meq. resin should be about 4 for strongly acid cation (160). As such, the amount of 10% w/v hydrochloric acid required to regenerate 350 cm^3 of Zerolit resin was predicted as follows:

Wet exchange capacity of Zerolit 225 SRC14
= 1.9 milliequivalent (meq)/cm^3.

Total exchange equivalent in 350 cm^3 of resin
= 1.9 x 350 meg.
= 665 meg.

Normal practice is to employ regenerants 4 times over

the required equivalent; hence equivalent of hydrogen ion required is

$$4 \times 665 = 2660 \text{ meg.}$$

and cm^3 of 10% w/v HCl required

$$= \frac{2660 \times 36.5 \times 100}{1000 \times 10}$$

$$= 970.9 \text{ cm}^3$$

Consequently, 1000 cm^3 of 10% w/v Hydrochloric acid was used to regenerate one batch of Zerolit resin. In ion exchange practice, recommended flow rates for regeneration (160) are 0.05 to 0.1 bed volume/minute. The flowrates calculated for regenerating 350 cm^3 resin was to be 17.5 cm^3 to 35 cm^3/minute. As the only means of controlling the regenerant's flow through the bed was by closing or opening of the screw clamp attached to the PVC tubing, the flowrates could therefore only be regulated to approximate values. These were measured by timing the amount of regenerant collected in the measuring cylinder, placed inside the filtering flask, over a fixed period of time. Furthermore, the flowrates varied with the height of regenerant above the resin bed. In order to maintain the initially set value, the level of regenerant was always kept approximately 3 cm above the resin bed.

Regeneration was followed by rinsing. In the literature (160), it is suggested that about 10 bed volumes of distilled water should be adequate, and the first bed volume of water wash should be at the same rate as the regenerant solution, and thereafter at about twice that rate. 3500 cm^3 of distilled water was used for rinsing each batch of Zerolit resin. At the end of the rinsing step, the sample of effluent from the funnel was collected and checked with a pH meter for the complete removal of excess acid.

The regeneration of the resin from a hydrogen form to a calcium form followed a similar procedure. 10% w/v calcium chloride solution was used as the regenerant. As calcium ion is bivalent, the amount of regenerant was predicted as

$$= \frac{2660 \times 111 \times 100}{1000 \times 10 \times 2} = 1476.3 \text{ cm}^3.$$

Hence, 1500 cm^3 of 10% w/v calcium chloride was used for treating each batch of Zerolit resin. According to the investigation by Boehringer Mannhein (65), the free H-equivalencies are only completely saturated with calcium when regeneration is carried out with a calcium chloride solution at 60°C or when the regeneration is carried out at room temperature with a calcium chloride solution, the pH of which is greater than 8. In order to

retain 3 - 5% of the hydrogen ions for future hydrolysis studies, the Zerolit resin was regenerated at room temperature and the pH value of the calcium chloride solution was found to be 5.5 - 6.0.

Procedures similar to previous regeneration and rinsing steps were adopted. At the end of the rinsing step, the pH of the effluent from the bed was checked to be 6.5 - 7.0 and this indicated a total removal of excess calcium chloride. The regenerated resin was subsequently transferred into a glass beaker containing distilled water and, to prevent the drying of the resin, 'Parafilm' sheet was wrapped tightly round the top of the beaker.

7.2. Column Packing Technique

The method employed for packing the SCCR4 columns was slurry packing. This included the placing of a large funnel on top of a column for the introduction of the packing, and the use of a vacuum pump, connected to the base of the column, for withdrawing water.

The column was initially filled with water, and the funnel was held in position with 'Parafilm' sheet. As the packing was introduced into the funnel, the vacuum pump was started simultaneously to create a flow of water

in the column. This method helps to minimize the settling of resin under gravity as this often results in segregation of the particles, because of the variation of settling velocity with particle diameter.

While the slurry was being introduced, the column was tapped sharply to ensure that the resin settled completely. This tapping was carried out in a random manner to avoid the creation of a standing wave in the column which would result in packing segregation. Also, while the column was being filled, distilled water was added continuously.

This packing procedure was stopped when a packed height of 65 cm was reached. The column inlet 'plunger' fitting (Section 6.2.2., 6.2.3) was replaced and the packed column was pumped with distilled water under pressure for 24 hours. At the end of this period, any drop in the level of packing was replenished so as to maintain a bed height of 65 cm.

The packed column was weighed and the total weight of wet resin in the column was determined from the difference in weight between a packed and an empty column. Similarly, the column volume of a bed height of 65 cm was obtained from the weight difference between an empty column and a column filled with water.

All the packed columns were subsequently mounted

onto the SCCR4 equipment, and with the pressure of the midget pneumatic cylinders being set at 250 kNm^{-2}, the system was commissioned with distilled water over a period of ten days. At the end of this period, the resin bed height of each column was measured and a drop of approximately 1 - 2 cm in bed heights were detected. This implies a decrease in column volumes. However any re-determination would require the emptying and repacking of resin beds. Because of time limitations, the new column volumes were predicted as follows:

$$V_R = \frac{V_{65}}{65} \times h \quad cm^3$$

V_R = Column volume with bed height h cm

V_{65} = Column volume with bed height 65 cm.

h = New bed height.

The calculated diameters (d) from

$$d = \sqrt{\frac{4}{\pi} \frac{V_{65}}{65}} \qquad (7.1)$$

varied between -0.8% to +0.67% from the nominal column diameter of 2.54 cm. Hence the above predicted new column volume were accepted. During future operations, the air pressure of the midget pneumatic cylinder was always maintained at 250 kNm^{-2} and no measurable change in bed heights was detected.

7.3. Comparison of Packed Columns

7.3.1. Theoretical Basis for Comparison

The general structure of a bed of spherical particles could be partly characterised by its fractional voidage, which is usually ~0.4. In elution chromatography this represents the fractional interstitial volume, V_o/V_{Total}, and the elution volume of a totally excluded species, V_o, is therefore a measure of the bed voidage. Comparison of V_o values obtained for columns of similar dimensions thus indicates their relative packed densities. A high voidage represents a more loosely-packed column.

Pressure drop, ΔP, through a packed bed is an alternative basis for comparing packed densities. For laminar flow and assuming no wall effect, Kozeny's equation (158) may be written:

$$\Delta P = \frac{K'' S_p^2 (1-\varepsilon)^2 \mu . l v}{\varepsilon^3} \qquad (7.2)$$

K'' = Kozeny's constant ($\pm$ 5)

S_p = Specific surface area of packing particles
= 6/dp for spheres

d_p = particle diameter

μ = fluid viscosity

l = bed length

v = average fluid velocity, defined as $\frac{1}{A}, \frac{dV}{dt}$.

V = Volume of fluid flowing in time, t.

A' = Total cross-sectional area of bed.

For spherical particles, Equation (7.2) becomes:

$$\Delta P = \frac{180\ (1-\varepsilon)^2 \mu.\ 1.v}{\varepsilon^2\ d_p^{\ 2}} \qquad (7.3)$$

Hence pressure drop readings of a series of columns, obtained at identical flow conditions, should provide a comparison of voidage and particle diameter:

$$\Delta P \propto \frac{(1-\varepsilon)^2}{\varepsilon^3\ d_p^{\ 2}} \qquad (7.4)$$

If the columns contain particles of a similar size, pressure drop readings should be proportional to $(1-\varepsilon)^2/\varepsilon^3$.

Furthermore, as in this research study, the separating mechanism relied on the distribution of fructose between the liquid mobile phase (void (V_o) + pore liquid (V_i))and the solid resin matrix (V_s); their values should ideally be constant for all columns in a continuous chromatographic machine. This ensures a constant migration rate for individual components through successive columns. However, a slight variation in $V_o + V_i$ and V_s values can be tolerated in the SCCR4 unit because the separating section consists of a series of columns and such variations are smoothed out

over the total separating section. As such, although the migration rate of a component through individual columns may vary, its average migration rate through the separation section of the SCCR unit would be essentially constant.

Finally, the main criteria for comparing the performance of batch chromatographic columns is usually based on their respective H.E.T.P. values. Fructose chromatograms were developed from all columns at a flowrate of (6.3 cm^3/min) which was the estimated elution flowrate likely to be employed in actual operations. The column and eluent temperature were maintained at 30°C. The variation of H.E.T.P. with temperatures at this flowrate was studied on column No.1 and column No.10.

7.3.2. Experimental Techniques

Starch, a polysaccharide with a large molecular size which forms no complexes with the calcium ions, was selected as the totally excluded species and its elution volume was taken as the void volume. Whereas the elution volume of glucose represents the void plus pore volume (Section 5.3.3.1.).

The apparatus used for the experiments is shown in Figure (7.2). Distilled water was pumped, via a

Fig. 7.2 Arrangement Of Equipment For Comparison Of SCCR4 Columns

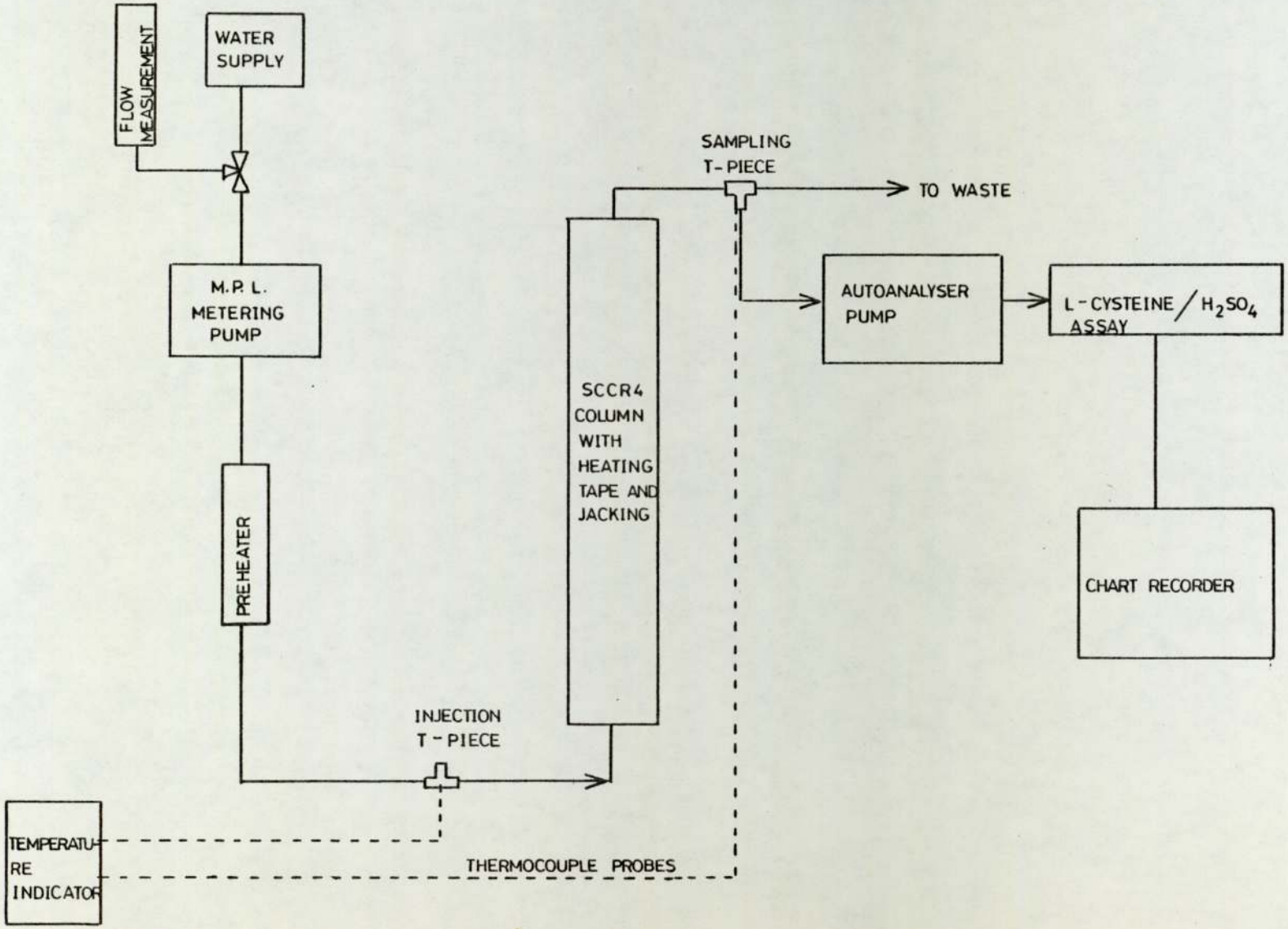

preheater, into the column, in situ in the SCCR4 unit, through the normal column fitting. A T-piece in the outlet line containing a silicone rubber septum, allowed a sampling needle, connected to the Technicon AutoAnalyser pump, to be introduced and a continuous sample stream removed. An automated cysteine-sulphuric acid assay was employed for developing chromatograms for starch, glucose and fructose. The column temperature was maintained by a heating tape and a fibre glass jacket. The temperatures of both eluent inlet and outlet, and the column wall were monitored by thermocouples.

Samples were introduced into the system through another T-piece, also containing a silicone rubber septum, in the mobile phase inlet line to the column. Sample injection was conducted with the use of a one cm^3 plastic syringe. The sample injection T-piece and product removal T-piece were positioned as close to the column as practically possible to minimize extra-column dispersion.

Elution of all samples was conducted at a flowrate of 6.3 cm^3/min, and a temperature of 30°C, these being the approximate mobile phase flowrate and temperature employed in the majority of SCCR4 runs during the research programme.

Samples of size 1 cm^3 and concentration 1 mg/cm^3 were used and the reproducibility of calculated V_o, V_R^G, V_R^F and H.E.T.P. values were determined by repeated injection of starch, glucose and fructose.

Results from this study revealed a low H.E.T.P. value for both column No.1 and No.10 and thus were selected for further investigation of temperature effect on the values of V_o, V_R^G, V_R^F and H.E.T.P. The temperature range investigated was from 20°C and 60°C.

The pressure drop for each SCCR4 column was recorded, at 25 $cm^3\ min^{-1}$, by the use of a mercury manometer.

7.3.3. Results and Discussion

The reproducibility of the experimental techniques for determination of V_o, V_R^G, V_R^F and H.E.T.P. values was found to be satisfactory. Values of V_o, V_R^G, V_R^F varied by $\pm$ 1% and H.E.T.P. values by $< \pm$ 2%. Results obtained from all ten columns are tabulated in Table (7.1).

V_o, V_R^G, V_R^F values (Table 7.1) for the SCCR4 columns varied by 12%, 5% and 4% respectively. The variation in Vo values stems mainly from the differences in column packing densities and illustrates the

Table 7.1 Characteristic Of SCCR 4 Columns

COLUMN NO.	COLUMN HEIGHT (cm)	V_{TOTAL} COLUMN VOLUME (cm^3)	WEIGHT OF WET RESIN (gm)	WET PACKING DENSITY (gm/cm^3)	ELUTION VOLUME cm^3			VOIDAGE $\varepsilon = \frac{V_O}{V_{TOTAL}}$	PERFORMANCE W. r. t. FRUCTOSE			PRESSURE DROP $kN\,m^{-2}$
					STARCH V_O	GLUCOSE V_R^G	FRUCTOSE V_R^F		NO. OF PLATES N	H.E.T.P. mm.	RELATIVE DISTRIBUTION COEFFICIENT K_D^F	
1	64	319	458	1.44	115.3	154.4	252.0	0.361	26	24.61	0.593	10.21
2	64	320	443	1.38	121.0	156.0	248.1	0.378	23	27.83	0.562	9.56
3	64	318	454	1.42	118.5	154.2	249.5	0.373	23	27.83	0.582	9.96
4	63	321	446	1.39	124.1	156.0	246.0	0.387	22	28.64	0.545	9.89
5	64	320	448	1.40	126.0	153.2	251.0	0.394	23	27.83	0.586	9.75
6	64	317	444	1.40	122.0	150.0	245.0	0.384	23	27.83	0.569	9.72
7	64	328	450	1.37	128.2	158.0	255.0	0.390	21	30.48	0.571	9.53
8	64	317	440	1.39	121.5	158.0	250.0	0.383	23	27.83	0.579	9.81
9	64	316	441	1.40	118.0	153.4	248.8	0.373	24	26.67	0 587	9.77
10	63	320	465	1.45	114.0	157.5	252.5	0.356	24	26.25	0.589	10.25

difficulty in producing uniformly packed large diameter chromatographic columns with a standard grade resin (Zerolit SRC14) having a wide size range (150μm to 300μm). However, as in this research, the total mobile phase in each column entered in the separation is the sum of the void (V_o) and pure (V_i) liquid ($V_R^G = V_o + V_i$), variation in V_o is compensated by only a 5% variation in V_R^G. This implies that each column contains an approximately equal volume of mobile phase. Similarly, a 4% variation in V_R^F represents the likely variation in the amount of calcium charge in individual columns. Furthermore, the variation in V_R^G and V_R^F is greatly reduced when we consider that the separating section is made up of nine columns, and we are really comparing the difference between one set of nine columns and another set of nine.

The maximum variations in V_R^G and V_R^F on this basis is 0.6% and 0.45% respectively.

Pressure drop readings for SCCR4 columns, recorded at 25 $cm^3\ min^{-1}$, show a variation of 8% which was mainly attributed to a variation in both the packed densities and bed height. The bed densities varied by 6% and the mean value (1.40) was found to be slightly higher than the values quoted in the literature, usually between 1.25 - 1.35 gm/cm^3 (160). This was the result

of pressure (250 kNm^{-2}) being applied, via the pneumatic cylinder and plunger, to the resin beds. Subsequent work on the SCCR4 unit has achieved higher bed densities with the application of 750 kNm^{-2} pneumatic pressure on the plunger units and better separation performance was recorded (161).

H.E.T.P. values of the SCCR4 columns varied by a maximum of 24%. This high value was caused by the variations in the extra-column dispersion incurred from column fittings and sampling T-pieces.

Figure (7.3) highlights the relationships of the H.E.T.P. values of SCCR4 columns with their corresponding pressure drop, voidage and packed density values. Column No.1 and No.10, with low H.E.T.P. values, have high packed densities, but low voidage. Whereas, the high H.E.T.P. value of column No.7 was accounted for by a high voidage and a low packed density. The corresponding pressure drop reading was expected and found to be low.

The effect of temperature on the H.E.T.P. values was studied with column No.1 and No.10 which have the lowest H.E.T.P. values. Figures (7.4, 7.5) illustrate a drop in H.E.T.P. values, for both glucose and fructose, with increasing temperature. Similar to previous findings from the analytical batch work (Section 5.3.3.3), the gain in efficiency with temperatures was more prominent with fructose than glucose. For both sugars,

Fig.7.3 Variations Of H.E.T.P., Voidage, Packing Density And Pressure Drop Among SCCR4 Columns

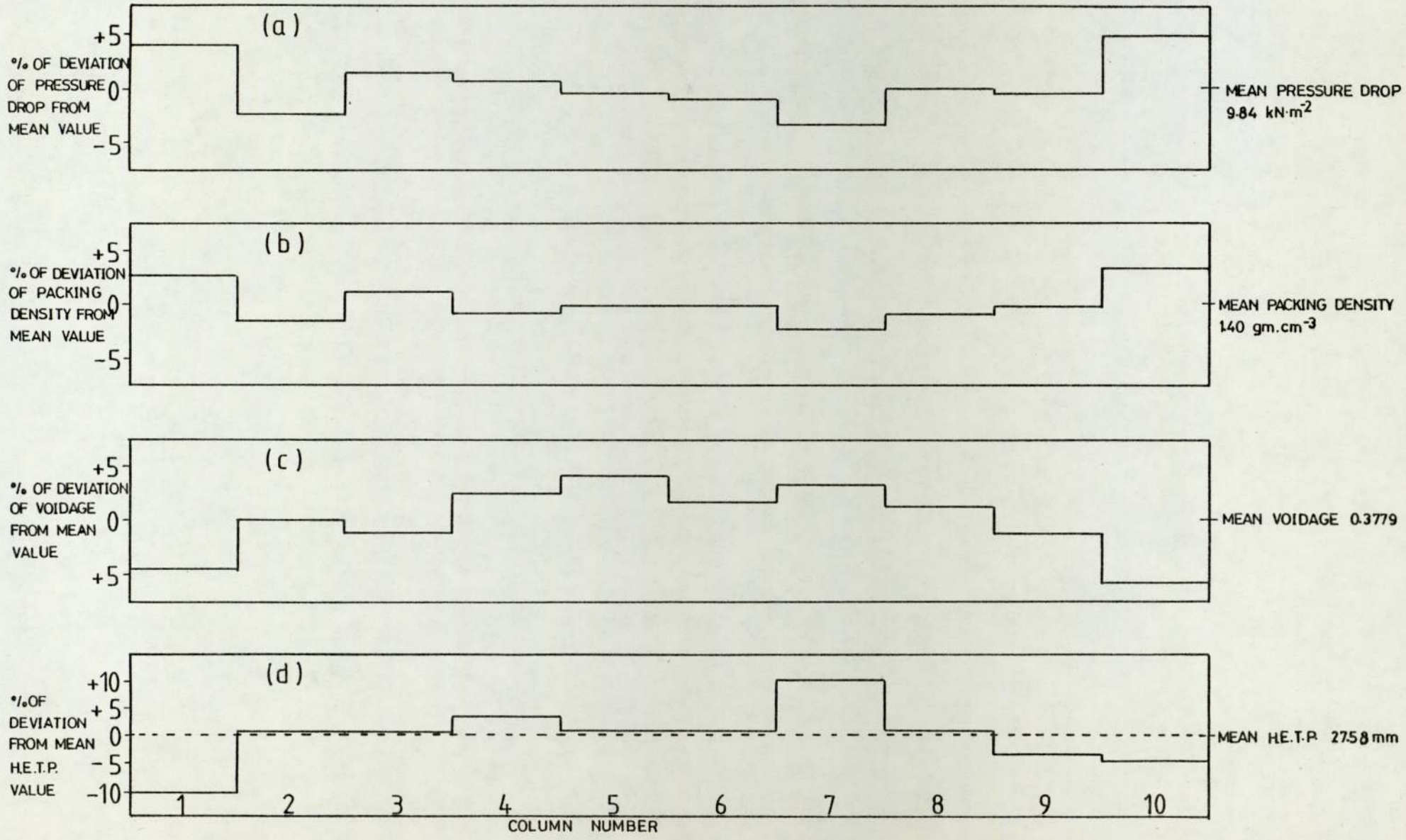

Fig. 7.4 Effect Of Temperatures On The H.E.T.P. Values Of Column (1)

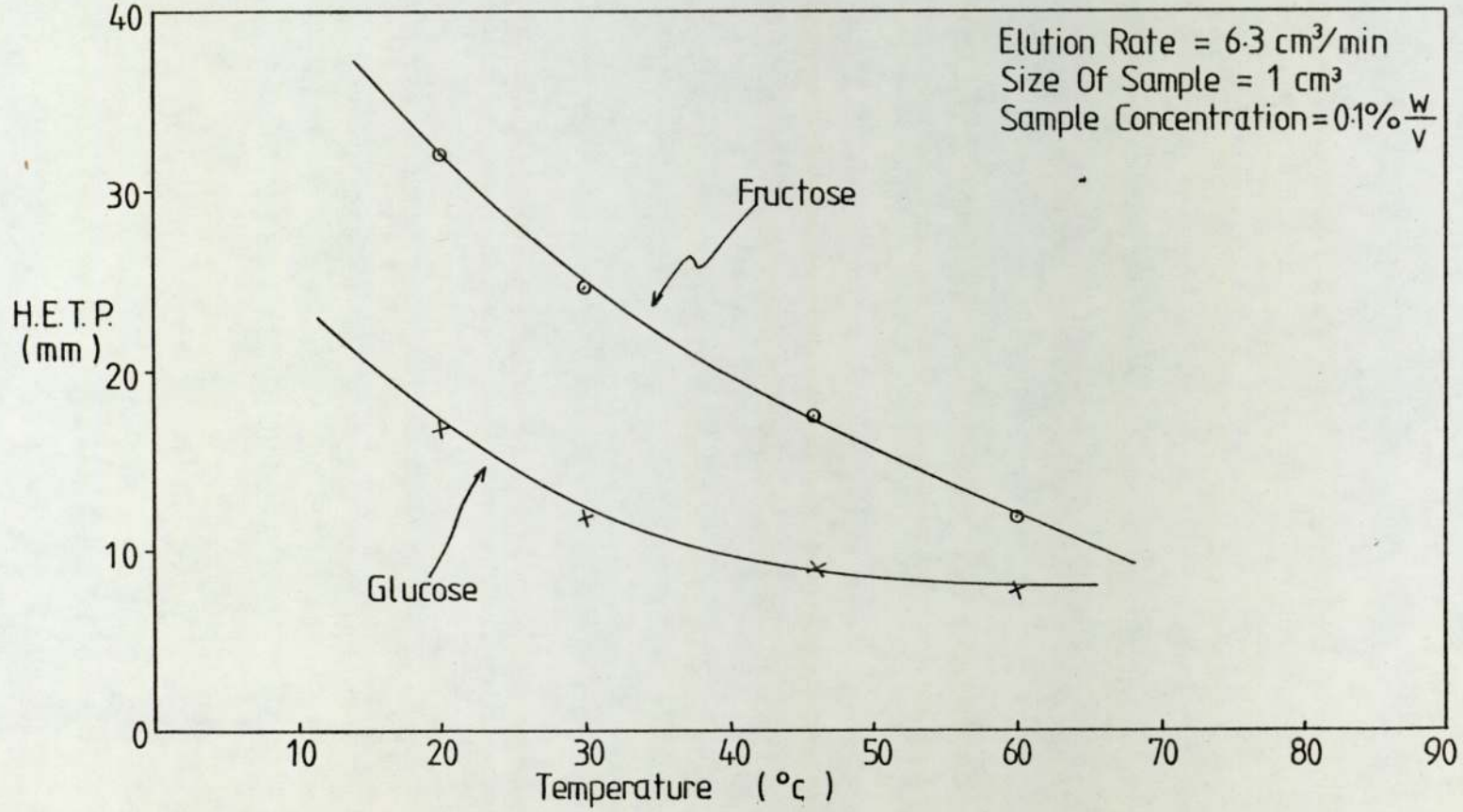

Fig. 7·5 Effect Of Temperatures On The H.E.T.P. Values Of Column (10)

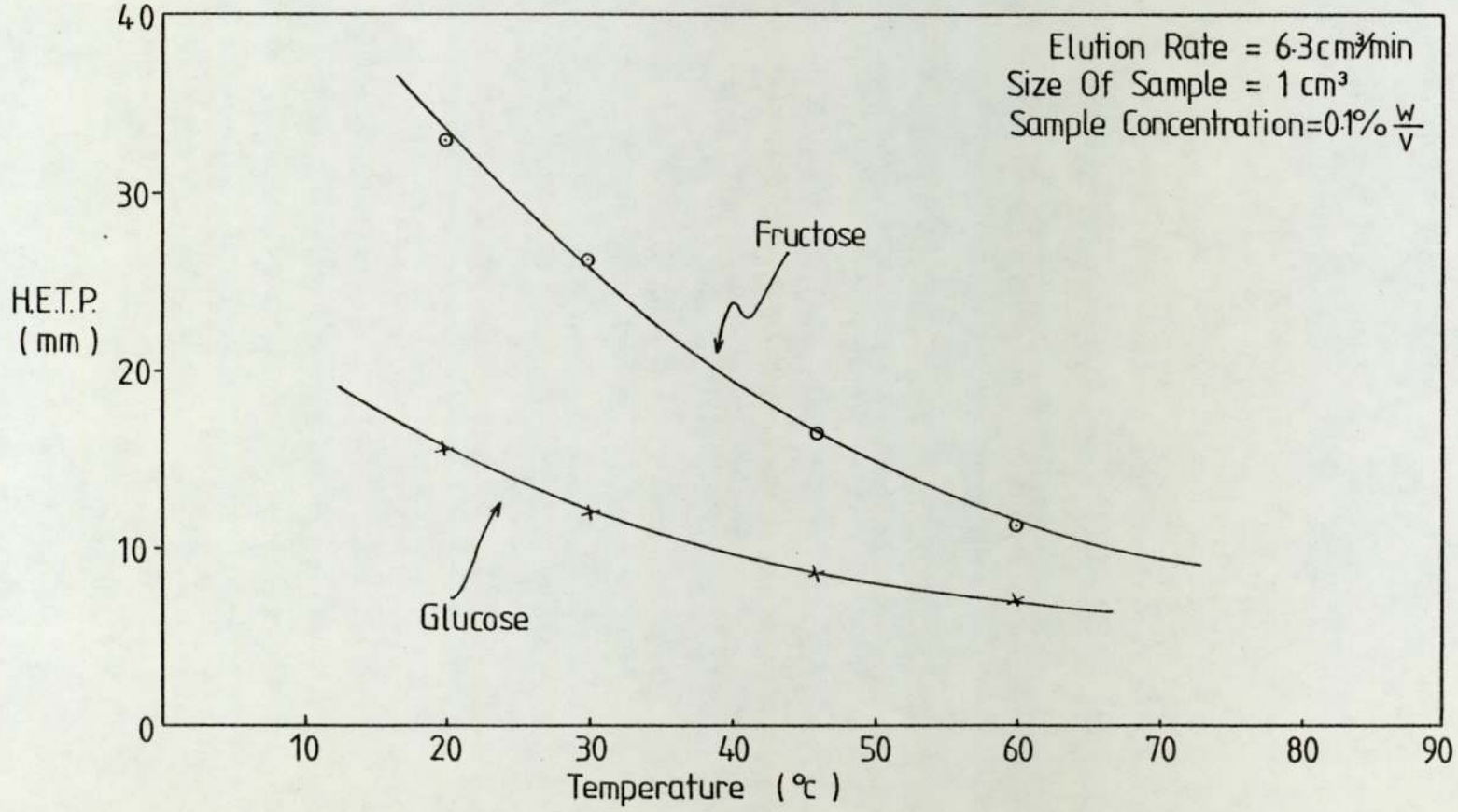

Table 7.2 Effect Of Temperature On H.E.T.P. Values

COLUMN NO. 1	TEMPERATURE °C	ELUTION VOLUME OF STARCH V_0 (cm³)	ELUTION VOLUME V_R (cm³)		NO. OF THEORETICAL PLATE N		H. E. T. P. (mm)		K_D^F
			GLUCOSE	FRUCTOSE	GLUCOSE	FRUCTOSE	GLUCOSE	FRUCTOSE	
BED HEIGHT 64 cm	20	115.3	154.4	273.0	38	20	16.8	32.0	0.72
	30	115.0	154.4	252.0	54	26	11.8	24.6	0.59
	46	115.4	153.5	229.95	70	38	9.1	16.8	0.46
	60	115.2	154.2	214.2	82	54	7.8	11.8	0.36
COLUMN NO. 10									
BED HEIGHT 63 cm	20	114.0	157.4	274.2	40	19	15.8	33.1	0.72
	30	114.3	157.5	252.5	52	24	12.1	26.2	0.58
	48	114.3	157.25	228.4	72	38	8.7	16.3	0.43
	60	114.2	157.5	215.8	90	56	7.0	11.25	0.36

the rate of decrease in H.E.T.P. values with increasing temperature was the highest within the range of 20° - 40°C, and implied a significant improvement on column dispersion.

However, the elution volume of fructose decreases with increasing temperature (Table 7.2). With the elution volume of glucose unaffected by temperature, this indicated a reduction in the peak-to-peak width between the two components' bands. Consequently, the advantage of separating glucose from fructose at elevated temperatures rests on weighing a reduction in H.E.T.P. values against a decrease in the peak-to-peak width.

7.4. Preliminary Separation of Fructose from Glucose

The objectives of the preliminary runs conducted with the SCCR4 unit may be summarized:

(i) To ensure that the pneumatic control unit and valves were functioning properly.

(ii) To ensure that the liquid inputs to the SCCR4 unit travelled in the correct directions which required the actuation of the appropriate valves. This was checked by means of a liquid balance for the unit.

(iii) To establish the approximate number of cycles for the equipment to achieve a pseudo-equilibrium state.

(iv) To check if the total sugar content of the products, when summed, equalled the total feed input values.

(v) To determine if the product purities were as expected from theoretical predictions of the operating conditions (Section 8.3).

(vi) To check leakage from column fittings, T-pieces and valves.

Four preliminary runs were carried out, and their conditions may be summarized:

Mobile Phase Flowrates	4.5 - 12.5 $cm^3\ min^{-1}$
Feed Flowrates	1 - 2 $cm^3\ min^{-1}$
Purge Flowrate	100 - 300 $cm^3\ min^{-1}$
Switching Interval	15 - 45 min

Feed Composition	1 - 10% w/v (50/50 Glucose and Fructose).
Time of Run	25 - 75 hours
Eluent Average Temperature	20 - 25°C
Purge temperature	20 - 70°C.

From the preliminary runs, it was found that an average of five to six cycles were required for establishing a pseudo-equilibrium state for the SCCR4 unit, and was independent of feed concentration. By elevating the purge liquid's temperature to 70°C, a more complete purging of SCCR4 columns was achieved. During the preliminary runs, the entire SCCR4 unit was found to be operating satisfactorily.

Chapter 8

Operation of the SCCR Unit on the Continuous Mode

8.1 Experimental Methods

8.1.1 Feed Preparation

Feed for all the SCCR4 runs was made up as a solution of glucose and fructose powders supplied by ICI Ltd. A detailed analysis of these glucose and fructose samples is given in Figure 1 of Appendix IV. Feed solution of a required concentration was prepared by dissolving the calculated amounts of glucose and fructose in distilled water. After stirring, a sample of the solution was introduced through the autoanalyser for the determination of the exact contents of glucose and fructose. The ease of dissolving the sugar powders varied depending on the concentration level required in the feed solution. Elevated temperatures were found to be necessary for preparing solutions of 50% w/v.

In order to prevent the growth of bacteria, moulds and other micro-organisms, in the sugar solutions, an inhibitor was needed. Sodium azide ($Na\ N_3$) in 0.02% w/v concentration was recommended by Fisons Ltd as being suitable.

For a polystyrene-sulphonated type resin (PSSR), the selectivity of ions increases with the valency of the ion (163). Consequently, the sodium ions (univalent) of the sodium azide will not displace the calcium ions (bivalent) from the resin. However, care must be taken when handling

sodium azide because solutions are toxic by skin absorption.

8.1.2 Start-up/Shut-down Procedures

The experimental runs with the SCCR4 machine lasted from 30 hours to 45 hours. As it was not convenient to operate the machine continually for such long time periods, each SCCR4 run was divided into separate consecutive daily operations ranging from 8 - 10 hours. When a continuous run was separated in such a manner, it is essential to establish that no significant change develops during the period that the machine is shut-down. This was the first fact that was established before any major experimental programme was commenced. Both the internal column concentrations and product concentrations for samples taken immediately before shut-down and after start-up indicated that no substantial change had occurred.

The details of start-up procedures are as follows:

(i) The distilled water in the isomantle was elevated to the required temperature and was maintained continuously at the desired temperature throughout the entire run by a thermostat switch.

(ii) A pneumatic supply was connected to the SCCR4

unit. The 'bias' and 'activity' pressures on the 'double acting' valves were set to the correct values. The on/off valve controlling the air supply to the midget pneumatic cylinders was opened slowly to allow a gradual building up of pressure in the cylinders. This action was necessary to avoid the full impact of the pneumatic cylinders which could have resulted in the breakage of the glass columns.

(iii) The fraction collector was set to collect the products as required.

(iv) The digital timer was set to the desired time interval. The mobile phase, the purge and the feed pumps were set to the required flowrates. The feed inlet lines were filled with feed solution and were connected to the columns for the run to commence.

(v) The digital millivoltmeter was switched on and the thermo-flask, employed as the thermocouple network's cold junction, was filled with iced water. For runs involving higher mobile phase temperatures, the column's heating tapes were switched on for 10 - 15 minutes before a run commenced so as to allow the columns to reach approximately the set temperature. The preheater for the mobile phase is only switched on when the run commences.

The shut down procedure included mainly the switching off of all equipments and immediately closely the inlet

taps of both the feed reservoir and the isomantle unit. This was to stop liquids 'syphoning' through the machine. The pneumatic supply to the SCCR4 unit was disconnected and the residual pressure was exhausted. The poppet valves were thus retained in the same position as during final sequencing operation. Finally, the outlet tubes of both product lines were plugged. Such shut-down procedure ensured no liquid flow with in the SCCR4 unit, and the only likely adverse effect was diffusion of sugars in individual columns or through the transfer lines between columns. Both effects were considered to be small due to the low liquid diffusivities of carbohydrate solutions.

8.1.3 Sampling Techniques

The sampling procedure adopted in the SCCR4 runs was to collect the products from one complete cycle, and then to switch over containers, using the fraction collector, to collect products from the next cycle. The maximum flowrates of products acquired during this research programme were 300 cm^3 min^{-1} and 6 cm^3 min^{-1} for the fructose-rich (purged) product and glucose-rich (mobile phase) product respectively. Bulk samples of both products were collected in plastic containers of 80 litres, and 6 or 10 litres capacity for the fructose-rich and glucose-rich products respectively. These samples

were weighed, and, after being thoroughly mixed, small samples were retained for the determination of the concentration of both glucose and fructose.

At the end of each experimental run, the mobile phase and feed pumps were disconnected from the unit and one additional cycle of the timing unit was conducted manually. During these periods, the sugar contents in each column was purged out at a high purge flowrate (-300 cm^3 min^{-1}) and collected in separate containers. These samples were weighed and, after thorough mixing, small samples were removed for analysis. This technique enabled the average column concentration profiles of glucose and fructose to be determined for a particular run condition.

8.2 Data Recorded During the SCCR4 Runs

8.2.1 Liquid Flowrates

Both the liquid outlet and inlet flowrates to the SCCR4 machine were measured frequently so as to indicate the proper functioning of both the pumps and the valves. A liquid balance was carried out every cycle to ensure that liquids were flowing at a constant rate and in the correct direction.

The feed flowrate was measured at least ten times per cycle, and the average value taken as the flowrate during the cycle.

8.2.2 Pressure Drop Data

The pressure of the mobile phase flow, the purge flow and the feed flow were recorded during every sequence of a cycle. It was observed that as the run proceeded the pressure drops for the mobile phase flow and feed flow increased and then reached a steady value. This was due to a steady build up of sugar concentration as the run proceeded. The rate of increase in pressure drop levelled off after cycle 5 which approximately coincided with pseudo equilibrium conditions.

8.2.3 Temperatures

The temperatures of the purge inlet and outlet were

checked at least once per sequence during a cycle. Due to a significantly large lag in the response of the thermostat switch of the isomantle, the purge inlet temperatures during a cycle could have a fluctuation of up to ± 5°C from the desired value. Therefore the purge temperature of a cycle was the average of various readings taken (both inlet and outlet) during a particular cycle. Similarly, the mobile phase temperatures of a cycle were the average value of various temperatures recorded, both at different locations along the SCCR4 separating section (Section 6.3.6) and over all sequences of a cycle. For experimental runs conducted without the use of the column heating tapes, the mobile phase temperature was mainly controlled by the temperature of the purge liquid. During the first cycle of each daily operation, the average temperatures of the mobile phase were recorded to be ambient. As the operation proceeded, the whole SCCR4 system was gradually warmed by the purge liquid and the average mobile phase temperatures increased to a steady value. Such variations in the mobile phase temperatures could result in slight changes in the separating efficiency of the SCCR4 machine during a day's operation. However, its effect over an entire experimental run was thought to be insignificant. For experimental runs conducted with the heating tapes in use, the purge

inlet temperature was adjusted to be similar to the column temperature so as to minimize its effect on the mobile phase temperature. It was observed that the temperature recorded in the transfer line of the mobile phase emerging from a column, was approximately 2 - 3^{o}C lower than the column's wall temperature. Had time permitted, a constant temperature enclosure would have been built to obtain more uniform temperature conditions.

8.3 The Selection of Experimental Operating Conditions

8.3.1 Introduction

The principle of operation of the SCCR4 unit was discussed in Chapter 5 and it has shown that if the packing of the column was moved counter-current to the direction of mobile phase flow at a correct rate, the slowest moving component can be made to travel with the packing, while the faster moving component with the mobile phase. The following sections deal with the development of a model for the prediction of theoretical operating conditions for the separation of a binary mixture (fructose/glucose) feed into two desired products.

8.3.2 The Idealized Case

A schematic diagram of the SCCR4 unit, illustrating the operating flowrates, is given in Figure 8.1. For a binary system, the rate of movement, r_{m_i}, of a component in the mobile phase is proportional to the fraction of its molecules in the mobile phase at equilibrium. Similarly, the rate of movement, r_{s_i}, of the same component in the stationary phase is proportional to the fraction of its molecules in the stationary phase at equilibrium

Fig. 8·1 Schematic Diagram Of SCCR4 Unit

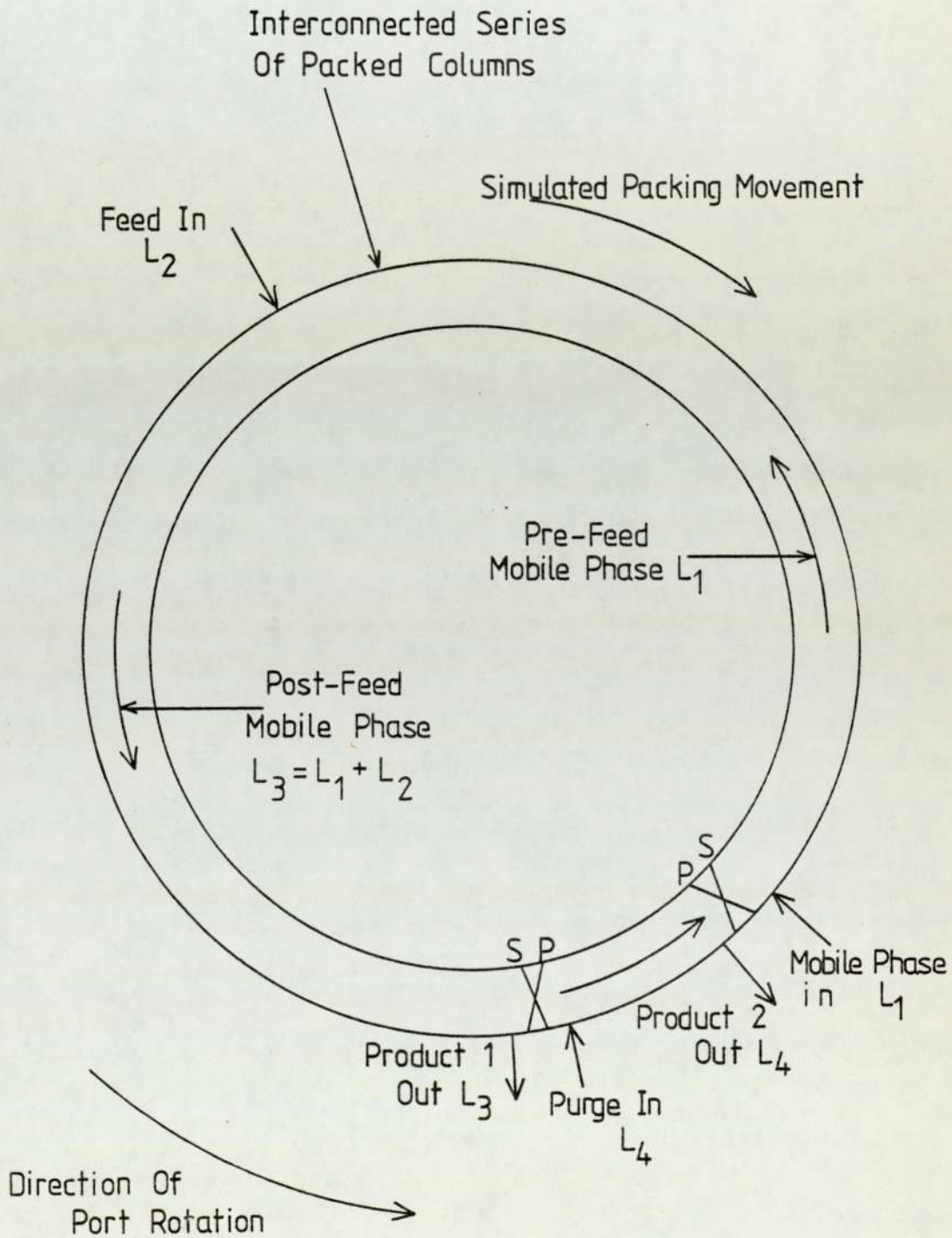

S-S Separation Section

Product 1 — Glucose-Rich

P-P Purge Section

Product 2 — Fructose-Rich

$$r_{m_i} = V_{m_{AV}} \quad \frac{A_m}{A_m + A_s K_{D_i}} \qquad (8.1)$$

$$r_{s_i} = V_{s_{AV}} \quad \frac{A_s K_{D_i}}{A_m + A_s K_{D_i}} \qquad (8.2)$$

$V_{m_{AV}}$ = average velocity of mobile phase = $\frac{L'}{A_m}$

L' = effective mobile phase flowrate

$V_{s_{AV}}$ = average velocity of stationary phase = $\frac{P}{A_s}$

P = stationary phase flowrate

A_m = average cross-sectional area of pores and interstices in column

A_s = average cross-sectional area of resin matrix in column.

In the SCCR4 machine, movement of the stationary phase is achieved by sequencing each packed column, by one position, at the end of every switching interval. As each column contains mobile phase in both the pores and interstices, the mobile phase rate is effectively reduced. Hence

$$L' = L_i - \frac{A_m . l}{S}$$

L' = effective mobile phase flowrate

$L_i = L_1$ or L_3 = recorded mobile phase flowrate.

l = length of one SCCR4 column

S = time of one sequencing interval.

A molecule will travel preferentially with the mobile phase if $r_{m_i} > r_{s_i}$ or

$$\frac{L'}{A_n} \cdot \frac{A_m}{A_m + A_s K_{D_i}} > \frac{P}{A_s} \cdot \frac{A_s K_{D_i}}{A_n + A_s K_{D_i}} \qquad (9.3)$$

or $\frac{L'}{P} > K_{D_i}$

Similarly a molecule will travel preferentially with the stationary phase if

$$\frac{L'}{P} < K_{D_i}$$

For complete separation of two components, 1 and 2:

$$K_{D_1} < \frac{L'}{P} < K_{D_2}$$

Also, for the least adsorbed component to be completely purged from the isolated section if:

$$L_4 > \frac{l(A_m + A_s . K_{D_i})}{s} \qquad (8.4)$$

or $\frac{L_4'}{P} > K_{D_i}$

where $L_4' = L_4 - \frac{A_m . l}{s}$

$P = \frac{A_s . l}{s}$

8.3.3 The Practical Case

Factors which cause departure from the idealized case are:

i) Chromatographic zone broadening.

ii) Finite column length

iii) The sequential nature of operation

iv) Finite feed flowrate

v) Finite feed concentration.

8.3.3.1 Zone Broadening

Zone broadening in chromatography was discussed in Chapter 2. This has the effect of causing a component with a K_D value K_{D_i} to elute from a chromatographic column over a range of K_D values, from $K_{D_i} - \delta_i$ to $K_{D_i} + \delta_i$, where $2\,\delta_i$ is the total baseline peak width, in K_D units. Therefore, the L'/P ratio must be restricted within a narrower range for a successful separation:

$$K_{D_1} + \delta_1 < \frac{L'}{P} < K_{D_2} - \delta_2 \qquad (8.5)$$

Also, in the purge section, the purge rate must be increased:

$$\frac{L_4}{P} > K_{D_2} + \delta_2 \qquad (8.6)$$

8.3.3.2 Finite Column Length

Column length is of prime significance in determining whether a successful separation can be achieved when operating the unit at specific flow conditions. As the $L'/_P$ ratio selected approaches either the value of K_{D_1} or K_{D_2}, the tendency for both components to move in opposing directions is reduced. The separation becomes increasingly difficult and a larger column length is necessary to achieve the same degree of separation. As such, for a finite column length, the range of $L'/_P$ values for a successful separation is narrower than that specified by K_{D_1} and K_{D_2}:

$$K_{D_1} + \delta_1 + \delta_1' < \frac{L'}{P} < K_{D_2} - \delta_2 - \delta_2' \qquad (8.7)$$

8.3.3.3 The Sequential Nature of the SCCR4 Unit

The counter-current movement of the stationary phase relative to the mobile phase is imposed by the discontinuous stepping of port functions around the ten linked columns. Such system of operation must further reduce the range of $L'/_P$ ratio

$$K_{D_1} + \delta_1 + \delta_1' + \delta_1'' < \frac{L'}{P} < K_{D_2} - \delta_2 - \delta_2' - \delta_2'' \qquad (8.8)$$

8.3.3.4 Finite Feed Flowrate

Figure 8.1 illustrates the existence of a pre-feed-point and a post-feed-point mobile phase flowrates (L_1 and $L_3 = L_1 + L_2$) during SCCR4 operations. This is because the feed has to be introduced in a finite volume. To minimize the effect of flow discontinuity, $L_1 >> L_2$. However, it is desirable to maintain a high L_2 so as to increase the feed throughput. Consequently, a compromise between throughput and product purity is necessary. The limit for complete separation is now defined by

$$K_{D_1} + \delta_1 + \delta_1' + \delta_1'' < \frac{L_1'}{P} < \frac{L_3'}{P} < K_{D_2} - \delta_2 - \delta_2' - \delta_2'' \qquad (8.9)$$

8.3.3.5 Finite Feed Concentration

There is a possible K_D (distribution coefficients of fructose) dependency on feed concentration. However, currently no experimental data on the subject is available. If such an effect is found, equation 8.9 would have to be modified accordingly.

8.3.4 Method Used for Selection of SCCR4 Settings

Equation 8.9 represents the ideal limits for the

resolution of two components. However, use of this equation demands detailed knowledge of the parameters involved, which in turn would require an extensive experimental and theoretical study. In practice, the operating conditions in the separating section were set with the mean value of $L_1'/_P$ and $L_3'/_P$ as follows;

$$K_{D_1} < \frac{L'_{mean}}{P} < K_{D_2}$$

In the purge section $\frac{L_4}{P} >> K_{D_2}$ was chosen to ensure a complete purging of the more adsorbed (Fructose) product. Table 8.1 shows the $\frac{L'}{P}$ values for all the experimental runs conducted during this research programme.

8.4 The Continuous Separation of Fructose from Glucose

8.4.1 Scope of Experimental Study

The objectives of the SCCR4 experimental programme may be summarized as follows:

i) Continuously separate a feed mixture containing approximately equal amounts of glucose and fructose into a glucose-rich product and a fructose-rich product.

ii) Investigate various operating conditions so as to reduce the loss of the fructose in the feed in the glucose-rich product stream.

iii) Determine the maximum throughput of glucose/fructose feed with the existing SCCR4 unit.

iv) To study the performance of SCCR4 unit under dilute feed concentration conditions.

v) Reduce the purge flowrate as far as practicable so as to increase the solid content of the fructose-rich product.

vi) Study the effect of mobile phase temperature on separation efficiency in terms of product's purities and loss of fructose in the feed in the glucose-rich product.

8.4.2 Experimental Operating Conditions

Table 8.1 summarizes the average experimental

Table 8.1 Experimental Operating Condition Of All SCCR4 Runs

RUN NUMBER	S SWITCH TIME	TEMPERATURE (AV.)		CONC. OF FEED		P PACKING SWITCH RATE	FEED FLOW RATE	ELUENT / FEED FLOW RATIO	SEPARATING SECTION							PURGE SECTION	
									PRE FEED SECTION			POST FEED SECTION			MEAN	FLOW	
		ELUENT	PURGE	GLUCOSE	FRUCTOSE				L_1	L_1'	L_1'/P	L_3	L_3'	L_3'/P	L'/P	L_4	L_4/P
	MIN	C°	C°	g. CM^{-3}	g. CM^{-3}	$CM^3\ MIN^{-1}$	$CM^3\ MIN^{-1}$		$CM^3\ MIN^{-1}$	$CM^3 MIN^{-1}$		$CM^3\ MIN^{-1}$				$CM^3 MIN^{-1}$	
45 - 1 - 4 - 29	45	29.5	70.0	0.23	0.22	3.66	1.0	4.1	4.1	0.65	0.18	5.1	1.65	0.45	0.315	300	82
49 - 1 - 6 - 29	30	29.5	70.0	0.24	0.25	5.48	1.0	6.3	6.3	1.13	0.20	7.3	2.13	0.39	0.29	293	53.5
49 - 2 - 4 - 29	30	29.5	70.0	0.24	0.25	5.48	2.0	3.05	6.1	0.93	0.17	8.1	2.93	0.53	0.35	293	53.5
49 - 3 - 6 - 29	30	29.5	70.0	0.24	0.25	5.48	3.0	2.03	6.1	0.93	0.17	9.1	3.93	0.72	0.445	293	53.5
49 - 3 - 6 - 20D	30	20.0	40.0	0.24	0.25	5.48	3.0	2.0	6.0	0.83	0.15	9.0	3.83	0.70	0.425	30	5.5
02 - 2.4 - 6 - 29	30	29.5	70.0	0.012	0.0095	5.48	2.4	2.54	6.1	0.93	0.17	8.5	3.33	0.60	0.385	289	52.3
52 - 2 - 6 - 38	30	38.0	34.0	0.27	0.25	5.48	2.0	3.05	6.1	0.93	0.17	8.1	2.93	0.53	0.35	210	38.3
52 - 2 - 6 - 44	30	44.0	46.0	0.27	0.25	5.48	2.0	3.05	6.1	0.93	0.17	8.1	2.93	0.53	0.35	290	52.9
52 - 2 - 6 - 65	30	65.0	70.0	0.27	0.25	5.48	2.0	3.05	6.1	0.93	0.17	8.1	2.93	0.53	0.35	290	52.9

operating conditions for fructose/glucose separations performed during this research programme. Details of individual run conditions are given in Tables (2-10) of Appendix 4. The experimental run number consists of four groups of digits as shown below;

49-2-6-29

The first group of digits, 49, signifies the feed concentration (w/v %); the second group, 2, refers to the feed flowrate; the third group, 6, refers to the mobile phase flowrate ($cm^3\ min^{-1}$); whilst the last group of digits, 29, represents the average mobile phase temperature (^oC).

Due to the possible industrial link of this research project with the glucose isomerase process, the experimental programme undertaken was aimed at maximizing throughput at feed concentrations of about 50% w/v. Hence, the concentrations of the feed solutions employed in SCCR4 study were all of approximately 50% w/v, except for Run No. 02-2-6-29, which was undertaken as a base case run under dilute feed concentration conditions.

Information obtained from preliminary runs that have not been recorded in the thesis indicated that, with a mobile phase flow/feed flow ratio between 4 - 6 and values of $L'_1/_P$ = 0.18 and $L'_3/_P$ = 0.75, would achieve

products of purities in the region of 90% w/w. Consequently, the first experimental run (No. 45-1-4-29) was conducted with a feedrate of 1 cm^3 min^{-1} and a mobile phase flowrate of 4.1 cm^3 min^{-1}. The switch time was set at 45 minutes so as to achieve the desired $\frac{L_1'}{P}$ and $\frac{L_3'}{P}$ values.

The next three runs (49-1-6-29, 49-2-6-29, 49-3-6-29) were conducted with an aim to determine the maximum throughput possible with the SCCR4 unit at fixed feed concentration, eluent rate and temperature conditions. From the previous run (45-1-4-29), it was realised that a switch time of 45 minutes had led to a cycle time of 7½ hours which would in turn result in a complete run (including feed preparation, final purging and product analysis) to last over three weeks. From a separate purging experiment conducted during the preliminary study, it was found that a time period between 25 - 30 minutes was sufficient for the complete purging of an SCCR4 column. Hence, in order to optimize on the overall operation time, it was decided to reduce the switch time by one third to 30 minutes. However, in order to maintain approximately the same $\frac{L_1'}{P}$ and $\frac{L_3'}{P}$ values, the mobile phase flowrate was increased by one-third to approximately 6 cm^3 min^{-1}. The feed concentration was 49% w/v (24% w/v glucose and 25% w/v fructose) and the feed flowrates were

1, 2, 3 cm^3 min^{-1} respectively for Run No. 49-1-6-29, 49-2-6-29 and 49-3-6-29. With the mobile phase flowrates of all three runs being kept at 6 cm^3 min^{-1}, their respective mobile phase/feed ratios were approximately 6/1, 3/1, and 2/1:

Run No. 49-3-6-20-D (the letter D signifies a lower purge rate) was conducted to investigate the effect of a reduced purge flowrate on the separation performance of the SCCR4 unit. From an individual viewpoint, a high solid content of fructose-rich product (purge product) would mean lower evaporation costs.

The effect of a low feed concentration on separation performance was studied in Run No. 02-2-6-29.

The final three experimental runs (52-2-6-38, 52-2-6-44, 52-2-6-65) were conducted with a view to examining the effect of mobile phase temperature on the performance of the SCCR4 unit. The average mobile phase temperatures of the three runs were 38°C, 44°C and 65°C respectively. To enable the results of these runs to be compared to that obtained previously with the lower mobile phase temperature of 29°C, the $\frac{L_1'}{P}$ and $\frac{L_3'}{P}$ values were set to be the same as Run No. 49-2-6-29.

8.4.3 Experimental Results and Discussions

Summaries of the experimental operating conditions

Table 8.2 Summaries Of Experimental Results Of SCCR4 Runs

RUN NUMBER	AVERAGE PRESSURE DROP			AVERAGE TEMPERATURE		FLOWRATES			FEED CONC.		G-RICH PRODUCT CONC.		F-RICH PRODUCT CONC.		G-RICH PRODUCT PURITY		F-RICH PRODUCT PURITY		MASS BALANCE (OUT/IN)		INPUT FRUCTOSE LOST IN GLUCOSE – RICH PRODUCT
	ELUENT	PURGE	FEED	ELUENT	PURGE	ELUENT	PURGE	FEED	G.	F.	G.	F.	G.	F.	G.	F.	G.	F.	G.	F.	
	$kN \cdot m^{-2}$			°C		$CM^3 \cdot MIN^{-1}$			$Mg \cdot CM^{-3}$		$Mg \cdot CM^{-3}$		$Mg \cdot CM^{-3}$		%		%		%		%
45 - 1 - 4 - 29	120	179.1	82.7	29.5	70.0	4.1	300	1.0	0.23	0.22	45	3.25	0.09	0.84	93.4	6.6	9.7	90.3	98.9	109.9	6.67
49 - 1 - 6 - 29	160.3	185.0	83.0	29.5	70.0	6.3	293	1.0	0.24	0.25	30	2.4	0.115	0.84	92.6	7.4	12.0	88.0	102.9	105.1	6.8
49 - 2 - 6 - 29	186.0	192.9	99.8	29.5	70.0	6.1	293	2.0	0.24	0.25	58	3.85	0.30	1.7	93.8	6.2	15.0	85.6	112.5	100.0	6.01
49 - 3 - 6 - 29	221.0	231.0	128.3	29.5	70.0	6.1	293	3.0	0.24	0.25	65	10.2	0.28	2.2	86.4	13.6	11.3	88.7	95.7	97.1	12.8
49 - 3 - 6 - 20D	280.0	73.0	129.0	20.0	40.0	6.0	300	3.0	0.24	0.25	65	5.2	3.6	21.9	92.6	7.4	13.4	86.6	99.7	93.6	6.5
02 - 24 - 6 - 29	102.0	150.5	50.1	29.5	70.0	6.1	287	2.4	0.012	00095	3.4	0.315	0.007	0.064	91.5	8.5	9.8	90.2	103.0	103.0	11.28
52 - 2 - 6 - 38	160.8	140.4	89.6	38.9	34.0	6.1	210	2.0	0.27	0.25	61	12.4	0.25	1.9	83.1	16.9	11.6	88.4	104.1	101.5	20.7
52 - 2 - 6 - 44	110.2	241.5	62.0	44.0	46.0	6.1	290	2.0	0.27	0.25	63	18.0	0.16	1.2	77.8	22.2	11.8	88.2	104.6	99.23	29.64
52 - 2 - 6 - 65	82.68	200.0	41.3	65.0	70.0	6.1	290	2.0	0.27	0.25	65	22.0	0.16	1.1	74.7	25.3	14.1	85.9	106.8	99.7	35.5

and results together with the concentration profiles for the nine runs conducted are given as Table (8.2) and Figure (8.2-8.10). In these profiles, the concentrations of glucose and fructose were obtained by dividing the amounts of glucose and fructose collected from individual columns at the end of each experimental run by the total mobile phase volume in a particular column. Given in Table 1 of Appendix 4 is an account of the amounts of glucose and fructose purged from each column at the end of all SCCR4 runs. Finally, a complete record of details of individual runs is to be found in Table 2 - 10 of Appendix 4.

8.4.3.1 Continuous Separation of Glucose/Fructose

The first experimental run (No. 45-1-4-29) recorded in detail in this thesis, was performed with a mobile phase/feed flow ratio of 4/1 and a mean $L'/_p$ value of 0.315. The purities of the glucose-rich and fructose-rich products were 93.4% w/w and 90.3% w/w respectively (Table 8.2). The amount of input fructose lost in the glucose-rich product was 6.67%. From the concentration profile (Figure 8.2), the 'cross-over' point of the two products' profiles was shown to be located in the feed column. The leading edge of the fructose profile dropped sharply, after the feed column, in the post-feed

Fig. 8.2 EXPERIMENTAL CONCENTRATION PROFILE OF RUN NO. = 45-1-4-29

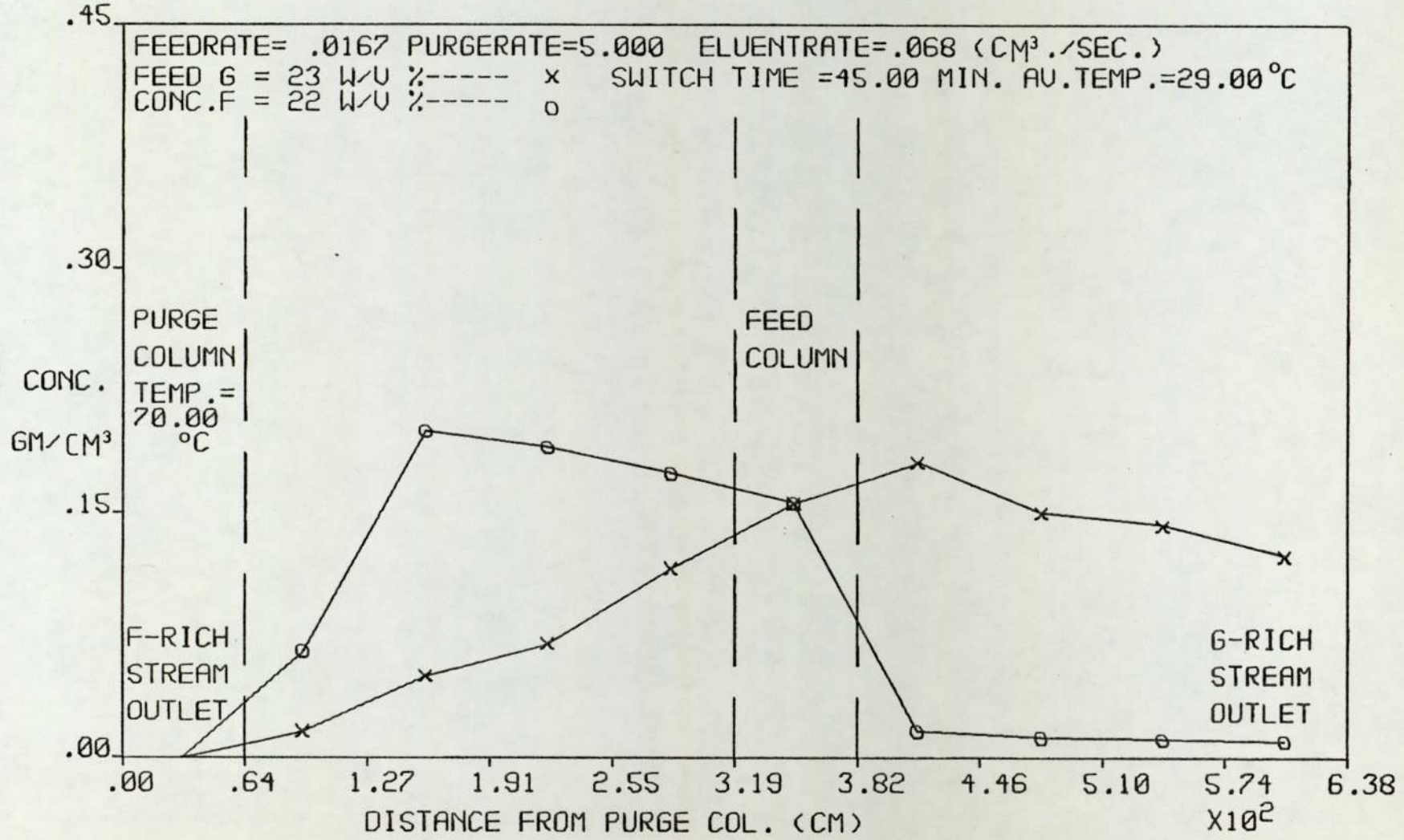

separation section and a glucose product purity of 93.4% w/w was obtained. The trailing edge of the glucose profile dropped less sharply but towards the fructose-rich outlet and led to a contamination of glucose in the fructose-rich product of 9.7% w/w. As such, this run was considered to be a successful indication of the possible use of the SCCR4 unit for glucose/fructose separations.

8.4.3.2 Change of Feedrate

Three experimental runs were conducted (No. 49-1-6-29, 49-2-6-29, 49-3-6-29) and the results (Table 8.2) show that by increasing the feedrate from 1 cm^3 min^{-1} to 2 cm^3 min^{-1}, no significant changes were observed in both the glucose-rich ($\sim$93% w/w) and the fructose-rich product ($\sim$85.0% w/w). Similarly, losses of input fructose to the glucose-rich product for both runs were approximately equal (6.8% for Run No. 49-1-6-29 and 6.01% for Run No. 49-2-6-29). However, from the concentration profiles (Figures 8.3, 8.4, 8.5), a difference in the location of the cross-over point was detected. In the concentration profile for Run No. 49-1-6-29 (Figure 8.3), the 'cross-over' point was found to be shifted slightly away from the feed column, towards the fructose-rich product outlet. In general, if the SCCR4 unit is operated under correct conditions, the optimum location of the cross-over point

Fig. 8.3 EXPERIMENTAL CONCENTRATION PROFILE OF RUN NO. = 49-1-6-29

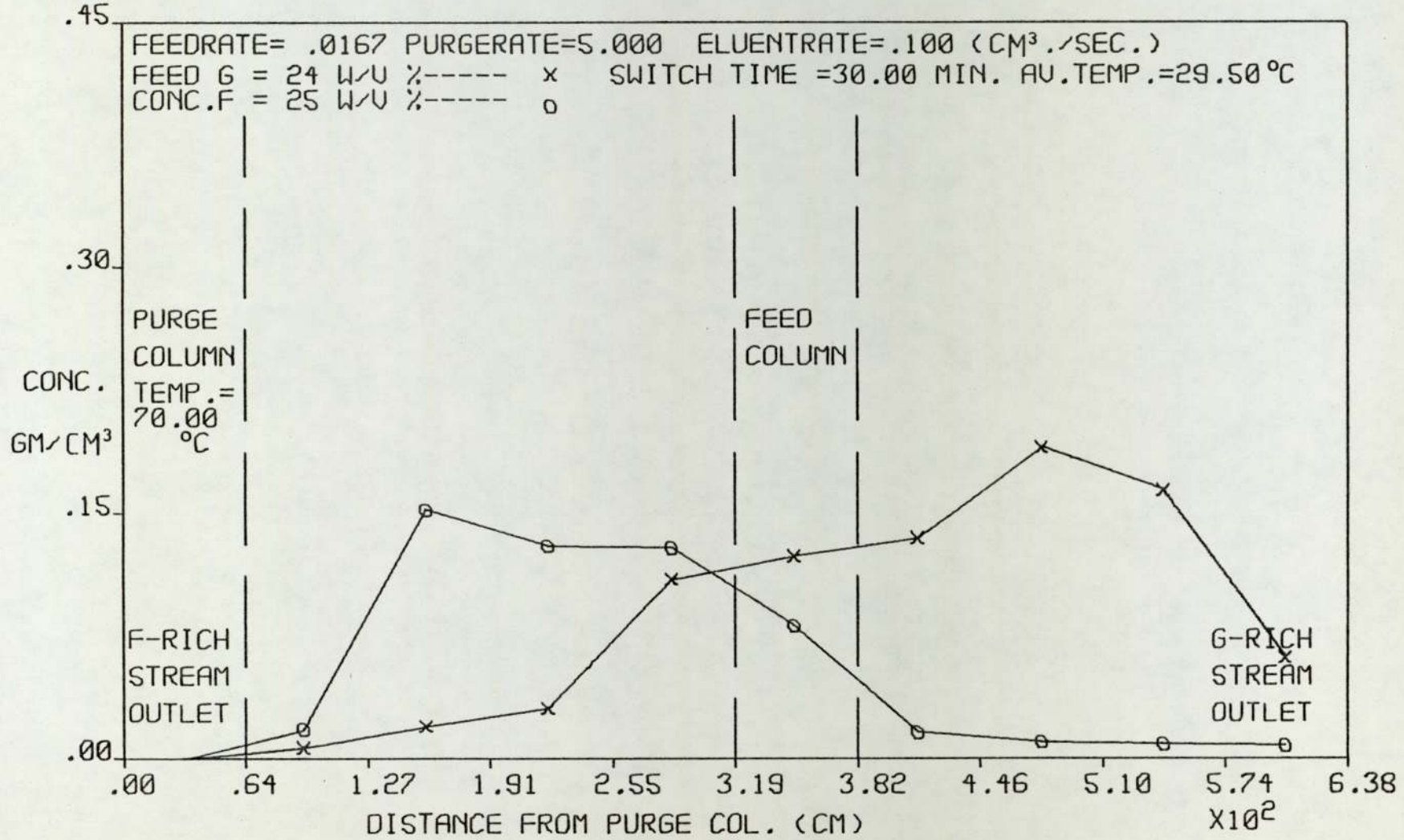

Fig. 8.4 EXPERIMENTAL CONCENTRATION PROFILE OF RUN NO. = 49-2-6-29

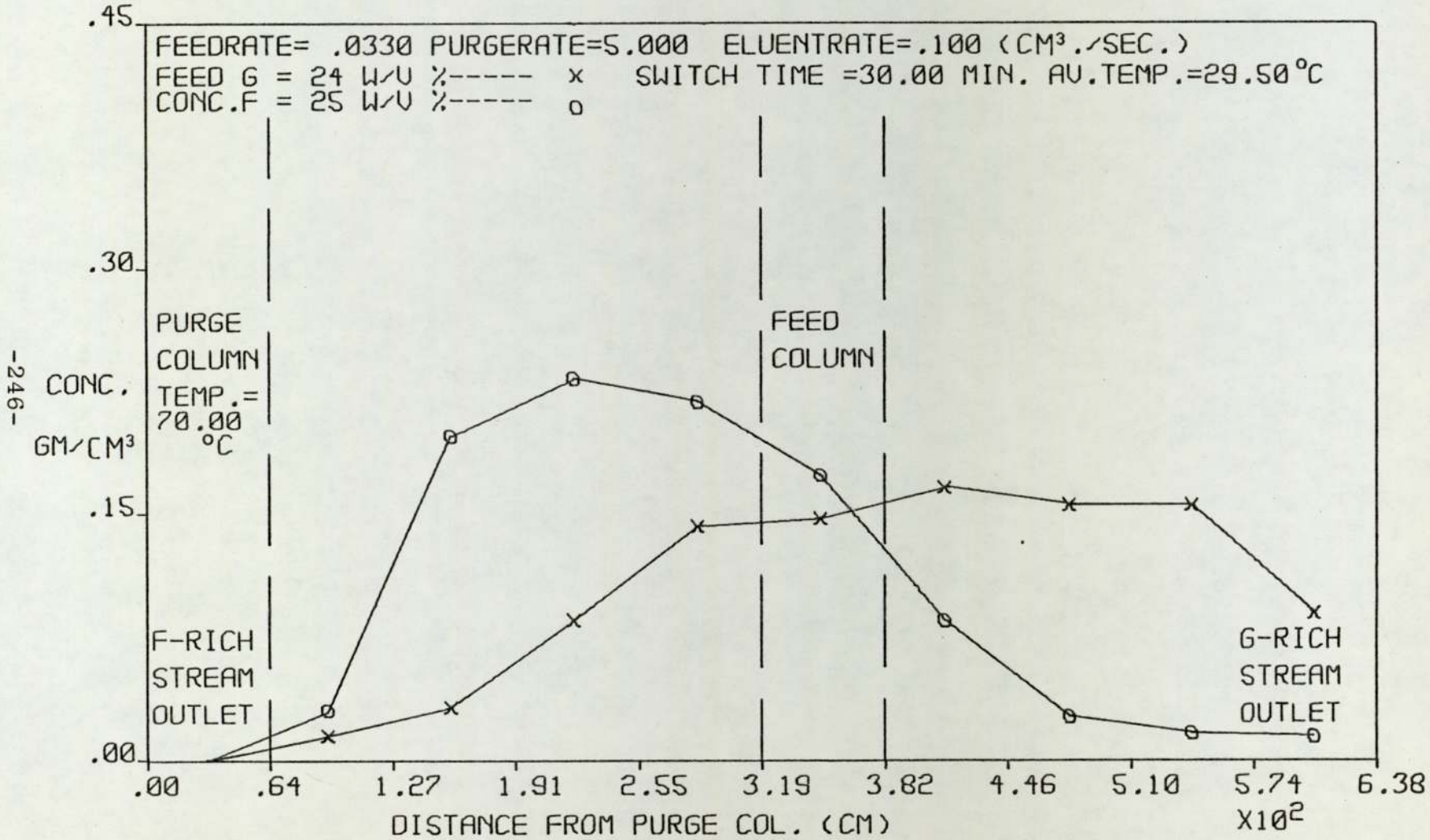

Fig. 8.5 EXPERIMENTAL CONCENTRATION PROFILE OF RUN NO. = 49-3-6-29

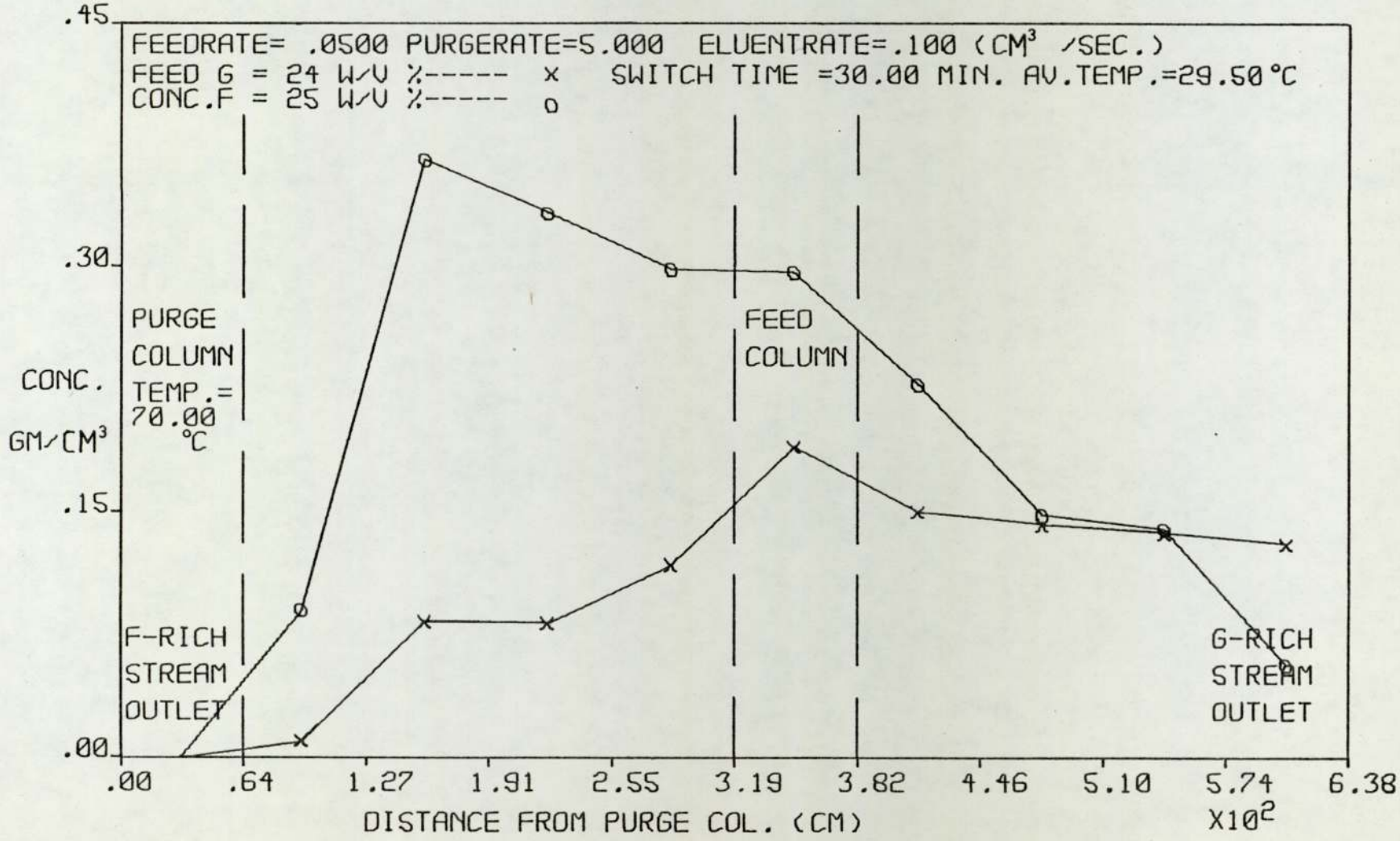

is thought to be in the feed column. A shift of this 'cross-over' point towards either the glucose-rich or fructose-rich product outlet could lead to a higher contamination of the corresponding product. However as the shift of the 'cross-over' point in Run No. 49-1-6-29 was very marginal, no significant deterioration in the fructose-rich products' purity was recorded. The reason for this shifting was the use of a lower value of $\frac{L'}{P}$ (0.29). In run No. 49-2-6-29, a higher $\frac{L'}{P}$ value (0.35) was employed and the 'cross-over' point was noted (Figure 8.4) to be in the feed column. While in Run No. 49-3-6-49, the $\frac{L'}{P}$ value was set to be even higher (0.445). Consequently the 'cross-point' was found to be pushed very close to the glucose-rich product outlet and resulted in the purities of this product dropping to 86.4% w/w. In addition, such a high post feed flowrate (9.1 cm^3/min) has also caused a higher loss of fructose in the glucose-rich product (12.8% w/w). In subsequent simulation work (Section 9.2) it was shown that under such operating conditions, a feedrate of 3 cm^3 min^{-1} of 49% w/w glucose/fructose was near to the maximum throughput possible with the SCCR4 unit. At a 4.5 cm^3 min^{-1} feedrate, the computer model (Section 9.4.2 and Figure 9.8, 9.9, 9.10) simulated a complete breakthrough of both solute profiles resulting in a high contamination of the glucose-rich product by fructose.

8.4.3.3 The Effect of Purge Flowrate

In all previous runs, a $(\frac{L_4}{P})$ value of 53 was used to ensure a complete purging of the isolated column. However, this had led to a very diluted fructose-rich product, approximately 0.2 - 0.25% w/v of total solids. Run No. 49-3-6-20-D was conducted under operating conditions similar to Run No. 49-3-6-29 except with the $\frac{L_4}{P}$ value being set at 5.5 and the purge temperature to 40°C. The lowering of the purge flowrate was expected to leave behind some fructose in the isolated column and thereby have a detrimental effect on the purity of the glucose-rich product. However, results from this run (Table 8.2), when compared with that of Run No. 49-3-6-29, revealed not only an improvement in the glucose-rich product purity (from 86.4% w/w for Run No. 49-3-6-29 to 92.6% w/w for Run No. 49-3-6-20-D), but also a reduction in the loss of input fructose in the glucose-rich product (from 12.8% for Run No. 49-3-6-29 to 6.5% for Run No. 49-3-6-20-D). These differences are thought to occur mainly from the fact that by employing a purge liquid temperature of 40°C, a lower mobile phase temperature (20°C) was achieved. In a subsequent experimental study (Section 8.4.3.5) it was established that as the mobile phase temperature increases, the 'cross-over' point of the

Fig. 8.6 EXPERIMENTAL CONCENTRATION PROFILE OF RUN NO. = 49-3-6-20-D

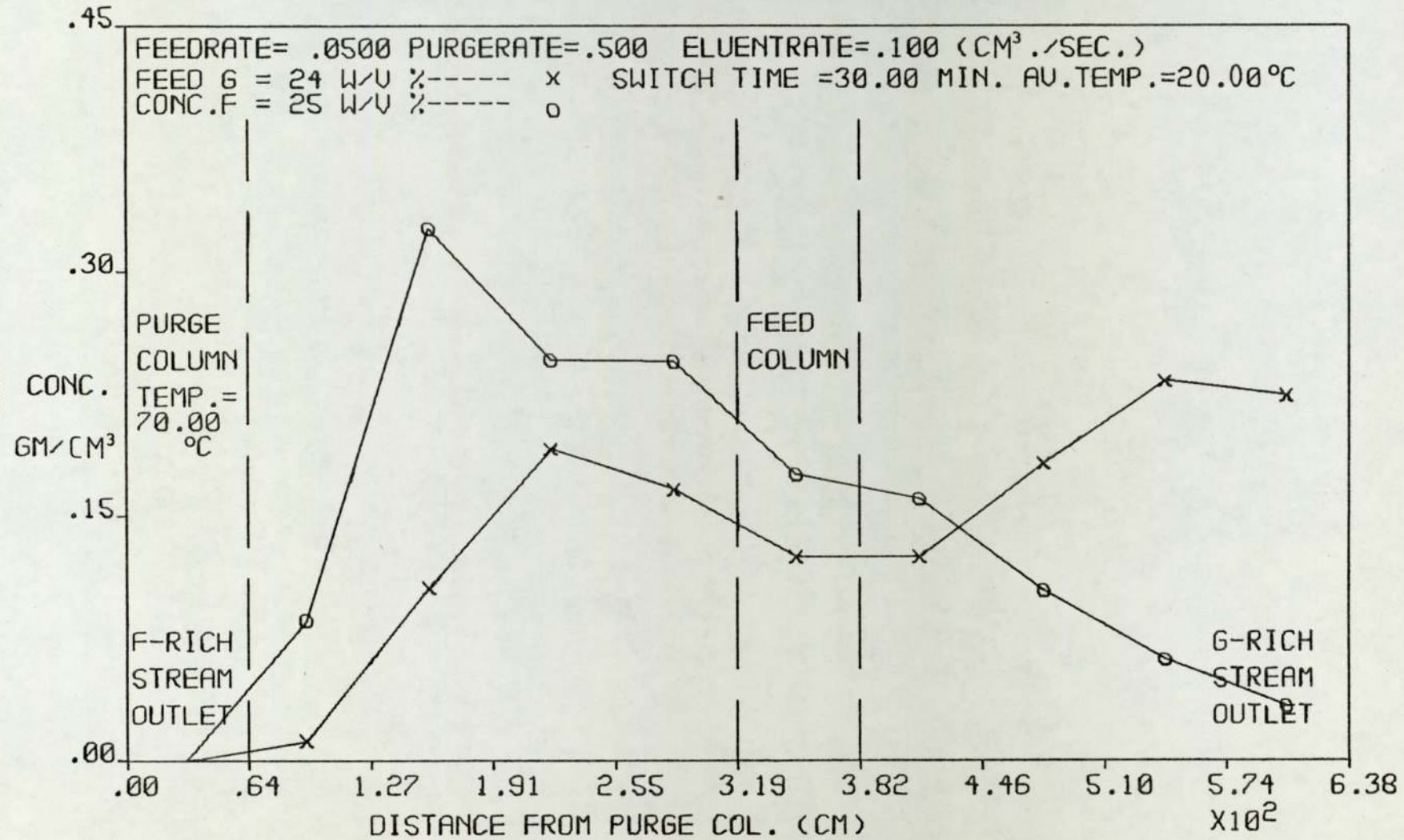

solute profiles shifts more towards the glucose-rich product outlet, resulting in a greater amount of fructose present in the glucose-rich product. As the mobile phase temperature dropped from 29°C to 20°C, the 'cross-over' point in the profile (Figure 8.6) for Run No. 49-3-6-20-D was found to be in the post feed point separation section but nearer to the feed column than that of Run No. 49-3-6-29. This accounts for an improvement in the glucose-rich product purity. Unfortunately, with the drop in the mobile phase temperature, a comparison of results between Run No. 49-3-6-20-D and Run No. 49-3-6-29 can not therefore be employed as a true representation of the effect of reducing purge flowrate on the separation performance of the SCCR4 unit. However, on the evidence that no significant deterioration was resulted in the fructose-rich product (86.6% w/w for Run No. 49-3-6-20-D and 88.7% w/w for Run No. 49-3-6-29) and that a total solid content of 2.5% w/w was achieved as the purge flowrate was reduced from 293 cm^3 min^{-1} to 30.0 cm^3 min^{-1}, the separation of a glucose/fructose feed solution into a fructose-rich product of 2-3% solid with the SCCR4 unit appeared possible.

8.4.3.4 The Study of the SCCR4 Unit Performance Under Dilute Feed Concentration Conditions

Run No. O2-2.4-6-29 was performed with a feed concentration of 1.2% w/w glucose and 0.95% w/w fructose and a mean $\frac{L'}{P}$ value of 0.385. In the previous experimental study on the effect of feedrate (Section 8.4.3.2), it was shown that as the mean $\frac{L'}{P}$ value increases from 0.35 (for Run No. 49-2-6-29; Figure 8.4) to 0.445 (for Run No. 49-3-6-29; Figure 8.5) the 'cross-over' point of solute profiles was shifted from the feed column into the post feed separation section next to the glucose-rich product outlet. With a mean $\frac{L'}{P}$ setting of 0.385, the profile 'cross-over' point of Run No. O2-2.4-6-29 was shown to be located in the post feed separation section between that of Run No. 49-2-6-29 and Run No. 49-3-6-29. Consequently, the purity of the glucose-rich product and the loss of fructose in the feed in glucose-rich product were shown to be between that of Run No. 49-2-6-29 and Run No. 49-3-6-29. (The purity of glucose-rich product and the loss of fructose in the feed in glucose-rich product were 93.8% w/w, 91.5% w/w, 86.4% w/w and 6.01% w/w, 11.28% w/w, 12.8% w/w respectively for Run No. 49-2-6-29, 49-3-6-29, O2-2.4-6-29).

However a comparison between the purities of the fructose-rich product of the above three experimental runs reveal a slight improvement for Run No. O2-2.4-6-29

Fig. 8.7

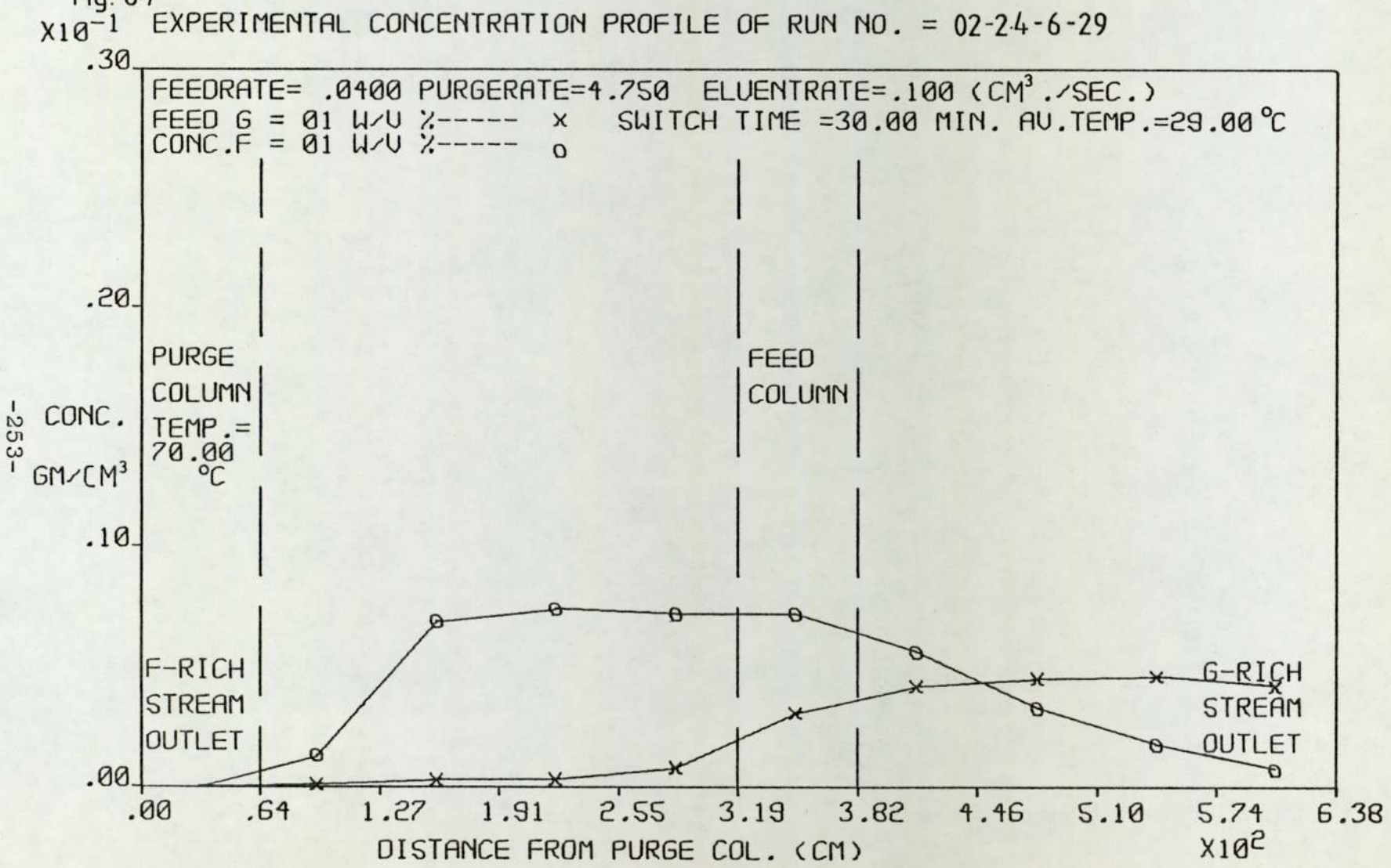
X10⁻¹ EXPERIMENTAL CONCENTRATION PROFILE OF RUN NO. = 02-24-6-29
FEEDRATE= .0400 PURGERATE=4.750 ELUENTRATE=.100 (CM³./SEC.)
FEED G = 01 W/V %----- x SWITCH TIME =30.00 MIN. AV.TEMP.=29.00 °C
CONC.F = 01 W/V %----- o
.30
.20
.10
.00
CONC. GM/CM³
PURGE COLUMN TEMP.= 70.00 °C
FEED COLUMN
F-RICH STREAM OUTLET
G-RICH STREAM OUTLET
.00 .64 1.27 1.91 2.55 3.19 3.82 4.46 5.10 5.74 6.38
DISTANCE FROM PURGE COL. (CM)
X10²

where dilute feed rate conditions prevailed. In the experimental concentration profile (Figure 8.7), such an improvement in the purity of the fructose-rich product was shown to be due to a sharper drop of the trailing edge of the glucose profile. This could probably stem from the fact that by reducing the feed concentration to 2% w/v, the concentrations of glucose and fructose in all columns were lowered substantially (Figure 8.7) which would have in turn altered the K_D values of the two components. Had time permitted, a full study of the feed concentration effect on both K_D values and SCCR4 separation performance would have been conducted. However, on the evidence of the results of Run No. O2-2.4-6-29, it appears that the SCCR4 unit performs better (in terms of fructose-rich product purity) under dilute feed concentration conditions.

8.4.3.5 The Effect of Mobile Phase Temperature

The flow settings of Run No. 49-2-6-29 were selected for experimental runs to investigate the effect of the mobile phase temperature on the separation performance of the SCCR4 unit. Results of runs (No. 49-2-6-29, 52-2-6-38, 52-2-6-44 and 52-2-6-65) are presented in Table 8.2 and reveal that by operating the SCCR4 unit with elevated mobile phase temperatures, the purity of

Fig. 8.8 EXPERIMENTAL CONCENTRATION PROFILE OF RUN NO. = 52-2-6-38

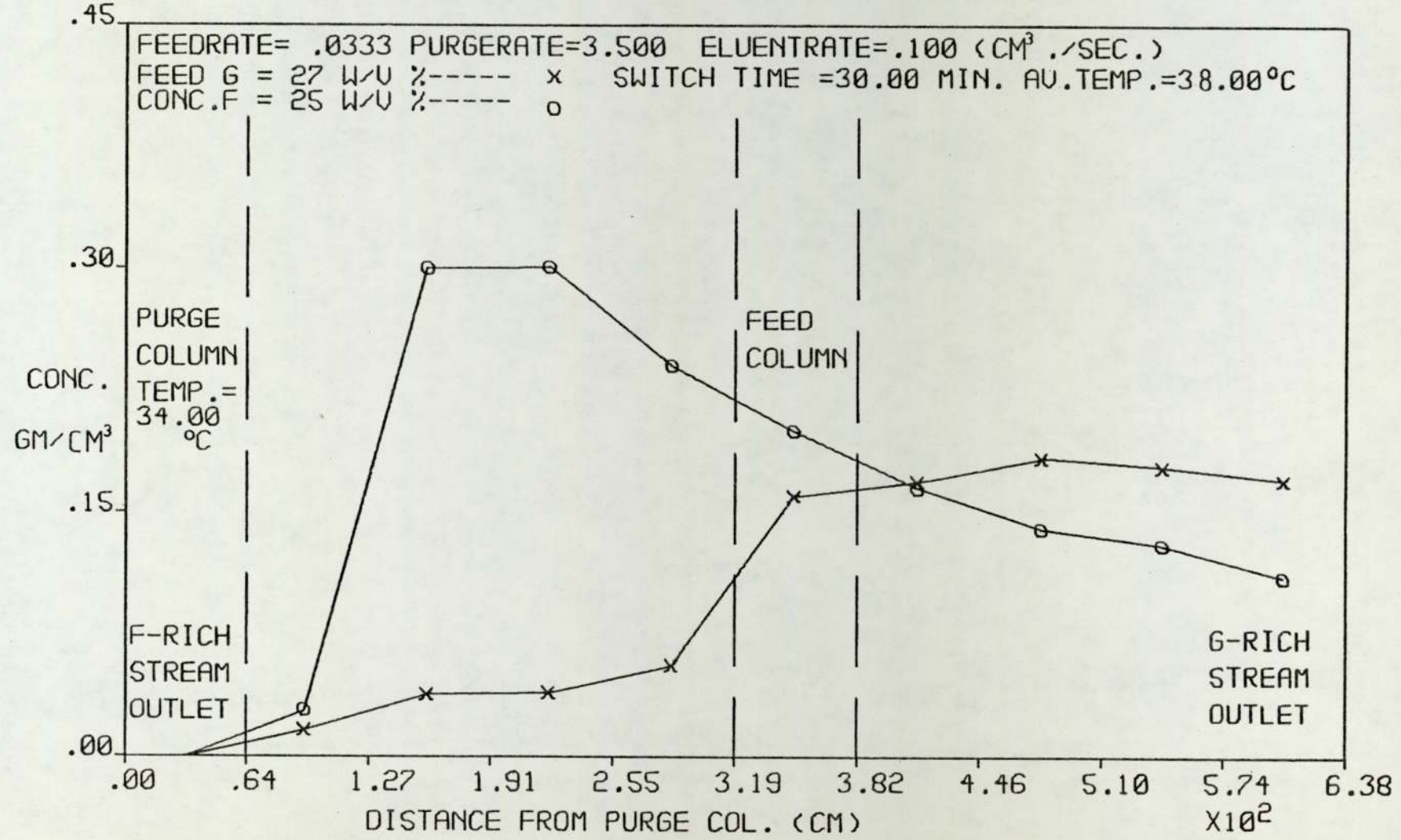

Fig. 8.9 EXPERIMENTAL CONCENTRATION PROFILE OF RUN NO. = 52-2-6-44

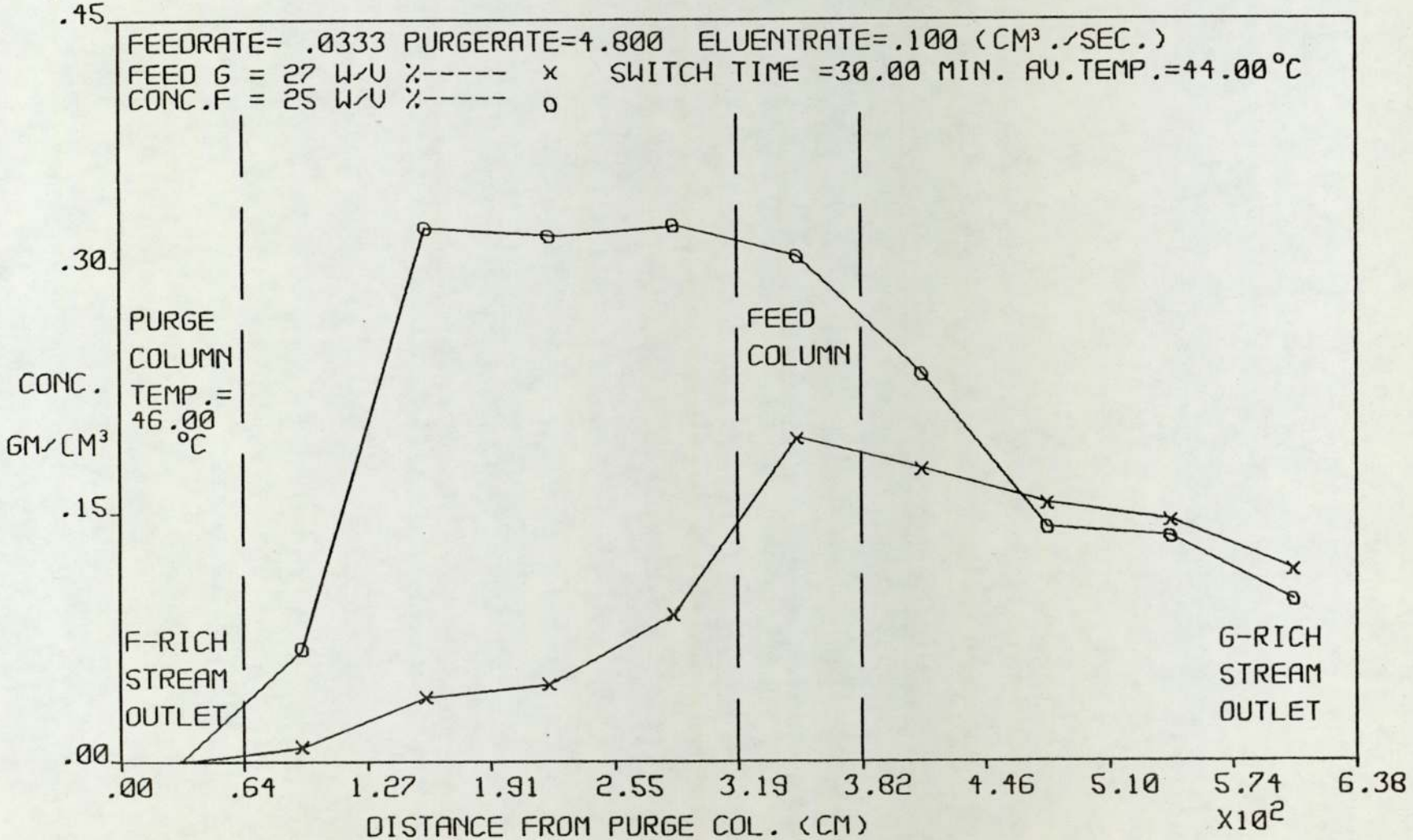

Fig. 8.10 EXPERIMENTAL CONCENTRATION PROFILE OF RUN NO. = 52-2-6-65

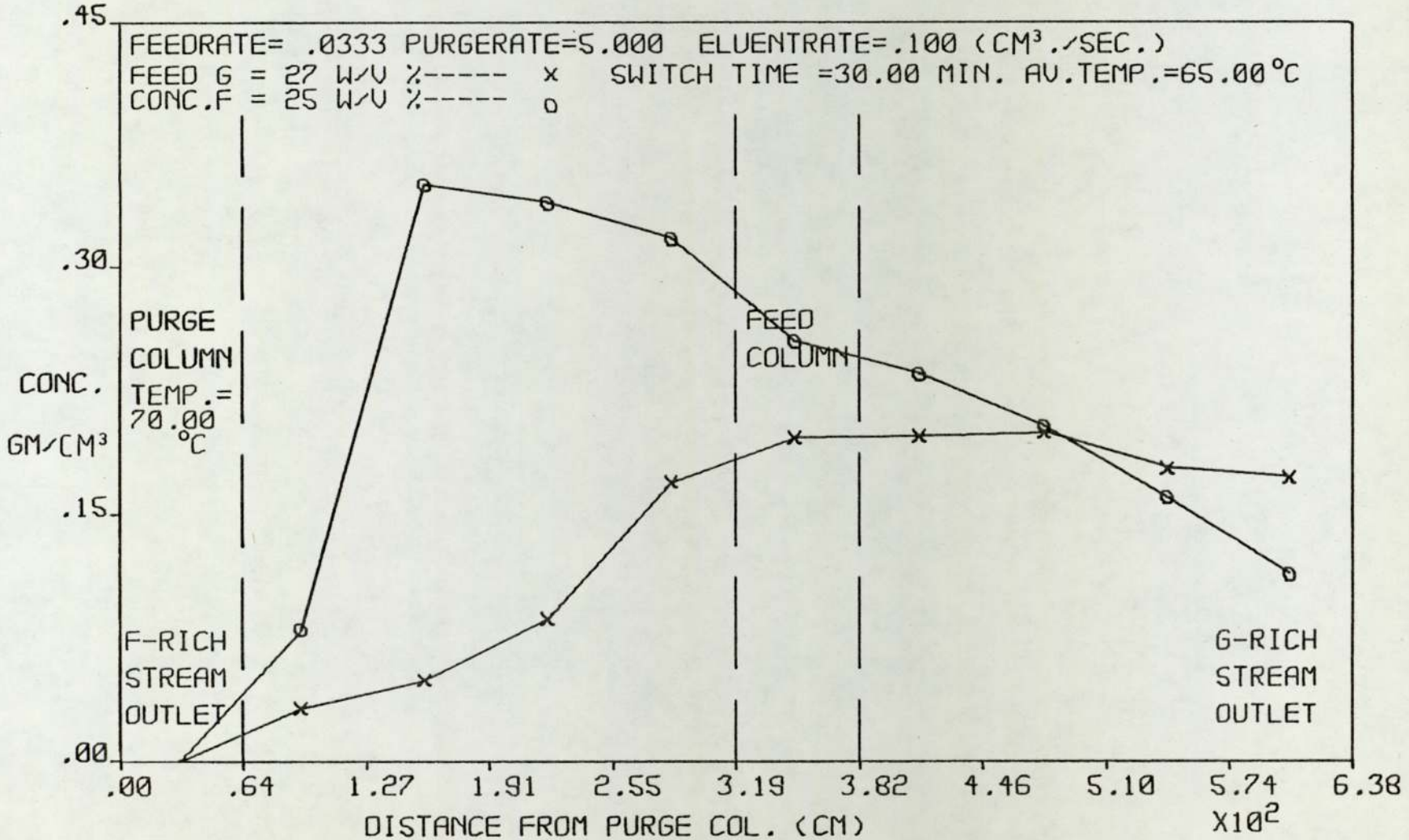

the glucose-rich product drops from 93.8% (at 29°C) to 74.7% (at 65°C). This was coupled with an increase in the loss of input fructose to the glucose-rich product namely, from 6.01% at 29°C to 35.5% at 65°C. However, the purity of the fructose-rich product remained unchanged (approximately 86 - 88% w/w).

The concentration profiles of these runs (Figures 8.4, 8.8, 8.9, 8.10) illustrates a gradual shift of the profile 'cross-over' point towards the glucose-rich product outlet as the mobile phase temperatures increases. In the results of the batch column work (Section 5.3), the K_D value of fructose was found to decrease from 0.617 to 0.456 as the mobile phase temperature increased from 25°C to 52°C. Such a decrease in the K_D value of fructose (K_{D_2}) will effectively reduce the operating range of the SCCR4 unit (Established in Section 8.3 to be between K_{D_1} and K_{D_2}) for possible separation of glucose/fructose. Hence, for experimental runs with a constant mean $\frac{L'}{P}$ setting of 0.35, the 'cross-over' point of the solute profiles are therefore expected to shift towards the glucose-rich product as the temperature of the mobile phase increases. As such, in order to offset the high loss of input fructose in the glucose-rich product in operations conducted with elevated mobile phase temperatures, it is necessary to alter the

corresponding $\frac{L'}{P}$ values so as to bring back the profiles 'cross-over' point into the feed column. Finally, the main benefit of increased operating temperature is a reduction in the pressure drop for both mobile phase and feed flow through the SCCR4 unit. Table 8.2, shows that by increasing the operating temperature from 29°C to 65°C, the mobile phase pressure drop through the equipment was reduced from 186.0 kN m^{-2} to 82.68 kN m^{-2}.

8.4.4 Comparison of the SCCR4 Unit's Performance with the Boehringer Batch Process

Table 8.3 lists some of the equipment features and results of the two processes. Information and results of the Boehringer process were extracted from British Patent No. 1085696. However, since results were obtained on different diameter columns packed with different resins, accurate comparison is not possible. Hence, the listed observations can only be employed as a general guideline to the performance of the two processes.

The main advantage of the batch process over the SCCR4 unit as constructed centred on the possibility of producing a pure fructose product with the batch unit. However, the maximum throughput of the SCCR4 unit on an

Table 8.3 Comparison Of The SCCR4 Unit With The Boehringer Batch Process

	Boehringer Batch Process	SCCR4 Process
No. Of Glass Columns Employed	6 × 15.24 cm I. D.	10 × 2.54 cm I. D.
Total Bed Length For Separation	9 metres	Approx. 5.75 metres
Resin	Dowex 50W×4 in Ca^{++}Form (4 % Linkage)	Zerolit 225 SRC 14 Ca^{++}Form (8 % Linkage)
Feed Concentration	50 % w/v	50% w/v
Maximun Throughput Per Unit Cross-Sectional Area	Based On A 10 Hrs. Run 6.90gm·hr^{-1}·cm^{-2}	16.83 gm·hr^{-1}·cm^{-2}
Mobile Phase Flowrate	1.64 cm^3·min^{-1}·cm^{-2}	Pre Feed = 1.2 Post Feed = 1.8 (cm^3·min^{-1}·cm^{-2})
Products Purities	Pure Glucose Or Pure Frucose Can Be Collected During Either The Inital Or Final Period Of Run	Glucose-Rich Product : 90% Fructose-Rich Product : 88%
Loss Of Input Fructose	30 ~ 40% w/w If Pure Fructose Is To Be Obtained	6 ~ 7% w/w At 29°C
Operating Temperature	60 °C	Between 29 °C ~ 65 °C More Preferrably At 29 °C
Mobile Phase Pressure Drop	Not Available	186 kN·m^{-2} At 29 °C

equivalent area basis was twice that of the batch process. Furthermore, the amount of input fructose lost in the glucose-rich product in SCCR4 operations could be maintained at approximately between 6 - 7% w/w. Whereas, in the batch process, if a pure fructose product was desired, the amount of input fructose lost in one pass through the batch equipment is expected to be about 30 - 40% w/w although this product could be recycled. Finally, a fructose-rich product of solid content 2.5% w/v was shown to be possible with the SCCR4 unit. Unfortunately, no information regarding the concentration of the fructose product from the batch process was published, and direct comparison cannot be made. However, in a study, by England (167) to compare the performance between batch and sequential chromatographic processes, the solid concentration of the purged product from the sequential process was found to be 2 - 3 times richer than that from the batch process when fractionating dextran by gel permeation chromatography.

From these preliminary studies, the SCCR4 type of system appears to provide more promising separation performance, but further experimental work and a proper economic study would need to be undertaken before the superiority of one system over the other can be established.

Chapter 9

Theoretical Treatment of the Continuous Counter-Current Chromatographic Process

9.1 Introduction

9.1.1 Model Based on the 'Equilibrium Stage or Plate' Concept

For the moving-bed form of continuous chromatography, a probabilistic model was proposed by Sciance and Crosser (166) to relate the degree of separation, operating conditions and required column length for a binary feed mixture. For the case when the feed is introduced into the mid-point of the column, the following equations were proposed:

$$\ln (u_Z)_A = \frac{l\, k''_A}{2u} (K_A - \psi) \qquad (9.1)$$

$$\ln \quad 1 - (u_Z)_B \quad = \frac{-l\, k''_B}{2u} (K_B - \psi) \qquad (9.2)$$

A refers to the faster moving component.

B refers to the slower moving component.

$(u_Z)_A$ = Bottom/feed mass flowrate ratio of A.

$(u_Z)_B$ = Tops/feed mass flowrate ratio of B.

k'' = rate constant of desorption.

u = average mobile phase velocity.

ψ = operating mobile phase/stationary phase velocity ratio.

l = required column length.

Use of the above equations rests on knowing values

of k''_A and k''_B. As published values are scarce and the experimental procedures for their determination are usually difficult, the application of this model is very restricted.

Based on the random walk approach (30), Al-Madfai (12) obtained an expression for predicting plate height in continuous 'moving column' counter-current chromatography, as follows

$$H = d_p + \frac{2D_m}{u} + \frac{2\gamma_1 \gamma_2}{(\gamma_1+\gamma_2)^2} \frac{(u + u_L)^2}{u\gamma_2 - u_L\gamma_1} \qquad (9.3)$$

where γ_1 = Rate of transfer of molecules from gas to liquid

γ_2 = Rate of transfer of molecules from liquid to gas

u_L = Stationary phase velocity.

When equation (9.3) is compared to a static column case, in which the plate height

$$H = dp + \frac{2D_M}{u} \frac{2\gamma_1 u}{(\gamma_1+\gamma_2)^2} \qquad (9.4)$$

the inclusion of a term in u_L in equation (9.3) accounts for the extra zone broadening caused by movement of the stationary phase.

Al-Madfai (12) also relates the number of

theoretical plates required to resolve a binary system employing a static column, N, to that, N_{cc}, required by a continuous chromatographic column through the two components' separation factor, α.

$$\frac{N_{cc}}{N} = 3\,(\alpha-1) \qquad (9.5)$$

N_{cc} = Number of counter-current theoretical plates.

N = Number of co-current theoretical plates (static column).

Equation (9.5) indicates that for difficult separations in which the separation factor, α, is below 1.33, fewer theoretical plates are necessary for the continuous case than for the static column. A similar study on the relationship between N_{cc} and N was conducted by Rony (164).

Following the work of Fitch et al. (115), Barker and Huntington (7) adapted the theory of stagewise liquid/liquid extraction given by Alder (165) to develop a relationship between product purity, the number of equilibrium stages and the difficulty of separation.

$$\log \frac{\psi_R}{\psi_S} = \log \frac{K_B}{K_A} + N_{cc}^{2} \left\{ \log \left(1-\frac{E_A}{f_A}\right) + \log \frac{E_B}{f_B} \right\} \qquad (9.6)$$

where ψ_R , ψ_S = the ratio of mobile phase/stationary phase flowrate in the 'rectifying' and 'stripping' sections respectively.

E_A , E_B = the mass production rates of components A and B in the top product.

f_A , f_B = the mass feedrate of components A and B to the column.

K_A , K_B = Partition coefficients for components A and B.

Using equation (9.6) Barker and Huntington obtained H.E.T.P. values of approximately 5 cm when separating benzene and cyclohexane on the circular, moving-column unit described in Chapter 4.

9.1.2 Model Based on the Transfer Unit Concept

Barker and Lloyd (4) employed the transfer unit concept of Chilton and Colburn in their treatment of the counter-current gas/liquid chromatographic process and derived the following equations:

$$(N_{oG})_R = \frac{1}{V_G/(KV_L - 1)} \ln \left\{ \frac{E_i/KV_L - C_1(V_G/KV_L - 1)}{E_i/KV_L - C_2(V_G/KV_L - 1)} \right\} \quad (9.7)$$

$$(N_{oG})_S = \frac{1}{(1-V_G/KV_L)} \ln \left\{ \frac{E_{ii}/KV_L - C_1(1-V_G/KV_L)}{E_{ii}/KV_L - C_2(1-V_G/KV_L)} \right\} \quad (9.8)$$

where

$(N_{oG})_R$, $(N_{oG})_S$ = the number of overall gas phase transfer units in the 'rectifying' and 'stripping' sections respectively.

E_i , E_{ii} = the mass flowrate of solute leaving in Product i and Product ii streams respectively.

C_1 , C_2 = Gas phase solute concentration at points 1, 2 in the column.

V_G , V_L = the gas and liquid volumetric flowrates.

K_o = Partition coefficient.

Experimental studies on a 2.5 cm diameter vertical moving-bed column (Section 4.3), with benzene, cyclohexane and methylcyclohexane as solutes and polyoxyethylene 400 diricinoleate as the solvent phase, was conducted by Barker and Lloyd (4). Their results indicated that the main resistance to mass transfer was in the gas phase. Furthermore, a first order relationship was found between the solvent (stationary) phase flowrate and the logarithm of H_{oG}.

9.1.3 Approach Employed for Simulating the Operation of the SCCR4 Chromatographic Unit

The theoretical treatment of counter-current chromatography described in Section 9.1.1. assumed a time steady state being reached. However, this assumption is only satisfied by the original continuous moving-bed type system. An additional variable, time, must be introduced for simulating sequential chromatographic type operations.

Sunal (16) developed a digital computer program for gas/liquid chromatography based on plate-to-plate calculations to describe the operation of the compact circular counter-current chromatograph reported in Chapter 4. A similar approach was also employed by Deeble (20) to simulate the operation of the SCCR1 gas-liquid chromatographic unit. In the present work, the concept of the plate model, employed by Sunal (16) and Deeble (20) for gas/liquid chromatography, has been adapted as a first attempt to simulate a semi-continuous counter-current liquid-solid chromatographic unit (SCCR4).

9.2 The Model

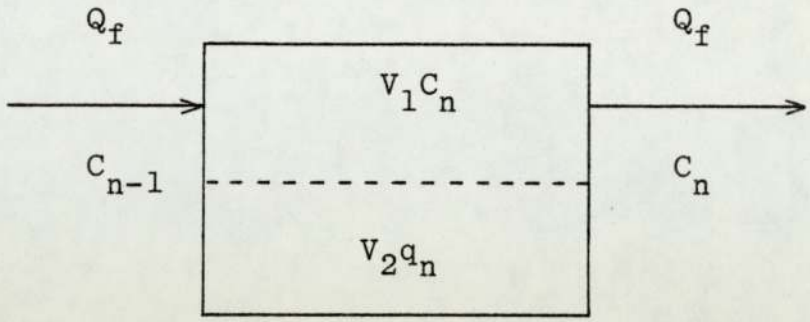

Plate n

The chromatographic column is considered to consist of a series of theoretical plates and a mass balance over plate n gives;

$$Q_f\ C_{n-1} = Q_f\ C_n + V_1 \frac{dC_n}{dt} + V_2 \frac{dq_n}{dt} \qquad (9.9)$$

Q_f = mobile phase volumetric flowrate

C = solute concentration in mobile phase

q = solute concentration in stationary phase

V_1 = Volume of mobile phase in a plate

V_2 = Volume of stationary phase in a plate

Substituting $K_D = q_n/C_n$; where K_D= Distribution coefficient;

$$Q_f\ C_{n-1} = Q_f\ C_n + (V_1 + K_D V_2) \frac{dC_n}{dt} \qquad (9.10)$$

Now, providing the time increment Δt is sufficiently small to allow C_{n-1} to be considered constant, integration of equation 9.10 yields

$$C_n = C_{n-1}\left(1 - e^{-\frac{Q_f.\Delta t}{(V_1+V_2K_D)}}\right) + C_n^o \cdot e^{-\frac{Q_f.\Delta t}{(V_1+V_2K_D)}}$$

(9.11)

where C_n^o = Initial concentration of solute in plate n.

The first term on the right-hand side of equation 9.11 represents the contribution to C_n from the $(n-1)^{th}$ plate to the n^{th} plate, while the second turn represents the contribution from material present on n^{th} plate at the beginning of the time increment.

For a feed plate, a mass balance yields a similar equation:

$$C_n = \left(\frac{Q_f\, C_{n-1} + F_f\, C_f}{Q_f + F_f}\right)\left(1 - e^{-\frac{Q_f.\Delta t}{V_1+V_2K_D}}\right) + C_n^o$$

$$e^{-\frac{Q_f.\Delta t}{V_1+V_2K_D}} \qquad (9.12)$$

where F_f, C_f = Feed flowrate and concentration.

($Q_f + F_f$ = Post feed point mobile phase flowrate)

The sequencing action of the SCCR4 unit was imposed onto the basic plate calculations by stopping

the concentration profile backwards, by one column, at the end of a sequencing interval. The above description of the computer model has considered only one solute to be present in the sequential unit. The inclusion of a second solute is achieved by duplicating the calculations at each plate with different variable names, it being assumed that the components do not interact. A flow sheet for the program used in this research is given in Figure 9.1. A listing of the programme together with all the variables, and a sample of the printout is provided in Appendix V.

Fig. 9.1 Flow Chart For The Computer Simulation Of The SCCR4 Unit

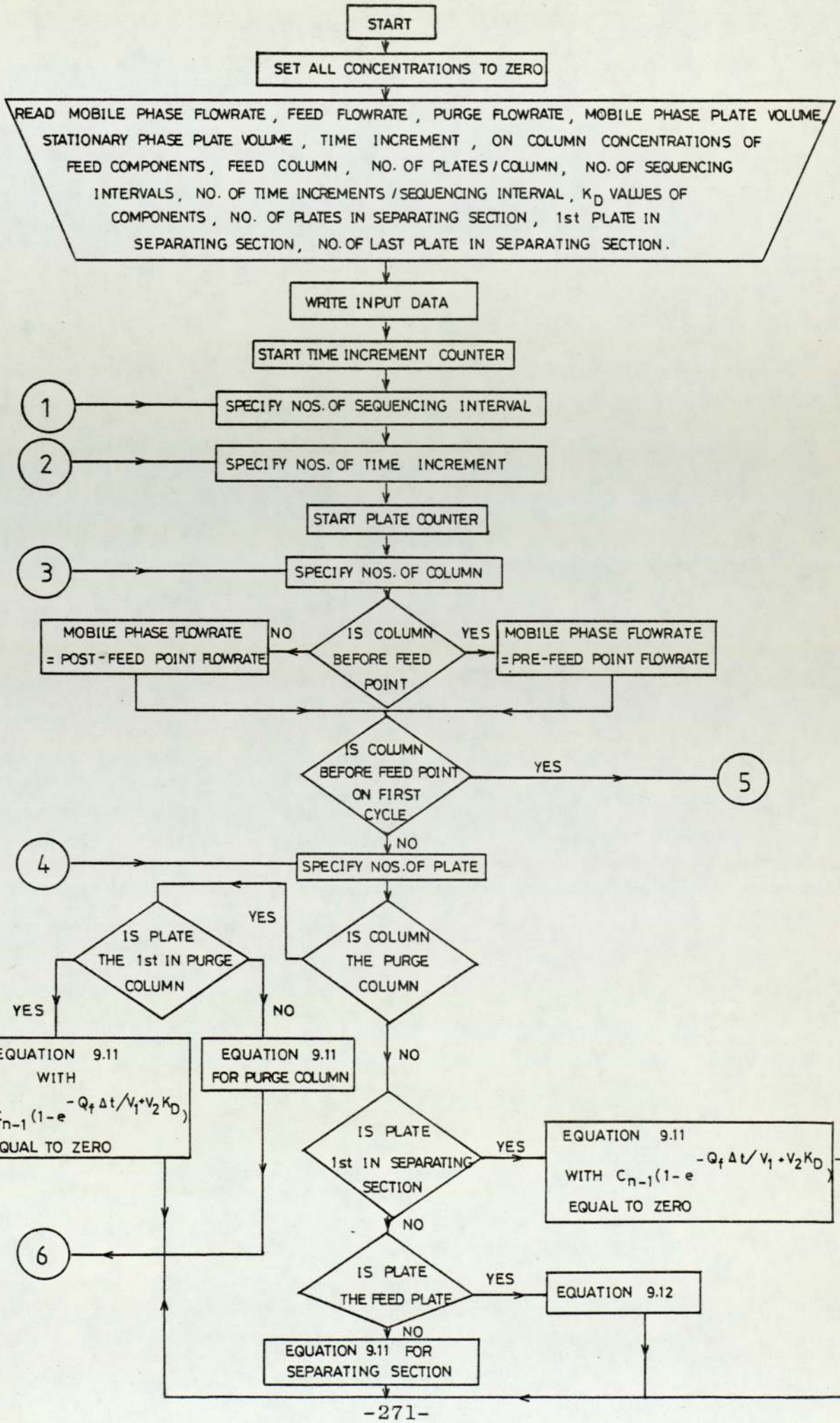

Fig. 9.1 (Contd.)

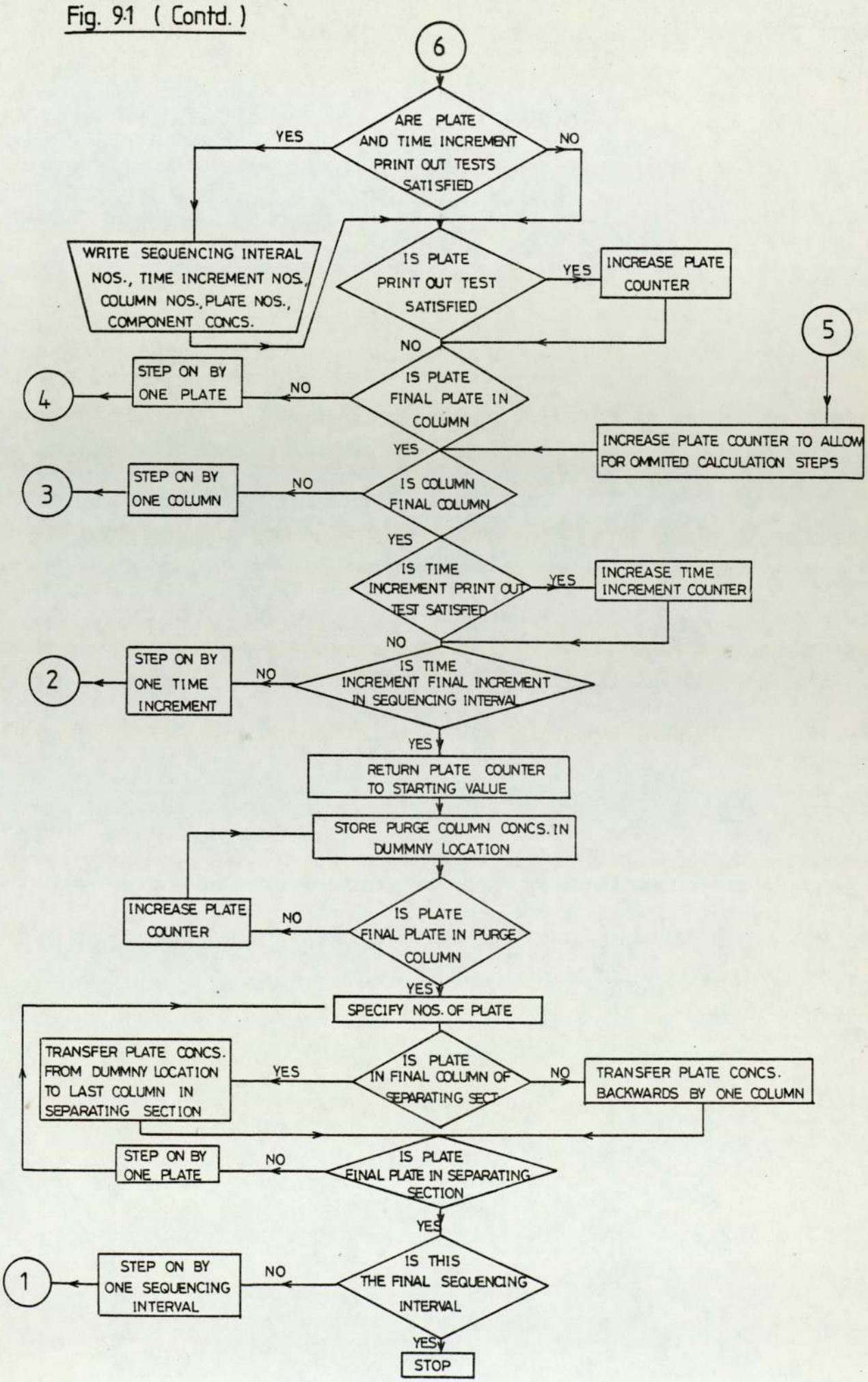
6
ARE PLATE AND TIME INCREMENT PRINT OUT TESTS SATISFIED
YES
NO
WRITE SEQUENCING INTERAL NOS., TIME INCREMENT NOS., COLUMN NOS., PLATE NOS., COMPONENT CONCS.
IS PLATE PRINT OUT TEST SATISFIED
YES
INCREASE PLATE COUNTER
NO
5
4
STEP ON BY ONE PLATE
NO
IS PLATE FINAL PLATE IN COLUMN
INCREASE PLATE COUNTER TO ALLOW FOR OMMITED CALCULATION STEPS
YES
3
STEP ON BY ONE COLUMN
NO
IS COLUMN FINAL COLUMN
YES
IS TIME INCREMENT PRINT OUT TEST SATISFIED
YES
INCREASE TIME INCREMENT COUNTER
NO
2
STEP ON BY ONE TIME INCREMENT
NO
IS TIME INCREMENT FINAL INCREMENT IN SEQUENCING INTERVAL
YES
RETURN PLATE COUNTER TO STARTING VALUE
STORE PURGE COLUMN CONCS. IN DUMMNY LOCATION
INCREASE PLATE COUNTER
NO
IS PLATE FINAL PLATE IN PURGE COLUMN
YES
SPECIFY NOS. OF PLATE
TRANSFER PLATE CONCS. FROM DUMMNY LOCATION TO LAST COLUMN IN SEPARATING SECTION
YES
IS PLATE IN FINAL COLUMN OF SEPARATING SECT
NO
TRANSFER PLATE CONCS. BACKWARDS BY ONE COLUMN
STEP ON BY ONE PLATE
NO
IS PLATE FINAL PLATE IN SEPARATING SECTION
YES
1
STEP ON BY ONE SEQUENCING INTERVAL
NO
IS THIS THE FINAL SEQUENCING INTERVAL
YES
STOP

9.3 Objectives of the Simulation Runs of the SCCR4 Unit

The computer runs were performed on a CDC 7600 digital computer, at the University of Manchester Regional Computer Centre. Results obtained were stored as data files on the ICL 1904S computer of the University of Aston, and subsequently transferred into graphical outputs with the aid of the specially developed GINO-F and GINO-Graph programs. The aims of the SCCR4 simulation work can be summarized as follows:

(i) Based on the results acquired in previous batch column studies (Section 5.3), concentration profiles were simulated for all the experimental runs conducted during this research programme. Comparisons made against the experimental profiles will serve to highlight the accuracy of the model.

(ii) To estimate the maximum throughput possible with the SCCR4 unit before breakthrough of product profiles occur.

(iii) To investigate the effect of the number of theoretical plates (N) (representing on-column dispersion) and K_D value of fructose (K_{D_2}) on separations. From experiments conducted with a batch column (Section 5.3.3) it was shown that by increasing the mobile phase

temperature, the K_D value of fructose decreases but the number of theoretical plates in the column increases. Hence, the equivalent effect of increasing operating temperature in SCCR4 separation performance can be simulated by a simultaneous variation of K_{D_2} and N.

The simulated concentration profile Run No consists of five groups of digits, e.g.

49-3-6-8-0.6

The first and second group of digits, 49 and 3, represent the feed concentration (% w/v) and flowrate (cm^3min^{-1}) respectively. The third group, 6, shows the mobile phase flowrate (cm^3min^{-1}) and the fourth group, 8, indicates the volume of resin matrix (cm^3) in each theoretical plate. Finally, the K_D value of fructose (K_{D_2}) employed in a simulation run is shown as the last group, 0.6.

9.4 Results and Discussion

9.4.1 Simulation of Profiles of the Experimental Runs Performed

Guided by the column characteristics and results obtained from the batch column work (Sections 5.3.3 and 7.3.3) the values of the following programme variables were set as:

V_1 = 8.00 cm^3

V_2 = 8.00 cm^3

N = 20 plates per column

K_{D_1} = 0.0

K_{D_2} = 0.6 at 29°C

Using the above data, concentration profiles were simulated for all experimental runs conducted at an average mobile phase temperature of approximately 29°C. A listing of these simulated profiles together with their corresponding experimental profiles, is given as Figure 9.2 to Figure 9.7 inclusive.

In general, good agreement, with regard to the location of the 'cross-over' point, was found between simulated and experimental profiles. In the computer simulation profiles of the fructose profile and the trailing edge of the glucose profile drop very sharply to zero after the 'cross-over' point. The simulation

Fig. 9.2 SIMULATED CONCENTRATION PROFILE FOR RUN NO. 45-144-294-8-0.6

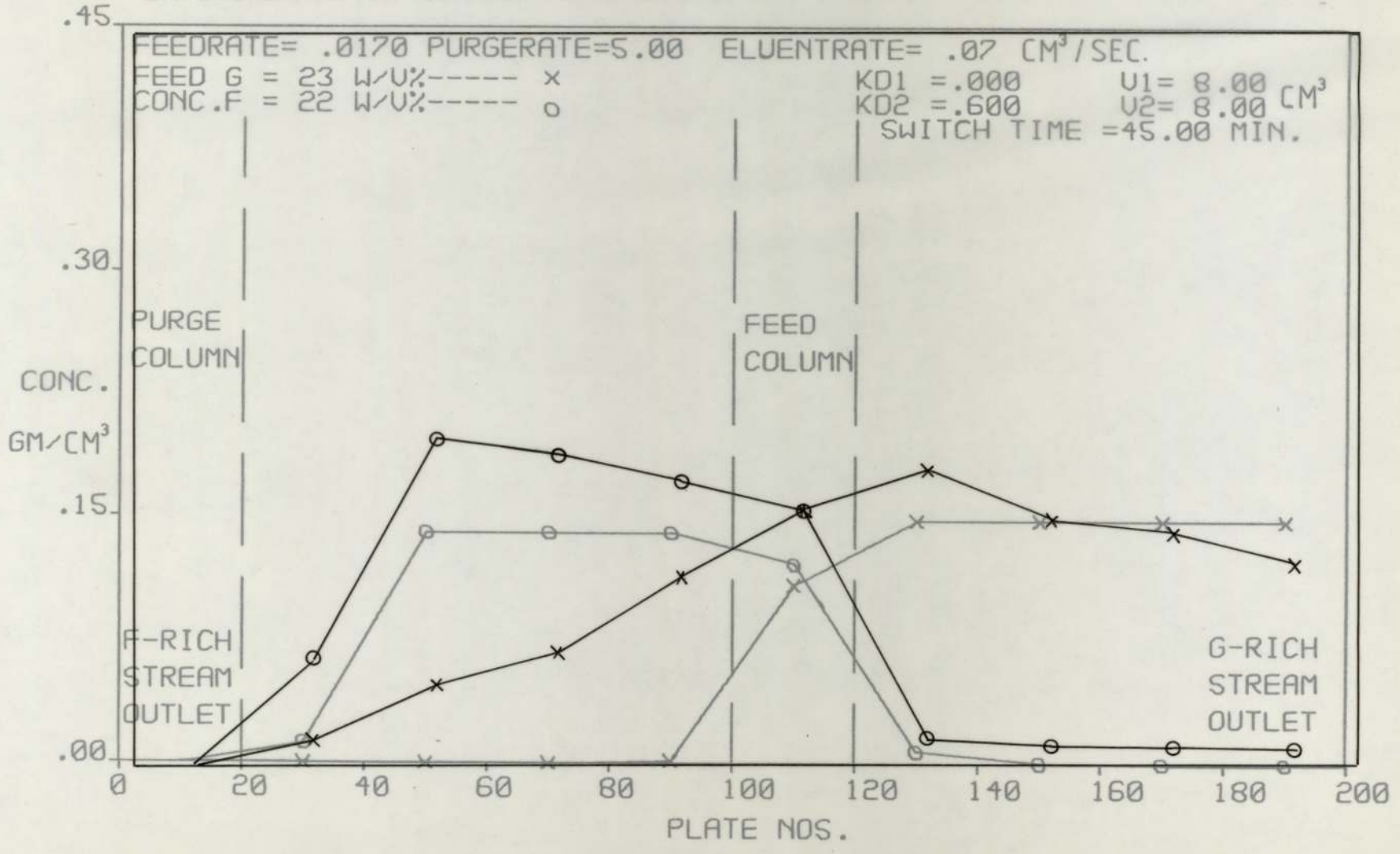

Fig. 9.2 SIMULATED CONCENTRATION PROFILE OF RUN NO. = 45-1-4-8-0.6

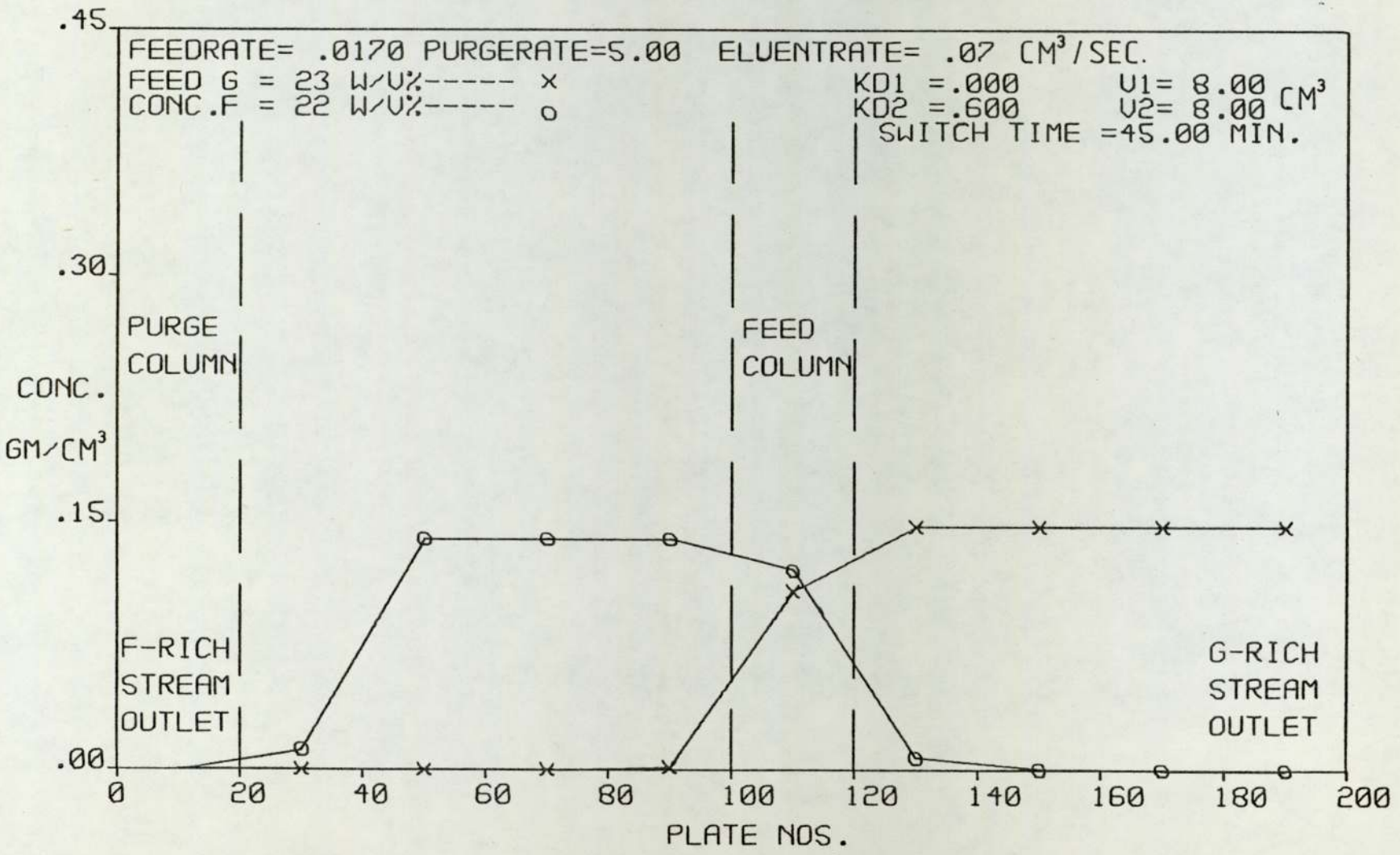

Fig. 93 SIMULATED CONCENTRATION PROFILE OF RUN NO. = 49-1-6-8-0.6

EXPERIMENTAL CONCENTRATION PROFILE OF RUN NO.= 49-1-6-29

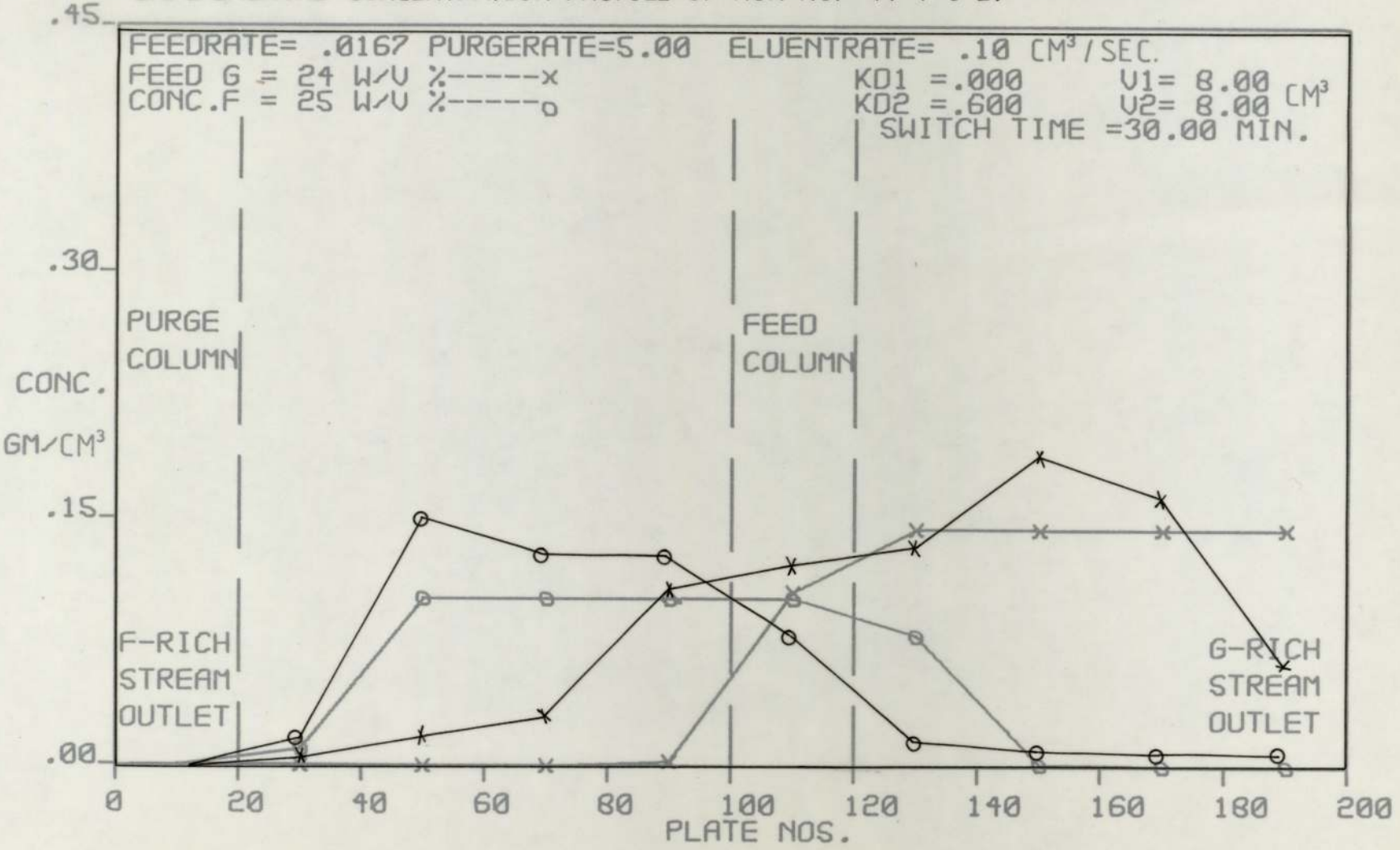

Fig. 9.3 SIMULATED CONCENTRATION PROFILE OF RUN NO. = 49-1-6-8-0.6

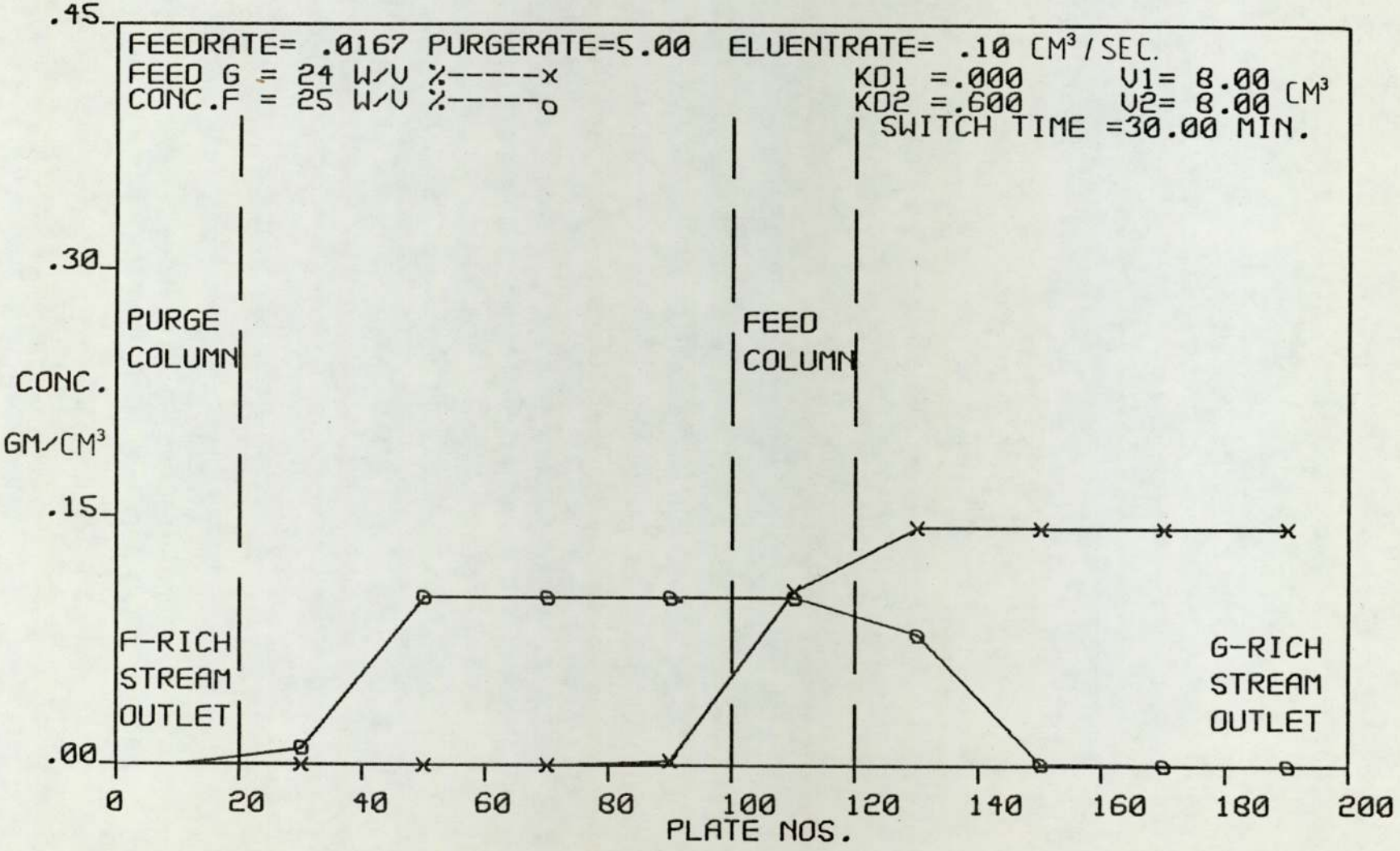

Fig. 9/ SIMULATED CONCENTRATION PROFILE OF RUN NO. = 49-2-6-8-0.6

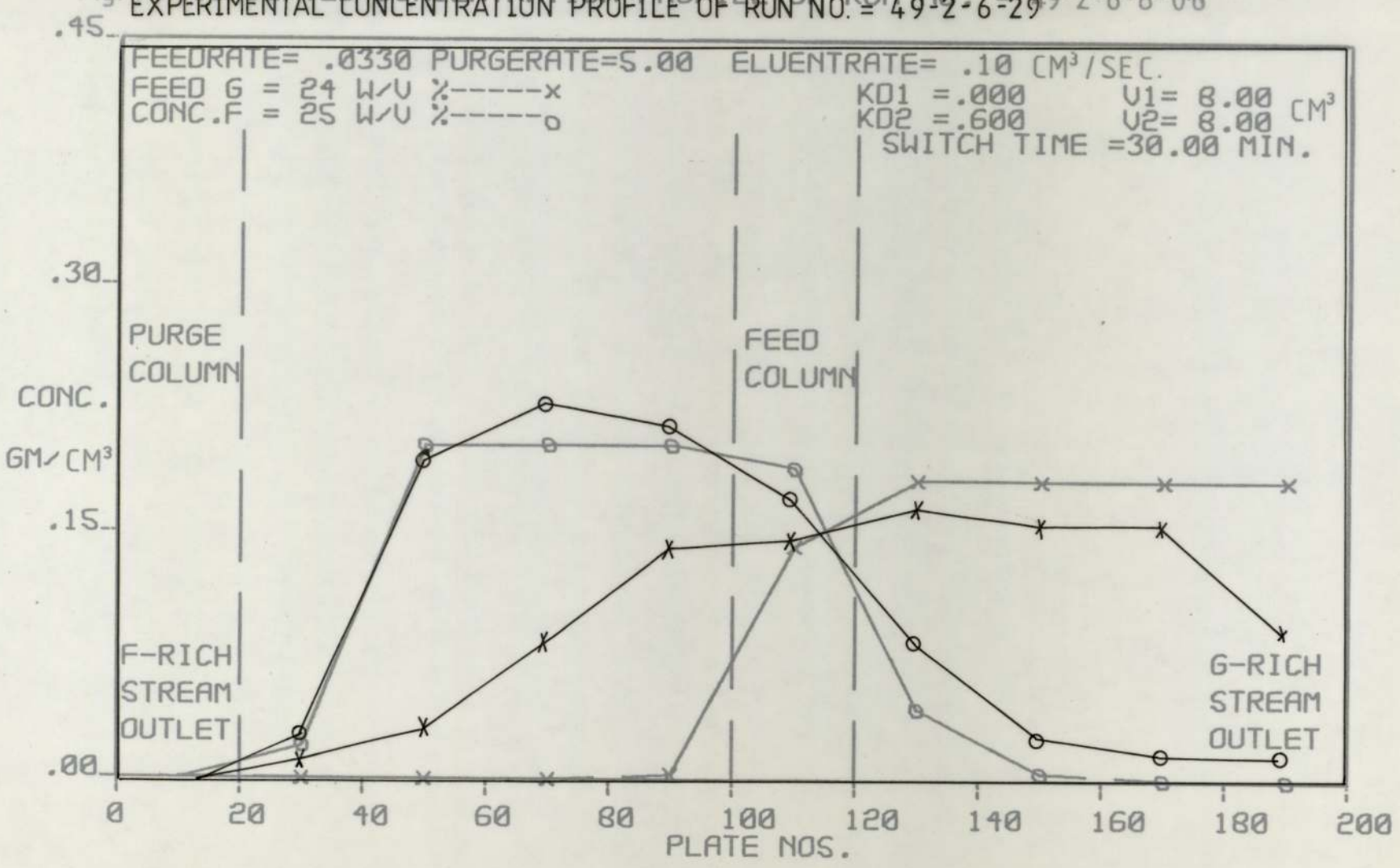

Fig. 9.4 SIMULATED CONCENTRATION PROFILE OF RUN NO. = 49-2-6-8-0.6

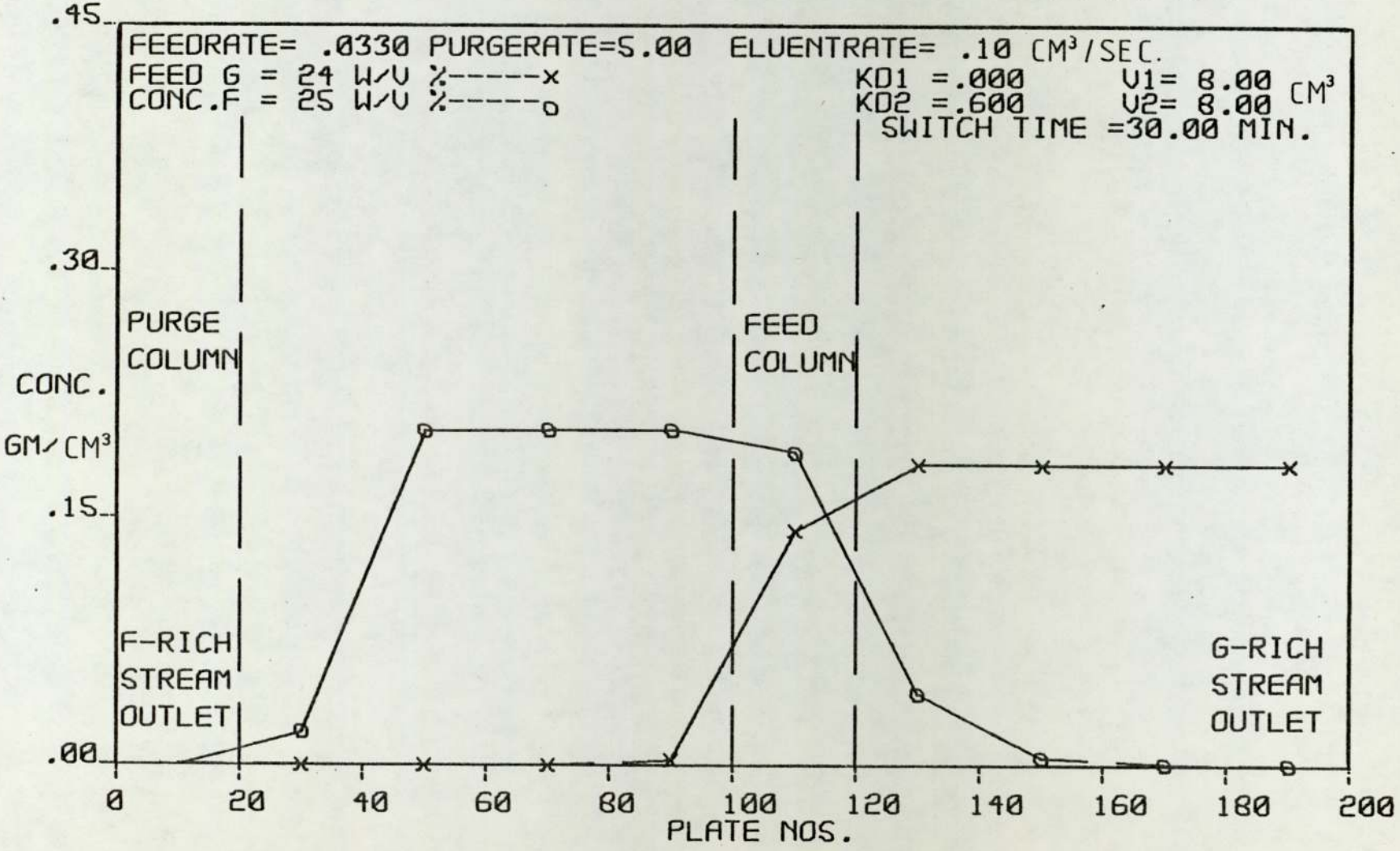

Fig. 9.5 SIMULATED CONCENTRATION PROFILE OF RUN NO. = 49-3-6-8-0.6

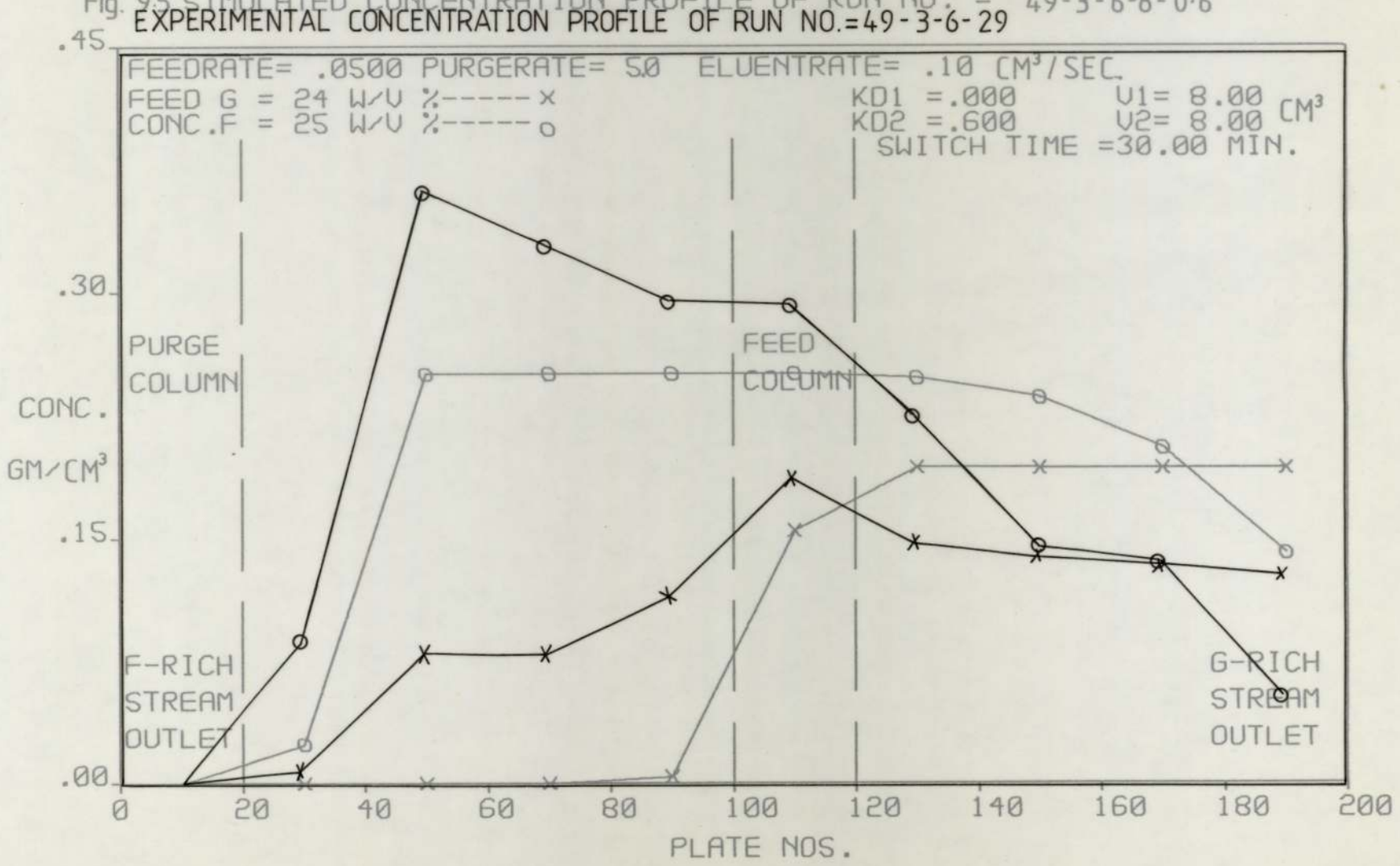

Fig. 9.5 SIMULATED CONCENTRATION PROFILE OF RUN NO. = 49-3-6-8-0.6

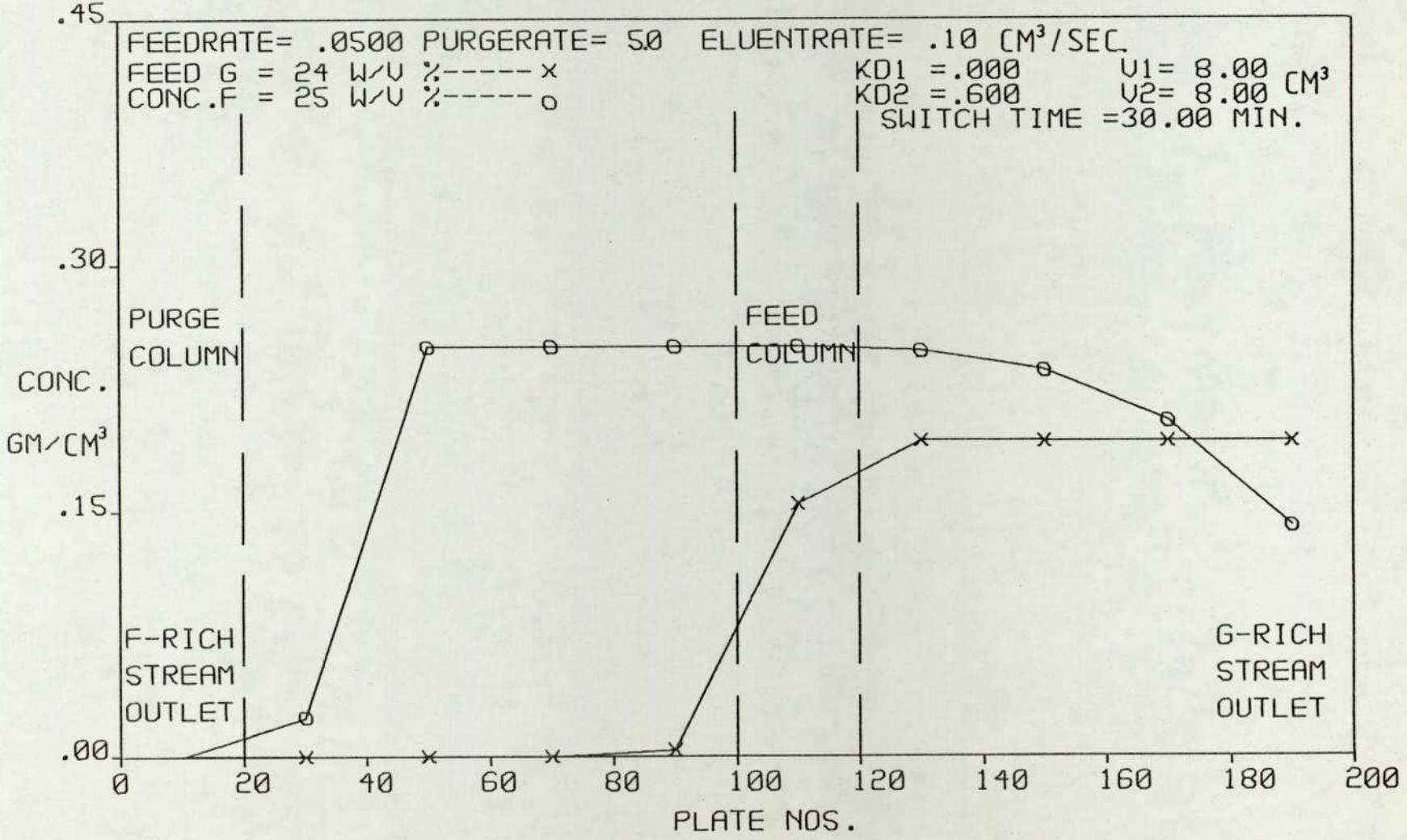

Fig. 96 SIMULATED CONCENTRATION PROFILE OF RUN NO. = 49-3-6-8-0.7-D

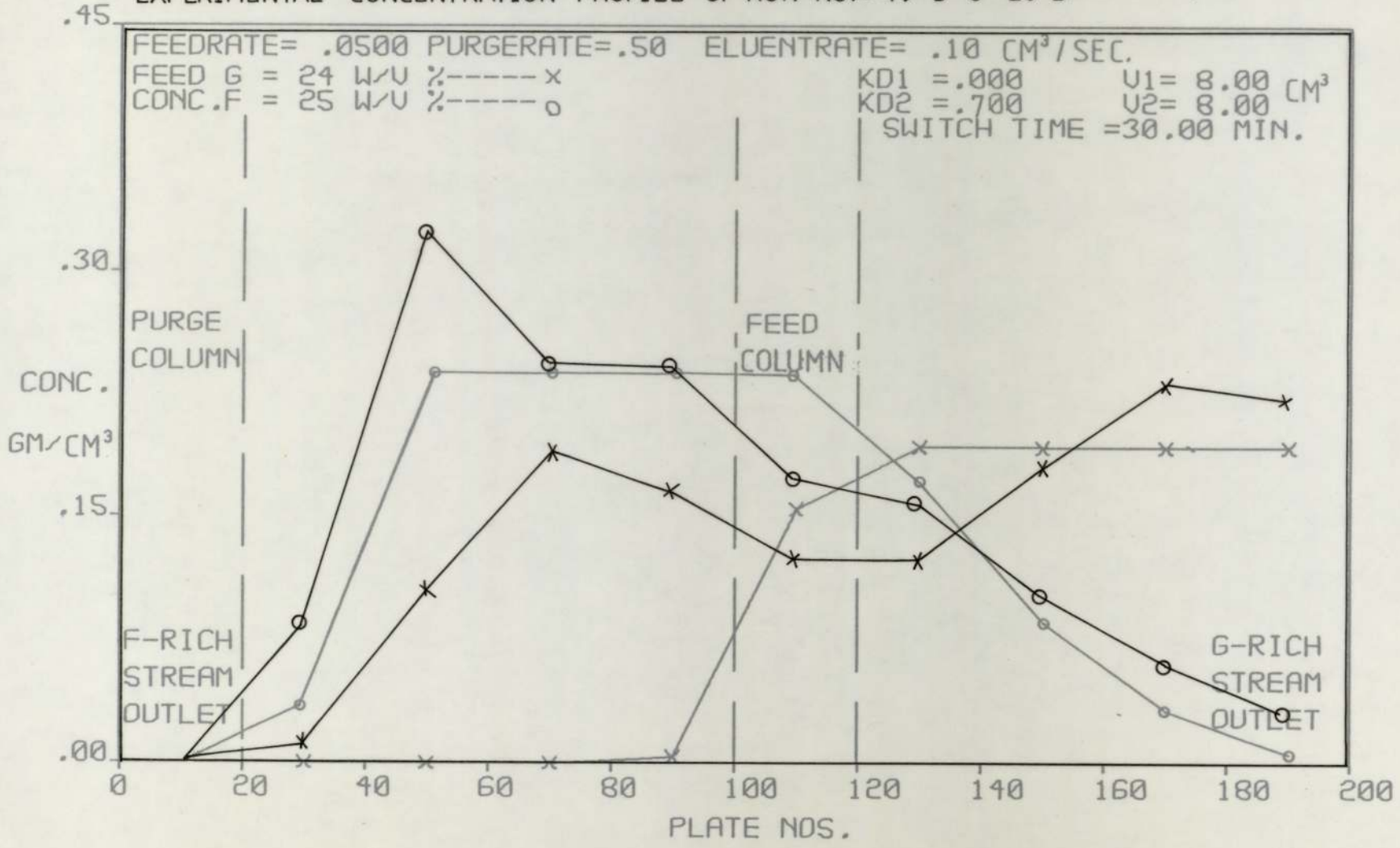

Fig. 9.6 SIMULATED CONCENTRATION PROFILE OF RUN NO. = 49-3-6-8-0.7-D

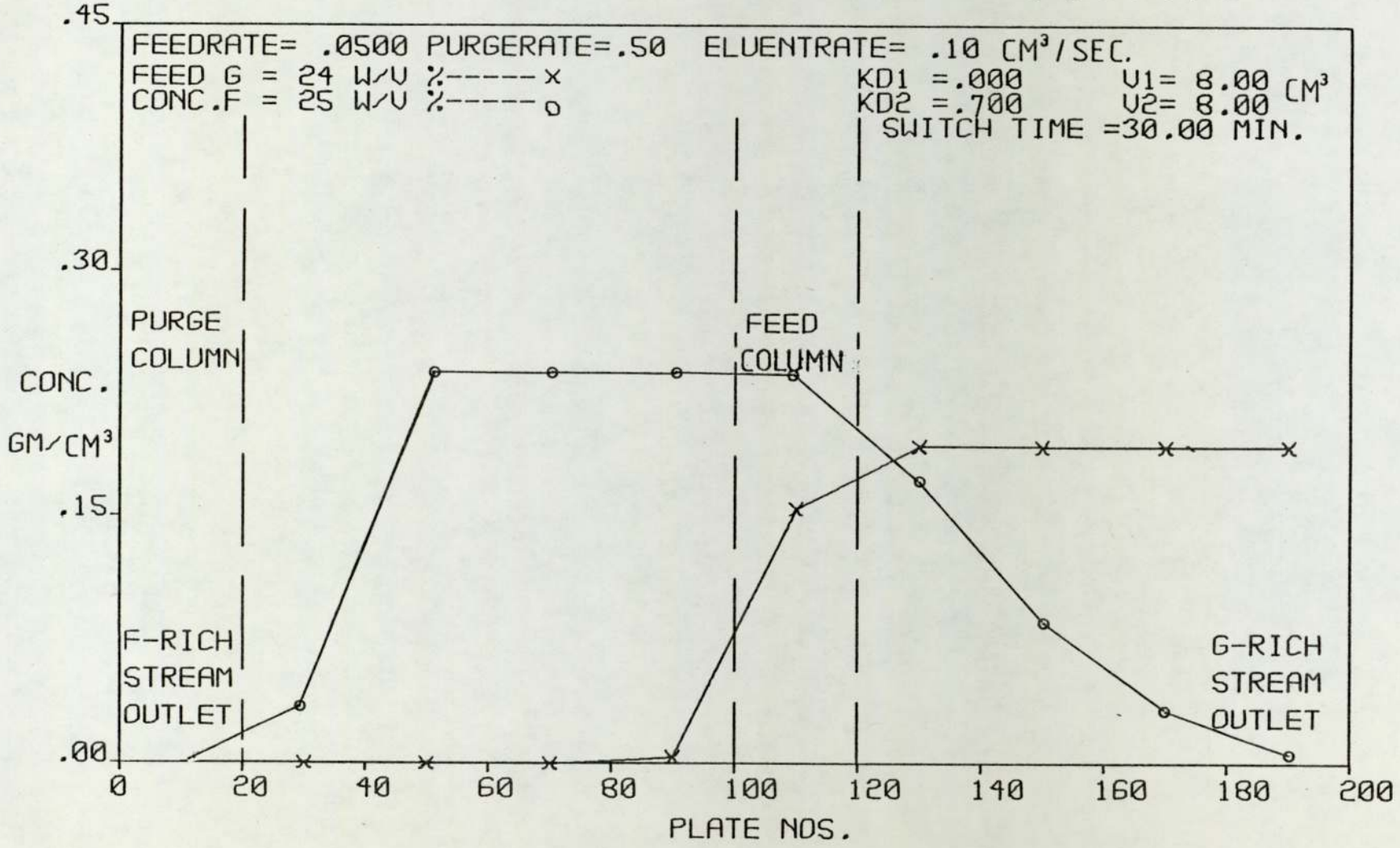

Fig. 97 SIMULATED CONCENTRATION PROFILE OF RUN NO. = 02-2-6-8-0.6

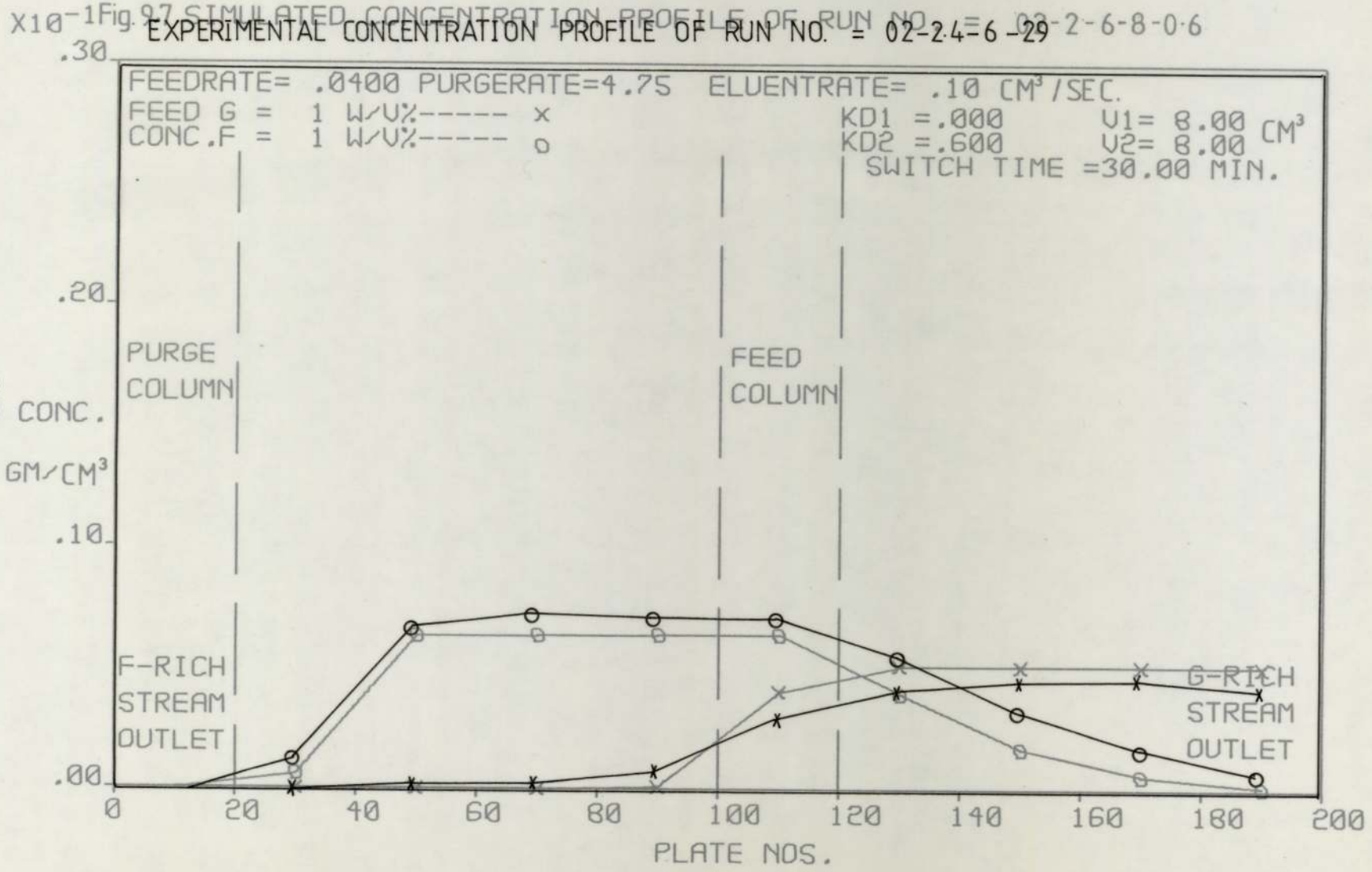

Fig. 9.7 SIMULATED CONCENTRATION PROFILE OF RUN NO. = 02-2-6-8-0.6

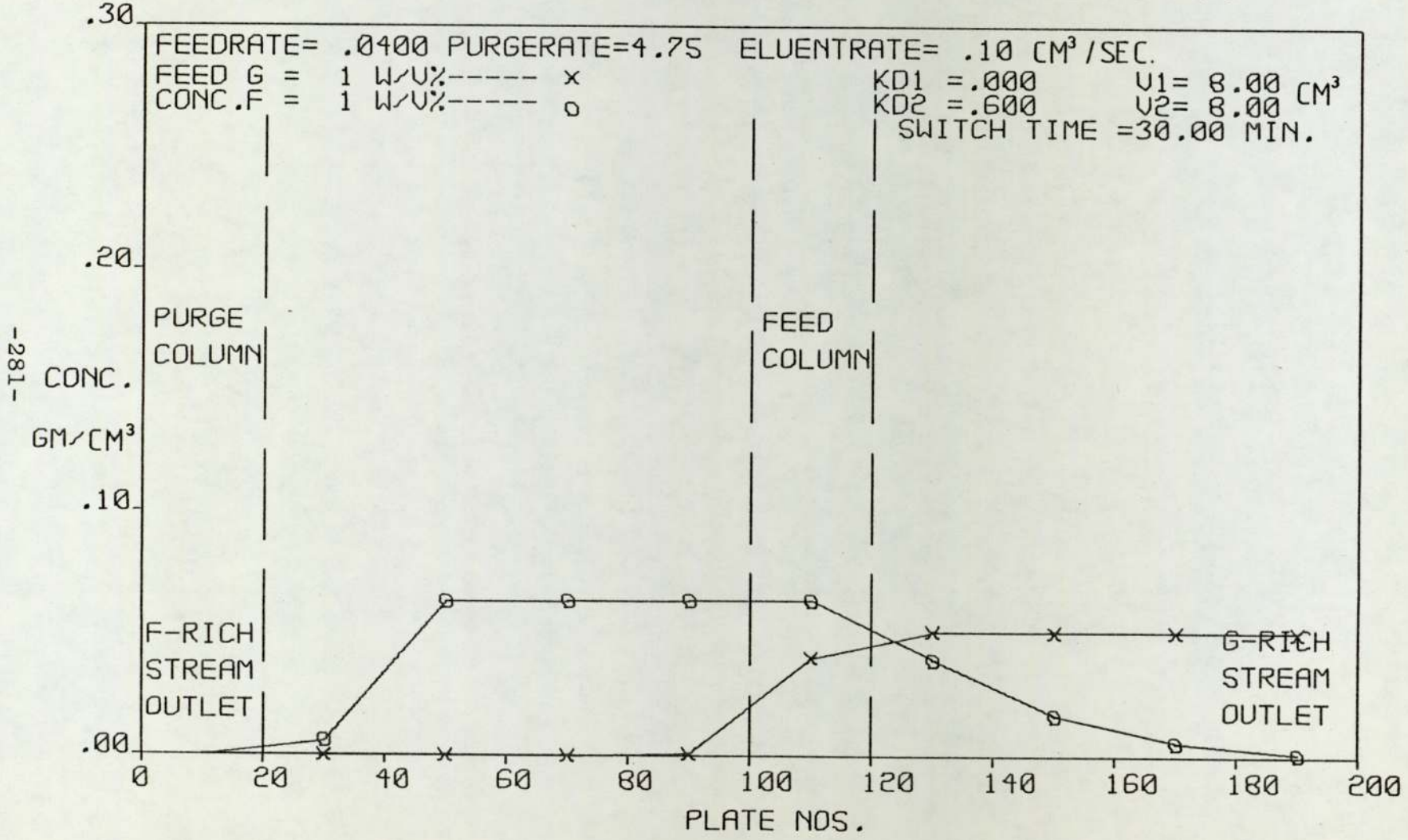

suggested that pure fructose and glucose products could be obtained readily within a separation length of approximately 3 to 4 columns. However, in the corresponding experimental profiles, the decline of the profile edges after the 'cross-over' point was much less sharp and never reached a zero value. Typically the products were contaminated to the extent of 8 - 10% of glucose or fructose. Such a discrepancy between the two groups of profiles could stem from the fact that no allowance was made in the programme for solute hold-up in the valves and the inter-column's transfer tubing (approximately 1 - 2% of the total mobile phase volume in a column). Also the model assumes instantaneous equilibrium conditions in each plate which in practice may not be the case. Similarly K_D could be concentration dependent, whereas the current model assumes a constant value in all columns. This probable K_D dependence on concentration could be the explanation for the best agreement achieved between the simulation and experimental profile for run No. 02-2.4-6-29. (Figure 9.7).

From the results of the above simulation work, it was established that 2½ cycles was necessary for the SCCR4 unit to achieve a pseudo-equilibrium state. In experimental operations, 5 to 6 cycles were required.

Listings of the computer run after 3 cycles and after 4 cycles are given in Figures 2 and 3 of Appendix V.

The simulation of profiles for experimental runs, conducted with higher than average mobile phase temperature, involved the use of different input values of K_{D_2} and N. These simulations are discussed in a later section, concerning the effect of these parameters on separations.

9.4.2. The Simulated Maximum Throughput Possible with the SCCR4 Unit

Figure 9.8 to 9.10 illustrate the changes in the simulated profiles as the feed rate was increased from 3 cm^3 min^{-1} to 6 cm^3 min^{-1}. Breakthrough of solute profiles occurred at a feed rate between 3 cm^3 min^{-1} and 4.5 cm^3 min^{-1}, suggesting that at the particular parameter settings chosen throughput of not much more than 3 cm^3 min^{-1} of feed could be achieved. Experimental run No. 49-3-6-29 (Figure 9.5) provides some support to the simulation findings.

9.4.3. The Effect of K_{D_2} (fructose) and N on Separations

The effect of K_{D_2} changes are shown in Figure 9.11. The flow settings for the simulation runs were selected

Fig. 98 SIMULATED CONCENTRATION PROFILE OF RUN NO. = 49-3-6-8-0·6

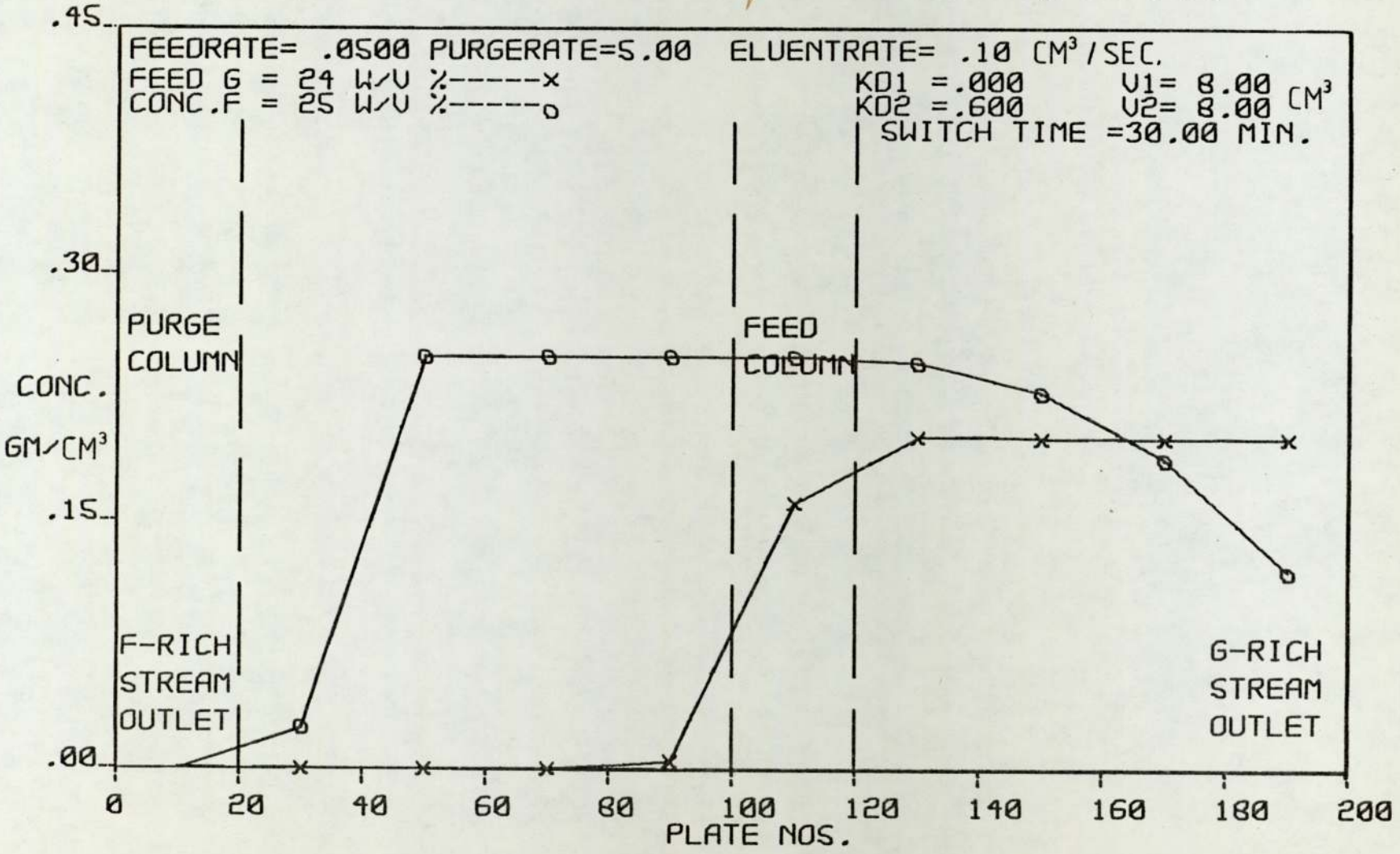

Fig. 9.9 SIMULATED CONCENTRATION PROFILE OF RUN NO. = 49-4·5-6-8-0·6

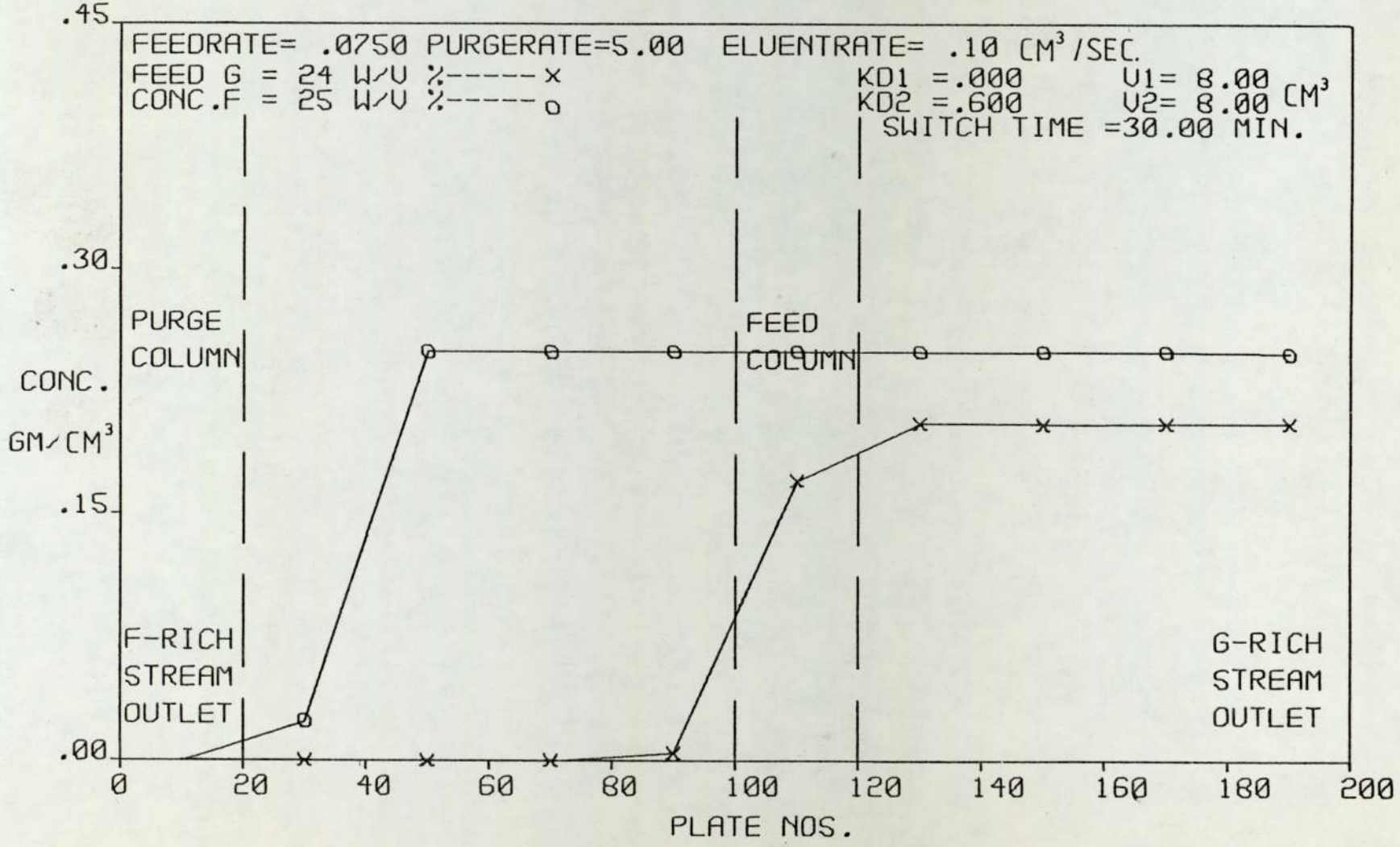

Fig. 9.10 SIMULATED CONCENTRATION PROFILE OF RUN NO. = 49-6-6-8-0.6

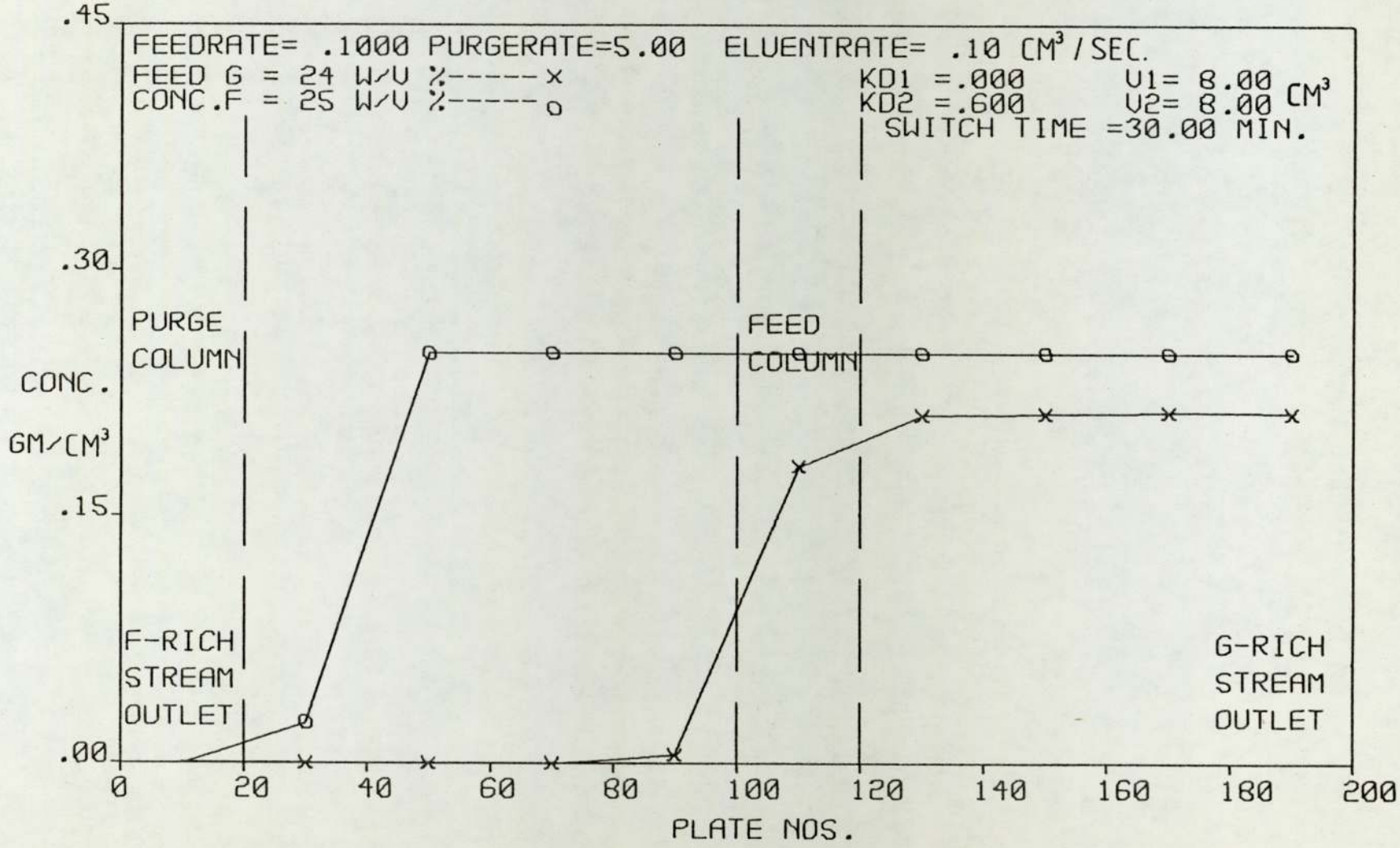

identically to that of the experimental runs conducted with elevated mobile phase temperatures. In the simulated profile, as the value of K_{D_2} decreases, the leading edge of the fructose profile spreads more into the post feed point separation section; and, at a K_{D_2} value of 0.4, a breakthrough of the fructose profile occurs.

Figure 9.11 to 9.13 illustrate the effect of N on the separation performance of SCCR4 unit. By increasing the number of theoretical plates per column from 20 (Figure 9.11) to 60 (Figure 9.13), the leading edge of the fructose profile (for the same K_{D_2} value e.g. K_{D_2} = 0.45) dropped more sharply in the post-feed point separation section and the 'cross-over' point moved closer towards the feed column. This represents a drop in the amount of the input fructose lost in the glucose-rich product. In the batch column work (Section 5.3.3) findings, it was shown that by eluting fructose at higher temperatures the K_D value of fructose decreases but the number of theoretical plates (N) in the column increases. From the computer model, an increase in N and a decrease in K_{D_2} have been established to have opposite effects on the simulated separation performance of the SCCR4 unit that is in terms of glucose-rich product contamination, and the

Fig. 9.11 SIMULATED CONCENTRATION PROFILE OF RUN NO. = 52-2-6-8-(WITH VARYING KD2)
AND WITH 20 THEORETICAL PLATES PER COLUMN

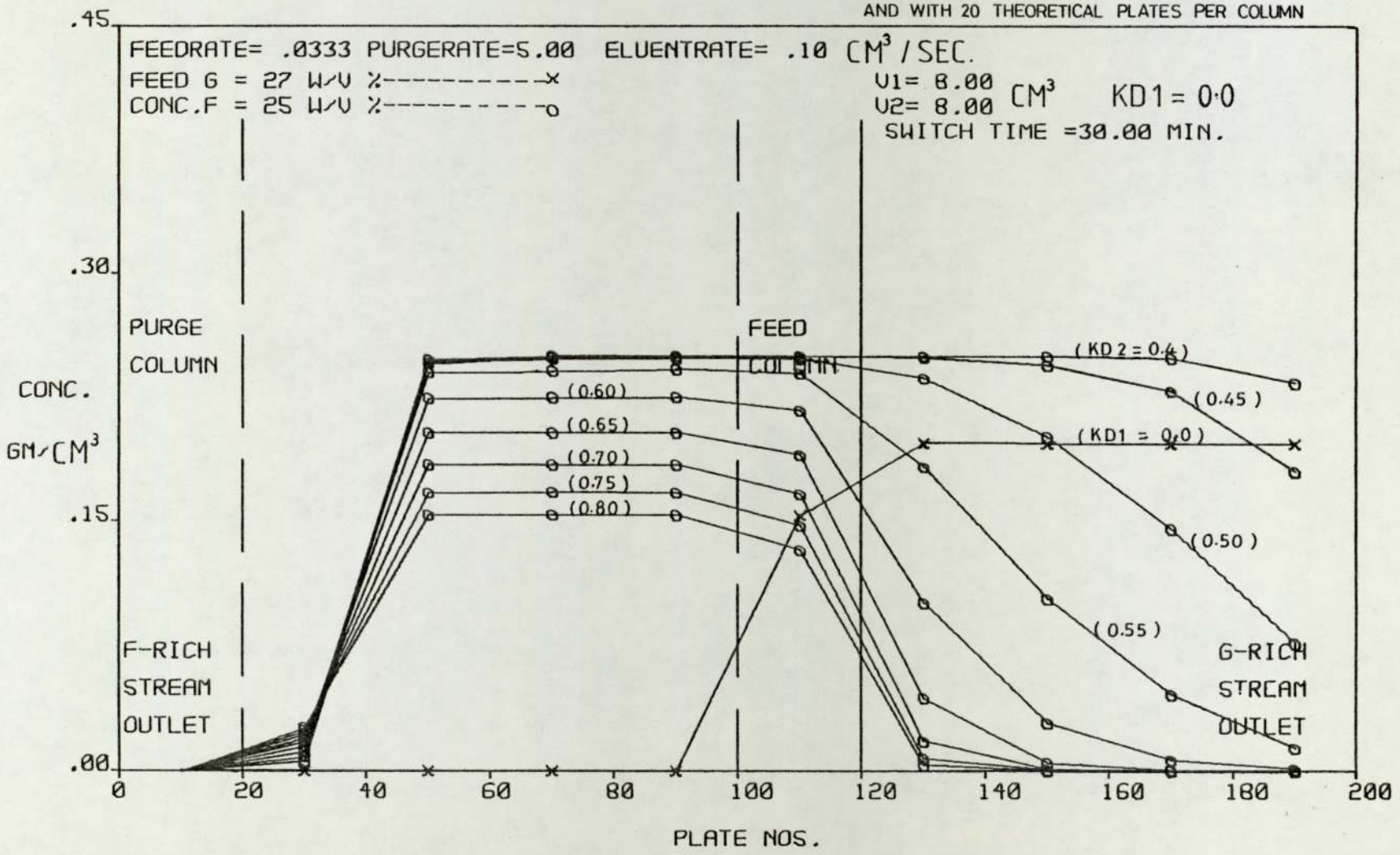

Fig. 9.12 SIMULATED CONCENTRATION PROFILE OF RUN NO. = 52-2-6-4- (WITH VARYING KD2)
AND WITH 40 THEORETICAL PLATES PER COLUMN

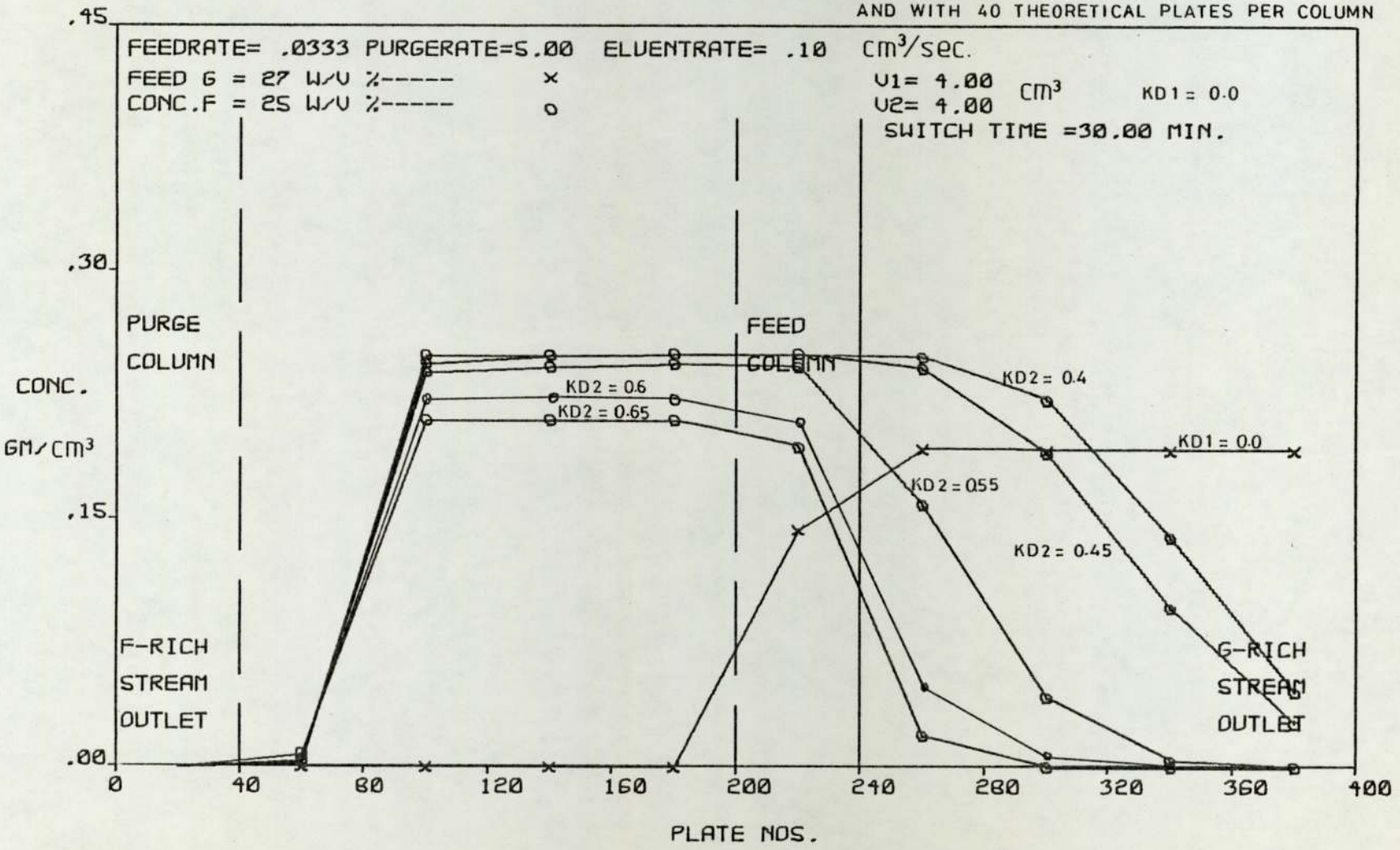

Fig. 9.13 SIMULATED CONCENTRATION PROFILE OF RUN NO. = 52-2-6-267- (WITH VARYING KD2)
AND WITH 60 THEORETICAL PLATES PER COLUMN

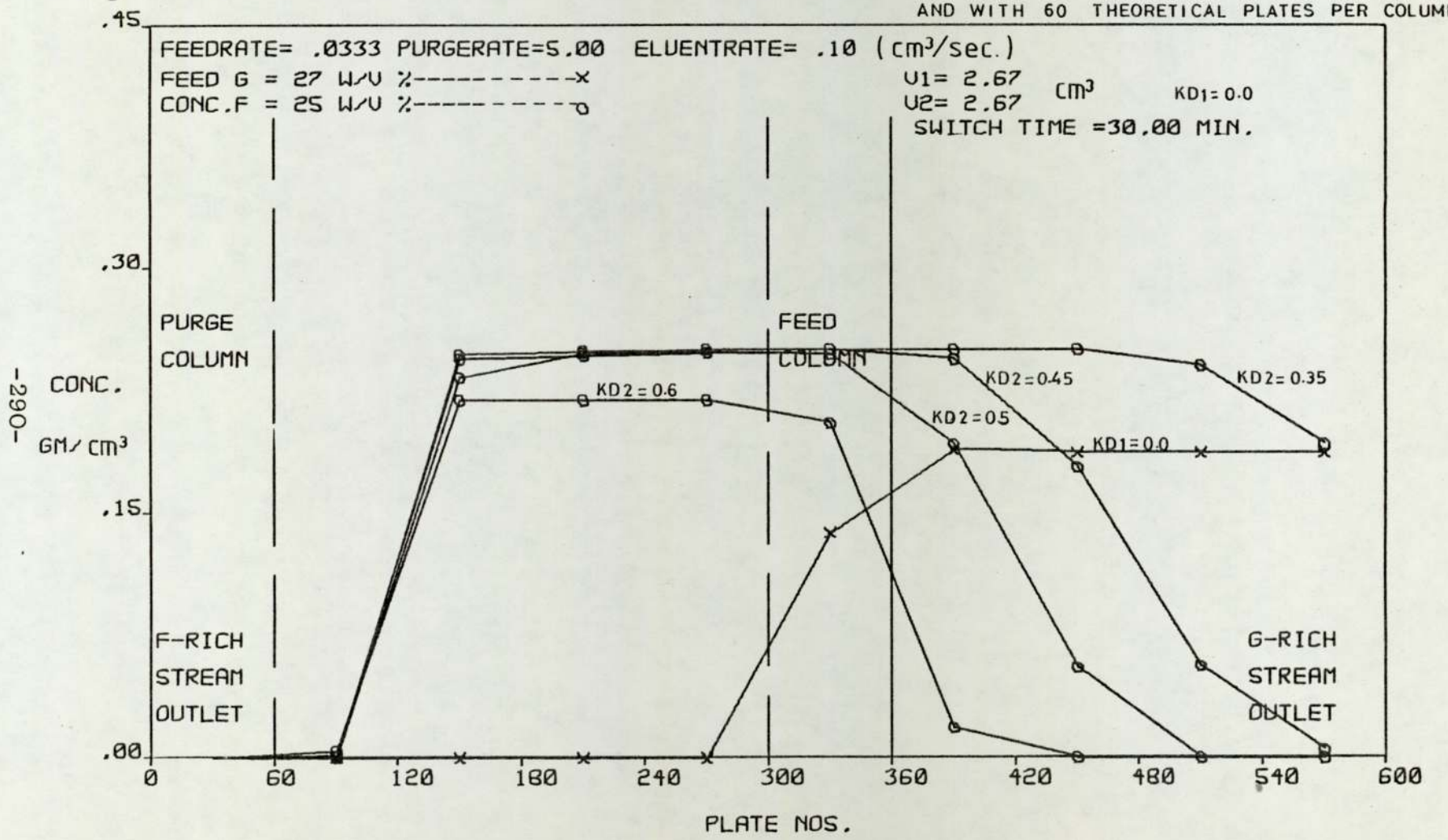

amount of input fructose lost in the glucose-rich product. Hence, operating the SCCR4 unit under fixed flow conditions but with higher mobile phase temperature, will result in a separation efficiency which is a compromise of the two effects.

Chapter 10

Conclusion and Recommendations for Future Work

10 Conclusions and Recommendations for Future Work

10.1 Conclusions

This research has shown for the first time that the principle of sequential chromatographic refining can be applied, on a preparative scale, to the separation of a solution containing equal amounts of glucose and fructose into glucose-rich and fructose-rich products of purities 74.7 - 93.8% w/w and 85.0 - 90.3% w/w respectively. At a mobile phase flowrate of 6 cm^3 min^{-1}, a throughput of 3 cm^3 min^{-1} of a 49% w/w feed solution has been achieved with the present SCCR4 unit. In comparison, on an equal cross-sectional area basis, this feed throughput (3 cm^3 min^{-1}) is approximately 2.5 times that of the equivalent Boehringer batch process.

Experimental work established that the 'cross-over' point between solutes profiles was influenced by the mobile phase temperature. Under constant flow conditions, the 'cross-over' point was shown to shift towards the glucose-rich product outlet as the temperature of the mobile phase increased. Shifting of the 'cross-over' point in such a manner has also accounted for a decrease in the recovery of the input fructose by the fructose-rich product. However, the adverse effect of operating at higher temperatures was compensated by a reduction in

the pressure drops for both the mobile phase and feed flows through the packed columns. Finally, under dilute feed concentration conditions, the separation performance (in terms of fructose-rich product purity) of the SCCR4 unit improved suggesting a possible K_D dependency with column concentration.

The results of the batch column study, conducted with an aim to acquire the equilibrium data and plate heights of use in the SCCR4 simulation work, revealed firstly an increase in the plate heights for both glucose and fructose as the mobile phase velocity increased; secondly, a decrease in the two components' peak-to-peak width and a reduction in on-column dispersion as the mobile phase temperature increased.

The results from the computer model, based on an equilibrium stage concept to simulate the liquid-solid chromatographic unit, indicated partial agreement with some of the experimental findings. The main discrepancy between the experimental and simulated sets of profiles existed in the shape of the trailing edge of the glucose profile. In the pre-feed separation section of an experimental profile, the glucose profile trailed, in a gradually diminishing fashion, towards the fructose-rich product outlet and thus accounted for the 8-12% contamination of this product. Whereas, in the corresponding simulated profile, the trailing edge of

the glucose profile dropped very sharply to zero in the pre-feed separation section and indicated a complete resolution of fructose from glucose. Such a disagreement served to highlight the imperfection of a theoretical plate model in which instantaneous equilibration is assumed. However, results from this model have established a shift of the profiles 'cross-over' point towards the glucose-rich product outlet as the mobile phase temperature increased. Furthermore, the model predicted, with the present SCCR4 unit and at a $\frac{L'_{mean}}{P}$ setting of 0.35, a breakthrough of solute profiles at a feedrate between 3 - 4.5 $cm^3\ min^{-1}$.

10.2 Recommendations for Future Work

Future work with the SCCR4 unit can be summarised as follows:

i) To study the effect of the location of the feed column on separation performance. In this research programme the feed was introduced into the fifth column of the separation section and this resulted in creating pre-feed and post-feed separating sections equivalent to 4 and 5 column lengths respectively. With the present pneumatic control valve system, feed can be introduced into any column within the separating section by

connecting the 'actuating' air supply tubing to the appropriate feed valve during a particular sequence. As such, the study of feed column location on separation performance could be conducted without entailing significant alteration of the SCCR4 unit. From the results of this research programme, (Figure 8.6) the contamination of the fructose-rich product was mainly caused by the spreading of the trailing edge of the glucose profile into the pre-feed column separation section. Hence, by shifting the feed column towards the glucose-rich product outlet and thus lengthening the pre-feed section, it may be possible to improve on the purity of the fructose-rich product.

ii) To study the effect of different feed concentrations on the separation performance of the SCCR4 unit. This work should be supported by separate batch column work investigating the dependency of K_D with carbohydrate concentration.

iii) To optimize the flow conditions for higher mobile phase temperature operations. In the present experimental study, it was shown that the 'cross-over' point of profiles shifted towards the glucose-rich product outlet as the mobile phase temperature increased causing a higher contamination of this product. In future, higher temperature operations could be performed at lower

(mean) $\frac{L'}{P}$ settings so as to offset the shift of the 'cross-over' point towards the glucose-rich product.

iv) To install an enclosure for constant temperature operations.

v) To employ lower $\frac{L_4}{P}$ settings so as to produce a higher solid content fructos-rich product. This can be achieved by operating with a lower purge flowrate or a higher packing switch rate. One possible means of achieving the latter is the isolation and purging of two consecutive columns during one sequence.

vi) To study the simultaneous hydrolysis and separation performance of the SCCR4 unit. As the Zerolit resin employed in this research was conditioned to retain 3 - 10% of free hydrogen ions, the SCCR4 unit is also designed with a view to separating sucrose solutions directly into a glucose-rich and fructose-rich product.

vii) To obtain a fructose-rich product from starch or corn hydrolysate.

viii) To incorporate more columns so as to attempt a complete separation of fructose from glucose.

Improvements on the computer simulation model include:

i) The allowance for K_D variation with concentration. In the present programme, K_D values were assumed to be independent of the mobile phase concentrations. Hence,

the substitution of the term, the rate of change of concentration in the solid phase over a time increment Δt, is as follows: (Section 9.2).

$$\frac{dq_n}{dt} = K_D \frac{dC_n}{dt}$$

where q_n = concentration of a component in the solid phase in plate n.

C_n = concentration of the same component in the mobile phase in plate n.

K_D = distribution constant.

If K_D is C_n dependent,

$$\frac{dq_n}{dt} = K_D \frac{dC_n}{dt} + C_n \frac{dK_D}{dt} \qquad (9.13)$$

Substituting equation 9.13 into equation 9.9 would result in a first order linear differential equation which will require a numerical analysis technique for its solution.

Alternatively one could use an empirical relationship between C_n and K_D obtained from analytical batch column studies. Its substitution into equation 9.13 and subsequently into 9.9 would lead to an equation involving a single differential term $\frac{dC_n}{dt}$.

ii) The use of a different K_D value for each theoretical plate along the separation section according to the plates' temperature. To effect this, a column temperature profile is necessary.

iii) The incorporation into the programme facilities to account for the liquid hold-up in the valves and transfer lines.

Appendix I

Fig. 1 Calibration Curve Of The Glucose Oxidase Assay

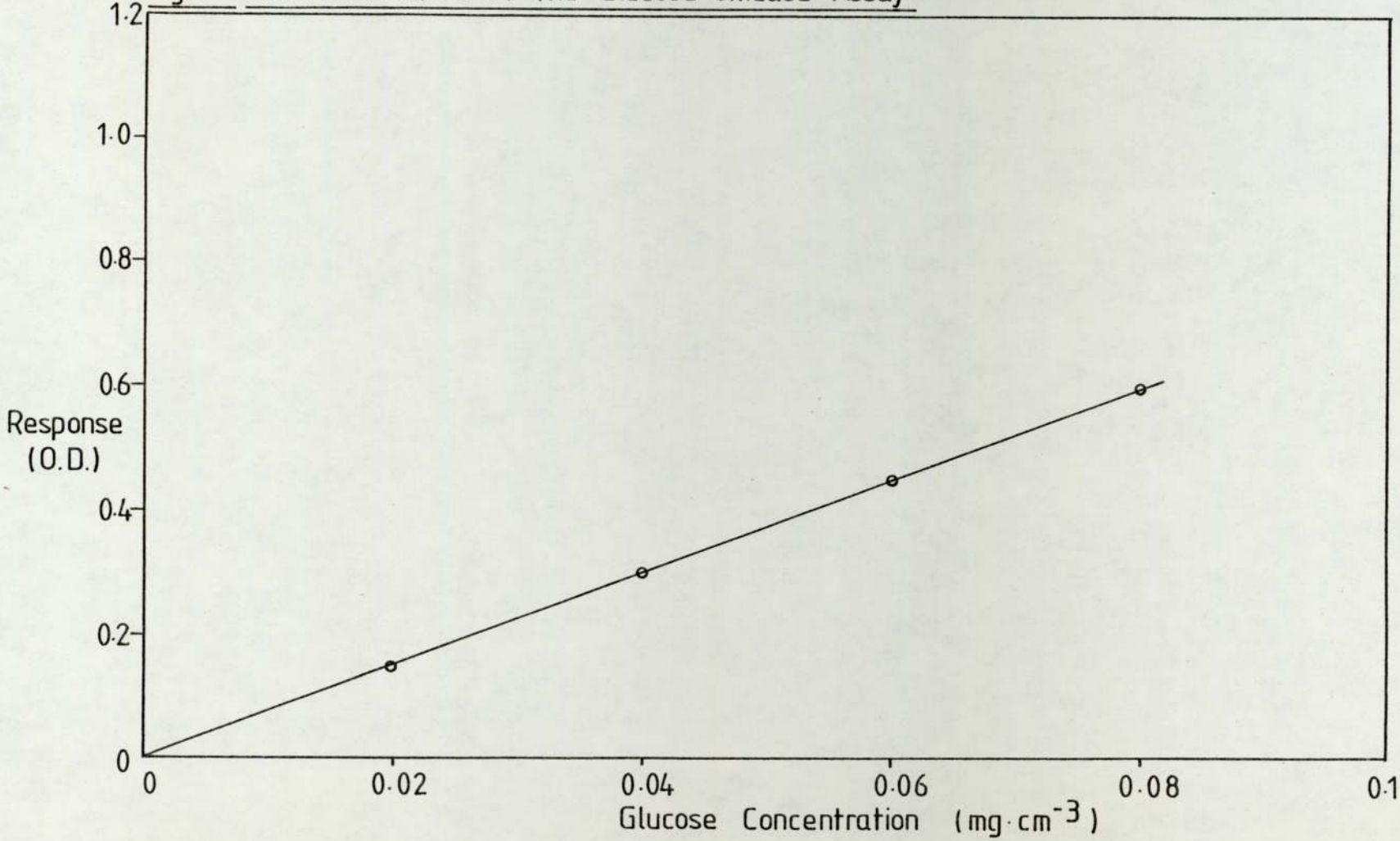

Fig. 2 Calibration Curve Of The Resorcinol Assay

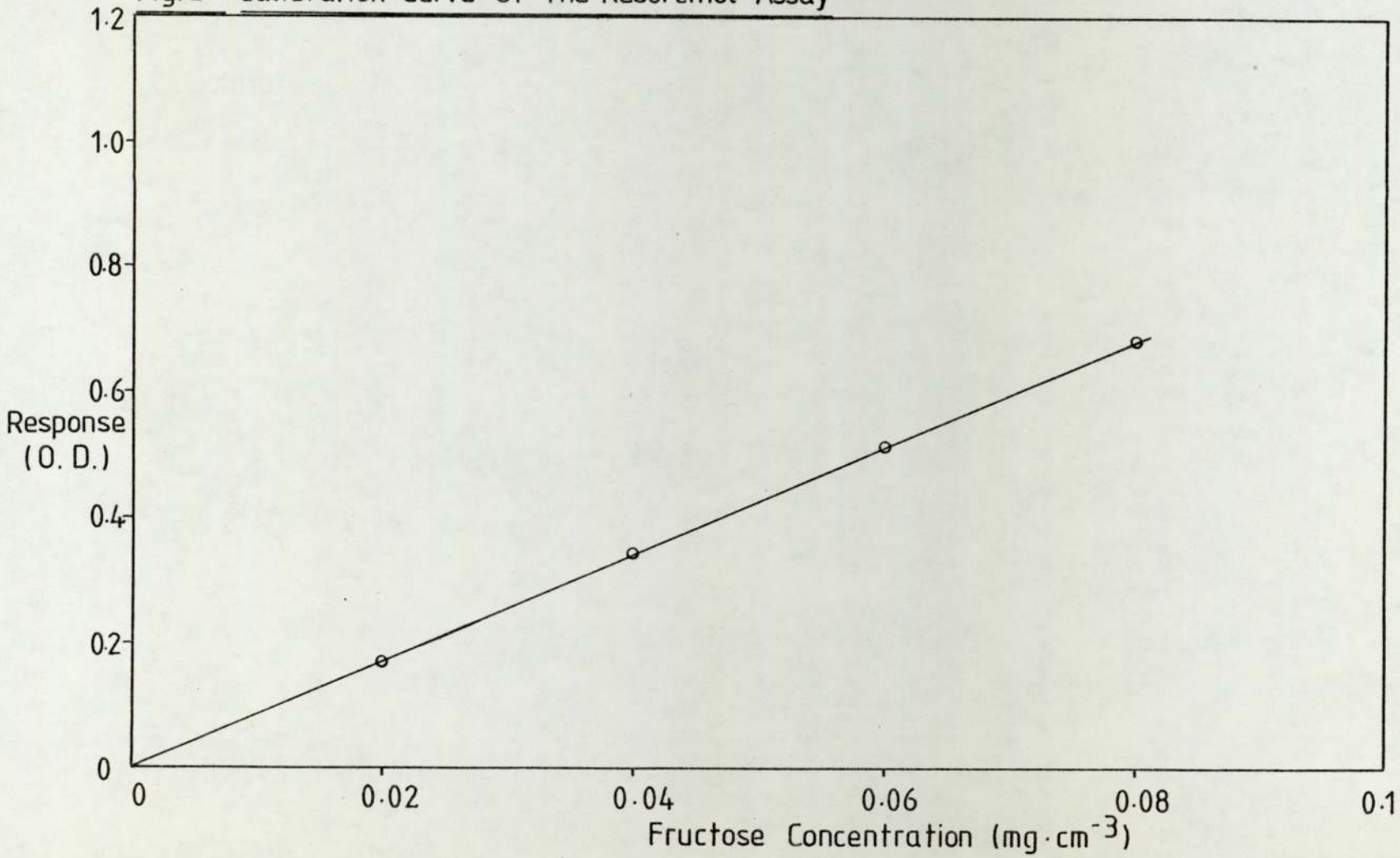

Fig. 3 Calibration Curve Of The Cysteine/Sulphuric Acid Assay

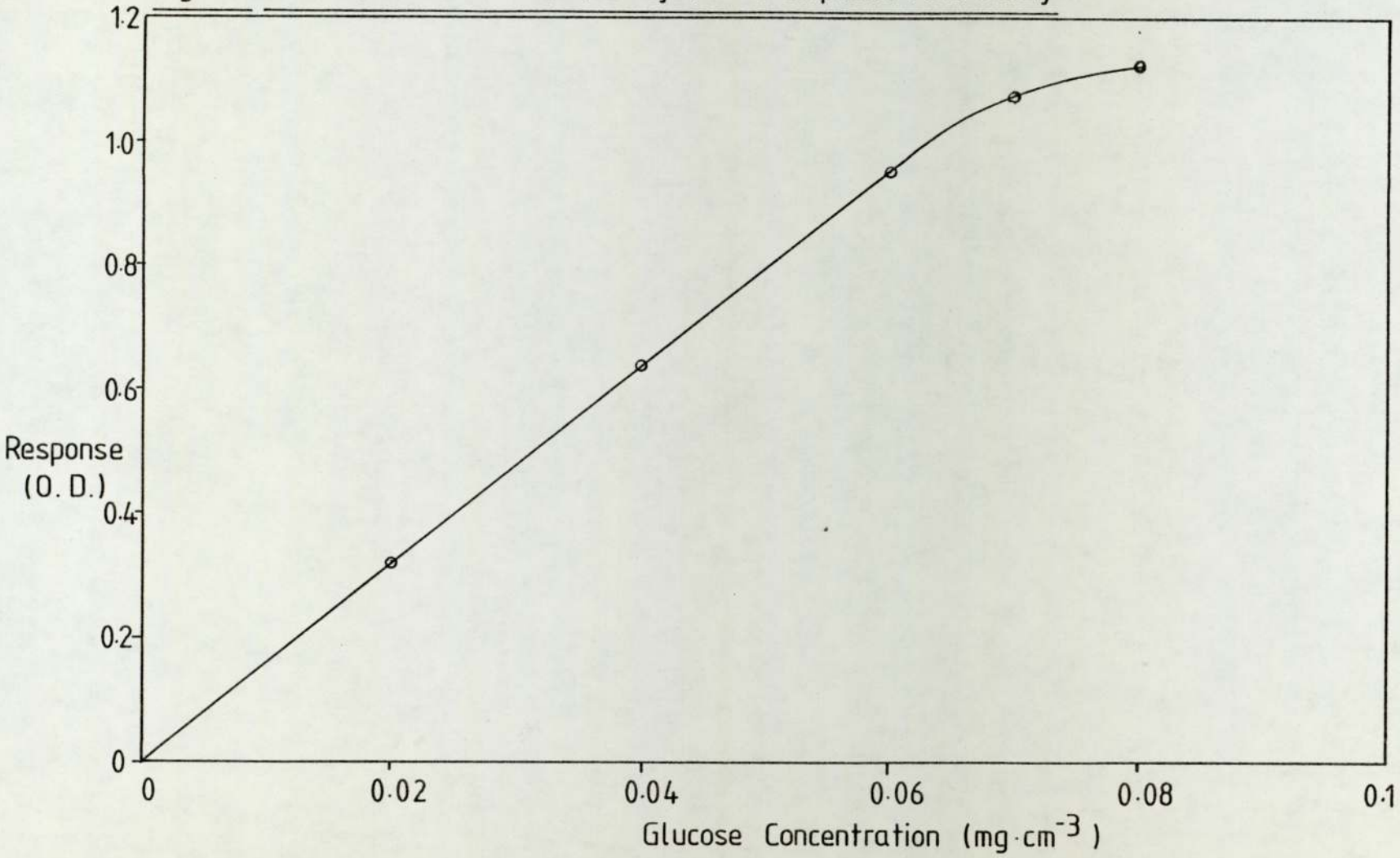

Appendix II

Fig.1 Calibration Curve For T_1 / T_2 (Nickel-Chromium/Nickel-Aluminium) Thermocouple

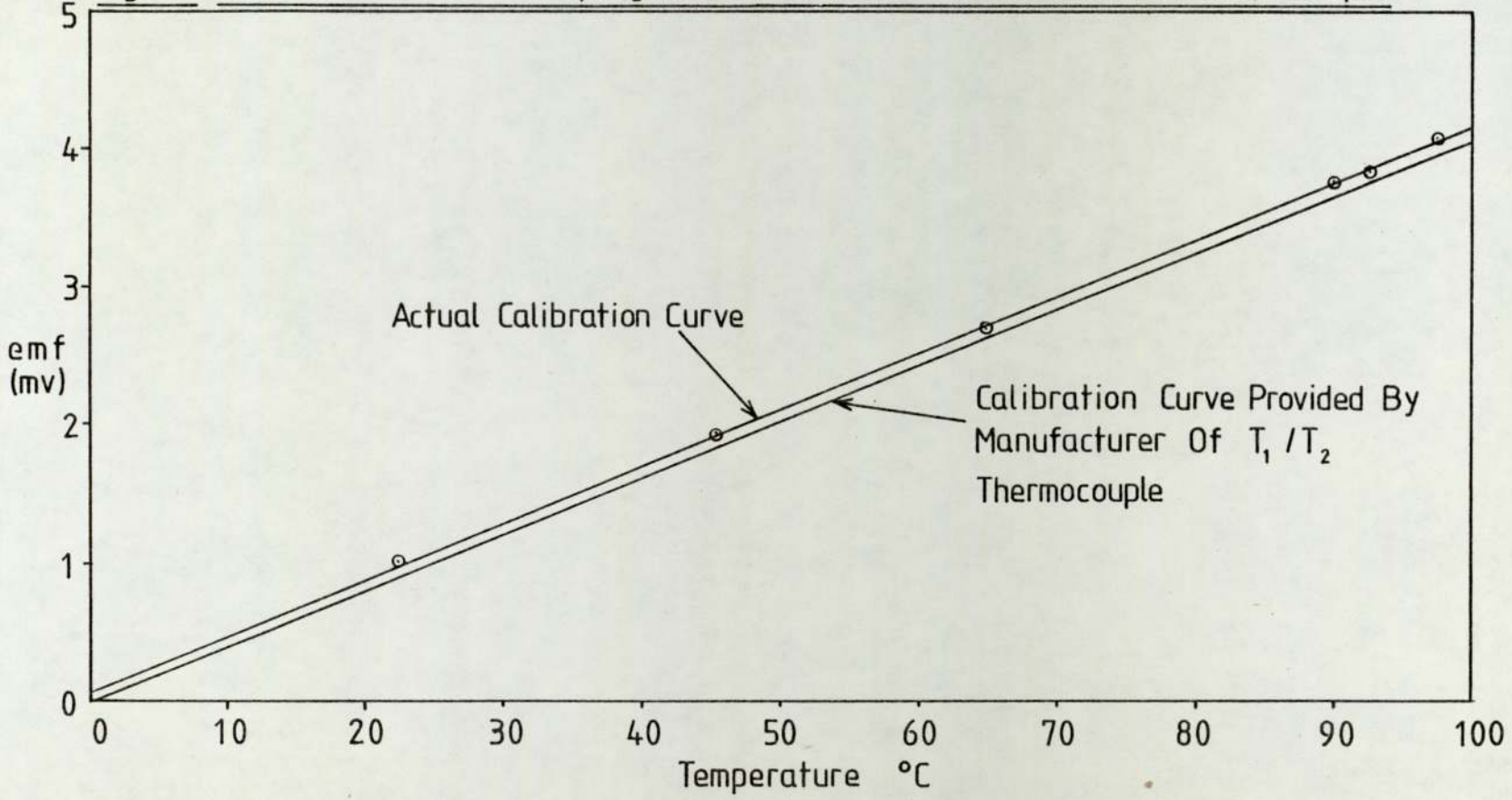

Appendix III

Fig. 1 Sieve Analysis Of Packing Sample

Size Range (μm)	Sample 1	Sample 2
	Weight Fraction	Weight Fraction
> 1204	0.0	0.0
1204 ~ 422	0.0	0.0
422 ~ 295	0.10	0.092
295 ~ 211	0.33	0.38
211 ~ 152	0.48	0.45
152 ~ 104	0.086	0.072
104 ~ 76	0.004	0.006
< 76	0.0	0.0

Appendix IV

Fig.1 Analysis Of Glucose & Fructose Sample used as Feed in SCCR4 Runs

Glucose Sample

Glucose	88.2 % w/w
Fructose	0.2
Xylose	0.4

Fructose Sample

Fructose	94.4 % w/w
Glucose	0.7
Unknown	2.6

Table 1 Details Of Product Distribution Profiles For All Runs

Run Number \ Column Number	Amount Of Products In Each Column (gm)																			
	Column 9		Column 10		Column 1		Column 2		Column 3		Column 4		Column 5		Column 6		Column 7		Column 8	
	G	F	G	F	G	F	G	F	G	F	G	F	G	F	G	F	G	F	G	F
45-1-4-29	—	—	2·36	10·05	7·56	30·86	10·76	29·79	17·58	26·83	24·34	24·34	27·58	2·60	22·50	1·95	22·59	1·74	18·96	1·74
49-1-6-29	—	—	0·79	2·99	2·93	23·16	4·68	19·97	16·81	19·74	19·34	12·48	20·38	2·38	28·35	1·65	25·75	1·78	9·48	1·74
49-2-6-29	—	—	2·36	4·73	4·79	30·42	19·03	35·88	21·59	33·90	22·78	27·14	25·19	13·17	23·40	4·05	24·65	2·53	14·55	2·37
49-3-6-29	—	—	1·73	14·18	12·66	56·05	12·79	51·48	18·50	45·64	29·17	45·86	22·89	33·99	21·00	21·90	21·33	21·65	20·38	8·85
49-3-6-20-D	—	—	1·73	13·55	16·21	49·87	29·33	37·44	25·44	37·00	19·65	27·14	18·99	24·34	27·00	15·45	36·18	9·80	35·01	5·37
02-2·4-6-29	—	—	0·02	0·20	0·04	1·05	0·05	1·15	0·15	1·12	0·46	1·14	0·63	0·84	0·67	0·50	0·73	0·28	0·67	0·12
52-2-6-38	—	—	2·49	4·41	5·79	46·01	6·15	46·80	8·64	37·00	24·65	31·04	25·88	25·60	27·60	20·85	27·97	20·38	26·70	17·22
52-2-6-44	—	—	1·18	10·63	6·33	49·40	7·33	49·30	13·42	47·80	30·42	47·42	26·96	35·23	23·25	21·00	23·07	21·33	18·33	15·48
52-2-6-65	—	—	5·00	12·29	7·41	53·88	13·42	52·73	26·06	47·80	30·42	39·00	30·18	35·24	29·55	30·00	27·97	24·81	27·02	17·85

Table 2 Operating Conditions Of Run No. (45-1-4-29)

CYCLE NO.	PERIOD OF OPS.	AVERAGE INLET PRESSURE			AVERAGE FLOWRATES (MEASURED)			AVERAGE TEMPERATURE		WEIGHT OF PRODUCT (COLLECTED)		AVERAGE PRODUCT DATA								MASS BALANCE [PRODUCTS OUT / FEED IN]	
												G – RICH PRODUCT CONC.		F – RICH PRODUCT CONC.		G – RICH PRODUCT PURITY		F – RICH PRODUCT PURITY			
		ELUENT	PURGE	FEED	ELUENT	PURGE	FEED	ELUENT	PURGE	G RICH PRODUCT	F RICH PRODUCT	G.	F.	G.	F.	G.	F.	G.	F.	G.	F.
	Hrs.	kN m^{-2}			CM^3 MIN^{-1}			°C		Kg.	Kg.	Mg. CM^{-3}		Mg. CM^{-3}		%		%		%	
1	0-7.5	89.0	140.0	62.0	3.95	300	0.933	28	70	2.2	131.82	—	—	—	—	—	—	—	—	—	—
2	7.5-15	100.0	158.5	70.0	4.12	297.5	1.009	30	70	2.17	131.8	11.88	2.0	0.09	0.35	85.6	14.4	20.5	79.5	36.37	50.98
3	15 – 22.5	105.0	159.3	78.0	4.13	298.0	1.015	30	70	2.20	131.8	41.25	3.1	0.045	0.65	93.0	7.0	6.5	93.5	96.21	92.04
4	22.5– 30	111.0	168.3	78.5	4.01	297.9	1.075	29.5	70	2.17	131.8	45.0	3.2	0.08	0.88	93.6	6.4	8.4	91.6	97.34	113.8
5	30 – 37.5	121	168.5	80.5	4.04	297.6	1.075	30.0	70	2.18	131.8	43.8	3.1	0.085	0.90	93.4	6.6	8.6	91.4	96.00	116.0
6	37.5 –45	120	179.1	82.7	4.10	297.0	1.074	29.5	70	2.18	131.8	45.0	3.25	0.09	0.84	93.4	6.6	9.7	90.3	98.93	109.9

Table 3 Operating Conditions Of Run No. (49-1-6-29)

CYCLE NO.	PERIOD OF OPS.	AVERAGE INLET PRESSURE			AVERAGE FLOWRATES (MEASURED)			AVERAGE TEMPERATURE		WEIGHT OF PRODUCT (COLLECTED)		AVERAGE PRODUCT DATA								MASS BALANCE [PRODUCTS OUT / FEED IN]	
												G - RICH PRODUCT CONC.		F - RICH PRODUCT CONC.		G - RICH PRODUCT PURITY		F - RICH PRODUCT PURITY			
		ELUENT	PURGE	FEED	ELUENT	PURGE	FEED	ELUENT	PURGE	G RICH PRODUCT	F RICH PRODUCT	G.	F.	G.	F.	G.	F.	G.	F.	G.	F.
	Hrs.	$kN\ m^{-2}$			$CM^3\ MIN^{-1}$			°C		Kg.	Kg.	$Mg.\ CM^{-3}$		$Mg.\ CM^{-3}$		%		%		%	
1	0 - 5	80.5	170.5	60.5	6.31	295	1.00	28.0	70.5	2.075	87.600	—	—	—	—	—	—	—	—	—	—
2	5 -10	110.8	178.1	67.0	6.30	293	1.01	29.0	70.0	2.083	87.690	—	—	—	—	—	—	—	—	—	—
3	10 -15	126.0	178.0	73.0	6.300	293	1.00	30.0	70.0	2.094	87.737	16.25	1.70	0.075	0.70	90.53	9.47	9.68	90.32	57.3	86.7
4	15 -20	152.8	182.8	79.5	6.301	293	1.00	29.5	70.0	2.122	87.734	18.75	1.85	0.072	0.713	91.02	8.98	8.95	91.05	64.1	89.5
5	20 -25	160.0	183.0	82.8	6.305	293	1.01	30.0	70.0	2.129	87.737	25.00	2.15	0.125	1.025	92.08	7.92	10.87	89.13	88.2	126.0
6	25 -30	160.3	185.0	83.0	6.300	293	1.00	29.0	70.0	2.135	87.738	30.00	2.40	0.115	0.840	92.59	7.41	12.04	87.96	102.9	105.1

Table 4 Operating Conditions Of Run No. (49-2-6-29)

CYCLE NO.	PERIOD OF OPS.	AVERAGE INLET PRESSURE			AVERAGE FLOWRATES (MEASURED)			AVERAGE TEMPERATURE		WEIGHT OF PRODUCT (COLLECTED)		AVERAGE PRODUCT DATA								MASS BALANCE [PRODUCTS OUT / FEED IN]	
												G - RICH PRODUCT CONC.		F - RICH PRODUCT CONC.		G - RICH PRODUCT PURITY		F - RICH PRODUCT PURITY			
		ELUENT	PURGE	FEED	ELUENT	PURGE	FEED	ELUENT	PURGE	G RICH PRODUCT	F RICH PRODUCT	G.	F.	G.	F.	G.	F.	G.	F.	G.	F.
	Hrs.	$kN\ m^{-2}$			$CM^3\ MIN^{-1}$			°C		Kg.	Kg.	$Mg.CM^{-3}$		$Mg.CM^{-3}$		%		%		%	
1 & 2	0–10	140·0	178·0	70·1	6·10	293	2·00	285	70·3	4910	175·00	—	—	—	—	—	—	—	—	—	—
3	10–15	168·1	180·0	85·0	6·10	293	2·02	28·0	70·1	2·451	87·045	52·00	3·50	0·22	1·45	93·7	6·3	13·2	86·8	100·7	88·97
4	15–20	173·1	184·0	90·0	6·11	293	2·01	29·5	70·5	2·425	87·045	62·00	5·00	0·37	1·80	92·5	7·5	17·1	82·9	103·8	111·9
5	20–25	175·1	185·0	95·0	6·10	293	2·04	30·0	71·0	2·430	87·00	66·00	4·80	0·34	1·80	93·2	6·8	15·9	84·1	129·3	109·9
6	25–30	186·1	191·9	98·0	6·11	293	2·02	29·8	70·0	2·462	87·00	64·00	4·50	0·29	1·60	93·4	6·6	15·3	84·7	125·7	99·2
7	30–35	185·5	190·0	97·9	6·05	288	2·00	29·5	70·1	2·450	86·136	60·00	3·80	0·38	1·80	94·0	6·0	17·4	82·6	124·8	109·6
8	35 40	186·0	192·9	99·8	6·05	290	2·08	29·5	70·0	2·460	86·20	58·00	3·85	0·30	1·70	93·8	6·2	15·0	85·0	112·5	100·0

Table 5 Operating Conditions Of Run No. (49-3-6-29)

CYCLE NO.	PERIOD OF OPS.	AVERAGE INLET PRESSURE			AVERAGE FLOWRATES (MEASURED)			AVERAGE TEMPERATURE		WEIGHT OF PRODUCT (COLLECTED)		AVERAGE PRODUCT DATA								MASS BALANCE [PRODUCTS OUT / FEED IN]	
												G - RICH PRODUCT CONC.		F - RICH PRODUCT CONC.		G - RICH PRODUCT PURITY		F - RICH PRODUCT PURITY			
		ELUENT	PURGE	FEED	ELUENT	PURGE	FEED	ELUENT	PURGE	G RICH PRODUCT	F RICH PRODUCT	G.	F.	G.	F.	G.	F.	G.	F.	G.	F.
	Hrs.	$kN\ m^{-2}$			$CM^3\ MIN^{-1}$			°C		Kg.	Kg.	$Mg.\ CM^{-3}$		$Mg.\ CM^{-3}$		%		%		%	
1	0 – 5	151·0	171·0	111·0	6·11	295	2·98	28·0	70·5	2·689	85·61	—	—	—	—	—	—	—	—	—	—
2	5–10	165·0	189·0	121·0	6·10	293	3·01	28·5	70·0	2·701	85·59	—	—	—	—	—	—	—	—	—	—
3	10–15	189·0	205·0	138·0	6·20	293	2·95	29	70·0	2·706	85·68	65·0	6·75	0·160	2·10	90·6	9·4	7·1	92·9	87·6	89·6
4	15–20	205·0	220·0	148·5	6·10	298	3·04	30	70·0	2·697	86·136	67·0	10·2	0·48	2·2	86·8	13·2	18·0	82·0	101·4	95·1
5	20 25	218·0	229·0	149·1	6·10	293	3·05	29	70·0	2·713	84·909	70·0	11·0	0·34	2·50	86·4	13·6	11·9	88·1	99·6	105·8
6	25–30	221·0	231·0	148·0	6·25	290	2·90	30	70·0	2·716	83·409	65·0	10·25	0·28	2·20	86·4	13·6	11·3	88·7	95·7	97·1

Table 6 Operating Conditions Of Run No. (49-3-6-20 D)

CYCLE NO.	PERIOD OF OPS.	AVERAGE INLET PRESSURE			AVERAGE FLOWRATES (MEASURED)			AVERAGE TEMPERATURE		WEIGHT OF PRODUCT (COLLECTED)		AVERAGE PRODUCT DATA								MASS BALANCE [PRODUCTS OUT / FEED IN]	
												G - RICH PRODUCT CONC.		F - RICH PRODUCT CONC.		G - RICH PRODUCT PURITY		F - RICH PRODUCT PURITY			
		ELUENT	PURGE	FEED	ELUENT	PURGE	FEED	ELUENT	PURGE	G RICH PRODUCT	F RICH PRODUCT	G.	F.	G.	F.	G.	F.	G.	F.	G.	F.
	Hrs.	$kN\ m^{-2}$			$CM^3\ MIN^{-1}$			°C		Kg	Kg	$Mg\ CM^{-3}$		$Mg\ CM^{-3}$		%		%		%	
1	0 – 5	210·0	61·0	89·8	6·00	29·0	3·01	21·0	39·0	2·65	8·974	—	—	—	—	—	—	—	—	—	—
2	5 –10	235·0	63·0	107·0	6·01	30·1	2·96	21·0	40·0	2·66	8·950	—	—	—	—	—	—	—	—	—	—
3	10–15	265·0	68·0	110·0	6·03	30·0	29·5	21·0	39·0	2·67	8·975	50·0	4·5	3·6	23·86	91·74	8·26	13·11	86·89	78·0	102·3
4	15–20	270·0	69·0	119·0	6·05	30·0	2·95	22·0	39·5	2·675	8·966	65·0	7·7	3·4	20·86	89·41	10·59	14·01	85·99	96·2	93·9
5	20–25	278·0	70·0	127·0	6·00	29·0	2·95	21·0	40·0	2·640	8·647	65·0	5·2	4·2	23·92	92·59	7·41	14·94	85·06	97·9	99·7
6	25–30	280·0	73·0	129·0	6·10	29·0	2·90	20·0	39·0	2·723	8·641	65·0	5·2	3·6	21·93	92·59	7·41	13·42	86·58	99·7	93·6

Table 7 Operating Conditions Of Run No. (02-2-6-29)

CYCLE NO.	PERIOD OF OPS.	AVERAGE INLET PRESSURE			AVERAGE FLOWRATES (MEASURED)			AVERAGE TEMPERATURE		WEIGHT OF PRODUCT (COLLECTED)		AVERAGE PRODUCT DATA								MASS BALANCE [PRODUCTS OUT / FEED IN]	
												G - RICH PRODUCT CONC.		F - RICH PRODUCT CONC.		G - RICH PRODUCT PURITY		F - RICH PRODUCT PURITY			
		ELUENT	PURGE	FEED	ELUENT	PURGE	FEED	ELUENT	PURGE	G RICH PRODUCT	F RICH PRODUCT	G.	F.	G.	F.	G.	F.	G.	F.	G.	F.
	Hrs.	kN m^{-2}			CM^3 MIN^{-1}			°C		Kg.	Kg.	Mg. CM^{-3}		Mg. CM^{-3}		%		%		%	
1 & 2	0—10	73·0	120·0	31·2	6·00	287	2·40	28·5	70·5	4·81	170·0	—	—	—	—	—	—	—	—	—	—
3	10—15	85·0	128·1	35·6	6·02	287	2·41	29·0	70·0	2·41	84·9	1·9	0·26	0·007	0·09	—	—	—	—	—	—
4	15—20	91·0	145·1	40·8	6·01	288	2·40	28·9	71·0	2·40	85·00	2·3	0·265	0·007	0·08	89·7	10·3	8·1	91·9	69·4	108·7
5	20—25	93·8	146·1	45·0	6·00	287	2·40	29·8	70·0	2·40	86·36	2·95	0·305	0·0065	0·07	90·6	9·4	8·5	91·5	90·9	99·1
6	25—30	99·5	145·0	49·9	6·00	287	2·45	29·5	70·1	2·50	86·36	3·40	0·315	0·007	0·064	91·5	8·5	9·8	90·2	103·0	103·0
7	30—35	100·0	148·0	50·8	6·10	287	2·40	29·5	70·0	2·554	86·36	3·25	0·300	0·006	0·058	91·5	8·5	9·4	90·6	102·1	87·7
8	35—40	102·0	150·5	50·1	6·10	287	2·35	29·5	70·0	2·515	85·91	3·05	0·350	0·006	0·059	91·0	9·0	9·3	90·7	96·8	88·7

Table 8 Operating Conditions Of Run No. (52-2-6-38)

CYCLE NO.	PERIOD OF OPS.	AVERAGE INLET PRESSURE			AVERAGE FLOWRATES (MEASURED)			AVERAGE TEMPERATURE		WEIGHT OF PRODUCT (COLLECTED)		AVERAGE PRODUCT DATA								MASS BALANCE [PRODUCTS OUT / FEED IN]	
												G - RICH PRODUCT CONC.		F - RICH PRODUCT CONC.		G - RICH PRODUCT PURITY		F - RICH PRODUCT PURITY			
		ELUENT	PURGE	FEED	ELUENT	PURGE	FEED	ELUENT	PURGE	G RICH PRODUCT	F RICH PRODUCT	G.	F.	G.	F.	G.	F.	G.	F.	G.	F.
	Hrs.	$kN\ m^{-2}$			$CM^3\ MIN^{-1}$			°C		Kg.	Kg.	$Mg.\ CM^{-3}$		$Mg.\ CM^{-3}$		%		%		%	
1	0–5	90·0	130·5	59·8	6·10	210	2·01	38·0	34·0	2·494	64·210	—	—	—	—	—	—	—	—	—	—
2	5–10	130·0	130·0	60·8	6·11	210	2·00	38·0	34·0	2·500	64·300	—	—	—	—	—	—	—	—	—	—
3	10–15	150·0	125·0	78·6	6·10	210	2·02	38·0	34·0	2·506	64·500	60·00	5·40	0·18	0·95	91·74	8·26	16·0	84·0	98·99	45·34
4	15–20	151·7	137·0	82·5	6·10	210	2·01	38·0	34·0	2·484	64·545	60·00	7·80	0·22	1·50	88·50	11·50	12·8	87·2	100·3	77·11
5	20–25	160·7	138·0	88·4	6·11	211	2·00	38·0	34·0	2·487	64·095	60·00	11·60	0·23	1·80	83·79	16·21	11·4	88·6	101·2	96·15
6	25–30	160·8	140·4	89·6	6·10	210	2·01	38·0	34·0	2·516	64·091	61·00	12·40	0·25	1·90	83·1	16·9	11·6	88·4	104·1	101·5

Table 9 Operating Conditions Of Run No. (52-2-6-44)

CYCLE NO.	PERIOD OF OPS.	AVERAGE INLET PRESSURE			AVERAGE FLOWRATES (MEASURED)			AVERAGE TEMPERATURE		WEIGHT OF PRODUCT (COLLECTED)		AVERAGE PRODUCT DATA								MASS BALANCE [PRODUCTS OUT / FEED IN]	
												G-RICH PRODUCT CONC.		F-RICH PRODUCT CONC.		G-RICH PRODUCT PURITY		F-RICH PRODUCT PURITY			
		ELUENT	PURGE	FEED	ELUENT	PURGE	FEED	ELUENT	PURGE	G RICH PRODUCT	F RICH PRODUCT	G.	F.	G.	F.	G.	F.	G.	F.	G.	F.
	Hrs.	$kN\ m^{-2}$			$CM^3\ MIN^{-1}$			°C		Kg.	Kg.	$Mg.\ CM^{-3}$		$Mg.\ CM^{-3}$		%		%		%	
1	0–5	75·0	210·0	45·0	6·10	290	2·00	42·5	46·0	2·460	86·90	—	—	—	—	—	—	—	—	—	—
2	5–10	78·0	220·0	50·0	6·11	291	2·00	44·0	46·1	2·480	87·01	—	—	—	—	—	—	—	—	—	—
3	10–15	98·0	230·5	54·0	6·10	293	2·02	43·8	45·5	2·476	86·99	46·0	8·00	0·085	1·90	85·2	14·8	8·7	91·3	74·1	64·75
4	15–20	105·5	239·5	58·0	6·10	293	2·00	44·0	46·1	2·480	86·89	64·0	12·00	0·098	1·05	85·7	14·3	8·6	91·4	103·2	80·66
5	20–25	109·0	240·5	61·0	6·10	292	2·01	44·1	45·8	2·500	86·91	62·0	17·00	0·15	1·20	80·5	19·5	11·1	88·9	103·2	97·4
6	25–30	110·2	241·5	62·0	6·10	290	2·00	44·0	46·0	2·470	87·00	63·0	18·00	0·16	1·20	79·6	20·4	11·8	88·2	104·6	99·23

Table 10 Operating Conditions Of Run No. (52-2-6-65)

CYCLE NO.	PERIOD OF OPS.	AVERAGE INLET PRESSURE			AVERAGE FLOWRATES (MEASURED)			AVERAGE TEMPERATURE		WEIGHT OF PRODUCT (COLLECTED)		AVERAGE PRODUCT DATA								MASS BALANCE [PRODUCTS OUT / FEED IN]	
												G RICH PRODUCT CONC.		F RICH PRODUCT CONC.		G RICH PRODUCT PURITY		F RICH PRODUCT PURITY			
		ELUENT	PURGE	FEED	ELUENT	PURGE	FEED	ELUENT	PURGE	G RICH PRODUCT	F RICH PRODUCT	G.	F.	G.	F.	G.	F.	G.	F.	G.	F.
	Hrs.	kN m^{-2}			CM^3 MIN^{-1}			°C		Kg.	Kg.	Mg. CM^{-3}		Mg. CM^{-3}		%		%		%	
1	0 – 5	61·00	145·0	30·8	6·10	290	2·00	64·9	70·0	2·430	86·89	—	—	—	—	—	—	—	—	—	—
2	5 – 10	69·00	165·0	35·0	6·11	295	2·01	65·1	70·0	2·441	86·99	—	—	—	—	—	—	—	—	—	—
3	10–15	78·00	170·0	35·8	6·10	293	2·00	65·0	70·0	2·440	87·00	63·0	18·00	0·16	0·80	77·7	22·3	16·67	83·37	103·4	75·68
4	15–20	79·00	189·8	39·0	6·10	293	2·01	65·0	70·0	2·453	86·951	65·1	21·01	0·15	1·00	75·6	24·4	13·04	86·96	106·0	91·87
5	20–25	80·72	199·0	40·3	6·09	291	2·00	64·8	70·1	2·439	86·98	64·5	22·08	0·16	1·15	74·5	25·5	12·24	87·78	105·7	102·6
6	25–30	82·68	200·0	41·3	6·10	290	2·001	65·0	70·0	2·450	86·951	65·0	22·00	0·16	1·100	74·7	25·3	14·1	85·9	106·8	99·7

Appendix V

Fig. 1 Programme Listing

```
      PRØGRAM PRØFILE(INPUT,ØUTPUT,TAPE1=INPUT,TAPE2=ØUTPUT)
      DIMENSIØN G(1500),F(1500),AG(150),AF(150),KD1(10),KD2(10)
      REAL KD1,KD2
      READ(1,319)L
  319 FØRMAT(I2)
      READ(1,3)CFLØW,FFLØW,SFLØW,V1,V2,DT
      READ(1,111)GFEED,FFEED
      READ(1,4)NFEED,NNBED,KTØTAL,KKINK,KKTYPE,NNTYPE
      READ(1,5)(KD1(J),KD2(J),J=1,L)
      DØ 317 J=1,L
      DØ 1 NN=1,1500
      G(NN)=0.0
      F(NN)=0.0
    1 CØNTINUE
      DØ 2 NN=1,150
      AG(NN)=0.0
      AF(NN)=0.0
    2 CØNTINUE
      WRITE(2,7)CFLØW,SFLØW,FFLØW,V1,V2
      WRITE(2,8)GFEED,FFEED,DT
      WRITE(2,9)NFEED,NNBED,KTØTAL,KKINK,KKTYPE,NNTYPE
      WRITE(2,11)KD1(J),KD2(J)
      NNTØT=NNBED*10
      NNNINE=NNBED*9+1
      NNFEED=(NFEED-1)*NNBED+1
      WRITE(2,12)
      KKSUM=1
      DØ 100 K=1,KTØTAL
      ISTKK=KKINK*(K-1)+1
      LSTKK=KKINK*K
      DØ 200 KK=ISTKK,LSTKK
      NNSUM=1
      DØ 300 N=1,10
      IF(N.LE.5)CFLØWC=CFLØW
      IF(N.GE.6)CFLØWC=CFLØW+FFLØW
      IF(N.LE.(NFEED-K))GØ TØ 500
      NNFST=NNBED*(N-1)+1
      NNLST=NNBED*N
      DØ 400 NN=NNFST,NNLST
      IF(N.EQ.1)GØ TØ 80
      IF((N.EQ.2).AND.(NN.EQ.NNFST))GØ TØ 40
      IF(NN.EQ.NNFEED)GØ TØ 50
      GØ TØ 60
   40 G(NN-1)=0.0
      F(NN-1)=0.0
      GØ TØ 70
   50 A=CFLØWC*DT
      IF(F(NN-1).LT.0.1E-10)F(NN-1)=0.0
      IF(F(NN-1).LT.0.1E-10)F(NN-1)=0.0
      RR=EXP(-A/(V1+V2*KD1(J)))
      SS=EXP(-A/(V1+V2*KD2(J)))
      G(NN)=(1.-RR)*((CFLØW*G(NN-1)+FFLØW*GFEED)/CFLØWC)+RR*G(NN)
      F(NN)=(1.-SS)*((CFLØW*F(NN-1)+FFLØW*FFEED)/CFLØWC)+SS*F(NN)
      GØ TØ 150
   60 IF(G(NN-1).LT.0.1E-10)G(NN-1)=0.0
      IF(F(NN-1).LT.0.1E-10)F(NN-1)=0.0
   70 A=CFLØWC*DT
```

Fig. 1 Cont.

```
      RR=EXP(-A/(V1+V2*KD1(J)))
      SS=EXP(-A/(V1+V2*KD2(J)))
      F(NN)=(1.-SS)*(F(NN-1))+SS*F(NN)
      G(NN)=(1.-RR)*(G(NN-1))+RR*G(NN)
      GØ TØ 150
   80 IF(NN.EQ.NNFST)GØ TØ 90
      IF(G(NN-1).LT.0.1E-10)G(NN-1)=0.0
      IF(F(NN-1).LT.0.1E-10)F(NN-1)=0.0
      GØ TØ 95
   90 G(NN-1)=0.0
      F(NN-1)=0.0
   95 A=SFLØW*DT
      RR=EXP(-A/(V1+V2*KD1(J)))
      SS=EXP(-A/(V1+V2*KD2(J)))
      G(NN)=(1.-RR)*(G(NN-1))+RR*G(NN)
      F(NN)=(1.-SS)*(F(NN-1))+SS*F(NN)
  150 IF((NN.EQ.(NNTYPE*NNSUM)).AND.(KK.EQ.(KKTYPE*KKSUM)))GØ TØ 160
      GØ TØ 170
  160 WRITE(2,161)K,KK,N,NN,G(NN),F(NN)
  170 IF(NN.EQ.(NNTYPE*NNSUM))NNSUM=NNSUM+1
  400 CØNTINUE
      GØ TØ 300
  500 NNSUM=NNSUM+NNBED/NNTYPE
  300 CØNTINUE
      IF(KK.EQ.(KKTYPE*KKSUM))GØ TØ 180
      GØ TØ 200
  180 KKSUM=KKSUM+1
      WRITE(2,185)
  200 CØNTINUE
      WRITE(2,190)
      WRITE(2,12)
      DØ 1500 NN=1,NNBED
      AG(NN)=G(NN)
      AF(NN)=F(NN)
 1500 CØNTINUE
      DØ 2000 NN=1,NNTØT
      IF(NN.GE.NNNINE)GØ TØ 2010
      NNADJ=NN+NNBED
      G(NN)=G(NNADJ)
      F(NN)=F(NNADJ)
      GØ TØ 2000
 2010 NNADJ=NN+1-NNNINE
      G(NN)=AG(NNADJ)
      F(NN)=AF(NNADJ)
 2000 CØNTINUE
  100 CØNTINUE
  317 CØNTINUE
    3 FØRMAT(5F10.5)
    4 FØRMAT(6I4)
    5 FØRMAT(2F10.5)
    7 FØRMAT(1H ,7HCFLØW= ,F8.3,4X,7HSFLØW= ,F8.3,4X,7HFFLØW= ,F8.3,4X
     1HV1= ,F10.5,4X,4HV2= ,F10.5)
    8 FØRMAT(1H ,8H GFEED= ,E13.6,4X,8H FFEED= ,E13.6,4X,4H DT= ,F10.5
    9 FØRMAT(1H ,7HNFEED= ,I2,1X,7HNNBED= ,I3,1X,8HKTØTAL= ,I3,1X,7HKK
     1K= ,I4,1X,8HKKTYPE= ,I3,1X,8HNNTYPE= ,I3)
   11 FØRMAT(1H ,5HKD1= ,E13.6,4X,5HKD2= ,E13.6)
  111 FØRMAT(2F10.5)
```

Fig. 1 Cont.

```
12 FØRMAT(1H,22X,1HK,14X,2HKK,15X,1HN,14X,2HNN,5X,14HGLUCØSE CØNC,
   1X,15H FRUCTØSE CØNC.)
161 FØRMAT(1HO,21X,I2,13X,I5,12X,I2,12X,I4,6X,F12.10,5X,F12.10)
185 FØRMAT(1H ,32HNEXT TIME INTERVAL FØR PRINT ØUT)
190 FØRMAT(1H1,23HNEXT SWITCHING INTERVAL)
    END
```

List of Symbols for SCCR4 Programme

G	Concentration of glucose (gm cm^{-3})
F	Concentration of fructose (gm cm^{-3})
V_1	Volume of mobile phase in each theoretical plate (cm^3)
V_2	Volume of stationary phase in each theoretical plate (cm^3)
CFLOW	Mobile phase flowrate (cm^3 sec^{-1})
FFLOW	Feed flowrate (cm^3 sec^{-1})
SFLOW	Purge flowrate (cm^3 sec^{-1})
KD1	Distribution coefficient of glucose
KD2	Distribution coefficient of fructose
DT	Length of time increment (sec)
GFEED	Glucose concentration in feed (gm cm^{-3})
FFEED	Fructose concentration in feed (gm cm^{-3})
NFEED	Number of feed column
NNBED	Total number of plates per column
KTOTAL	Total number of sequences
KKINK	Number of time increments within a sequencing interval
KKTYPE	Number of time increments between print-outs
NNTYPE	Number of plates between print-outs
NN	Counter for number of plates
N	Counter for number of columns
NNTOT	Number of final plate in separating section, or total number of plates

NNNINE	First plate in last column of separating section
NNFEED	Number of feed plate
KKSUM	Time increment counter used for print-out condition
K	Counter for number of sequencing intervals
ISTKK	First time increment in sequencing interval
LSTKK	Last time increment in sequencing interval
KK	Counter for number of time increments
NNSUM	Counter used for plate print-out condition
CFLOWC	Post feed mobile phase flowrate (cm^3 sec^{-1})
NNFST	First plate in a column
NNLST	Last plate in a column

Fig. 2 Print Out After 3 Cycles

K	KK	N	NN	GLUCØSE CØNC.	FRUCTØSE CØNC.
30	27000	1	10	0.0000000000	0.0000000000
30	27000	1	20	0.0000000000	0.0000000000
30	27000	2	30	0.0000000000	.0100013829
30	27000	2	40	.0000000023	.0915953244
30	27000	3	50	.0000000584	.1012094561
30	27000	3	60	.0000008958	.1012541015
30	27000	4	70	.0000127835	.1012549687
30	27000	4	80	.0001768613	.1012463307
30	27000	5	90	.0024100346	.1011259636
30	27000	5	100	.0281144417	.0934845054
30	27000	6	110	.1058712568	.0786422333
30	27000	6	120	.1370655806	.0178630350
30	27000	7	130	.1439309260	.0006811434
30	27000	7	140	.1437245061	.0000184864
30	27000	8	150	.1437176879	.0000005026
30	27000	8	160	.1436957002	.0000000124
30	27000	9	170	.1436612977	0.0000000000
30	27000	9	180	.1436062904	0.0000000000
30	27000	10	190	.1434421056	0.0000000000
30	27000	10	200	.1297896900	0.0000000000

Fig.3 Print Out After 4 Cycles

K	KK	N	NN	GLUCØSE CØNC.	FRUCTØSE CØNC.
40	36000	1	10	0.0000000000	0.0000000000
40	36000	1	20	0.0000000000	0.0000000000
40	36000	2	30	0.0000000000	.0100029889
40	36000	2	40	.0000000029	.0916060570
40	36000	3	50	.0000000672	.1012151465
40	36000	3	60	.0000009601	.1012566522
40	36000	4	70	.0000131419	.1012561386
40	36000	4	80	.0001784406	.1012468774
40	36000	5	90	.0024152675	.1011262230
40	36000	5	100	.0281253246	.0934846350
40	36000	6	110	.1058828646	.0786423031
40	36000	6	120	.1370791618	.0178630721
40	36000	7	130	.1439495912	.0006811540
40	36000	7	140	.1437518937	.0000184882
40	36000	8	150	.1437581959	.0000005028
40	36000	8	160	.1437563109	.0000000125
40	36000	9	170	.1437533387	0.0000000000
40	36000	9	180	.1437488189	0.0000000000
40	36000	10	190	.1436681593	0.0000000000
40	36000	10	200	.1301021750	0.0000000000

NOMENCLATURE

A	Eddy diffusion mass transfer resistance terms in Van Deemter equation
A'	Column area
A_m	Average cross-sectional area of proes and interstices in column of the SCCR4 unit
A_s	Average cross-sectional area of resin matrix in column of the SCCR4 unit
B	Axial diffusion mass transfer resistance term in Van Deemter equation
C_s	Stationary phase mass transfer resistance term in Van Deemter equation
C_m	Mobile phase mass transfer resistance term in Van Deemter equation
C	Solute concentration in mobile phase
C_1, C_2	Gas phase solute concentration at point 1, 2 in the column in Barker and Lloyd's H.T.U. model
C_{n-1}, C_n	Concentration of solute in mobile phase of plate n-1 and n in SCCR4 simulation model
C_n^o	Initial concentration of solute in plate n used in SCCR4 simulation model
C_f	Feed concentration used in SCCR4 simulation model
D	Diffusion coefficient
d_p	Mean particle diameter
D_m	Mobile phase molecular diffusivity
D_s	Stationary phase molecular diffusivity

d	Thickness of stationary phase liquid film
d_c	Diameter of column
D_r	Radial diffusion coefficient
E	Eddy diffusivity
E'	Enzyme
E_p	Production rate of a given component in Pretorious and de Clerk equation
E_A, E_B	The mass production rates of components A and B in the top products employed in Barker and Huntington relationship between product purity, number of plates and difficulty of separation
E_i, E_{ii}	Mass flowrate of solute leaving in product i and product ii streams respectively in Barker and Lloyd's H.T.U. model
F'	Mobile phase flowrate
F_M	Fractional volume of mobile phase
F_s	Fractional volume of stationary phase
F	Fructose
f_A, f_B	The mass feedrate of components A and B to the column employed in Barker and Huntington's relationship between product purities, N and difficulty of separation
F_f	Feed flowrate used in the simulation study of SCCR4 unit
g'	Configuration factor of the packing

G	Glucose
H	Plate height
H'	Intrinsic plate height for packing as measured on an analytical column
H'_c	Plate height obtained for large diameter column without mixing devices
H'_{CN}	Plate height obtained for the same diameter column with mixing devices
h	New bed height of SCCR4 column
I_o	Intensity of radiation incident upon a sample
I	Intensity of radiation emerging from the sample
K_D	Equilibrium distribution coefficient
K'	Capacity factor
K^1	Average K_D value of two components = $\frac{\frac{1}{2}(V_{R_1}+V_{R_2})-V_M}{V_M}$
K	Constant factor in relationship between intrinsic viscosity and molecular weight
K_D^G	Distribution coefficient of glucose
K_D^F	Distribution coefficient of fructose
K''	Kozeny's constant
k''	Rate constant of desorption
K_A, K_B	Partition coefficient for components A and B used in Barker and Huntington's relationship between product purity, number of plates and difficulty of separation

K_o	Partition coefficient for a component in Barker and Lloyd's H.T.U. Model
L_m	Distance migrated in the Random Walk model
l	Length of a packed column
l'	Step length in Random Walk model
L_1	Pre-feed mobile phase flowrate in SCCR4 unit
L_3	Post-feed mobile phase flowrate in SCCR4 unit
L'	Effective mobile phase flowrate in SCCR4 unit
L_4	Purge flowrate in SCCR4 unit
m	Total mass of component in sample in Pretorious and de Clerk's equation
Δ_m	Mass of component lost
N	Number of theoretical plates
n'	Number of steps in Random Walk model
N_{min}	Minimum number of theoretical plates for achieving resolution
n_1	Number of mixing devices in a column
N_{cc}	Number of counter-current theoretical plates
$(N_{OG})_S$, $(N_{OG})_R$	Number of overall gas phase transfer units in the stripping and rectifying sections respectively in Barker and Lloyd's H.T.U. model
P	Stationary phase flowrate in SCCR4 unit
g	solute concentration in stationary phase used in SCCR4 simulation model
Q	Production rate in Timmin's equation

Q_f Mobile phase flowrate used in SCCR4 simulation model

R_s Resolution

R Fraction of time of solute in the mobile phase

r_c Radius of column

r_{m_i} Rate of movement of component with mobile phase in SCCR4 unit

r_{m_s} Rate of movement of component with stationary phase in SCCR4 unit

S_p Specific surface area of packing particles used in Kozeny's equation

S Time of one sequencing interval of the SCCR4 unit

t_R Elution time of a component

t_o Elution time of non-retained component

t_D Diffusion time

T' Transmittance

u Mobile phase velocity

V Average fluid velocity used in Kozeny's equation

$(u_z)_A$, $(u_z)_B$ Mass flowrate ratio of component A and B used in the equilibrium stage model of Sciance and Crosser

u_L Stationary phase velocity

V_R Elution volume of a component

V_M Total volume of the mobile phase in a SCCR4 column

V_s	Volume of stationary phase in a SCCR4 column
V	Volume of fluid flowing in time, t
V_i	Pore volume
V_o	Void volume (Elution volume of starch)
V_{TOTAL}	Total column volume
V_G, V_L	The gas and liquid volumetric flowrates in Barker and Lloyd's H.T.U. model
V_1, V_2	Volume of mobile and stationary phase respectively in one theoretical plate employed in SCCR4 simulation study
$V_{m_{AV}}$	Average velocity of mobile phase in SCCR4 unit
$V_{s_{AV}}$	Average velocity of stationary phase in SCCR4 unit
W	Solute band width of a component
$W_{h'/e}$	Peak width at 1/e of peak height used to calculate N
W_{t_o}	Total chromatogram width/sample at column outlet in production equation for co-current chromatographic operation
W_i, W_α, W_β	Factors used in chromatographic theoretical plate height equation to allow for non-uniformity of velocity profile and packing structure
X	Concentration of feed in mobile phase during injection
Z	Distance along a column of length L
σ	Standard Deviation
λ	Packing characterisation term for eddy diffusivity
α'	Constant for packing geometry

α	Relative retention factor
γ'	Labyrinth factor to allow for the torous flow path
γ_1, γ_2	Rate of transfer of molecules from gas to liquid and from liquid to gas respectively used in Al-Madfai's model for predicting plate height in continuous 'moving column' counter current chromatography
ϕ	Column porosity
ρ	Mobile phase density
η_L	Mobile phase utilisation efficiency
ε_L	Column utilisation efficiency
ε	Voidage
μ	Fluid viscosity
ψ	Operating mobile phase/stationary phase velocity ratio
ψ_R, ψ_S	The ratio of mobile phase/stationary phase flowrate in the rectifying and stripping sections respectively used in Barker and Huntington's relationship between product purity, number of theoretical plates and difficulty of separation
δ_i, δ_i', δ_i''	Series of factors to correct theoretical operating $L'/_P$ limits of the SCCR4 unit.

REFERENCES

1. P.E. Barker and D. Critcher, Chem. Eng. Sci., 13, 82 (1960).
2. D. Critcher, Ph.D. Thesis, University of Birmingham, 1963.
3. P.E. Barker and D. Lloyd, Symposium on the Less Common Means of Separation, 1963, Inst. Chem. Eng., London, 1964, p.68.
4. D. Lloyd, Ph.D. Thesis, University of Birmingham, 1963.
5. P.E. Barker and D. Lloyd, U.S. Patent 3,338,031.
6. P.E. Barker and D.H. Huntington, J. Gas Chromatog. 4, 59, (1965).
7. D.H. Huntington, Ph.D. Thesis, University of Birmingham, 1967.
8. P.E. Barker and D.H. Huntington, Dechema Monograph, 62, 153 (1969).
9. P.E. Barker and Universal Fisher Eng. Co. Ltd., British Patent Applications 33630/65; 43629/65, 5764/68, 44375/68.
10. P.E. Barker and S. Al-Madfai, J. Chromatog. Sci, 7, 425 (1969).
11. P.E. Barker and S. Al-Madfai, Proc. 5th International Symposium on Advances in Chromatography, Las Vegas, 1969, Preston Technical Abstracts Co., Evanston, Illinois, 1969, p.123.
12. S. Al-Madfai, Ph.D. Thesis, University of Birmingham, 1969.

13. P.E. Barker, "Preparative Gas Chromatography", A. Zlatkis, Ed., Wiley-Interscience, London, 1971, p.325.

14. B.W. Hatt, Ph.D. Thesis, University of Birmingham, 1970.

15. P.E. Barker, S.A. Barker, B.W. Hatt and P.J. Somers, Chem. and Proc. Eng., 52 (1), 64 (1971).

16. A.B. Sunal, Ph.D. Thesis, University of Aston in Birmingham, 1973.

17. P.E. Barker and R.E. Deeble, paper presented at Symposium on Less Common Means of Separation, Inst. of Chem. Eng., London, 1972.

18. P.E. Barker and R.E. Deeble, Anal. Chem., 45, 1121, (1973).

19. P.E. Barker and R.E. Deeble, British Patent Appl. 27786/72, and U.S. Patent Appl. 368,584.

20. R.E. Deeble, Ph.D. Thesis, University of Aston in Birmingham, 1974.

21. J.F. Ellison, Ph.D. Thesis, University of Aston in Birmingham, 1976.

22. A.N. Williams, Ph.D. Thesis, University of Aston in Birmingham, 1976.

23. P.E. Barker, B.W. Hatt and F.J. Ellison, "Chromatography of Synthetic and Biological Polymers", Vol.1, pp. 218-238, 1977.

24. B.W. Hatt and A. Knoechelmann, Private communication.

25. J.J. Kirkland, Modern Practice of Liquid Chromatography, Wiley-Interscience, 1971.

26. A.T. James and A.J.P. Martin, Biochem. J., 50, 679, (1952).

27. E.Glueckauf, Trans. Faraday Soc., 51, 34 (1955).

28. L. Lapidus and N.R. Amundson, J. Phys. Chem., 56, 984 (1952).

29. J.J. Van Deemter, F.J. Zuiderweg and A. Klinkenberg, Chem. Eng. Sci., 5, 271 (1956).

30. J.C. Giddings, "Dynamics of Chromatography, Part I, Principles and Theory", Edward Arnold Ltd., London, 1965.

31. J.C. Giddings, W.A. Mainwaring and M.N. Myers, Science, 154, 146 (1966).

32. O. Grubner, "Advances in Chromatography Vol.6", R.A. Keller and J.C. Giddings, Eds., Marcel Dekkor Inc., New York, 1968, p.173.

33. J.C. Giddings, J. Chem. Ed., 35, 588 (1958).

34. J.C. Giddings and H. Eyring, J. Phys. Chem., 59, 416 (1955).

35. J.C. Giddings, J. Gas Chromatog., 1 (1), 12 (1963).

36. J.C. Giddings, J. Gas Chromatog., 1 (4), 38 (1963).

37. J.C. Giddings and G.E. Jensen, J. Gas Chromatog., 2 (9), 290 (1964).

38. A. Einstein., Ann. der Physik, 17, 549 (1905).

39. S.J. Angyal, Inst. J. Chem., 1972, 25, pp 1957-66.

40. S.J. Angyal, and M.E. Evan, Carbohydrate Research, 25 (1972), 43-48.

41. S.J. Angyal, D. Greeves and J.A. Mills, Aust. J. Chem., 1974, 27, 1447-56.

42. S.J. Angyal and R.J. Hickman; Aust. J. Chem. 1975, 28, 1279-87.

43. S.J. Angyal, C.L. Bodkin and F.W. Parrish; Aust. J. Chem, 1975, 28, 1541-9.

44. S.J. Angyal, Journal of Pure Applied Chem., 1973, 35, 131-146.

45. F.W. Parrish, S.J. Angyal, M.E. Evan and J.A. Mills, Carbohydrate Research, 45 (1975), 73-83.

46. K. Torssell, J.H. McClendon and G.F. Somers., Acta. Chem. Scand, 12 (1958) No.7.

47. E.O. Von Lippman; Abstract from J.A. Rendleman Jr., Carbohydrate Chem., 1966, 21, 209.

48. H. Vogel and A. Georg; Abstract from J.A. Rendleman Jr., Carb. Chem., 1966, 21, 209.

49. S. Matsuura, J. Chem. Soc. Japan, Pure Chem. Sect., 49, 247 (1928).

50. O. Wiklund, Zucker, 8, 266 (1955).

51. N.V. Lebedev, Chem. Abstract, 54, 4012 (1960) and 55, 14952 (1961).

52. P.J. Charley, Abstract from J.A. Hendleman, Jr., Carb. Chem., 1966, 21, 212.

53. K. Nishizawa and Y. Hachihama; J. Soc. Chem. Ind. Japan, 36, 497 (1933).

54. J.A. Rendleman, Jr., J. Org. Chem, 31, 1839 (1966).

55. Naffia and Frege, Abstract from J.A. Rendleman, Carb. Chem, 1966, 21, 220.

56. J.M. Stokes and R.H. Stokes, J. Phys. Chem, 60, 217 (1956), 62, 497 (1958).

57. K.B. Domovs and E.H. Freund, J. Dairy Sci., 43, 1216 (1960).

58. R. Tatuki., U.S. Patent No. 3671316.

59. R.H. Smith and B. Tollens, Ber., 33, 1277 (1900).

60. L.M.J. Verstraeten, Adv. Carb. Chem., 1967, 22, 229-305.

61. P.J. Antikainen, Finn. Chem. Lett., 1974, 4, 159-64.

62. J.K.N. Jones, R.A. Wall and A.O. Pittet, Can. J. Chem., 1960, 38, 2285-9.

63. J.K.N. Jones, R.A. Wall, Can. J. Chem. 1969, 38, 2290.

64. The Colonial Sugar Refining Co., Brit. Pat. 1,083,500, September, 1967.

65. C.F. Boehringer and Soehme GmbH; British Patent 1085696, October, 1967.

66. BMA process pamphlet by Boehringer Mannheim GmbH, 1968.

67. J.K. Dale and D.P. Langlosis; U.S. Patent, 2,201,609.

68. R.O. Marshall and E.R. Kooi, Science 125-648 (1957).

69. R.O. Marshall, U.S. Patent 2,950,228 (1960).

70. N. Tsumara and T. Sato., Agri. Biol. Chem., 25:616 (1961).

71. M. Natake and S. Yoshimura., Agri. Biol. Chem. 27:342, (1963).

72. Y. Takasaki., Agri. Boil. Chem., 30:1247 (1966).

73. T. Sato and N. Tsumura., Agri. Boil. Chem., 29:1129 (1965).

74. T. Sato and N. Tsumura., Japan Patent 17640.

75. Y. Takasaki and O. Tanabe., U.S. Patent 3616221.

76. Y. Takasaki, Y. Kosugi and A. Kanbayashi., Fermentation Advances, Academic Press, New York p.561 (1969).

77. N.H. Mermelstein., Food Tech., 29 (6), 20 (1975).

78. J.D. Harden, Food Engineering (12) : 59 (1972); (1): 65 (1973).

79. Lloyd et al., (1972) U.S. Patent 3694134.

80. Thompson et al., (1974) U.S. Patent 3788945.

81. Financial Times, February, (1975).

82. L. Zittin., M.H. Nielsen., Die Starke, 1975, 27 (7), 236.

83. I. Yasushi., Japan Patent 75,160,479, (1975).

84. J.C. Giddings., J. Gas Chromatog., 1 (4), 38 (1963).

85. J.C. Giddings and G.E. Jensen, J. Gas Chromatog., 2, (9), 290 (1964).

86. F.H. Huyten, W. Van Beersan and G.W.A. Rijinders, "Gas Chromatog. 1960", R.P.W. Scott, Ed., Butterworths, London, 1960, pp.224.

87. G.M.C. Higgins and J.F. Smith, "Gas Chromatog 1964", A. Goldup, Ed., Inst. of Petroleum, London, 1965, p.94.

88. G.W.A. Rijinders, "Advances in Chromatography Vol.3", Marcel Dekler, New York, 1966, p.215.

89. E. Bayer, K. Hupe and H. Mack, Anal. Chem. 35, 492 (1963).

90. A.B. Littlewood, Anal. Chem. 38, 2 (1966).

91. S.T. Sie and G.W.A. Rijinders, Anal. Chem. Acta., 38, 3 (1967).

92. V. Pretorius and K. de Clerk, "Preparative Gas Chromatography", A. Zlatkis and V. Pretorius, Eds., Wiley - Interscience, London, 1971, p.1.

93. S.F. Spencer and P. Kucharski, Facts and Methods, 7, (4), 8 (1966).

94. J.H. Knox, "Advances in Gas Chromatography", A. Zlatkis and L. Ettre, Eds., Preston Technical Abstracts Co., Illinois, 1966.

95. J.R. Conder and J.H. Purnell, Chem. Eng. Prog. Symp. Ser., 91 (65), 1 (1969).

96. J.R. Conder and J.H. Purnell, Chem. Eng. Sci., 25, 353 (1970).

97. F. Helfferich, J. Chem. Educ., 41, 410 (1964).

98. J.H. Purnell, J. Chem. Soc., 1268 (1960).

99. C.L. Guillemin., J. Chromatog. 12, 163 (1963), 30, 222 (1967).

100. J. Albrecht and M. Verzele., J. Chromatog. Sci., 8, 586 (1970).

101. L.R. Snyder, Anal. Chem., 39, 698 (1967).

102. R.S. Timmins, L. Mir and J.M. Ryan, Chem. Eng., 76, 170 (1969).

103. S.M. Gordon, G.J. Krige and V. Pretorius, J. Gas Chromatog., 2, 241 (1964)., 2, 246 (1964); 2, 285 (1964), 3, 87 (1965).

104. J.R. Conder, paper presented at Symposium on Less Common Means of Separation, Inst. Chem. Eng., London, 1972.

105. W.N. Musser and R.E. Sparks, J. Chromatog. Sci., 9, 116 (1971).

106. J. Albrecht and M. Verzele, J. Chromatog. Sci., 9 745 (1971).

107. A.B. Carel and G. Perkins Jr., J. Anal. Chem. Acta., 34, 83 (1966).

108. A.B. Carel, R.E. Clement and G. Perkins Jr., J. Chromatog. Sci., 7, 218 (1969).

109. R.E. Pescar, "Preparative Gas Chromatography", A. Zlatkis and V. Pretorius, Eds., Wiley-Interscience, London, 1971, p.73.

110. M.J. Golay, "Gas Chromatography", H.J. Noebels, R.F. Wall, N. Brenner, Eds., Academic Press, New York, 1961.

111. L. Mir, J. Chromatog. Sci., 9, 436 (1971).

112. J.W. Amy, L. Brand and W. Baitinger, 12th Pittsburg Conference of Analytical Chemistry and Applied Spectroscopy, Pittsburgh, Pennsylvania, 1961.

113. G.J. Friscone, J. Chromatog., 6, 97 (1961).

114. B.J. Bradley and P.F. Tiley, Chem. Ind. (London), 18, 743 (1963).

115. G.R. Fitch, M.E. Probert and P.F. Tiley, J. Chem. Soc., 4875 (1962).

116. D.W. Pritchard, M.E. Probert and P.F. Tiley, Chem. Eng. Sci., 26, 2063 (1971).

117. W. Kuhn, E. Narten and M. Thurkauf, 5th World Petroleum Congress; 1958, Section 5, paper 5, p.45.

118. W. Kuhn, E. Nanten and M. Thurkauf, Helv. Chem. Acta., 41, 2135 (1958).

119. S. Turina, V. Krajovan and T. Kostonaj, Z. Anal. Chem., 189, 100 (1962).

120. R.L. Pigford, B. Baker III and D.E. Blum, Ind. Eng. Chem. Fundamentals, 8, 144 (1969).

121. R.L. Pigford, B. Baker III and D.E. Blum, Ind. Eng. Chem. Fundamentals, 8, 848 (1969).

122. R.H. Wilhelm and N.M. Sweed, Science, 159, 522 (1968).

123. E.J. Tuthill, J. Chromatog. Sci., 8, 285 (1970).

124. P.C. Wankat, Separat. Sci., 9, 85 (1974).

125. P.C. Wankat, Ind. Eng. Chem. Fundamentals, 14 (2), 102 (1975).

126. A.J.P. Martin, Discussion Faraday Soc., 7, 332 (1949).

127. J.C. Giddings, Anal. Chem., 34, 37 (1962).

128. D. Dinelli, S. Polezzo and M. Taramasso, J. Chromatog., 7, 447 (1962).

129. D. Dinelli, M. Taramasso and S. Polezzo, U.S. Patent, 3,187,486.

130. M. Taramasso and D. Dinelli, J. Gas Chromatog., 2, 150 (1962).

131. M. Taramasso and F. Sallusto and A. Guerra, J. Chromatog. 20, 226, (1965).

132. M. Taramasso, J. Chromatog., 49, 27 (1970).

133. J.B. Fox Jr., R.C. Calhoun and W.J. Eglinton, J. Chromatog., 43, 48 (1969).

134. J.B. Fox Jr., J. Chromatog., 43, 55 (1969).

135. R.A. Nicholas and J.B. Fox Jr., J. Chromatog, 43, 61 (1969).

136. U.S. Patent 3,078,647 (1963).

137. U.S. Patent 3503712 (1970).

138. M.V. Sussman, K.N. Astill, R. Bombach, A. Cerrulo and S.S. Chen., Ind. Eng. Chem. Fundamentals, 11, 181 (1972).

139. M.V. Sussman, K.N. Astill and R.N.S. Rathore., J. Chromatog. Sci., 12, 91 (1974).

140. H. Schultz, "Gas Chromatography" (1962), M. Van Swaay, Ed., Butterworths, London, 1963, p.225.

141. R.P.W. Scott, "Gas Chromatography", (1958), D.H. Desty, Ed., Butterworths, London, 1958, p.189.

142. W.L. Nelson, "Petroleum Refinery Engineering", McGraw-Hill, New York, 1958.

143. U.S. Patent 2,869,672.

144. H. Pichler and H. Schultz, Bremmstoff Chem., 39, 48 (1958).

145. U.S. Patent 3,016,107 (1959).

146. D. Glasser, "Gas Chromatography 1966", R.B. Littlewood, Ed., Inst. of Petroleum, London, 1967 p.119.

147. U.S. Patent 2,893,955 (1959).

148. Unidev leaflet on Sequential Separation, Unidev Ltd., Crawley, Sussex.

149. P. Carr., Unilever Ltd., paper presented at 8th International Symposium on Advances in Chromatography, Toronto, 1973.

150. L. Szepesy, Zs. Sebestyen, I. Feber and Z. Nagy, J. Chromatog., 108, 285 (1975).

151. D.B. Broughton, Chem. Eng. Prog., 64 (8), 60 (1968).

152. D.B. Broughton, R.W. Neuzil, J.M. Pheris and C.S. Brearley, Chem. Eng. Prog, 66 (9), 70 (1970).

153. S. Liodakis, Ph.D. Thesis, University of Aston, 1977.

154. P. Somers, Birmingham University, private communication.

155. W. Yaphe and G.P. Arsenault, Anal. Biochem., 13 (1965), 143.

156. S.A. Barker, B.W. Hatt and P.J. Somers, Carbohyd. Res., 26 (1973) 41.

157. S.A. Barker, Anal. Biochem., 26 (1968) 219.

158. J.M. Coulson and J.F. Richardson, "Chemical Engineering Vol.2 - Unit Operations", Pergammon Press, Oxford, 1968, p.6.

159. E.Glueckauf, "Ion-exchange and its Applications", Soc. Chem. Ind., London, 1956, p.34.

160. "Ion Exchange Properties", published by BDH Ltd,,

161. C. Chuah, private communication.

162. Tswett, Trav. Soc. Nat. Varsovia, No.6, 14 (1963).

163. K. Dorfner, "Ion Exchangers : Properties and Applications", Ann arbor science publishers inc. 1972.

164. P.R. Rony, Separation Science, 5, (2), 1970.

165. L. Alder, "Liquid-liquid Extraction", Elsevier, Amsterdam, 1959.

166. C.T. Sciance, O.K. Crosser, A.I. Chem. Eng. Journal, 12 (1), 100, 1966.

167. K. England, University of Aston, unpublished work.

168. A.J.P. Martin and R.L.M. Synge, Biochem. J., 35, 1358 (1941).